Investigating the Human-*M. tuberculosis* interactome to identify the host targets of ESAT-6 and other mycobacterial antigens

by
Natalie Bruiners

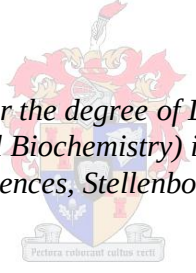

Dissertation presented for the degree of Doctor of Philosophy in Medical Sciences (Medical Biochemistry) in the Faculty of Medicine and Health Sciences, Stellenbosch University

Promotor: Prof Nicolaas Claudius Gey van Pittius
Co-promotor: Prof Robin Mark Warren

December 2012

DECLARATION

By submitting this dissertation electronically, I declare that the entirety of the work contained therein is my own, original work, that I am the owner of the copyright thereof (unless to the extent explicitly otherwise stated) and that I have not previously in its entirety or in part submitted it for obtaining any qualification.

Date: 6 Augustus 2012

Signature: Natalie Bruiners

ABSTRACT

The causative agent of human tuberculosis, *Mycobacterium tuberculosis*, is an intracellular pathogen that secretes virulence factors, namely ESAT-6 and CFP-10, as substrates of the ESX-1 secretion system. It is hypothesised that these substrates interact with host proteins in a targeted manner in order to elicit a required immune response, and they have been shown to be involved in processes related to pro-inflammatory responses, necrosis, apoptosis, membrane lysis and cytolysis. However, the biological function of ESX-1 substrates during host-pathogen interactions remains poorly and incompletely understood. Therefore, the present study was designed to gain insight into the role of the ESX-1 secretion system substrates in host-pathogen interactions and to identify how *M. tuberculosis* mediates the response of the human host.

In this study, a cDNA yeast two-hybrid library was constructed from human lung mRNA, to identify mycobacterial-host protein-protein interactions that occur within the lung alveoli. The ESX-1 secretion system substrates, ESAT-6 and CFP-10, were cloned in-frame into the pGBKT7 vector, which was used in the yeast two-hybrid system to screen the lung cDNA library in *Saccharomyces cerevisiae*. The ESAT-6 and CFP-10 screens identified 79 and 19 positive colonies, respectively. Of the total number of clones characterised, only two in-frame inserts were identified with the ESAT-6 screen, corresponding to the human proteins filamin A and complement component 1, q subcomponent, A chain (C1QA). In addition, the screen with CFP-10 also identified C1QA as binding partner.

Subsequent *in vitro* and *in vivo* experiments were unable to confirm the putative interactions of C1QA with ESAT-6 and CFP-10. However, the interaction between filamin A and ESAT-6 was demonstrated and confirmed by both *in vivo* co-localisation and co-immunoprecipitation. Furthermore, the degradation of filamin A in the presence of ESAT-6 was shown to be reflective of cytoskeleton remodelling and the induction of cell death. The work presented here suggests that as ESAT-6 gains access to the cytosol, it initiates cell death by inducing destabilisation of the cytoskeleton cell structure. This may possibly be driven by the interaction of ESAT-6 and filamin A.

Finally, we also initiated an investigation of the identified putative binding partners (filamin A and C1QA) as possible genetic markers for genetic susceptibility studies to tuberculosis. A

case-control analysis was performed involving 604 cases, of which 109 were Tuberculous Meningitis (TBM), and 486 were controls from the South African Coloured (SAC) population within the Ravensmead-Uitsig catchment area. The results of this analysis demonstrated a novel association of a regulatory variant (rs587585) located upstream of the *C1QA* gene and demonstrated an increasing trend towards increased values in tuberculosis patients with the associated genotype.

This study has contributed significantly to our understanding of human-mycobacterial host-pathogen protein-protein interactions and has opened the way for future studies further exploring the consequences and function of the identified ESAT-6-filamin A interaction. It has also led to the identification of a novel genetic association with tuberculosis. Finally, it demonstrates the usefulness of the yeast two-hybrid system to identify potential protein-protein (host-pathogen) interactions that can lead to additional important and exciting research questions.

OPSOMMING

Die organisme wat tuberkulose veroorsaak, *Mycobacterium tuberculosis*, is `n intrasellulêre patogeen wat virulensie faktore afskei, naamlik ESAT-6 en CFP-10, as substrate van die ESX-1 sekresiesisteem. Daar word vermoed dat hierdie substrate met gasheerproteïene in ‘n teiken wyse interaksie het om `n vereiste immuunreaksie voort te bring. Hierdie substrate is betrokke by prosesse soos pro-inflammatoriese reaksies, nekrose, apoptose, membraanlise en sitolise. Die biologiese funksie van die ESX-1 substrate tydens gasheer-patogeen interaksies word egter tans swak en onvolledig verstaan. Daarom was die huidige studie ontwerp om insig te bekom oor die rol hiervan in gasheer-patogeen interaksies en om te identifiseer hoe *M. tuberculosis* die reaksie teenoor die gasheer bemiddel.

In hierdie studie was `n komplementêre deoksiribonukleïensuur (kDNS) gis twee-hibried biblioteek gemaak vanaf long boodskapper ribonukleïensuur (bRNS) om proteïen-proteïen interaksies wat in die long plaasvind, te identifiseer. Die substrate van die ESX-1 sekresiesisteem, ESAT-6 en CFP-10, is in volgorde gekloneer in die pGBKT7 vektor en is gebruik om die long kDNS biblioteek in *Saccharomyces cerevisiae* te ondersoek. In die soeke na interaksies met ESAT-6 and CFP-10, was 79 en 19 positiewe kolonies onderskeidelik geïdentifiseer. Van die aantal klone, was slegs twee volgordes in-leesraam geïdentifiseer met ESAT-6. Hierdie proteïene het ooreengestem met filamin A en “complement component 1, q subcomponent, A chain” (C1QA). Bykomend hiertoe, is C1QA ook geïdentifiseer as ‘n bindende vennoot met CFP-10.

Daaropvolgende *in vitro* and *in vivo* eksperimente kon nie die vermeende interaksie van C1QA met ESAT-6 en CFP-10 bevestig nie. Maar die interaksie tussen filamin A en ESAT-6 kon wel gedemonstreer word deur die gebruik van mede-lokalisering en mede-imunopresipitasie. Die afbreek van filamin A in die teenwoordigheid van ESAT-6 is ook aangetoon en blyk ‘n weerspieëling te wees van sitoskelet hermodellering en die induksie van seldood. Die werk wat hier aangebied word, dui daarop dat soos ESAT-6 toegang kry tot die sitosol, inisieër dit seldood deur die destabilisaisie van die sitoskelet selstruktuur. Dit word moontlik aangedryf deur die interaksie van ESAT-6 met filamin A.

Laastens het ons `n ondersoek van die geïdentifiseerde bindingsvennote (filamin A and C1QA) as moontlike genetiese merkers vir genetiese vatbaarheidsstudies vir tuberkulose uitgevoer. `n Pasiënt-kontrole studie is gedoen waarby 604 individue ingesluit is, waarvan 109 gediagnoseer is met Tuberculosis Meningitis (TBM), en die ander 486 kontrole individue was van die Suid Afrikaanse Kleurling (SAC) bevolking binne die Ravenmead-Uitsig opvanggebied. Die resultate het ‘n nuwe assosiasie van ‘n regulerende variant (rs587585) wat stroomop van die *C1QA* geen gelokaliseer is, getoon. Hierdie variant het `n verhoogde neiging in tuberkulose pasiënte met die geassosieërde genotipe getoon.

Hierdie studie het `n beduidende bydrae gemaak tot ons begrip van menslike-mikobakteriese gasheer-patogeen proteïen-proteïen interaksies. Hierdie resultate het die weg oopgemaak om die gevolge en funksie van die geïdentifiseerde ESAT-6-filamin A interaksie verder te ondersoek. Dit het ook aanleiding gegee tot die identifikasie van `n genetiese assosiasie met tuberkulose. Om saam te vat, hierdie werk bewys die bruikbaarheid van die gis twee-hibriede sisteem, om potensiële proteïen-proteïen interaksies te ontdek wat die moontlikheid het om aanleiding te gee tot addisionele navorsingsvrae.

ACKNOWLEDGEMENTS

Lord, to You be all the glory, honour and praise.

Mama and papa, thanks you so much for all your support and words of encouragement and for always believing in me no matter what. Baie lief vir my dada en my noeksie!!!

Heinrich, my ou stouter…jou suster is baie lief vir jou. Dankie dat ek jou altyd kon bel en net kan ontlaai oor enige iets!

Richard my boeta dankie vir jou ondersteuning en die goeie tye saam op kampus.

Natasha en Graeme dankie vir al die fun times en dat julle altyd aan my snert luister. Julle twee is legends!!!

Mugeleigh dankie vir die grootste geskenk ooit, jou gebede.

My supervisor, Nico, thanks for all the support, guidance, proofreading and allowing me to run with ideas.

My co-supervisor, Rob, thanks for all you support, guidance, proofreading, fun and jokes.

Eileen van Helden and Marlo Möller Karstens, thank you for your valuable input.

Craig Kinnear and Hanlie Moolman-Smook for your guidance with the yeast two-hybrid.

To everyone in Lab 424, thank you for making my experience one to remember. Thank you for the support and pushing me with words of encouragement "Nearly there", "Remember, you are?? AWESOME!!!" and "You can do this!" You are all amazing beautiful people!

Olivia, Jeska, Hanlie (en jou Ouma), Jacques, Nasstasja, Neal, Francios, Nyameka and Herby thanks for all your prayers.

Suereta Fortuin, Leanie Kleynhans Cornelissen, Gaynor Gardiner, Andrea Gutschmidt, Liezl Bloem, Lynsey Isherwood, Tatiana Super, Marika "Lady" Bosman, thank you for all your support and encouragement!

The National Research Foundation, the Harry Crossley Foundation, Ernst and Ethel, Medical Research Council of South Africa, Stellenbosch Postgraduate funding and Professor Paul van Helden for financial support.

TABLE OF CONTENTS

DECLARATION ii
ABSTRACT iii
OPSOMMING v
ACKNOWLEDGEMENTS vii
TABLE OF CONTENTS viii
LIST OF TABLES xv
LIST OF FIGURES xvii
LIST OF APPENDICES xxii
ABBREVIATIONS xxiii

CHAPTER 1

1. Introduction 2

1.1. The varied lifestyles of intracellular pathogens 2

1.2. *Mycobacterium tuberculosis* 4
1.2.1. A brief history 4
1.2.2. TB incidence 5
1.2.3. Bacteriology 6
1.2.4. The course of *M. tuberculosis* infection 8

1.3. Genome of *Mycobacterium tuberculosis* 9
1.3.1. ESX-1 secretion system 11
1.3.2. Structural characteristics of CFP-10 and ESAT-6 13
1.3.3. Role of the ESX-1 secretion system and virulence 15
1.3.4. Host binding partners of ESAT6 16
1.3.4.1. Syntenin-1 16
1.3.4.2. Toll-like receptor 2 17
1.3.4.3. Phenylalanine-rich peptides 17
1.3.4.4. Laminin 18

1.4. Mycobacterial virulence strategies inside macrophages 18
1.4.1. Survival during phagosomal acidification 18

Page

1.4.2. Inhibition of phagosome-lysosome fusion and "phagosomal maturation" 20
1.4.3. Other mechanisms of survival 21

1.5. Interaction of *Mycobacterium tuberculosis* with the macrophage 22
1.5.1. Complement receptors 22
1.5.2. Mannose receptors 25
1.5.3. Surfactant receptors 26
1.5.4. Toll-Like receptors 28
1.5.5. Nucleotide-binding oligomerisation domain-like receptors 30
1.5.6. Other 31

1.6. Systematic approach to understanding tuberculosis 31
1.6.1. Human genetic variation and host susceptibility 32
1.6.2. Strain variation and the influence on host response 35
1.6.3. Tuberculosis and HIV co-infection 39
1.6.4. Complexity of interactome analysis 40

1.7. The present study 40
1.7.1. Problem statement 40
1.7.2. Hypothesis 41
1.7.3. Aim 41
1.7.4. Objective 42

CHAPTER 2

2 Materials and Methods 44

2.1 Strains, plasmids and cell lines 44
2.1.1 Bacterial strains 44
2.1.1.1 *M. tuberculosis strain* 44
2.1.1.2 *Escherichia coli XL-1 blue* 44
2.1.2 *Saccharomyces cerevisiae* strains 44
2.1.3 Plasmids 45
2.1.4 Human cell lines 45

2.2 Generation of competent cells 46
2.2.1 Electro-competent *E. coli* XL-1 cells 46
2.2.2 Chemically competent yeast cells 46

2.3 Polymerase Chain Reaction (PCR) 47
2.3.1 Primer design 47
2.3.2 Generation of PCR inserts 47

2.4 PCR amplification 47
2.4.1 Amplification of insert fragments 47
2.4.2 Colony PCR 48
2.4.3 cDNA amplification 48

2.5 Agarose gel electrophoresis 49

2.6 Automated DNA sequencing and analysis 49
2.6.1 DNA sequencing 49
2.6.2 Analysis of DNA fragments 50

2.7 Generation of constructs 50
2.7.1 pGemT-easy cloning 50
2.7.2 Restriction digest 51
2.7.3 Shrimp alkaline phosphatase treatment 52
2.7.4 DNA ligation 52

2.8 Plasmid transformation 52
2.8.1 Bacterial plasmid transformation 52
2.8.2 Yeast plasmid transformation 53

2.9 Plasmid purification methods 53
2.9.1 Bacterial plasmid purification 53

2.9.2 Yeast plasmid purification 54

Page

2.10 Tissue culturing human cell lines 54
2.10.1 Culturing from frozen stocks 54
2.10.2 Splitting the cell culture 54
2.10.3 Differentiation of THP-1 cells 54
2.10.4 Generating stock cultures 55

2.11 *In vivo* treatments 55
2.11.1 Etoposide-induced apoptosis 55

2.12 Protein transfection 55

2.13 Evaluation of yeast strains and constructs 56
2.13.1 Phenotypic assessment of yeast strains 56
2.13.2 Testing the DNA-BD construct for transcriptional activation 56
2.13.3 Toxicity test of transformant yeast strains 57

2.14 Yeast two-hybrid analysis 57
2.14.1 Principles of the yeast two-hybrid (Y2H) technique 57
2.14.2 Library construction 58
2.14.3 Establishment of bait culture 59
2.14.4 Yeast two-hybrid assay 60

2.15 *In vivo* microscopy 61
2.15.1 Tissue culturing and staining for microscopy 62
2.15.2 Fluorescence microscopy and *in vivo* co-localisation 63

2.16 *In vivo* co-immunoprecipitation 63
2.16.1 Principle 63
2.16.2 Preparation of cell lysates 64
2.16.3 Membrane protein extraction 64
2.16.4 *In vivo* semi-endogenous co-immunoprecipitation 65
2.16.5 Western blot analysis 65

2.17 Case-Control study 66
2.17.1 Patient and control cohort 66

Page

2.17.2 Demographics of the study cohort 67
2.17.3 Promoter screening for functional variants 67
2.17.4 SNP selection 68
2.17.5 TaqMan SNP genotyping 68
2.17.6 Real Time PCR amplification 69
2.17.7 Allelic discrimination 69

2.18 ELISA assay 70

2.19 Statistical Analysis 70

CHAPTER 3

3 Yeast two-hybrid analysis to identify host binding partners of ESAT-6 and CFP-10 73

3.1 Results 73

3.1.1 Construction of lung cDNA library 73
3.1.1.1 Integrity of lung RNA 73
3.1.1.2 cDNA amplification 74
3.1.1.3 Library construction 75

3.1.2 Bait construction 76
3.1.2.1 Amplification of ESAT-6 and CFP-10 76
3.1.2.2 pGem-T-easy ligation and colony PCR 76
3.1.2.3 Construction of pGBKT7 constructs 77

3.1.3 Testing of pGBKT7 constructs 78
3.1.3.1 Testing pGBKT7 constructs for toxicity 78
3.1.3.2 Testing pGBKT7 constructs for transcriptional activation 80

3.1.4 Yeast two-hybrid screen 80
3.1.4.1 ESAT-6 80
3.1.4.2 CFP-10 82

Page

3.2 Discussion 83

CHAPTER 4

4 Verification studies of ESAT-6 and CFP-10 binding partners 91

4.1 Results 91

4.1.1 Recombinant mycobacterial proteins 91

4.1.2 Transfection of recombinant proteins into cultured cells 92

4.1.3 Detection of endogenous proteins 94

4.1.4 *In vivo* co-localisation of C1QA with ESAT-6 and CFP-10 95

4.1.5 Co-immunoprecipitation of C1QA with ESAT-6 and CFP-10 96

4.1.6 *In vivo* co-localisation of filamin A and ESAT-6 98

4.1.7 *In vivo* co-immunoprecipitation of filamin A and ESAT-6 104

4.1.8 Effect of ESAT-6 on Jurkat cells and endogenous filamin A 105

4.1.9 Cytotoxicity and cell death mediated by ESAT-6 108

4.2 Discussion 109

CHAPTER 5

5 Association studies of the C1Q gene cluster 115

5.1 Results 115

5.1.1 FLNA gene 115

5.1.1.1 PCR amplification of the promoter of *FLNA* 115

Page

5.1.1.2 Sequence analysis 116

5.1.2 *C1QA* gene 117

5.1.2.1 TaqMan allelic discrimination results 118

5.1.2.2 Genotype and allele frequencies 119

5.1.3 Linkage disequilibrium and haplotype analysis 122

5.1.4 C1QA ELISA 124

5.1.4.1 Analysis of normality 124

5.1.4.2 Group and subgroup analyses 124

5.2 Discussion 126

CHAPTER 6

6 CONCLUSION 131

REFERENCES 138

APPENDICES 159

LIST OF TABLES

Chapter 2

Table 2.1: Plasmids used in this study 45

Table 2.2: Primers used in this study. 48

Table 2.3: Starting product size and required concentration for sequencing reactions 50

Table 2.4: Nutritional requirements for AH109 and Y187 56

Table 2.5: Primary and secondary fluorescence labelled antibodies for use as immunofluorescent microscopy 62

Table 2.6: Summary of fluorescent filters 63

Table 2.7: Primary and secondary antibody combinations for the detection of proteins using Western blot analysis. 66

Table 2.8: Selected dbSNP used for this study and the TaqMan assay used to type the particular variant. 66

Chapter 3

Table 3.1: Testing pGBKT7-ESAT-6 and pGBKT7-CFP-10 constructs for transcriptional activation of reporter genes. 80

Chapter 5

Table 5.1: HapMap MAF of the five selected SNPs. 118

Table 5.2: Genotype and allele frequencies of the *C1Q* gene variants in the control, tuberculosis and Tuberculous Meningitis group. 120

Table 5.3: Results from association analyses of rs587585, rs665691, rs172378, rs12033074 and rs631090. 121

Table 5.4: Haplotype pairs of rs587585 and rs665691. 123

Table 5.5: Results of haplotype associations. 123

Chapter 6

Table 6.1: Variations of Y2H systems and their specificities. 135

LIST OF FIGURES

Chapter 1

Figure 1.1: Estimated TB incidence rates, by country, in 2010. 6

Figure 1.2: Microbial characteristics of *M. tuberculosis.* 7

Figure 1.3: Representation of the mycobacterial cell wall 8

Figure 1.4: Schematic representation of the genomic organisation of the five ESAT-6 gene cluster regions of *M. tuberculosis.* 11

Figure 1.5: Proposed model for secretion of substrates using Type VII secretion system. 12

Figure 1.6: Solution structure of the ESAT-6·CFP-10 protein complex. 14

Figure 1.7: Host cell receptors involved in *M. tuberculosis* infection. 24

Figure 1.8: Interplay of factors influencing tuberculosis disease. 32

Figure 1.9: Illustrates the genetic variation across a population. 33

Figure 110: Genes involved in TB susceptibility. 35

Figure 1.11: Global phylogeography of *M tuberculosis.* 36

Figure 1.12: Selection of MTBC isolates representative of global genetic diversity. 38

Figure 1.13: MTBC isolates and their varying ability to induce the production of pro-inflammatory cytokines. 38

Chapter 2

Figure 2.1: Principle of the yeast two-hybrid assay 57

Figure 2.2: Lung cDNA library construction using homologous recombination in yeast 58

Figure 2.3: Schematic flow diagram of the Y2H analyses and verification studies 60

Figure 2.4: Principle of *in vivo* co-immunoprecipitation. 64

Figure 2.5: Distribution of gender and age of the study cohort 67

Figure 2.6: Allelic discrimination 69

Chapter 3

Figure 3.1: Assessment of RNA integrity and purity. 73

Figure 3.2: 1.2 % TAE Agarose gel electrophoresis image of size fractionated ds cDNA before and after purification. 74

Figure 3.3: Screening of randomly selected yeast colonies. 75

Figure 3.4: 1.5% TAE agarose gel of PCR products of ESAT-6 and CFP-10. 76

Figure 3.5: Screening of white pGem-T-ESAT-6 and pGem-T-CFP-10 colonies. 77

Figure 3.6: Construction of pGBKT7-ESAT-6 and pGBKT7-CFP-10 constructs. 78

Figure 3.7: Recombinant pGBKT7-ESAT-6 and pGBKT7-CFP-10 constructs in Y187 yeast strains. 79

Figure 3.8: Growth rate of pGBKT7-ESAT-6 and pGBKT7-CFP-10. 79

Figure 3.9: 1.5% TAE agarose gel of PCR products of candidate clones identified during the ESAT-6 screen. 81

Page

Figure 3.10: Heterologous mating to re-test the interactions of ESAT-6. 81

Figure 3.11: 1.5% TAE agarose gel of PCR products of candidate clones identified during the CFP-10 screen. 82

Figure 3.12: Heterologous mating to re-test the interaction of CFP-10 and C1QA of six randomly selected clones. 83

Figure 3.13: Representation of FLNA. 86

Figure 3.14: Structure of C1Q. 87

Chapter 4

Figure 4.1: Western blot of ESAT-6 and CFP-10. 91

Figure 4.2: Western blot of Jurkat lysates transfected with recombinant ESAT-6. 92

Figure 4.3: Western blot of differentiated THP-1 lysates treated with recombinant ESAT-6 and CFP-10. 93

Figure 4.4: Cytolysis of differentiated THP-1 by recombinant ESAT-6. 94

Figure 4.5: Western blot detection of prey proteins. 95

Figure 4.6: *In vivo* localisation of endogenous C1QA. 96

Figure 4.7: *In vivo* co-immunoprecipitation of C1QA with CFP-10 and ESAT-6. 97

Figure 4.8: Non-specific background correction for ESAT-6 and filamin A. 98

Figure 4.9: *In vivo* co-localisation of ESAT-6 and filamin A. 99

Figure 4.10: Example of co-localising pixels. 100

Page

Figure 4.11: Measurement of co-localisation coefficient of ESAT-6 and filamin A. 101

Figure 4.12: Spectral profile of ESAT-6, filamin A and the cell nuclei. 102

Figure 4.13 Inclusion bodies with ESAT-6. Figure 4.14: XYZ section through THP-1 cells containing ESAT-6 inclusion bodies 103

Figure 4.14: XYZ section through THP-1 cells containing ESAT-6 inclusion bodies. 104

Figure 4.15: *In vivo* co-immunoprecipitation filamin A and ESAT-6. Figure 4.16: Expression levels of filamin A in the presence of ESAT-6 and CFP-10. 105

Figure 4.16: Expression levels of filamin A in the presence of ESAT-6 and CFP-10. 106

Figure 4.17 Expression level of filamin A and β-tubulin in the presence of CFP-10. 107

Figure 4.18 Expression level of filamin A and β-tubulin in the presence of ESAT-6 and etoposide. 108

Figure 4.19: Comparison of THP-1 nuclear morphology in treated and untreated with recombinant ESAT-6. 109

Chapter 5

Figure 5.1: 1% TAE Agarose gel electrophoresis image of the PCR products of the FLNA promoter. 115

Figure 5.2: Sequence alignment of TB cases to the reference sequence of *FLNA*. 116

Figure 5.3: Representative result for a TaqMan allelic discrimination plot. 119

Figure 5.4: LD structure for rs587585, rs665691, rs172378, rs12033074 and rs631090. 122

Figure 5.5: Representation of the ELISA data distribution. 124

Figure 5.6: Levels of C1QA distribution between groups and subgroups. 125

Figure 5.7: Levels of C1QA distribution stratified according to subgroups and rs587585 genotypes. 125

Chapter 6

Figure 6.1: Illustration and description of the set of six Gateway-compatible yeast two-hybrid pGBKT7 bait vector and pGADT7 prey vector. 133

LIST OF APPENDICES

1. Preparing buffers and media for *E. coli* cultures 159

2. Maps of vectors used in this study 163

3. Tissue culturing 166

4. Electro-competent *E. coli* 168

5. cDNA generation and library construction 172

6. Electrophoresis solutions, loading dyes and agarose gels 178

7. Promega Wizard® SV PCR, Gel and Plasmid Clean-up, High yield DNA extraction from larger volumes of bacterial culture and Yeast plasmid extraction 179

8. Bait Construction 183

9. Transform into yeast 186

10. Testing of DNA-BD Fusions 188

11. Yeast Two-Hybrid Assays 192

12. Verification and Analyses of Positive Interactions 196

13. Protocol for Immunofluorescence-Labelling of Cultured Cells 199

14. SDS polyacrylamide gel electrophoresis and Western blotting 201

15. Sandwich ELISA protocol 206

16. Haplotype frequencies 209

ABBREVIATIONS

°C	degree Celsius
µF	Microfarad
µFd	Capacitance
µg	microgram
µL	Microliters
µm	Micrometers
µM	Micromolar
3’	3 prime
3-AT	3-aminotrizole
5’	5 prime
5-FoA	5-fluoroorotic acid
A	Adenine
ATPases	adenosine triphosphatase
AD	activation domain
Ade	Adenine
ADE2	Phosphoribosylaminoimidazole carboxylase gene
AIDS	acquired immune deficiency syndrome
ANOVA	analysis of variance
APC	antigen presenting cells
ART	anti-retroviral therapy
ASC	apoptosis associated spec
AUG	start codon
BacA	Bacitracin
BACTEC	culture system to detect microbial growth from blood specimens
BAL	bronchoalveolar lavage
BCG	Bacille Calmette Guérin
BD	binding domain
BIR	baculovirus inhibitor of apoptosis repeat
BLAST	Basic local alignment system tool
BLASTN	Basic local alignment system tool (nucleotides)
BLASTP	Basic local alignment system tool (proteins)
bp	Basepair
BS^3	suberic acid bis (3-sulfo-N-hydroxysuccinimide ester) sodium salt
C	Carboxyl
C	cytosine
C1q	complement component 1 q
C1QA	complement component 1 q chain A
C1qB	complement component 1 q chain B
C1qC	complement component 1 q chain C
C1r	complement component 1 r
C1s	complement component 1 s

C3	complement 3
C3b	cleavage product of C3
C3bi	complement protein fragment of C3
C4b	cleavage product of C4
Ca^{2+}	calcium
CARD	caspase activation and recruitment domain
CCL2	chemokine(C-C motif) ligand 2
CD14	cluster of differentiation 14
CD148	receptor-type protein tyrosine phosphatase
CD209	gene encoding DC-SIGN
CD4	cluster of differentiation 4
CD63	53 kDa type III lysosomal glycoprotein
cDNA	complementary deoxyribonucleic acid
CEU	Utah residents with ancestry from northern and western Europe
CFP10	10kDa culture filtrate protein
cfu	colony forming units
CH50	total hemolytic complement
CHB	Han Chinese in Beijing, China
Cl	confidence interval
cm^3	cubic centimeter
CO2	Carbon dioxide
CO-IP	co-immunoprecipitation
CpG	cytosine phosphate guanosine
CR1	complement receptor 1
CR3	complement receptor 3
CR4	complement receptor 4
CRs	complement receptors
D'	measure of linkage disequilibrium
dATP	deoxyadenosine triphosphate
DC-SIGN	dendritic cell-specific intercellular adhesion molecule-3 grabbing non-non- integrin
dbSNP	single nucleotide polymorphism database
dCTP	deoxycytidine triphosphate
dGTP	deoxyguanosine triphosphate
dH_2O	distilled water
DMSO	dimethyl sulfoxide
DNA	Deoxyribonucleic acid
DOTS	directly observed treatment and short-course
ds	double stranded
dT	stretch of deoxythymidine
dTTP	deoxythymidine triphosphate
E. coli	Escherichia coli
EccA1	gene name for locus Rv3868

EccB1	gene name for locus Rv3869
EccCa1	gene name for locus Rv3870
EccCb1	gene name for locus Rv3871
EccD1	gene name for locus Rv3877
EccE1	gene name for locus Rv3882c
EDTA	ethylenediaminetetraacetic acid
EEA1	early endosome autoantigen 1
ELISA	Enzyme-linked immunosorbent assay
ER	endoplasmic reticulum
ESAT6	6kDa early secreted antigenic target
ESAT-6•CFP-10	1:1 dimer complex of ESAT6 and CFP10
EspA	ESX-1 secretion-associated protein A,
espACD	operon encoding EspA, C, and D
EspB	ESX-1 substrate protein B
EspC	ESX-1 substrate protein C
espD	ESX-1 substrate protein D
EspR	ESX-1 substrate protein R
ESX	early secretory antigenic target 6 system 1
esxA	gene encoding the 6kDa early secreted antigenic target
esxB	gene encoding the 10kDa culture filtrate protein
EtBr	Ethiumbromide
extRD1	extended region of difference 1
FcγR	fragment, crystallisable gamma receptor
FLNa	filamin A
FLNB	filamin B
FLNC	filamin C
G	Guanosine
GAL4	transcriptional activator encoding galactose-metabolizing enzymes
glm	general linear model
GST	glutathione s-transferase
GTPase	guanosine triphosphatase
H+	hydrogen isotope
H_2O	Water
H_2O_2	hydrogen peroxide
H_2SO_4	sulphuric acid
H37Ra	attenuated *Mycobacterium tuberculosis* strain
H37Rv	virulent *Mycobacterium tuberculosis* strain
HA	hemagglutinin
HapMap	haplotype map
HCB	Han Chinese in Beijing
HCI	hydrochloric acid
HI-FBS	heat-inactivated fetal bovine serum
His	Histidine

HIS3	imidazoleglycerolphosphate dehydratase gene
HIV	human immunodeficiency virus
HLA	human leukocyte antigen
hVPS34	class III PI 3-kinase
ID	Identification
IDT	Integrated DNA Technologies
IFNGR	interferon gamma receptor
IFN-γ	gamma interferon
IgG	immunoglobulin G
IgM	immunoglobulin M
IL-10	interleukin-10
IL-12	interleukin 12
IL-1β	interleukin-1 beta
IL-5	interleukin-5
IL-5Rα	interleukin-5 receptor alpha
in vitro	latin for 'within glass'
in vivo	latin for 'within the living'
IRAK4	interleukin-1 receptor-associated kinase 4
IRF	interferon regulatory factors
JPT	Japanese in Tokyo
kb	Kilobases
kDa	Kilodalton
kV	Kilovolts
LAM	Lipoarabinomannan
LB	Luria Bertani
LD-PCR	long distance PCR
Leu	Leucine
LEU2	3-isopropylmalate dehydratase
LiCl	lithium chloride
LJ	Lowenstein Jenson
LM	Lipomannan
Ltd	Limited
M	Molar
mAb	monoclonal antibody
MAF	minor allele frequencies
ManLAM	mannose-capped lipoarabinomannan
MBL	mannose binding lectin
MDP	muramyl dipeptide
MEL1	Alpha-galactosidase gene
µg/mL	micrograms per milliliter
mg/mL	milligram per milliliter
MGB	minor groove binder

$MgCl_2$	magnesium chloride
MHC	major histocompatibilty complex
min	Minute
mL	Milliliters
mM	Millimolar
mm	Millimeter
mM	Millimolar
MR	mannose receptor
mRNA	messenger ribonucleic acid
MSMD	Mendelian susceptibility to mycobacterial disease
Mtb	*Mycobacterium tuberculosis*
MTBC	*Mycobacterium tuberculosis* complex
MycP1	mycosin 1
MyD88	myeloid differentiation primary response gene 88
N	Amino
n	sample number
NaCl	sodium chloride
NaPO4	sodium phosphate
NCBI	National Center for Biotechnology Information
NF-κβ	nuclear factor kappa beta
ng	nanograms
ng/µL	nanograms per microliter
NHS	N-hydroxysuccinimide
NIAID	National Institute of Allergy and infectious Diseases
NLR	NOD like receptors
NLRP3	NLR family, pyrin domain containing 3
nM	Nanomolar
NOD	nucleotide binding oligomerisation domain
NOS2A	nitric oxide synthase 2
NRAMP1	natural resistance-associated macrophage protein 1
NZB	New Zealand Black
OD600	optical density at 600nm
OmpA	outer membrane protein a
OR	odds ratio
P	Probability
p53	tumor protein 53
PAMPs	pathogen associated molecular pattern
PBS	phosphate buffer saline
PCR	polymerase chain reaction
PEG	polyethylene glycol
pen-strep	penicillin-streptomycin
pH	potential of hydrogen
PI	Phosphatidylinositol

PI(3)P	phosphatidylinositol-3-phosphate
PIMs	phosphatidyl-myo-inositol mannosides
PknG	serine/threonine kinase G
PMA	phagosomal maturation
PMA	phorbol 12-myristate 13-acetate
pmol	Picomol
pmol/µL	pmol per microliters
PPAR-γ	peroxisome proliferator-activated receptor gamma
PPI	protein -protein interactions
PRRs	pattern recognition receptors
Pty	Property
PVDF	polyvinylidene difluoride
QDO	quadruple drop-out
r^2	coefficient of determination
Rab	small GTP-binding proteins
Ras	family of related small GTPases
RD	region of difference
RIP2	receptor-interacting protein 2
RNA	ribonucleic acid
RNI	reactive nitrogen intermediates
ROI	reactive oxygen intermediates
rpm	revolutions per minute
RPMI 1640	Roswell Park Memorial Institute formulation 1640
RT	reverse transcriptase
Rv2136c	possible conserved transmembrane protein
Rv3671c	possible serine protease membrane protein
Rv3874	6 kDa early secreted antigenic target
Rv3875	10 kDa culture filtrate protein
SAC	South African Coloured
SAP	shrimp alkaline phosphatase
SapM	28 kDA acid phosphatase
SCINEX-P	Screening for interactions between extracellular proteins
SD	synthetic dropout
SD	standard deviation
SDS	Sequence detection systems
sec	Second
SLE	systemic lupus erythematous
SMART	Switching Mechanism at 5' end of RNA Transcript
SNP	single nucleotide polymorphisms
SOC	Super Optimal broth with Catabolite repression
SOS	human Son-of-sevenless gene
Sox4	SRY-related HMG-box 4 (transcription factor)
SP110	nuclear body protein

Sp-A	surfactant protein A
Sp-D	surfactant protein D
Sp-R120	210-kDa receptor
SV40	simian vacuolating virus 40
T	Timidine
TA	single 3'-overhanging thymine residue on each blunt end
TACO	tryptophan aspartate rich coat protein
TAE	Tris acetate EDTA
TB	Tuberculosis
TBM	Tuberculous Meningitis
TDO	triple drop-out
TE/LiAc	lithium acetate
TFG-β	transforming growth factor gamma
Th1	T helper cell
THP1	Human acute monocytic leukemia cell line
TLR	toll-like receptor
Tm	melting temperature
TMB	3, 3´, 5, 5´ - tetramethyl-benzidine
TNFα	tumour necrosis factor alpha
Tris	tris(hydroxymethyl)aminomethane
Trp	tryptophan
TRP1	phosphoribosyl-anthranilate isomerase
UBG	ultraviolet, blue, green
Ura	Uracil
VDR	vitamin D (1,25- dihydroxyvitamin D3) receptor
via	by way of
VII	7
w/v	weight/volume
WHO	World Health Organisation
X-α-gal	5-bromo-4-chloro-3-indolyl alpha-D-galactopyranoside
Y2H	yeast two-hybrid
YPDA	yeast peptone dextrose adenine
YRI	Yoruba in Ibadan
α	Alpha
λ	Lamda
μM	Micrometers
Ω	Ohms

Chapter 1

“We dance round in a ring and suppose,
But the secret sits in the middle and knows.”
Robert Frost

1 Introduction

1.1 The varied lifestyles of intracellular pathogens

Intracellular pathogens replicate either in the cytosol or in specialised phagosomal compartments to establish an infection niche. In doing so, microbes need to develop mechanisms to gain entry into host cells, as well as to escape the unfavorable effects of host immunity. Among the first lines of defense are the skin and mucosal epithelial cells of the respiratory, alimentary and urogenital tract. Once pathogens cross these physical barriers, the innate immune response is activated, to eliminate or contain infection (Kapetanovic and Cavaillon, 2007). Cellular components that mediate innate immunity includes epithelial cells, goblet cells, dendritic cells, airway macrophages, neutrophils, pneumocytes and secreted products such as antimicrobial peptides, inflammatory mediators, mucin and secretory immunoglobulin's (Sethi and Murphy, 2008). Of these cell types, macrophages are more permissive to intracellular pathogens due to their inherent function of engulfing foreign particles and initiating an immune response.

Macrophages, also known as professional phagocytes, regulate body homeostasis by engulfing necrotic and apoptotic cellular debris, in a silent non-inflammatory action, to aid in tissue development and maintenance. In a similar way, these cells act as alert signals for the innate immune response by recognising and engulfing invading pathogens and regulating activation of the acquired immune response (Yates et al., 2005). Beyond question, activated macrophages provide the most hostile niche for pathogen replication.

Once inside the phagosome, pathogens need to adapt to the hostile environment but it also offers most micro-organisms the ability to escape humoral recognition by circulating antibodies and complement. Some pathogens reside in the phagosome and maintain features of either early-endosomes or late-endosomes by diverting the endocytic pathway, normally targeted by lysosomal compartments (Cossart and Roy, 2010). A few pathogens, like *Brucella abortus* and *Legionella pneumophila,* avoid lysosomal vesicles by using an alternative route through the endoplasmic reticulum (ER) to disguise the phagosomal membrane as an ER membrane (Kumar and Valdivia, 2009).

A selected number of bacteria succeeds in escaping from the phagosome and replicate within the cytosol. This is true for *Listeria monocytogenes*, *Shigella flexneri*, *Rickettsia conorii* and *Francisella tularensis*. Once entry into the cytosol has been established, pathogens need to circumvent autophagy. Autophagy is a conserved event in which double layers of cellular membrane encapsulate unwanted cytosolic particles and degrade them by fusion with lysosomal vesicles (Cossart and Roy, 2010). In escaping autophagy, pathogens rapidly replicate, and employ actin polymerisation to establish intra- and inter-cellular distribution. Actin motility is employed by *Listeria* and *Shigella*, which hijack host protein complexes to produce actin comet tails for escape. These host protein complexes, which are considered uniquely for actin motility, have also been connected to autophagy recognition (Mostowy and Cossart, 2011).

However, pathogens within the phagosome are challenged by phagolysosome fusion, which is designated to dispose of microbial invaders. Several intracellular pathogens like *Salmonella*, *Chlamydia* and *Mycobacterium* have developed various strategies for inhibiting phagolysosome fusion (Duclos and Desjardins, 2000; Deretic et al., 2006). Whether pathogens truly inhibit phagolysosome fusion, is open for debate, since authors suggest that it is rather a continual communication with the endocytic pathway delaying the event (Drecktrah et al., 2007; Pryor and Raines, 2010). However, it is clear that proteins and lipids involved in the regulation of lysosomal trafficking are targeted by secretory products of the pathogen (Pryor and Raines, 2010). Mycobacteria seem to be more proficient in this survival mechanism (Nguyen and Pieters, 2005).

Macrophages are long-lived compared to neutrophils (which live for a much shorter lifespan and are also professional phagocytes) (Allen, 2003). Therefore, inhabiting macrophages provides a much more stable timeframe for intracellular replication. In the final step of replication and spread, pathogens need to be released from their replication niche in order to transmit to other cells. Examples of cell-to-cell spread have been observed with *Listeria*, malaria plasmodia and *Toxoplasma gondii* (Mounier et al., 1990; Sibley, 2004). Malaria and *T. gondii* strictly require being within host cells compared to *Listeria*, *Mycobacterium tuberculosis*, *Brucella spp.* and *Salmonella enterica*, which have developed the capacity to exist in the extracellular environment prior to entering new host cells. Microbes like these can even live in an abiotic milieu for longer periods of time. Despite the fact that *M. tuberculosis* is ultimately seen as an intracellular

bacterium, it flourishes in the extracellular debris of granulomas, reaching up to 10^{13} bacilli (Kaufmann, 2011) and can persist asymptomatically in the human host for years.

1.2 *Mycobacterium tuberculosis*

1.2.1 A brief history

Robert Koch (1843-1910) had variable research interests and studied multiple organisms responsible for anthrax, plague, cholera, malaria, sleeping sickness and numerous animal diseases such as rinderpest and surra of cattle and horses. Regardless of this wide range of interests, his name is usually associated with the development of staining and culture methods for bacteria and for the isolation of the slow-growing agent of tuberculosis – *Mycobacterium tuberculosis* (Taylor et al., 2003). His work on *M. tuberculosis* was presented to the Physiological Society of Berlin in March 1882 (Ligon, 2002).

A few years later, in 1895, Wilhelm Konrad Röntgen discovered X-rays and together these two scientific achievements were applied to clinical medicine. From 1905, doctors could start making a precise diagnosis by demonstrating abnormalities in a patient's chest radiograph and isolating tubercle bacilli from sputum (Murray, 2004). During the 1880s, Louis Pasteur developed a method to intentionally attenuate the virulence of a living microbe to generate a successful vaccine; the first was against fowl cholera and later against rabies and anthrax (Pasteur et al., 2002). In 1908, Albert Calmette and Camile Guérin applied Pasteur's technique to generate a vaccine against tuberculosis. By a fortunate discovery, they learned that growth in ox bile diminished virulence of *M. bovis* and by performing 230 serial passages they isolated a single colony unable to cause fatal tuberculosis in a number of animals – among these were guinea pigs, rabbits, cows, horses, monkeys and chimpanzees (Dubos, 1986). The vaccine was called Bacille Bilié Calmette et Guérin, shortened to Bacille Calmette Guérin (BCG). In 1921, BCG vaccination was given to a number of babies and young children and by 1924 the vaccine demonstrated apparent protection with fewer side effects. It has been commonly observed that BCG immunisation is helpful in infants, providing protection against severe forms of tuberculosis, particularly miliary and meningeal disease (Dubos, 1986; Murray, 2004).

Much hope was placed on mass vaccination; but this was quickly shattered by the lack of BCG's protective effects. There has been no consensus about the usefulness of BCG vaccination, as BCG-induced immunity does not prevent subsequent development of infection; it only retards the spread (Gomes et al., 2004). Anti-tuberculous drugs was introduced in the 1940s (streptomycin) and 1950s (isoniazid), these and several other antibiotics were used as a clinical regimen (Lönnroth et al., 2009). Today, many countries document increases in multidrug resistant strains and in some cases now resistance to all available drugs (Velayati et al., 2009). Furthermore, no new drugs have been licensed since the identification of ethambutol in the 1960s (Comas and Gagneux, 2011). With the increasing prevalence of drug resistance and TB-human immunodeficiency virus (HIV) co-infections, there is an urgent need for new control strategies, improved diagnostics, effective drugs, shorter treatments and better vaccines (Kaufmann and Parida, 2007).

1.2.2 TB incidence

The World Health Organisation (WHO) – Global Tuberculosis Control 2011 Report – estimated that during 2010 there were an estimated 8.8 million incident cases (range, 8.5 – 9.2 million). The greatest proportion of incident cases occurred in Asia (59%) and Africa (26%), with smaller rates occurring in regions of the Eastern Mediterranean (7%), Europe (5%) and America (3%) (Figure 1.1). The five countries that had the largest TB incidence in 2010 were India (range, 2.0-2.5 million), China (range, 0.9-1.2 million), South Africa (range, 0.4-0.59 million), Indonesia (range, 0.35-0.52 million) and Pakistan (range, 0.33-0.48 million). Of the reported 8.8 million cases in 2010, the best fit estimate of people living with TB-HIV co-infection was 1.1 million (13%). Strikingly, approximately 82% of the HIV-positive individuals were from the African Region (Global Tuberculosis Control 2011 Report).

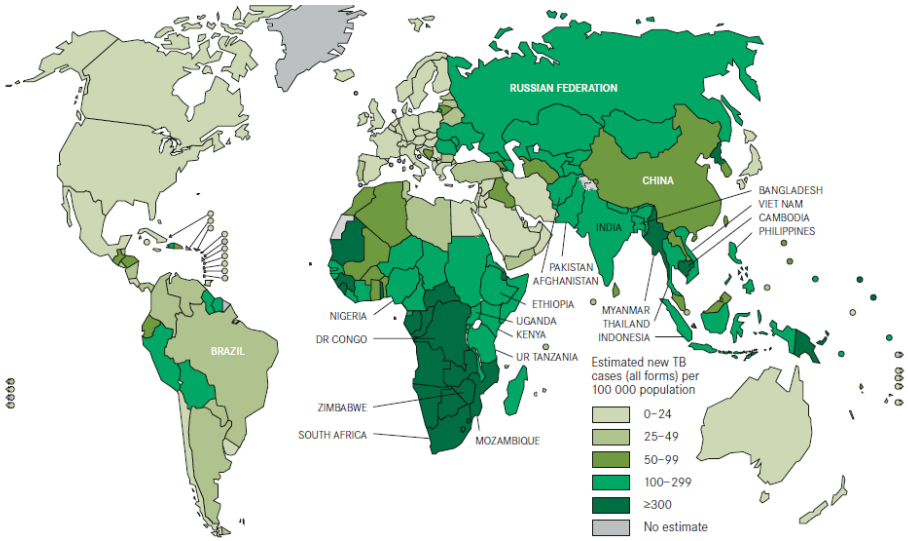

Figure 1.1: Estimated TB incidence rates, by country, in 2010 (WHO report 2011).

Global TB control programs primarily focus on understanding transmission through early detection and effective treatment. Although control measures such as BCG vaccination and the WHO Directly Observed Treatment Short-Course (DOTS) strategy have been implemented, the rise in HIV transmission and the emergence of drug resistant phenotypes are still troublesome. However, since the addition of DOTS into the Stop TB strategy, the approach led to the treatment of 36 million patients between 1995 and 2008 and prevention of up to 8 million deaths (Ahmad, 2011). A combination of disease surveillance and computational modeling predicts that the 1990 targets of prevalence and mortality could be halved by 2015. The probability is, that if these targets are reached and maintained, the rate of disease will decrease, which will require a set of effective interventions that are both cost-effective and capable of producing effects on larger scale (Dye and Floyd, 2006). In 2005, the African Health Ministers at the 55th Session of the WHO Regional Committee for Africa in Maputo declared tuberculosis as an "Emergency", ensuring immediate and determined efforts to combat the disease (Chaisson and Martinson, 2008).

1.2.3 Bacteriology

Tuberculosis is caused by a number of closely related Gram-positive bacilli in the genus of Mycobacterium, known as the *Mycobacterium tuberculosis* complex (MTBC). The MTBC

consists of a number of species and subspecies that include *M. tuberculosis*, *M. africanum*, *M. bovis*, *M. canetti*, *M. caprae*, *M. microti*, *M. pinnipedi* and recently discovered *M. mungi* (Alexander et al., 2010).

M. tuberculosis is a non-motile rod shaped bacterium (Figure 1.2A). The rods are 2-4 micrometers (µm) in length and 0.2-0.5 µm in width. *M. tuberculosis* is an obligate aerobe. For this reason, it is classically found within well-aerated upper lobes of the lungs, where it functions as an intracellular facultative pathogen. The tubercle bacilli has extremely slow doubling times of ~20 hours (Todar, 2011), compared to the closely related *M. marinum* that doubles every ~ 4 hours (Ramakrishnan and Falkow, 1994). As a result, *M. tuberculosis* can establish its niche within the host before recognition by host immunity.

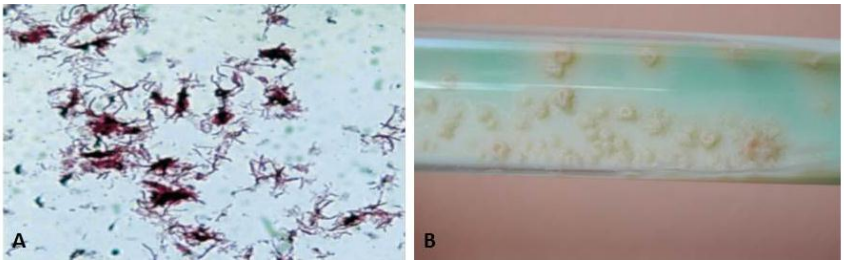

Figure 1.2: Microbial characteristics of *M. tuberculosis* – (A) Acid-fast staining of rod shaped *M. tuberculosis* recovered from glass culture tubes (Taylor et al., 2003). (B) Colonies of *M. tuberculosis* are rough, waxy, thick, wrinkled, have an irregular margin, and are faintly buff-coloured (Ojha et al., 2008).

Traditionally, *M. tuberculosis* is grown on Lowenstein Jensen (LJ) culture media requiring several weeks before the bacilli can be isolated, resulting in delay of treatment. A faster result is nowadays obtained using Middlebrook medium or the BACTEC™ MGIT™ 960 System. Colonies of *M. tuberculosis* have an unusual, waxy coat on the cell surface that primarily consists of mycolic acids (Figure 1.2B) (Todar, 2011). This distinct feature highlights the large number of enzymes involved in lipid metabolism (Guo et al., 2010). It is also the dense lipid cell wall that makes the cells impermeable to gram staining, hence the use of acid fast staining techniques for identification (Figure 1.2A) (Misawa, 1952).

The majority of the cell wall components consist of peptidoglycans and lipids. The lipid component primarily consists of hydrophobic mycolic acids, which are α-branched lipids and

makes up 50% of the dry weight of the mycobacterium (Figure 1.3). As a result, mycobacteria are slow growers due to the impaired entry of nutrients through the thick layer of mycolic acids, but it also provides resistance to cellular degradation processes within the human host (Brennan and Nikaido, 1995). Mycolic acids are dispersed mostly at the external portions of the cell wall, while the internal portions mostly consist of arabinogalactan, phosphatidyl-myo-inositol mannosides (PIMs) and peptidoglycans. Adjacent to the mycolic acids are other composites such as mannose-capped lipoarabinomannan (ManLAM), the related lipomannan (LM) and mannosylated glycoproteins. The outer capsule and surface of the bacilli presents with mannan and arabinomannan caps (Torrelles and Schlesinger, 2010).

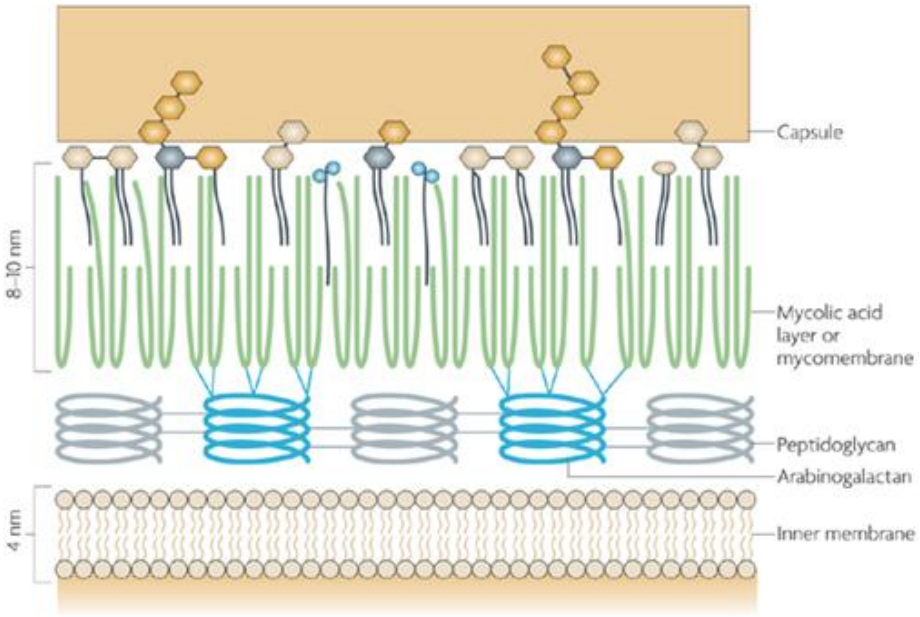

Figure 1.3: Representation of the mycobacterial cell wall. The cell wall consists primarily of a large cell-wall complex that comprises of three covalently linked structures i.e. mycolic acids (green), arabinogalactan (blue) and peptidoglycan (grey). The mycolic acids are covalently linked and results in a hydrophobic layer of low fluidity, referred to as the mycomembrane (Abdallah et al., 2007).

1.2.4 The course of *M. tuberculosis* infection

The first stage of tuberculosis begins with the inhalation of *M. tuberculosis* containing aerosols into the respiratory tract. Once in the lung, the bacilli are phagocytized by alveolar macrophages resident in the lung airways (Cooper, 2009). During this stage, the destruction of the

mycobacteria depends on the intrinsic bactericidal capacity of alveolar phagocytes and the virulence spectrum of the inhaled *M. tuberculosis* strain. During the initial infection, the bacillus multiplies in the lung, causing limited inflammation. Infection is established by employing multiple survival strategies within macrophages (Fatty et al., 2003), as well as the initial interactions with host cells. These survival mechanisms include triggering anti-inflammatory responses, blocking reactive oxygen and nitrogen production, and reducing acidification of *M. tuberculosis*-containing phagosomes (Flynn and Chan, 2001; Cooper, 2009).

During the persistent phase of infection, the bacilli escape bactericidal properties and multiply, resulting in the destruction of alveolar macrophages. This prompts a localised inflammatory response that results in the supply of neighbouring mononuclear cells from blood vessels, providing new host cells for the bacterial growth (Russell et al., 2010). The monocytes mature into either antigen presenting cells, alveolar macrophages or dendritic cells. Alveolar macrophages ingest, but do not kill the bacteria, allowing them to effectively grow with limited tissue damage. T lymphocytes are activated and recruited 2-3 weeks post infection via antigen presenting dendritic cells travelling from the site of infection (Kleinnijenhuis et al., 2011).. The recruited T cells form the building blocks of the early granuloma, where macrophages become activated to kill intracellular *M. tuberculosis* (Ulrichs and Kaufmann, 2006; Sasindran and Torrelles, 2011). Continued activation of T cells leads to the formation of granulomas, which are the pathological signature of this disease, and subsequently to the emergence of cell-mediated immunity. This marks the latent stage of infection, where growth and spread to additional tissue sites are limited. The third and final stage is when latent and controlled infection is activated. The two main reasons for activation of disease is marked by (1) a decline in the host's immunity due to genetic, environmental or biological causes and (2) failure to maintain and develop immune signals, resulting in lung cavitation and development of disease (Sasindran and Torrelles, 2011).

1.3 Genome of *Mycobacterium tuberculosis*

Tuberculosis research has made great advances since the publication of the *M. tuberculosis* H37Rv genome in 1998 (Cole et al., 1998). Since then, sequences from *M. bovis*, *M. bovis* BCG, *M. microtti*, *M. africanum* and a large number of other strains have either been finished or are in

the process of completion. The genome of the laboratory strain, H37Rv, was revealed to possess a sequence length of 4, 411, 529 bp (Cole et al., 1998). Comparative genomics have revealed a number of polymorphisms across various members of the MTBC that adds to the phenotypic diversity observed across the various strains. Larger polymorphic regions, those greater than 0.5 kb, have also been identified between strains and are termed regions of difference (RD loci).

Mahairas and colleagues applied subtractive hybridisation to identify regions of difference that accounted for the avirulent phenotype observed in *M. bovis* BCG (Mahairas et al., 1996). Their studies showed three regions of difference in the genome of H37Rv that were absent from *M. bovis* BCG. Of these regions, RD3 corresponded to one (PhiRv1) of the two prophages elements (PhiRv1 and PhiRv2), and were found to be varied among *M. tuberculosis* clinical and laboratory strains. RD2 was only deleted from isolates of *M. bovis* BCG that was re-cultured from 1925. Lastly, and most importantly, RD1 was found to be deleted from all *M. bovis* BCG strains and were only present in the ancestral pathogenic strains, leading to the hypothesis that this deletion caused the attenuation of BCG. However, complementation assays with RD1 into modern BCG strains did not reconstitute the full virulent phenotype of *M. bovis* BCG (Mahairas et al., 1996).

With the completion of the genome, other differences were found in BCG-duplicated regions (Brosch et al., 2000), and lineage specific deletions and point mutations (Behr et al., 1999) that all appeared to contribute to the attenuation of BCG (Brosch et al., 2007). However, many mechanisms are specific to *M. tuberculosis*, one of which is dependent on a fully functional RD1 locus together with an effective two-component regulatory system (Frigui et al., 2008). The RD1 locus is situated in a cluster of genes that are part of a specialised secretion system named the ESX-1 secretion system (Hsu et al., 2003; Pym et al., 2003; Stanley et al., 2003; Brodin et al., 2004; Guinn et al., 2004). The individual genes encoded by this locus have been shown by several groups to participate in virulence (Hsu et al., 2003; Pym et al., 2003; Sassetti and Rubin, 2003; Stanley et al., 2003; Guinn et al., 2004).

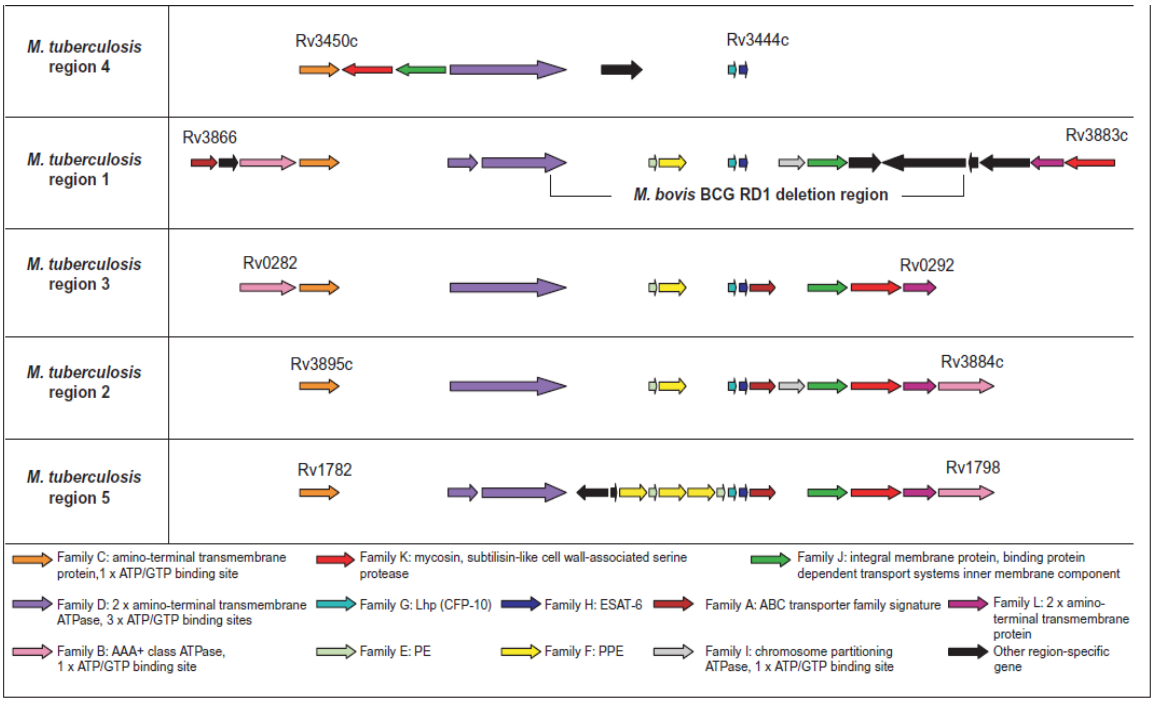

Figure 1.4: Schematic representation of the genomic organisation of the five ESAT-6 gene cluster regions of *M. tuberculosis* (ESX-1 to - 5) (Gey van Pittius et al., 2001).

1.3.1 ESX-1 secretion system

M. tuberculosis has five specialised ESX secretion systems (ESX-1 to ESX-5, Figure 1.4), which have been dubbed Type VII secretion systems (Abdallah et al., 2007). The ESX systems are named after the first known secretion product of the ESX systems, the 6kDa early secreted antigenic target (ESAT-6). The trademark of these systems is that they secrete products with homology to ESAT-6 (Feltcher et al., 2010).

The proteins associated with the ESX-1 secretion system can broadly be classified into three groups, namely – (1) secreted, (2) regulatory and (3) structural proteins. Combining computational results with those known from literature, Das and colleagues proposed a model for secretion of proteins through the ESX-1 secretion machinery. The model is depicted in Figure 1.5 (Das et al., 2011).

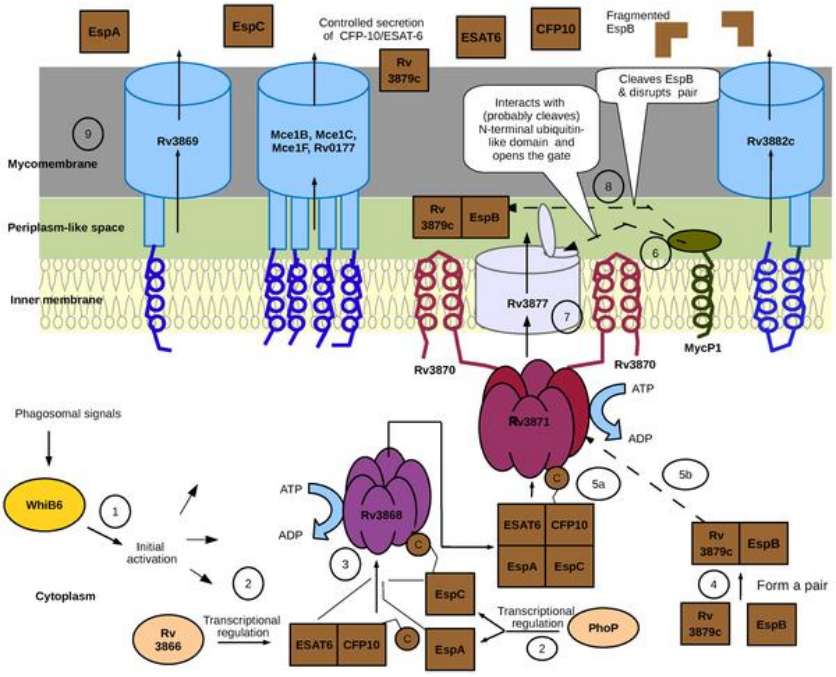

Figure 1.5: *Proposed model for secretion of substrates (CFP-10, ESAT-6, EspA, EspC, EspB) using Type VII secretion system*. The various steps involved are indicated by numbers and are described below: (1) Initial activation by WhiB6; (2) Transcriptional regulation of the secretory proteins by Rv3866 and PhoP; (3) Multimeric assembly of secretory proteins by Rv3868; (4) Pairing up of secretory protein EspB with Rv3879c; (5a) Recruitment of CFP-10/ESAT-6/EspA/EspC multimer by Rv3870 and Rv3871 to the inner membrane pore (Rv3877); (5b) Recruitment of EspB/Rv3879c pair by Rv3870 and Rv3871 to the inner membrane pore (Rv3877); (6) Interaction of MycP1 with Rv3877; (7) Inner membrane translocation of secretory proteins; (8) Cleavage of EspB by MycP1; (9) Mycomembrane translocation of secretory proteins. The dashed arrows show interaction between the components connected by the arrow (Das et al., 2011).

The ESX-1 system functions to secrete effector proteins, including the 10kDa culture filtrate protein (CFP-10 also known as esxB) directly into the host phagosome or cytosol (Stanley et al., 2007; Lewinsohn et al., 2006). In addition to ESAT-6 and CFP-10, four other substrates are secreted by the ESX-1 system: EspR, EspA, EspB and EspC (Gao et al., 2004; Fortune et al., 2005; MacGurn et al., 2005; McLaughlin et al., 2007; Xu et al., 2007). EspR is a transcriptional activator that regulates the secretion of the system and are found to influence the expression of the e*spACD* loci, which in turn regulates export of the ESAT-6·CFP-10 complex. The secretion of EspR is dependent on activation of the ESX-1 system that results in reduced expression of *espACD* genes (Blasco et al., 2011). So, when the pathway is inactive, the cytosolic concentration of EspR increases, causing expression of the *espACD* loci (Raghavan et al., 2008).

Additionally, EspA secretion is dependent on the secretion of the ESAT-6·CFP-10 complex and *vice versa* (Fortune et al., 2005).

The ESX-1 locus contains two cytoplasmic AAA ATPases, EccA1 and EccCb1, that probably supply energy for the secretion process and are involved in targeting products for secretion (Stanley et al., 2003; Luthra et al., 2008). Eccb1 binds the C-terminal signal peptide of CFP-10 and EccA1 binds the C-terminal region of EspC, these binding abilities are required for secretion of both the ESAT-6·CFP-10 complex and EspC (Champion et al., 2006; DiGiuseppe Champion et al., 2009).

EccD1 is a multi-transmembrane protein that is proposed to be involved in the formation of the transmembrane pore for the translocation of mycobacterial proteins and virulence factors (Brodin et al., 2005). The integral membrane protein, EccCa1, interacts with ATPase EccCb1 (Stanley et al., 2003). EccB1 and EccE1 are predicted to be transmembrane proteins located in the periplasm of the cell wall (Krogh et al., 2001). EspD has been shown to interact with EccE1 and is required for the secretion of the ESAT-6·CFP-10 complex (MacGurn et al., 2005). Mycosin-1 (MycP1) is a transmembrane protein and is located in the cytoplasmic membrane of the cell wall. MycP1 is a serine protease that has been shown to cleave EspB after translocation and has been shown to be essential for ESX-1 secretion (Ohol et al., 2010).

The ESX-1 secretion apparatus is a unique system, in that secretion of substrates is mutually dependent on all substrates of the system (Fortune et al., 2005; Abdallah et al., 2007) and deletion of any part of the system causes attenuation of the organism (Hsu et al., 2003; Stanley et al., 2003; Guinn et al., 2004; Wards et al., 2000).

1.3.2 Structural characteristics of CFP-10 and ESAT-6

The open reading frames encoding for ESAT-6 and CFP-10 lie in an operon and are co-transcribed. The protein products form a tight 1:1 complex (Renshaw et al., 2002; Lightbody et al., 2004). Renshaw and colleagues determined the structure of the ESAT-6·CFP-10 complex (Figure 1.6) and revealed that the inner core had a well-defined complex of two similar helix-

turn-helix hairpin structures for each individual protein, which lie parallel to each other, forming a four helix bundle. The contact surface between CFP-10 and ESAT-6 is hydrophobic in nature (Renshaw et al., 2005) and the complex formation stabilises the protein, which is important for secretion, as CFP-10 contains a C-terminal signal peptide that targets the whole complex for secretion.

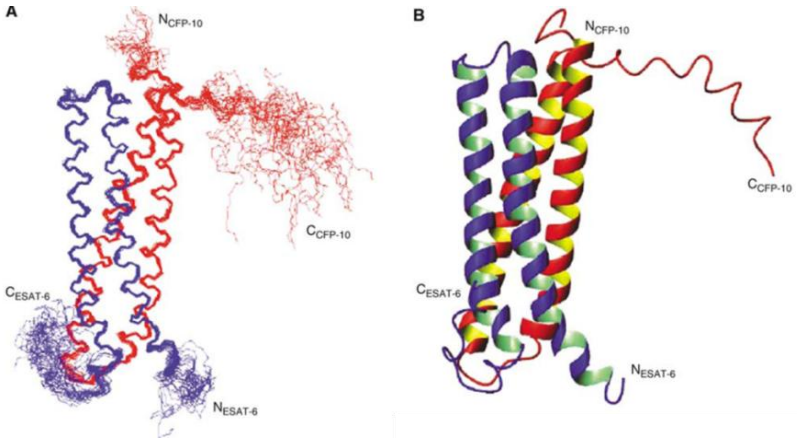

Figure 1.6: Solution structure of the ESAT-6·CFP-10 protein complex. (A) A best-fit superposition of the protein backbone, with CFP-10 shown in red and ESAT-6 in blue. (B) A ribbon representation of the backbone topology of the ESAT-6·CFP-10 complex based on the converged structure closest to the mean, which illustrates the two helix–turn–helix hairpin structures formed by the individual proteins (Renshaw et al., 2005).

It has been demonstrated that once ESAT-6 and CFP-10 associate as a complex; it is the C-terminus of CFP-10 that is responsible for the binding to host cells. This was illustrated by truncation of CFP-10 (residues 1-86) bound to full length ESAT-6 and full length CFP-10 bound to ESAT-6 with residues 1-84 being deleted. The deletion of CFP-10 residues impaired the binding of the complex to macrophage host cells, while the deletion of ESAT-6 showed no distinguishable difference when compared to the wild-type complex (Renshaw et al., 2005). Thermodynamic analyses revealed that binding between ESAT-6 and CFP-10 can take place below any melting temperature (T_m) of the complex, which is 53.4°C. An interesting observation was the loss of binding capacity to phospholipid membranes upon complex formation. Moreover, ESAT-6 adopted a more helical structure and enhanced thermal stability compare to CFP-10 or the complex, in the presence of phospholipid membranes. The processes that govern this observation and whether these features of ESAT-6 are observed on the surface of macrophages remain unknown. With respect to biochemical stability, the complex was found to be more

resistant to proteolytic cleavage by trypsin. The work presented by Meher *et al.*, demonstrates overall structural change, enhanced thermodynamic and biochemical stability upon complex formation and highlight features involved in the physiological role of ESAT-6, CFP-10 and/or the complex in host cells (Meher et al., 2006).

1.3.3 Role of the ESX-1 secretion system and virulence

The ESX-1 secretion system is a major virulence determinant of *M. tuberculosis*. Described ESX-1 effects are related to suppression of pro-inflammatory responses, necrosis, apoptosis, membrane lysis and cytolysis (Simeone et al., 2009). It has long been thought that ESAT-6 and CFP-10 are the effector molecules of the system, but additional proteins are also secreted and may serve as effector substrates of the ESX-1 machinery.

The most documented function of ESAT-6 in literature is linked to lysis of cell membranes. It has been demonstrated that deletion mutants of ESAT-6 did indeed multiply in macrophages but were unable to spread to uninfected macrophages (Guinn et al., 2004). In addition, deletion mutants displayed reduced invasiveness due to the lack of cytolytic ability. The interaction of ESAT-6 and CFP-10 is dependent on pH and conversion to a more acidic environment leads to dissociation of the complex (de Jonge et al., 2007). Moreover, ESAT-6 has a greater ability to disrupt and lyse liposomes, whereas CFP-10 does not. Therefore, it is thought that the biological function of ESAT-6 is dependent on the acid environment within the phagosome (de Jonge et al., 2007). In contrast, Lightbody et al., demonstrated that the complex between ESAT-6 and CFP-10 showed no decrease in stability and appeared to be more stable at lower pH (Lightbody et al., 2008). These observed inconsistencies could be explained by the fact that Guinn et al., used acetylated ESAT-6 from culture filtrates (Guinn et al., 2004), whereas the latter study used non-acetylated ESAT-6 expressed from *Escherichia coli* (Lightbody et al., 2008). Furthermore, blot overlay assays demonstrated that CFP-10 primarily interacted with non-acetylated ESAT-6, with less binding affinity to acetylated ESAT-6 (Okkels et al., 2004).

Literature suggests that *M. tuberculosis* remains in the phagosome, inhibiting maturation and phagosomal acidification, but escape from the phagosome remains to be elucidated. Lee and

colleagues showed that the metabolic status of *M. tuberculosis* correlates with the degree of phagosomal maturation. They demonstrated that compartments occupying mycobacteria differ markedly from fully matured phagolysosomes. They showed that metabolically active *M. tuberculosis* is less fusiogenic with lysosomes than metabolically inactive *M. tuberculosis*. In addition, they also observed that 5 days post infection, 25% of *M. tuberculosis* was found in the cytosol of macrophages without phagosomal membranes (Lee et al., 2008). This confirms the finding of van der Wel and coworkers who proposed translocation of *M. tuberculosis* from the phagosome to the cytosol (van der Wel et al., 2007).

In summary, the ESX-1 secretion system is clearly involved in pathogenicity and host-cell interactions, but there are still many details outstanding on the biology of these secretion systems and the function of the secreted products thereof. The elucidation thereof will have important consequences for the development of vaccines and therapeutic agents.

1.3.4 Host binding partners of ESAT-6

ESX-1 mediated secretion occurs early during infection before uptake into phagocytes, therefore secreted products can engage host receptors of alveolar macrophages and dendritic cells, as well as host components of the phagosome and cytosol. These interactions take place between secretory products of *M. tuberculosis* and the host cells at the primary site of infection; in order for infection to be established. In the following sections we discuss findings of ESAT-6 interactions with host proteins and the role of these interactions in the host-pathogen relationship.

1.3.4.1 Syntenin-1

Syntenin-1 is a host protein which functions in multiple roles related to vesicular trafficking, cytoskeletal dynamics, protein turnover, cell adhesion and signaling pathways involved in cell differentiation (Bernfield et al., 1999; Lander and Selleck, 2000; Yoneda and Couchman, 2003; Sarkar et al., 2004). Syntenin-1 was reported to interact with CD148, a transmembrane protein tyrosine phosphatase (Harrod and Justement, 2002). Numerous investigators observed negative regulation of T cell activation by CD148, demonstrating that it might play a role in the inhibition

of T cell immune responses (de la Fuente-García et al., 1998; Tangye et al., 1998). Syntenin-1 was identified to also interact with interleukin (IL)-5Rα and SRY-related HMG-box 4 (Sox4). The interaction of syntenin-1 with IL-5Rα was required for IL-5 mediated activation of transcription factor, Sox4 (Geijsen et al., 2001). This mechanism demonstrates that syntenin-1 acts as an adaptor molecule. Consequently, authors speculated that the interaction of ESAT-6 with syntenin-1 might contribute to the ability of *M. tuberculosis* to induce impairment in T cell activation and pro-inflammatory response, to facilitate escape from sterilising immunity (Schumann et al., 2006). Further validation studies are required to understand the functional role of ESAT-6 and syntenin-1 in the infection process.

1.3.4.2 Toll-like receptor 2

ESAT-6 binds directly to toll-like receptor 2 (TLR2) on the surface macrophages, leading to inhibition of nuclear factor (NF)-κβ and interferon regulatory factors (IRF) by inhibiting the ligand-mediated recruitment of interleukin-1 receptor-associated kinase 4 (IRAK4) to myeloid differentiation primary response gene 88 (MyD88). Pathak and coworkers provided evidence for a direct interaction on the extra-cytosolic side of the plasma cell membrane between TLR2 and ESAT-6, resulting in suppressed assembly of TLR signaling molecules inside cells required for efficient activation of the innate immune responses during tuberculosis infection (Pathak et al., 2007).

1.3.4.3 Phenylalanine-rich peptides

Kumar and coworkers used a human lung protein library and demonstrated that peptides with a high presence of phenylalanine residues displayed preferential binding to ESAT-6 (Kumar et al., 2009). None of these peptides were classified as host proteins. Further experimental data demonstrated that phenylalanine rich peptides (referred to as Hcl1), affected growth and pathogenesis of *M. tuberculosis*. Additionally, microarray data illustrated that these peptides altered regulation of mycobacterial genes and influenced growth and survival of mycobacteria negatively. These findings present the hypothesis that Hcl1 may function as an antimicrobial peptide or that it interacts with other mycobacterial protein(s) leading to the interference of

normal cellular processes of *M. tuberculosis* (Kumar et al., 2009). The binding of ESAT-6 to phenylalanine-rich peptides is not essential for *M. tuberculosis*, but presents rather as a potential drug-like target against the pathogen.

1.3.4.4 Laminin

ESAT-6 also interacts with laminin found on the surface of epithelial lungs cells (Kinhikar et al., 2010). The alveolar epithelial surface is covered by both type 1 and type 2 pneumocytes both of which express laminin on their basolateral surface (Dunsmore and Rannels, 1996). *In vivo* work demonstrated an upregulation of *ESAT-6* transcripts in pneumocytes, and the binding of ESAT-6 to laminin, followed by lysis of pneumocyte membranes by either free or bacterium-bound ESAT-6. This scenario suggests that *M. tuberculosis* invades epithelial cells and that the invasive phenotype upregulates ESAT-6 expression, increasing the ability of *M. tuberculosis* to bind to cells expressing laminin on their surface, to facilitate dissemination by directly damaging a small number of alveolar cells (Kinhikar et al., 2010).

1.4 Mycobacterial virulence strategies inside macrophages

Normally, after uptake of foreign particles, macrophages become activated, resulting in a course of action aimed at killing the foreign particles. These include gradual acidification of phagosomes, phagosome-lysosome fusion, induction of reactive oxygen intermediates (ROI) and reactive nitrogen intermediates (RNI), as well as antigen presentation (Roxas and Li, 2009). Together these efforts ensure that the immune system functions properly and is capable of handling foreign particles such as parasites, bacteria and viruses. This is not always the case and *M. tuberculosis* has developed the capacity to escape natural sterilising immunity.

1.4.1 Survival during phagosomal acidification

Mycobacterial particles are internalised within the lung macrophage through the process of phagocytosis. Viable bacilli can survive and replicate inside this harmful environment, as the phagosomes do not completely mature into phagolysosomes (Pieters and Gatfield, 2002). In these

non-activated macrophages, *M. tuberculosis* is capable of preventing the fusion of the phagosome with acidic lysosomes, causing the phagosome to remain at a mild pH of ~6.2. The reduced acidification (or lack thereof) is due to the exclusion of the vacuolar H^+ -ATPase-containing vesicles (Stewart et al., 2005; Rohde et al., 2007). Under physiological exposure to interferon gamma (IFN-γ) the fusion block is relieved and macrophages fuse with lysosomes, acidifying the *M. tuberculosis*-containing compartment to a pH of ~4.5 (Schaible et al., 1998; Via et al., 1998; MacMicking et al., 2003). Mycobacterial survival at a low pH in activated macrophages demonstrates the ability of *M. tuberculosis* to resist acid conditions.

During the early 1900s, Metchnikoff hypothesised that the lipid rich cell wall of *M. tuberculosis* serves as an important barrier against entry of protons (Metchnikoff, 1905). This observation (proposed more than 100 years ago) did not receive much interest. More recently, Vandal *et al*., sought to identify essential genes linked to the ability of *M. tuberculosis* to survive at a low pH (Vandal et al., 2008). In this study Vandal and colleagues screened 10 100 *M. tuberculosis* transposon mutants and identified 34 mutants (containing transposons in 21 genes) unable to survive at low pH. A total of 15/21 transposons represented genes involved in cell wall functions, such as peptidoglycan and lipoarabinomannan biosynthesis. Two acid sensitive transposon mutants were isolated, containing insertions in *Rv2136c* and *Rv3671c*. These two mutants were unable to sustain a neutral intra-bacterial pH during the acid test *in vitro*, as well as inside IFN-γ activated murine macrophages. In the same way, both mutants were severely attenuated for growth in mice and the bacterial load was cleared from both lung and spleen of mice during the chronic stage of infection (Vandal et al., 2008, 2009b, 2009a). *Rv2136c* encodes a putative bacitracin resistance protein, a homolog of *Escherichia coli* BacA. BacA is an undecaprenyl pyrophosphate phosphatase involved in peptidoglycan biosynthesis (Cole et al., 1998; El et al., 2004). *Rv3671c* encodes for a membrane-associated serine protease and may protect *M. tuberculosis* against acid by modifying the bacterial cell envelope by regulating protein or lipid control, and/or serving in signaling pathways that may help the bacterium resist extracellular stress (Vandal et al., 2009a).

Another cell wall component, *OmpA*, a pore forming protein or porin, is also important for acid resistance and virulence of *M. tuberculosis* (Raynaud et al., 2002). A deletion mutant of *OmpA*

showed that *M. tuberculosis* was strongly affected by its ability to grow at reduced pH, but not under normal growth conditions. It was observed that the permeability of this mutant was affected at pH 5.5 and that uptake of serine was at a minimum (Molle et al., 2006). The data indicated that *OmpA* might function at two levels: (a) as a pore-forming protein with properties of a porin and (b) in enabling *M. tuberculosis* to respond to reduced environmental pH (Raynaud et al., 2002).

The identification of acid responsive genes, as well as the change in expression profiles of mycobacterial transcripts or proteins, indicates that low pH triggers important signals critical for adaptation and survival that equips the bacterium to survive within this stress environment (Vandal et al., 2009a).

1.4.2 Inhibition of phagosome-lysosome fusion and "phagosomal maturation"

The phenomenon termed phagosomal maturation arrest (PMA) was first described by Armstrong and Hart, demonstrating that roughly 70% of *M. tuberculosis*-containing phagosomes fail to localise with lysosomal trackers (Armstrong and Hart, 1971).

To accomplish this goal, mycobacteria maintain features of an early endosome. These features are characteristic of a neutral pH due to exclusion of the host vacuolar H^+ -ATPase pump and lysosomal markers such as CD63 and recycling of cell surface molecules (Briken, 2008). The phagosome containing *M. tuberculosis* has small Rab GTPases distinctive of early endosomes (Rab4, Rab5 and Rab14) but not in the case of late endosomes and lysosomes (Kyei et al., 2006). Additional means by which *M. tuberculosis* inhibits phagosomal maturation is by the retention of host tryptophan aspartate rich coat protein (TACO), also known as coronin-1. The recruitment of coronin-1 to the surface of phagosomes prevents delivery to lysosomes. *M. tuberculosis* infected mice deficient in coronin-1 were unable to inhibit phagosome-lysosomal fusion (Ferrari et al., 1999; Jayachandran et al., 2007).

Host products involved in the formation and maturation of phagosomes are known as phosphatidylinositol (PI) 3-kinases (Vieira et al., 2001). The glycosylated *M. tuberculosis* phosphatidylinositol mannose-capped lipoarabinomannan (ManLAM), that closely resembles the equivalent of the mammalian lipid form, serves as an inhibitor of PI 3-kinases. This counterpart is

responsible for blocking the delivery of lysosomal components from the trans-Golgi network, aimed at mycobacterium-containing phagosomes, by preventing the accumulation of phosphatidylinositol-3-phosphate (PI(3)P) (Fratti et al., 2003). The inhibitory effect of mycobacterial ManLAM increases cytosolic Ca^{2+} and possibly accounts for the known Ca^{2+} block associated with phagocytosis of *M. tuberculosis*. Thus, the action of ManLAM prevents the binding of PI3 kinase hVPS34 with calmodulin that is required for downstream recruitment of early endosome autoantigen 1 (EEA1). EEA1, together with Syntaxin 6, is necessary for the delivery of lysosomal compartment from the trans-Golgi network to the phagosome. As a result, mycobacterial PMA is accomplished by ManLAM-mediated disruption of Ca^{2+}/calmodulin-dependent regulation of PI(3)P and EEA1 on phagosomes (Vergne et al., 2003).

Numerous other mycobacterial products are involved in the inhibition of phagosomal maturation; these include trehalose dimycolate and sulpholipids, 28 kDA acid phosphatase (SapM) and the serine/threonine kinase G (PknG) (Rohde et al., 2007). Additionally, a mutant defective in the secretion of ESAT-6/CFP-10 during *M. marinum* infection of murine macrophages demonstrated a higher percentage of association with acidified compartments. These results suggested that secretion of ESAT-6/CFP-10 contributes to the arrest of phagosome maturation and promotes survival of mycobacteria within macrophages (Tan et al., 2006).

1.4.3 Other mechanisms of survival

Apart from the *M. tuberculosis* subversion strategies discussed above, several other mechanisms exist for survival of *M. tuberculosis*. For example, apoptosis normally leads to the killing of pathogens by removing the replication niche and plays a key role in the immune responses against *M. tuberculosis*. However, the bacterium has been found to inhibit cell apoptosis (Velmurugan et al., 2007). Induction of apoptosis exerts an anti-microbial effect and prevention of macrophage apoptosis appears to be a virulence strategy for *M. tuberculosis* (Keane et al., 2000). Other mechanisms involve the inhibition of macrophage response to IFN-γ by manipulating signaling events downstream of the receptor through the 19-kDa lipoprotein (Pennini et al., 2006).

M. tuberculosis can also inhibit the expression of MHC class II on macrophages to prevent antigen presentation to CD4+ T cells by blocking transport and presentation of molecules, resulting in the inhibition of IFN-γ responses (Noss et al., 2001; Pecora et al., 2006; Gehring et al., 2004). Another possible virulence strategy is the exploitation of actin, as actin serves as a scaffolding protein of endosomes during interactions with phagosome and has been related to the delay of phagosomal maturation (Anes et al., 2003).

1.5 Interaction of *Mycobacterium tuberculosis* with the macrophage

The interaction of *M. tuberculosis* with host cells is complex and remains to be completely elucidated (Kleinnijenhuis et al., 2011). Various studies suggest that multiple pathways may be employed simultaneously during the uptake of *M. tuberculosis.* Host receptors which are mainly involved in the recognition of *M. tuberculosis* are summarised in Figure 1.7 and will be discussed briefly in the following sections.

1.5.1 Complement receptors

Complement receptors (CRs) are expressed on macrophages and facilitate phagocytosis of intracellular pathogens (Aderem and Underhill, 1999). Receptors for complement on the surface of macrophages include CR1, a monomeric transmembrane protein that binds complement components C3b and C4b. CR3 and CR4 (which are heterodimeric proteins) bind C3bi and glucan, leading to recognition of complement-opsonised and in some cases unopsonised pathogens (Ernst, 1998). *M. tuberculosis* activates complement via the alternative pathway, resulting in C3 deposition on the surface of *M. tuberculosis* and is initiated by the alternative pathway in the presence of high complement proteins. However, when these proteins decrease, the classical pathways play a greater role in the deposition of C3 on the surface of the mycobacterium via covalent linkages in the forms of C3b and C3bi (Ferguson et al., 2004). Entry of *M. tuberculosis* via CR3 can be beneficial, resulting in prevention of macrophage activation (Caron and Hall, 1998). The interaction of CR3 with its active compound does not prompt a respiratory burst, as in the case of Fc receptors; thus leading to a less stressful event for successful entry. Several studies have indicated that signaling during CR3 routing suppresses IL-

12 production by macrophages (Sutterwala et al., 1997; Karp et al., 1996; Marth and Kelsall, 1997). This cytokine is required for the differentiation of naïve T cells into Th1-type cells, which is required for host defenses against invading pathogens like *M. tuberculosis.*

Furthermore, entry of *M. tuberculosis* via CR3 is strictly reliant on the presence of membrane cholesterol at the host plasma surface (Gatfield and Pieters, 2000; Peyron et al., 2000). The presence of cholesterol also prevents fusion of lysosome with mycobacterial phagosome, ensuring intracellular survival of M. tuberculosis (Gatfield and Pieters, 2000; Jayachandran et al., 2007).

In addition, *M. tuberculosis* may utilise host membrane cholesterol for both carbon and energy during chronic stage of infected macrophages (Pandey and Sassetti, 2008). This strongly supports the idea that *M. tuberculosis* engages selective receptors, resulting in an appropriate signaling event advantageous to the pathogen by avoiding degradation inside the macrophages. However, *in vitro* and *in vivo* studies exhibited no substantial difference in the phenotype between CR3 deficient and wild-type mice with respect to bacterial burden and pathology (Hu et al., 2000). Even though the evidence contradicts the role of CR3 on the course of tuberculosis infection, it is thought that CR4 may function as an important player in the uptake of *M. tuberculosis* during the early stages of infection.

Human alveolar macrophages are reported to have more CR4 than CR1 or CR3. The effect of blocking CR4 with antibodies had a much greater effect on the phagocytosis of *M. tuberculosis* compared to antibodies blocking CR1 and CR3. This may correlate to the observation that CR4 and mannose receptors are the most highly expressed receptors on the surface of alveolar macrophages (Sasindran and Torrelles, 2011) and participate more frequently in the phagocytosis of *M. tuberculosis.*

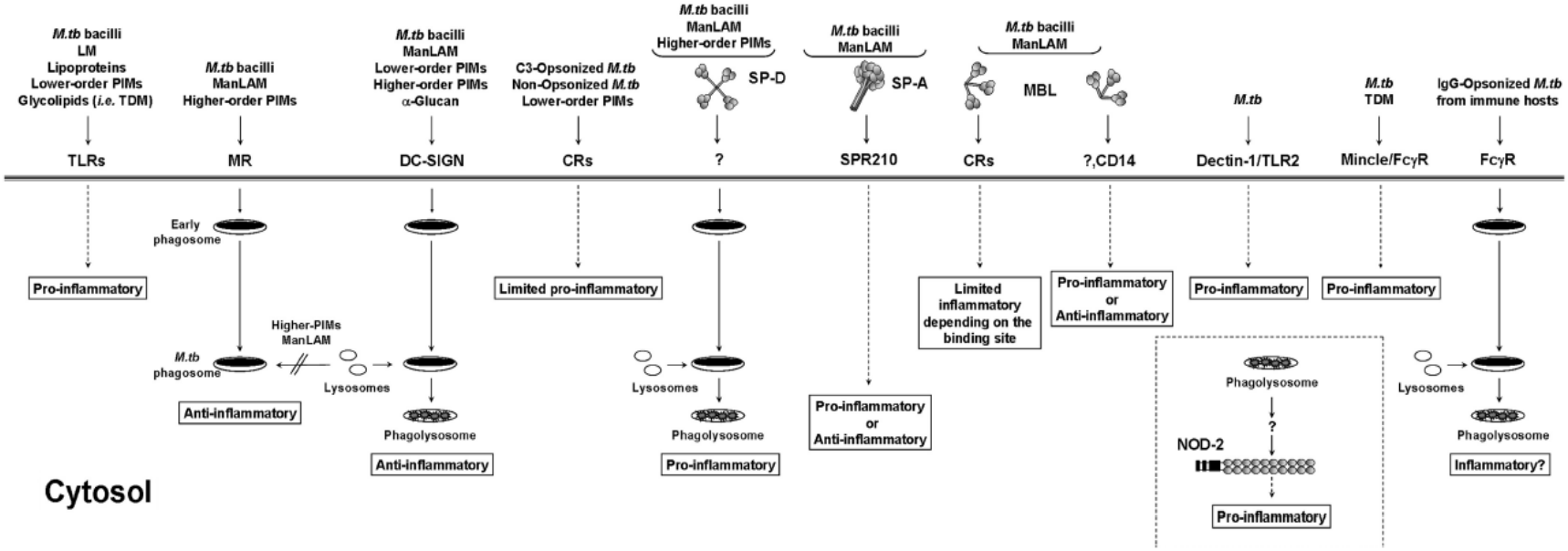

Figure 1.7: Host cell receptors involved in *M. tuberculosis* infection. TLR, Toll-like receptor; MR, mannose receptor; DC-SIGN, dendritic cell-specific intercellular adhesion molecule-3 grabbing non-integrin; CR, complement receptor; SP-A and SP-D, surfactant protein-A and -D; SpR210, 210-kDa receptor; MBL, mannose binding lectin; Dectin-1, dendritic cell associated C-type lectin-1; Mincle, macrophage-inducible C-type lectin/FcγR, fragment,crystallizable gamma receptor; NOD-2, nucleotide binding oligomerisation domain-like receptor (Sasindran and Torrelles, 2011).

1.5.2 Mannose receptors

The *M. tuberculosis* cell envelope is particularly rich in a wide variety of unique mannose-containing biomolecules, including mannose-capped lipoarabinomannan (ManLAM), the related lipomannan (LM), higher-order phosphatidyl-myo-inositol mannosides (PIMs), arabinomannnan, mannan, and mannosylated glycoproteins (Torrelles and Schlesinger, 2010). These molecules are incorporated into the plasma membrane and acts as ligands on the surface of *M. tuberculosis*. Mannose-containing molecules are situated in a perfect structural position, to mediate interactions between the macrophage and the pathogen (Torrelles and Schlesinger, 2010). The most abundant mannose structure in the cell envelope is ManLAM, which is implicated as a key factor in virulence and immunopathogenesis (Brennan and Nikaido, 1995; Nigou et al., 2003). ManLAM and higher-order PIMs habour terminal mannosyl elements ideally located in such a way, that they interact with mannose receptors on the surface of macrophages and dendritic cells (Schlesinger et al., 1994). The mannose receptor has been implicated in homeostatic processes, such as clearance of endogenous products and cell adhesion, as well as pathogen recognition and antigen presentation (Taylor et al., 2005).

Literature suggest that mannosylation of mycobacterial surfaces contributes to host cell recognition and immune responses (Horn et al., 1999). The terminal mannose caps of ManLAM bind to the macrophage C-type lectin mannose receptor (MR), and facilitate phagocytosis of mycobacteria by human macrophages (Schlesinger, 1993; Schlesinger et al., 1994). The binding of cell wall mannose caps induces peroxisome proliferator-activated receptor γ (PPARγ) expression through engagement of the mannose receptor. PPARγ is a transcriptional factor that regulates inflammation and is expressed in activated alveolar macrophages and macrophage-derived foam cells. The recognition of *M. tuberculosis* via MR causes up regulation of PPARγ activity, which induces an alternative activation state of alveolar macrophages, to enhance intracellular survival (Rajaram et al., 2010).

The recognition of PIMs by the MR has also been demonstrated by a study which showed that *M. smegmatis* strains expressing higher-order PIMs associated more with macrophage MR compared to wild type strains (McCarthy et al., 2005). The importance of higher-order PIMs and ManLAM

in *M. tuberculosis* infection have also been illustrated in a comparative study investigating the quantities of PIMs associated with virulent *M. tuberculosis* Erdman, virulent *M. tuberculosis* H37Rv and non-virulent *M. smegmatis* mc^2155, and attenuated *M. tuberculosis* H37Ra (Torrelles et al., 2006). The results demonstrated that *M. tuberculosis* strains had significantly more higher-order PIMs compared to *M. smegmatis*. Furthermore, the results showed that virulent *M. tuberculosis* strains had more higher-order PIMs than the attenuated *M. tuberculosis* H37Ra (Torrelles et al., 2006). In addition, virulent *M. tuberculosis* acquired more cell wall lipoglyco-conjugates with α (1-2) mannosylated termini. These terminal caps resemble those of mannose N-linked oligosaccharides of newly produced glycoproteins in eukaryotic cells. It has been shown that host molecules released in circulation 'of such an order' are effectively scavenged by macrophage MR through pinocytosis to regulate homeostasis. This may represent a form of exploiting structural similarities by increasing α (1-2) mannosylated units on the surface of *M. tuberculosis* to facilitates preferential engagement of the MR for survival in macrophages (Martinez-Pomares et al., 2001).

Variation in ManLAMs, as well as PIMs, with respect to length, structure and avidity for the MR varies in degree between mycobacterial strains (Valdivia-Arenas et al., 2007). This leads to the hypothesis that host-adapted mycobacterial strains may expose heavily mannosylated ManLAM and greater amounts of higher-order PIMs in order to bind MR and other C-type lectins. These strains are found to be optimised for phagocytosis by engaging both MR and complement receptors. Uptake of these strains by the mannose-containing biomolecule/MR pathway provides a safe entry for the pathogen with minimal cytokine responses and effective trafficking of the bacteria. These strains grow more slowly and are more successful during the infection process, contributing likely to latent infection rather than active disease (Torrelles and Schlesinger, 2010).

1.5.3 Surfactant receptors

Airway and pulmonary macrophages are the sites where the initial inoculum of *M. tuberculosis* resides and are the first line of cellular defense. Pulmonary surfactants, which play important roles in innate immunity, enhance the binding of *M. tuberculosis* to epithelial cells or alveolar macrophages (Ferguson and Schlesinger, 2000). These surfactants are termed collectins, which

include structurally related proteins such as MBL and C1q (Vandivier et al., 2002). These proteins have the ability to regulate the initial interaction between *M. tuberculosis* and the macrophage.

Surfactant protein (Sp)–A and –D regulate the early events of mycobacterial infection. Sp-A has been shown to increase binding and uptake of *M. tuberculosis* through direct interaction on the surface of macrophages, which upregulates MR activity (Ernst, 1998). Downing and colleagues demonstrated that HIV infected individuals had increased amounts of Sp-A in bronchoalveolar lavage (BAL) fluid and demonstrated enhanced attachment of *M. tuberculosis* to murine alveolar macrophages (Downing et al., 1995). When BAL fluid was depleted of Sp-A, the attachment was lost, and it was again restored with the addition thereof (Downing et al., 1995). Sp-A is known to function as an opsonin that allows for opsonisation of *M. tuberculosis* through recognition via its specific receptor, Sp-R210. The recognition of Sp-R210 leads to the secretion of anti-inflammatory cytokines like interleukin-10 (IL-10) and transforming growth factor (TFG) - β that facilitates the suppression of cell-mediated immunity against *M. tuberculosis* (Samten et al., 2008). It has been shown that Sp-A also up regulates the expression of macrophage MR and contributes to the survival of *M. tuberculosis* by preventing phagosome maturation. In this instance, Sp-A may add to the establishment of successful infection (Sasindran and Torrelles, 2011).

Sp-D, on the other hand, has been shown to block the uptake of mycobacterial strains into macrophages (Ferguson et al., 1999). Recent evidence suggests that Sp-D has high affinity for *M. tuberculosis* ManLAM and PIMs (Ferguson et al., 1999; Carlson et al., 2009). Opsonisation and aggregation of *M. tuberculosis* reduces phagocytosis via the action of Sp-D. Equally, opsonisation of *M. tuberculosis* via Sp-D results in increased phagosome-lysosomal fusion, leading to reduced intracellular growth (Ferguson et al., 2006). These observations may therefore link various concentrations of surfactant proteins to developmental risk of tuberculosis.

1.5.4 Toll-Like receptors

Toll-like receptors (TLRs) are a family of pattern recognition receptors (PRRs), essential for immunity against a variation of intracellular pathogens (Akira et al., 2006). TLRs are expressed on the surface of macrophages (for example TRL2 and 4) as well as inside cell compartments (for example TLR8 and 9), but the most important function is on antigen presenting cells (APC) (Kawai and Akira, 2010). The recognition of *M. tuberculosis* structures by TLRs activates innate immunity and enhances adaptive immunity by regulating the secretion of multiple pro-inflammatory cytokines and anti-bacterial effector molecules (Hou et al., 2008). The interactions of TLRs and mycobacterial components are more complex than that of other bacteria in that different TLRs interact with different bacterial components.

TLR2 alone or as a heterodimer with either TLR1 or TLR6 have been shown to recognise mycobacterial cell wall glycolipids like LAM, LM, 38kDa and 19kDa mycobacterial glycoproteins and PIMs as triacylated (TLR2/TRL1) or diacylated (TLR2/TRL6) lipoprotein structures (Thoma-Uszynski et al., 2001; Means et al., 2001; Jones et al., 2001). TLR2 is known to be an important regulator of the innate immune response through its mechanisms on tumour necrosis factor (TNF)-α production in macrophages (Underhill et al., 1999; Bafica et al., 2005). TLR2 is also associated with the release of IL-1β and IL-12 (Pompei et al., 2007; Kleinnijenhuis et al., 2009). Deletion mutants of TLR2 in mice have demonstrated defective granuloma formation. When challenged with high doses of bacilli, these mutants showed greatly enhanced susceptibility to mycobacterial infection compared wild-type mice (Reiling et al., 2002; Drennan et al., 2004).

Heat shock proteins secreted by various *M. tuberculosis* species activate TLR4 (Ohashi et al., 2000; Bulut et al., 2005). In murine models, macrophages deficient in TLR4 showed less, but not completely abolished production of TNFα (Li and Cherayil, 2004). *In vivo* murine studies have demonstrated conflicting results on the function of TLR4 in recognition of *M. tuberculosis* when different mouse strains were used (Reiling et al., 2002). In comparison to TLR2 mutant mice, TRL4 mutants showed similar susceptibility profiles when compared to wild-type mice (Reiling et al., 2002). In contrast, Abel and colleagues, demonstrated higher mycobacterial growth in the

spleen, liver and lungs as well as a low survival rate in the TLR4 mutant compared to the wild-type mice (Abel et al., 2002). A body of evidence therefore illustrates conflicting results with respect to TLR4 and *M. tuberculosis*. Recently, simultaneous activation of TLR2 and TLR4 signaling pathways were shown to induce apoptosis and necrosis of macrophages in response to *M. tuberculosis* via different signaling mechanisms (Sánchez et al., 2010). Further work is required to understand the precise processes and to elucidate these conflicting results.

TLR9 recognises unmethylated CpG (cytosine phosphate guanosine) motifs of pathogen-derived DNA (Hemmi et al., 2000). Bafica and colleagues investigated the immunostimulatory effect of CpG islands and their recognition by TLR9 and demonstrated that mycobacterial DNA does indeed stimulate pro-inflammatory and Th1 responses to live *M. tuberculosis in vitro* and *in vivo* (Bafica et al., 2005). *M. tuberculosis* infected TLR9 mutant mice exhibited only minor increases in pulmonary bacilli and decreased survival at a low dose challenge, presenting with enhanced susceptibility when challenged with a high inoculum, comparable to TLR2 mutant mice (Bafica et al., 2005). In contrast to TLR2 mutant mice, those deficient in TLR9 did not illustrate major changes in granuloma formation or production of TNFα by antigen presenting cells (APC) (Bafica et al., 2005). Even though TLR9 and TLR2 mutant mice revealed similar changes in restricting growth at both low and high inoculum challenge, they displayed different immune responses to the pathogen *in vivo* (Bafica et al., 2005).

TLR8 is able to identify circulating single-stranded RNA from pathogens such as RNA viruses (Heil et al., 2004). Davila *et al*., demonstrated significant increases in transcript expression during the acute phase of tuberculosis infection, suggesting a possible functional role of TLR8 during *M. tuberculosis* infection (Davila et al., 2008). *In vivo* studies revealed an increase in protein levels of THP-1 cells after infection with *M. bovis* BCG (Davila et al., 2008). To date, this was the only study addressing the possible role of TLR8 during *M. tuberculosis* infection, with ligands and signaling properties remaining unknown.

From several lines of evidence it has become clear that TLRs communicate during the host defense against mycobacteria, which supports the notion that complex polygenic events involve

multiple, rather than single TLR pathways during innate immunity to human infections (Bafica et al., 2005).

1.5.5 Nucleotide-binding oligomerisation domain-like receptors

Nucleotide-binding oligomerisation domain-like receptors (NLRs) are cytosolic regulators of the pro-inflammatory immune response and have been implicated in *M. tuberculosis* infection (Shi et al., 2003). Structurally, the C-terminal domain consists of a series of leucine repeats that recognise pathogen associated molecular pattern (PAMPs) leading to receptor activation of the molecule (Proell et al., 2008). The N-terminal region consists of an effector domain of CARD (caspase activation and recruitment domain) or BIR (baculovirus inhibitor of apoptosis repeat). The CARD regions of NLRs (NOD1 and NOD2) recruit receptor-interacting protein 2 (RIP2) via CARD-CARD binding, which activates recruitment of NF-*κ*B (Dufner et al., 2006). NODs sense bacteria by recognising peptidoglycans in their cell wall. NOD1 recognises a diaminopimelic acid (Chamaillard et al., 2003) and NOD2, a muramyl dipeptide (MDP) (Girardin et al., 2003). In most bacteria, MDP is *N*-acetylated, but in mycobacteria and Actinomycetes MDP is *N*-glycolylated (Adam et al., 1969). In animal studies, *N*-glycolyl MDP was a more potent stimulator of the immune response, than N-acetyl MDP (Coulombe et al., 2009).

The stimulation of macrophages with the NOD2 ligand, MDP, followed by *M. tuberculosis* and BCG infection significantly increases the production of both TNF-α and IL-1β. The signaling cascades downstream via recognition of MDP with BCG increases the regulation of RIP2 and NF-*κ*B, but the latter are decreased with *M. tuberculosis*, likely as a mechanism to dampen the innate immune response (Brooks et al., 2011). The down regulation in RIP2 and NF-*κ*B with *M. tuberculosis* is possibly due to the lack of RD1 in BCG, which is responsible for the secretion of ESAT-6 and CFP-10 (Abdallah et al., 2007). These virulence factors have been shown to inhibit reactive oxygen species (ROS) NF-κB activation (Ganguly et al., 2008). Furthermore, *in vitro* studies using NOD2 deficient human macrophages demonstrated that NOD2 controlled the growth of both *M. tuberculosis* and BCG, whereas growth of BCG was only controlled in murine macrophages (Brooks et al., 2011).

1.5.6 Other

Other receptors present on macrophages are the Fcγ receptors, which binds immunoglobulin G (IgG) opsonised *M. tuberculosis* in the presence of a specific humoral response (Maglione et al., 2008b). Phagocytosis of *M. tuberculosis* and other particles via the FcγR leads to ROS activation and a pro-inflammatory immune response (Maglione et al., 2008a; Haberzettl et al., 2008). Previous studies have demonstrated that FcγR-mediated phagocytosis of IgG coated latex beads led to rapid phagosomal maturation, followed by acidification of the phagosomal compartment within 5 minutes. FcγR-mediated uptake of *M. tuberculosis* may be one of the pathways that are favoured by the host to mount an effective macrophage response before adaptive immunity is activated (Ernst, 1998).

In addition to all these, many other proteins and receptors can facilitate the interaction between the macrophage and the pathogen. Scavenger receptors bind polyanionic macromolecules and particles, including lipopolysaccharides of gram-negative bacteria and lipoteichoic acid of gram-positive bacteria (Krieger et al., 1993; Dunne et al., 1994). However, the role of scavenger receptors in the recognition of *M. tuberculosis* has not been extensively studied, but a few studies have shown involvement (Zimmerli et al., 1996; Neyrolles et al., 2006). Purified class A scavenger receptors bind *M. tuberculosis* and sulfolipids from *M. tuberculosis* compete with other ligands for binding to class A receptors (Ernst, 1998). Recently, class A receptor and macrophage receptor with collagenous structure (MACRO) have been involved in the binding of *M. tuberculosis* cord factor (Bowdish et al., 2009). Another receptor that recognises lipopolysaccharides of gram-negative and gram-positive bacteria is CD14, a phosphatidylinositol glycan-linked membrane protein (Pugin et al., 1994). CD14 can bind LAM of *M. tuberculosis* (Bernardo et al., 1998), while DC-SIGN, mannose binding lectin and possibly dectin-1 bind other motifs on mycobacterial surfaces.

1.6 Systematic approach to understanding tuberculosis

The course of *M. tuberculosis* infection is determined by mycobacterial and human genetic factors, the environment and their shared interactions. Given the complexity of *M. tuberculosis*

infection, a systematic approach is necessary to increase our understanding of the interplay of all the factors involved in this disease (Figure 1.8). The challenge of understanding *M. tuberculosis* infection at a systems biology level requires multidisciplinary data, which are used to construct predictive models. In order to generate such models, a clearer understanding of the biological mechanisms operating during host-pathogen interactions is required. In humans, susceptibility to tuberculosis is multifactorial, polygenic and displays population heterogeneity (Singh et al., 1983; Blackwell et al., 1997; Bellamy et al., 1998; Bellamy et al., 1999, 2000; Hoal-Van Helden et al., 1999; Greenwood et al., 2000; Roth et al., 2004). Accompanying the human susceptibility profile, are strain-specific genetic variation that can cause different pathological signatures of this disease. In this section the role of strain variation of *M. tuberculosis* and human genetic susceptibility that contribute to tuberculosis, will briefly be discussed.

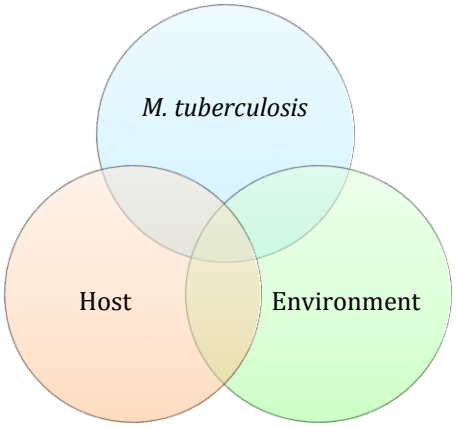

Figure 1.8: Interplay of factors influencing tuberculosis disease. The host represents all genetic and immunological factors; *M. tuberculosis* represents strain variation, drug resistance and virulence strategies. The environment represents all factors associated with co-morbidities, nutrition, urbanisation, globalisation, socio-economics and TB control effects. The overlap between these factors is described as "Systems Epidemiology" (Comas and Gagneux, 2009).

1.6.1 Human genetic variation and host susceptibility

The role of susceptibility and adaptation to the bacterium has been equally observed in Qu'Appelle Indians and illustrates the function of host genetics (Möller et al., 2010). When initially exposed to the bacterium, 10% of this population died due to the lack of innate resistance as a consequence of no previous historical exposure to the bacilli. Within 40 years more than half

of the families were eliminated. The observed reduction in annual death rate (0.2%) is proposed to be indicative of a strong selection against TB susceptibility genes within the population (Motulsky, 1989). This idea is reasonable, because Europeans also have a greater resistance to tuberculosis than individuals from African descent, probably due to the centuries of contact with tuberculosis (Dubos, 1986). A study in a nursing home in the United States demonstrated that individuals from African descent were twice as likely as individuals from European descent within the same environment to be infected with *M. tuberculosis* (Stead et al., 1990). It therefore does appear that genetic factors in certain populations contribute to disease susceptibility.

Host genetic factors explain partly why some individuals within a population display varying vulnerability to *M. tuberculosis*. Among these individuals, only 10% develop clinical tuberculosis, while the majority of the population control *M. tuberculosis* effectively. A tragic event in 1926 supports this observation. In Lubeck (Germany), 251 infants within the first 10 days of life were immunised by mistake with virulent *M. tuberculosis* (instead of BCG). The outcome of this event left some babies remaining unaffected (n = 47) whereas others developed severe clinical disease (n = 127) and some died (n = 77) (Dubos, 1986). This demonstrated that a wide range of responses to infection with *M. tuberculosis* exist within a population (Figure 1.9).

Figure 1.9: The direction of the arrow illustrates the genetic variation across a population. Some individuals never become infected; others are infected and never develop disease, while others are infected and develop active clinical disease.

Twin studies support the observed effect of host genetics on disease susceptibility. In these studies, disease concordance were found to be higher in monozygotic (essentially identical in genetic makeup) than dizygotic twins (Simonds, 1965; Comstock, 1978; Sørensen et al., 1988). Since monozygotic twins strongly tend to have a similar environment, it may be indicative that genetic factors are playing a major role in the patterns of tuberculosis development. Van der Ejik

and colleagues reanalysed the data presented by Simonds, (1963) and Comstock, (1978) to reconsider the role of environmental vs. genetic factors in determining the concordance of *M. tuberculosis* infection in twin studies. Environmental factors (i.e. intensity of exposure to the tubercle bacilli) outweighed the importance of genetic factors (van der Eijk et al., 2007). Intensity of exposure was defined as sputum positivity, physical proximity between twin pairs, contagiousness of disease and living together. Giving the findings, the analyses did not include the reanalysis of genetic factors and their effect on disease concordance in twins. Furthermore, data demonstrates that environmental factors may play a more important role than genetic factors in the variability of responses to mycobacterial subunit vaccines, but that genetic factors play a central role in the regulation of immune response to *M. tuberculosis* (Newport et al., 2004). This observation, provided by twin studies (Simonds, 1965; Comstock, 1978; Sørensen et al., 1988), supports the initial assumption that host genetics contribute to tuberculosis susceptibility.

Additional evidence for the involvement of genetics in host susceptibility was the discovery of individuals with the rare human syndrome of Mendelian susceptibility to mycobacterial disease (MSMD) (Altare et al., 1998). Individuals with MSMD have impaired cell-mediated immunity and show increase susceptibility to poorly pathogenic mycobacteria (non-tuberculous mycobacteria (NTM) and BCG), as well as *Salmonella* (Kumararatne, 2006). Mutation analyses reveal that these individuals contain variations in genes related to the IL-12/IL-23/IFN-γ axis (Casanova and Abel, 2002; Fieschi et al., 2003; Filipe-Santos et al., 2006). These individuals present as ideal cases for whole genome mapping of susceptibility loci in the general population.

The most popular method of studying host susceptibility to tuberculosis is population-based case-control studies, having a greater power to detect variation in genes with small rather than linkage studies, given an adequate sample size (Risch and Merikangas, 1996). A number of genes have been investigated for their involvement in TB susceptibility and are illustrated in Figure 1.10. Of these, *HLA*, *NRAMP1*, *IFNγ*, *NOS2A*, *SP110*, *CCL2*, *MBL*, *CD209*, *VDR* and *TLR* have been associated with tuberculosis, some repeatedly, whereas others demonstrated no association in other populations or not at all (Möller et al., 2010). Even though several genes have been implicated in tuberculosis susceptibility, it is necessary to remember that other genes, the environment and *M. tuberculosis* can influence the progression of disease (Möller et al., 2010).

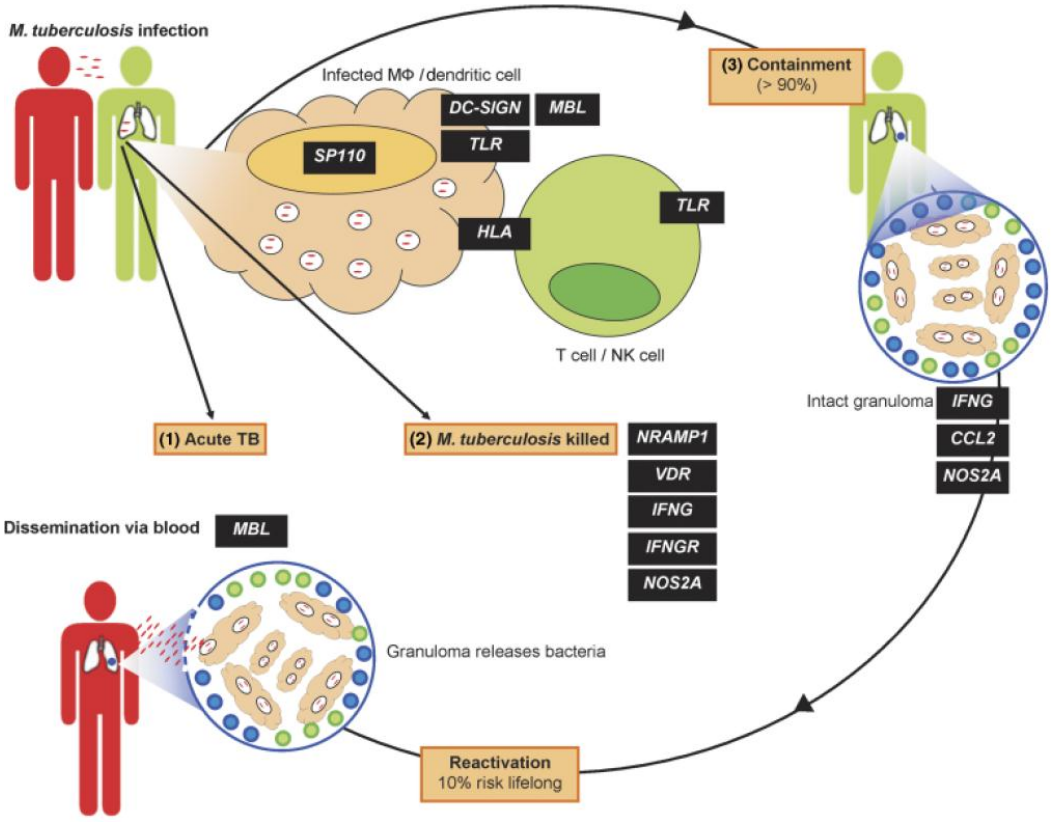

Figure 1.10: Genes involved in TB susceptibility. Simplified representation of the different outcomes after *M. tuberculosis* infection and some of the genes that may be involved at the various stages of infection. *HLA* (human leukocyte antigen), *NRAMP1* (natural resistance-associated macrophage protein 1), *IFN*γ (gamma interferon gamma), *NOS2A* (nitric oxide synthase 2), *SP110* (nuclear body protein), *CCL2* (chemokine (C-C motif) ligand 2), *MBL* (mannose binding lectin), *CD209* (gene encoding toll-like receptor DC-SIGN), *VDR* (vitamin D (1,25-dihydroxyvitamin D3) receptor) and *TLR* (toll-like receptor) (Möller et al., 2010).

1.6.2 Strain variation and the influence on host response

Genetic variation in pathogenic species may influence the outcome of disease. For example, genes encoding for toxins in staphylococci (Scholl et al., 1989) and streptococci (Mollick et al., 1993), the distribution of pathogenicity islands in enteric bacterial pathogens (Karaolis et al., 1998), the naturally occurring lipid A mutants in *Neisseria meningitidis* that cause low activity of lipopolysaccharides (Fransen et al., 2009), capsular variation in *Haemophilus influenza* (Kapogiannis et al., 2005) and *Streptococcus pneumonia* (Brueggemann et al., 2003). In *M. tuberculosis*, genetic variation primarily evolves by deletion, duplication and insertion events, as

well as single nucleotide polymorphisms (SNPs) (Nicol and Wilkinson, 2008). This sort of genetic variation among the global strains led to the emergence of six phylogenetically distinct lineages, with a strong association between lineage and geographical origin of the strain (Figure 1.11) (Gagneux et al., 2006).

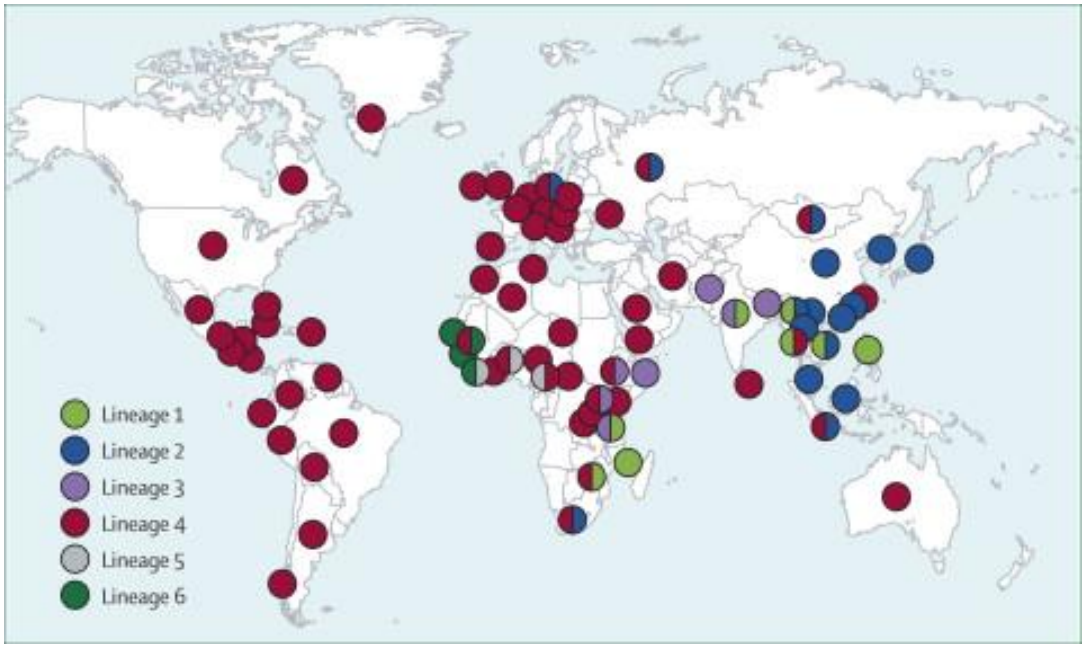

Figure 1.11: Global phylogeography of *M tuberculosis.* The coloured dots indicate the dominant lineage in each country (Gagneux et al., 2006).

Several lines of evidence suggest that particular strains of *M. tuberculosis* demonstrate differences in immunogenicity and virulence (Nicol and Wilkinson, 2008; Coscolla and Gagneux, 2010; Kumar et al., 2010). For example, the difference in virulence of CD1551 and HN878 *M. tuberculosis* strains is linked to specific variation in their lipid cell wall (Gagneux and Small, 2007). Lipid extracts from strain HN878 and related W/Beijing isolates preferentially induce Th2 immunity. Whereas CDC1551 induces strong expression of proinflammatory cytokines and other molecules associated with macrophage activation and Th1 protective immunity (Manca et al., 2004).

Moreover, most studies on pathogenesis have focused on laboratory strains H37Rv and Erdman, paying little attention to clinical strains segregating more frequently in a population. Recently, Portevin and colleagues evaluated macrophage response to 26 *M. tuberculosis* clinical isolates

representative of the global diversity of MTBC and their ability to induce an inflammatory response (Figure 1.12) (Portevin et al., 2011). They demonstrated that genetically diverse strains of MTBC vary widely in their ability to induce an early inflammatory response during infection of human macrophages and that the differences can be linked to the different MTBC lineages. The authors found that strains belonging to the more 'modern' lineage produced significantly more pro-inflammatory responses compared to 'ancient' lineages. Although the inflammatory response differed widely between the various strains, the cytokine profiles demonstrated a trend in the conservation of responses between the eight donors (Figure 1.13).

The findings presented by Portevin *et al*., support the model by which the more 'modern' lineages might progress more rapidly to active disease and transmit more easily to new hosts by evading early immune recognition. Once this observation is confirmed, it will be consistent with the thought that 'modern' lineages adapted under high population densities, which increased selection of virulence and transmission factors of *M. tuberculosis* (Comas and Gagneux, 2011). In support of this observation, a study in Gambia showed that patients infected with 'modern' strains were more likely to progress to active disease compared to those infected with *M. africanum*, a member of the ancient lineage (de Jong et al., 2008). If this hypothesis holds true, the current impact of globalisation, urbanisation and population growth should impact on the virulence of MTBC in the future (Comas and Gagneux, 2011).

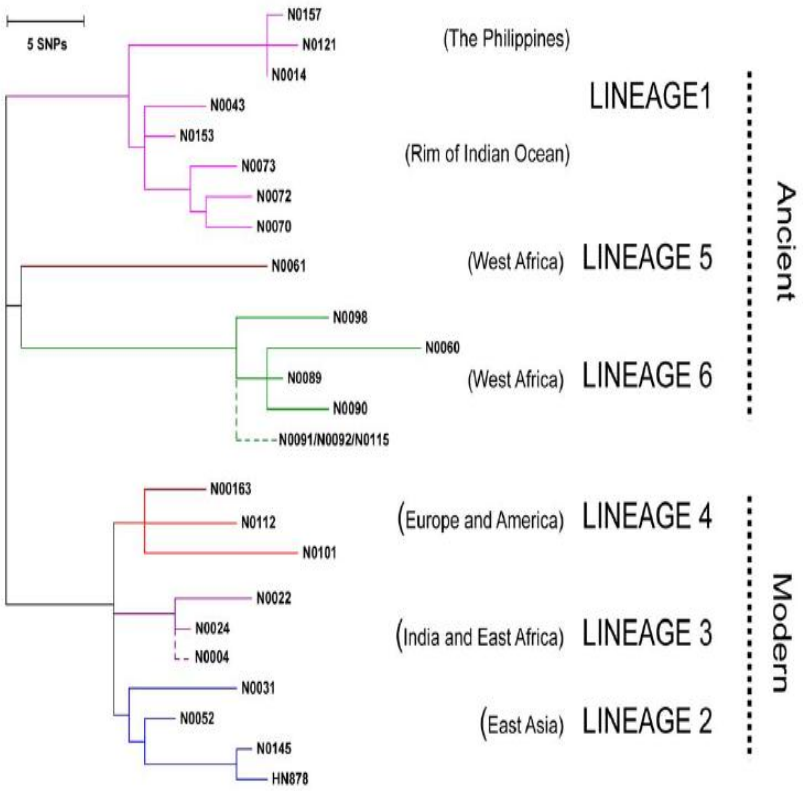

Figure 1.12: Selection of MTBC isolates representative of global genetic diversity (Portevin et al., 2011).

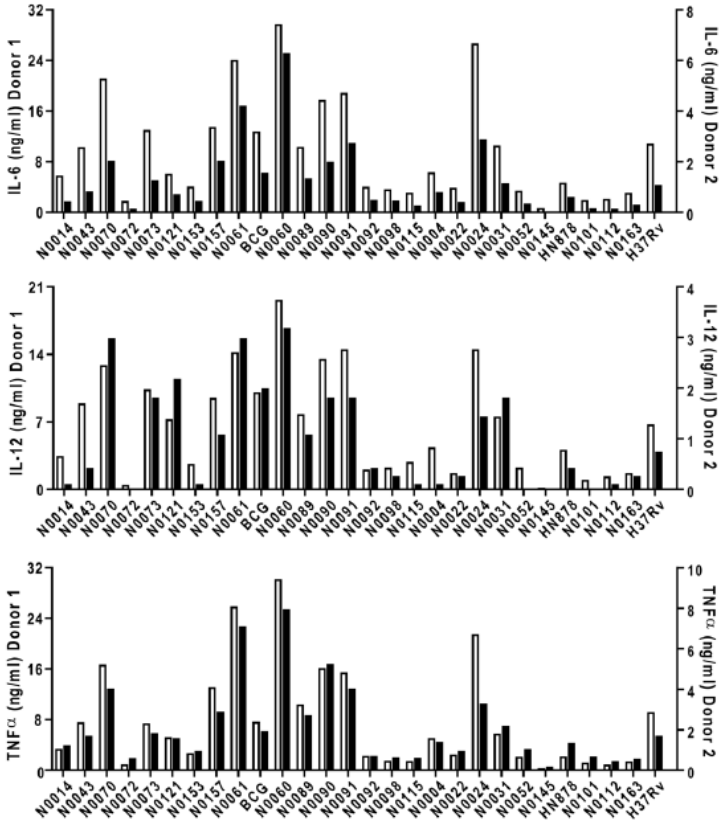

Figure 1.13: MTBC isolates and their varying ability to induce the production of pro-inflammatory cytokines (Portevin et al., 2011).

1.6.3 Tuberculosis and HIV co-infection

Tuberculosis and HIV co-infection is of global concern and should be addressed since the dynamics of epidemiology, clinical manifestation and management of both infections are different and more complex when present simultaneously. However, our knowledge of the interactive mechanism of the two pathogens in the human host has many gaps and need to be filled in order to address preventative measures against the two diseases.

The most powerful known risk factor for the predisposition of *M. tuberculosis* infection and progression to active disease is infection with HIV (Sawant et al., 2011). The risk of reactivation in latent tuberculosis patients increases with 20-fold (Mofenson and Laughon, 2007). In TB patients, tuberculosis is the most common cause of AIDS-related death (Sterling et al., 2010). Therefore, tuberculosis/HIV co-infection interacts to accelerate the weakening of host immune responses, leading to subsequent death, if left untreated (Pawlowski et al., 2012).

The reduction of CD4+ T cells is the main feature of AIDS and is an important contributor to the increase risk of TB reactivation in latently infected individuals and susceptibility to a TB contact (Geldmacher et al., 2012). Factors that facilitate the progression of tuberculosis disease in HIV infected individuals are the upregulation of entry receptors for *M. tuberculosis* on macrophages (Rosas-Taraco et al., 2006), the manipulation of macrophages bactericidal pathways (Spear et al., 1990), down regulation of chemotactic receptors (Wahl et al., 1989) and a tipped Th1/Th2 balance (Havlir and Barnes, 1999). In HIV infection, TNFα-mediated macrophage apoptotic response to *M. tuberculosis* is impaired, which facilitates bactericidal survival (Patel et al., 2007).

In the light of understanding human/*M. tuberculosis* interactions it is important to note the interactions between *M. tuberculosis* and HIV exist. The mere presence of HIV substantially shifts this spectrum in favour of bacillary replication and progression to active disease. This highlights the urgent need to understand the interactive role of both diseases.

1.6.4 Complexity of interactome analysis

The interaction of *M. tuberculosis* with the human host is an example of a balanced biological system (van Crevel et al., 2002) that allows for communication with various receptors, where the bacilli uses host macrophages for replication (Yates et al., 2005) and yet these cell structures remain stable in housing this deadly pathogen. Once inhaled, uptake is facilitated by multiple receptors (discussed in section 1.5), which are present on the cell surface of host cells. These initial interactions determine the subsequent fate of the bacilli (Sasindran and Torrelles, 2011). At the interface, cross-talk consists of numerous pathological strategies to successfully invade their host, to acquire nutrients, and to evade host immune defenses (Kleinnijenhuis et al., 2011); this introduces the existence of high level complexity that translates into dynamic interconnected actions. These types of strategies often involve direct protein-protein interactions and the formation of protein complexes. Host-pathogen protein-protein interactions (PPIs) play important roles in initiating infection (Kumar and Nanduri, 2010). Understanding the complex structure of vital PPIs during host-pathogen response can be targeted during drug treatment to relieve PPIs important for mycobacterial persistence (Mészáros et al., 2011). The identification of interactions between proteins is typically studied using traditional biochemical and genetic experiments, focusing only on one protein or pathway. Larger scale experiments, such as yeast-two-hybrid and tandem affinity purification, enable more comprehensive detection at the cost of significant false-negative and false-positive error rates (Hart et al., 2006; Davis et al., 2007).

Much remains to be learned about the vast majority of network interactions between the human host and mycobacterial proteins. These are fundamental areas in need of attention and could be addressed using approaches described by the field of systems biology, such as system-level snapshots of host-pathogen interactions, and have the potential to address numerous questions related to mycobacterial entry, escape and persistence.

1.7 The present study

1.7.1 Problem statement

To date, there is considerable evidence about the mechanisms of *M. tuberculosis* persistence, but little is known about host-pathogen PPIs. *M. tuberculosis* is an intracellular pathogen that

secretes a number of virulence factors that interact with human proteins (i.e. receptors, ligands and cytosolic proteins) in a targeted manner to elicit a required response. Substrates of the ESX-1 system have been shown to contribute to mycobacterial virulence. However, the biological function of ESX-1 substrates during host-pathogen interaction remains poorly and incompletely understood.

The present study was designed to gain insights into the role of host-pathogen interactions and to identify novel proteins that may contribute to the knowledge of how *M. tuberculosis* secretory substrates, ESAT-6 and CFP-10, interact with human host proteins. The knowledge of protein-protein interaction will prove helpful to understand (a) how *M. tuberculosis* evades the host immune response, and (b) the role of *M. tuberculosis* secreted virulence factors during the infection process.

1.7.2 Hypothesis

M. tuberculosis has developed various mechanisms to persist in the human host and is well documented in literature. However, the host-pathogen PPI's involved in the initiation and establishment of infection are poorly understood. It is therefore hypothesised that secreted proteins of *M. tuberculosis* during infection interact with host proteins in a targeted manner in order to elicit a pathogen required response. The focus of this study was to investigate how *M. tuberculosis* secretory substrates, ESAT-6 and CFP-10, interact with human host proteins.

1.7.3 Aim

The aim of the project was to investigate human/M. tuberculosis host-pathogen interactions in order to understand how secreted proteins of M. tuberculosis mediate their effects within the human host macrophage.

1.7.4 Objectives

In this study a high-throughput yeast two-hybrid approach was employed to identify host interacting binding partners of secretory antigens, ESAT-6 and CFP-10 and the putative interactions were then verified.

The objectives of this study were:

a) To identify host targets of ESAT-6 and CFP-10 using the yeast two-hybrid approach
b) To verify putative interactions

Throughout the study, a third objective was identified.

c) To perform genetic screens of identified putative candidate genes in a case/control setting to identify association with disease.

Chapter 2

Materials and Methods

2 Materials and Methods

All protocols were approved by the Health Research Ethics Committee of the Faculty of Medicine and Health Sciences, Stellenbosch University (project number 2003/151/N).

2.1 Strains, plasmids and cell lines

2.1.1 Bacterial strains

2.1.1.1 M. tuberculosis strain

Genomic DNA from *M. tuberculosis* H37Rv reference strain, kindly provided by Prof RM Warren, University of Stellenbosch, South Africa, was extracted as described previously (Warren et al., 2006). The isolated genomic DNA was used to generate PCR inserts of mycobacterial gene products (section 2.4.1).

2.1.1.2 Escherichia coli XL-1 blue

E. coli XL-1 blue strains were obtained as a kind gift from Prof NC Gey van Pittius, University of Stellenbosch, South Africa. *E. coli* strain was grown in Luria-Bertani (LB, 1% tryptone, 0.5% yeast extract, 1% NaCl, pH 7.0) liquid media or agar plates at 37°C. LB was supplemented with either 50 μg/mL kanamycin or 100 μg/mL ampicillin depending on the type of transformed plasmid (see Appendix 1A for culturing conditions).

2.1.2 *Saccharomyces cerevisiae* strains

S. cerevisiae strains Y187 and AH109 were supplied with the MATCHMAKER Two-Hybrid System 3 (Clontech Laboratories Inc., Palo Alto, CA). The pGBKT7 bait constructs were transformed into Y187 strains, while the cDNA library was transformed into AH109. The yeast strains were grown at 30°C in yeast peptone dextrose adenine (YPDA: 2% 1% yeast extract, Difco bacto-peptone, 2% dextrose or glucose, 0.003% adenine hemisulfate) or synthetic dropout (SD: 2% glucose, 0.007% yeast nitrogen base) liquid media or on agar plates. Selection in yeast was performed using amino acid dropout mixtures according to manufacturer's recommendation

(e.g. LEU$^-$ dropout lacks leucine and is encoded by the *LEU2* gene of pGADT7) (see Appendix 1B for culturing conditions).

2.1.3 Plasmids

The plasmids used in this study are summarised in Table 2.1, with a short description, outlining the specific use of each vector (see Appendix 2 for vector maps). The experimental procedure will be discussed in the sections that follow.

Table 2.1: Plasmids used in this study

Vector	Description	Source
pGemT easy	For cloning of PCR products; confers ampicillin resistance.	Promega
pGBKT7	Expresses proteins fused to amino acids 1-147 of the GAL4 DNA binding domain (BD); carries kanamycin resistance for selection in *E. coli* and *TRP1* nutritional maker for selection in yeast; serves as bait construct in the traditional yeast two-hybrid (Y2H) assay.	Clontech
pGADT7-Rec	Expresses proteins fused to the GAL4 activation domain (AD); carries ampicillin resistance for selection in *E. coli* and *LEU2* nutritional marker for selection in yeast; engineered for the construction of GAL4/cDNA libraries by homologous recombination in yeast; serves as 'preys' in the traditional Y2H screen.	Clontech
pGADT7-SV40	Expresses the SV40 large-T antigen in yeast; serves as a positive control; interacts with murine p53	Clontech
pGBKT7-p53	Expresses murine p53 in yeast; serves as a positive control; interacts with SV40	Clontech
pGBKT7-Lam	Expresses the human laminin C in yeast; serves as a negative control.	Clontech

2.1.4 Human cell lines

Immortalised human monocytic leukemia (THP-1) and T lymphocyte (Jurkat) cell lines (kindly provided by Dr. Katharina Ronacher-Mansvelt, University of Stellenbosch, South Africa) were used to verify the results obtained from the Y2H screening. These verification analyses were performed using *in vivo* co-localisation (section 2.15) and co-immunoprecipitation (section 2.16). Cell lines were incubated in a 37°C, 5% CO_2 incubator (Farma International, Miami, Florida) in Roswell Park Memorial Institute formulation (RPMI) 1640 media (Sigma, St. Louis, MO)

supplemented with 10% heat inactivated fetal bovine serum (HI-FBS) (GIBCO Laboratories, Grand Island, NY) and 1% penicillin-streptomycin (pen-strep) solution (Sigma, St. Louis, MO) (see Appendix 3 for general tissue culture conditions).

2.2 Generation of competent cells

2.2.1 Electro-competent *E. coli* XL-1 cells

A glycerol stock culture of *E. coli* XL-1 was thawed and inoculated into 50 ml LB media containing tetracycline (10 µL/mL) and incubated overnight in a 37°C shaking incubator at 3000 rpm for a starter culture. Following incubation, 250 mL pre-warmed LB media containing tetracycline was inoculated with 1/100 of the starter culture. The 250 mL culture was incubated at 37°C for 3 – 4 hours with shaking until OD_{600} of 0.7 was reached. Harvesting and washing of cells were performed with ice cold 10% glycerol solution. The cell pellet was re-suspended in 2 mL 10% glycerol. Aliquots (100 µL per tube) were frozen in a liquid nitrogen bath and stored at -80°C until further use (see Appendix 4A for a detailed protocol).

2.2.2 Chemically competent yeast cells

A small amount of frozen cells (AH109 or Y187) were scraped from the stock cultures and inoculated with a sterile loop onto YPDA agar plates. The plates were incubated facing down at 30°C until colonies appeared (~3 days). A single isolated colony was re-streaked on selection media lacking essential amino acids. A stock plate was prepared by re-streaking the isolated colony on an YPDA agar plate. The verified stock plate was used to propagate competent yeast cells, displaying the expected phenotypes (section 2.13.1). Following verification of yeast phenotypes, an isolated colony was inoculated in YPDA media and incubated at 30°C until an OD_{600} of 0.4 – 0.5 was reached. The yeast cells were washed with sterile deionised H_2O and re-suspended in a final solution of 1.1X TE/LiAc (Lithium acetate). The competent cells were used directly following preparation (see Appendix 4B for a detailed protocol).

2.3 Polymerase Chain Reaction (PCR)

2.3.1 Primer design

Primers were designed according to the sequences published on Tuberculist for *M. tuberculosis* genes (http://genolist.pasteur.fr/TubercuList/) and NCBI for human genes (http://www.ncbi.nlm.nih.gov/). The primer sequences were analysed for self-complementarity, primer-primer complimentary and melting temperature compatibility using IDT Oligonucleotide Tools online service (http://eu.idtdna.com/analyzer/Applications/OligoAnalyzer/). The primers were synthesised according to the standard protocol by Whitehead Scientific (Pty.) Ltd.

2.3.2 Generation of PCR inserts

PCR amplification of the full-length ESAT-6 and CFP-10 genes from *M. tuberculosis* H37Rv was performed with primer sets listed in Table 2.2. The generated PCR fragments were subsequently used for TA cloning into the cloning vector pGemT-easy, followed by sub-cloning into the pGBKT7 bait vector (Table 2.1). Enzyme restriction sites are underlined in Table 2.2.

2.4 PCR amplification

2.4.1 Amplification of insert fragments

All PCR reactions were performed in a total volume of 50 µL containing 1 µL of genomic DNA, 20 pmol of each primer set (listed in Table 2.2), 2.5 mM of each dATP, dCTP, dTTP and dGTP (Promega, Madison WI, USA), 5 µL of 10X PCR buffer, 4 µL of 25 mM $MgCl_2$, 10 µL of 5X Q-solution and 0.2 µL of HotStar Taq Polymerase (Qiagen, Hilden, Germany) and sterile dH_2O to a final volume of 50 µL. Parameters for cycling included: initial denaturing 95°C for 15 min, 35 cycles of 95°C for 30 sec; Tm according to Table 2.2 for 30 sec; and 72°C for 1 min, a final extension step of 72°C for 10 min were performed using a GeneAmp® PCR System 2720 thermal cycler (Applied Biosystems, Forster City, CA, USA). The PCR products were stored at -20°C until further use.

Table 2.2: Primers used in this study. Primer pairs for

Gene	Primer Sequence [5'-3']	Tm (°C)	Ta (°C)	bp	Used for Sequencing
ESAT-6	F: GAATTCATGACAGAGCAGCAGTGGAAT	45			
	R: CTGCAGATCCCGTGTTTCGCTATTCT	47	54	339	No
CFP-10	F: GAATTCATGGCAGAGATGAAGACCGAT	59			
	R: CTGCAGTGACATTTCCCTGGATTGC	60	60	414	No
FLNA	F: CTGACAAGTCTTATGGGAACC	53			
	R: CCGAGAGTGGGAGCTACTCAT	58	55	1181	Yes
Vector	**Primer Sequence [5'-3']**	**Tm (°C)**	**Ta (°C)**		
pGBKT7	F: TCATCGGAAGAGAGTAGT	49			
	R: GTCACTTTAAAATTTGTATAC	42	50		Yes
pGADT7	F: CTATTCGATGATGAAGATACCCCACCAAACCC	61			
	R: GTGAACTTGCGGGGTTTTTCAGTATCTACGAT	61	61		Yes
T7	F: TAATACGACTCACTATAGGG				
Sp6	R: GATTTAGGTGACACTATAG	NA	NA		Yes

NA - T7 and Sp6 were only used for sequencing reaction.

(1) ESAT-6 and CFP-10 were used to generate PCR fragments for plasmid cloning, (2) FLNA were used to amplify the promoter region of FLNA gene (1kb from ATG start site), followed by sequence analysis, (3) pGBKT7, pGADT7, and T9 and Sp6 (specific for pGemT constructs) were used to verify recombinant vectors using either PCR or sequence analysis to test conformity by bidirectional sequencing. Enzyme restriction sites are underlined: GAATTC-EcoRI and CTGCAG-PstI.

2.4.2 Colony PCR

Colony PCR amplification was done to select for recombinant plasmids, which were subsequently subjected to restriction enzyme digestion to verify successful cloning. PCR reactions for both bacterial and yeast colony PCR was performed as described in section 2.4.1, with the genomic DNA being replaced with a toothpick amount of bacterial or yeast cells.

2.4.3 cDNA amplification

Lung messenger RNA (mRNA) (cat# 636105, Clontech Laboratories Inc., Palo Alto, CA) was purchased from Clontech Laboratories and was copied into double stranded (ds) cDNA using Clontech BD SMART (Switching Mechanism at 5' end of RNA Transcript) technology (Clontech Laboratories Inc., Palo Alto, CA). During the first strand synthesis, cDNA was generated by converting mRNA into single strand cDNA using an oligo (dT) CDS III Primer (5'-ATT CTA GAG GCC GAG GCG GCC GAC ATG-d(T)30VN-3' [N = A, G, C, or T; V = A, G, or C]). As amplification reached the 5'-terminus, the enzyme terminal transferase activity added a stretch of

deoxycytidine to the 3' end of the cDNA. Thereafter, the SMART III™ Oligonucleotide primer was added (5'- AAG CAG TGG TAT CAA CGC AGA GTG GCC ATT ATG GCC GGG -3'), which base-paired with the deoxycytidine stretch, creating an extended template. The CDS III and SMART III anchors served as priming sites for the universal sense (5'- TTC CAC CCA AGC AGT GGT ATC AAC GCA GAG TGG -3') and anti-sense (5'-GTA TCG ATG CCC ACC CTC TAG AGG CCG AGG CGG CCG ACA -3') primers during Long Distance PCR (LD-PCR). After amplification, the ds cDNA was purified with a BD CHROMS SPIN™ TE-400 column, following the manufacturer's directions (Clontech Laboratories Inc., Palo Alto, CA) (see Appendix 5 for a detailed protocol).

2.5 Agarose gel electrophoresis

All products generated by PCR amplification and restriction enzyme analyses (with EcoRI and PstI) were subjected to electrophoresis as follows: 5 µL of product was mixed with 5 µL of loading buffer (Fermentas, Burlington, Canada). Each sample was loaded on 1% w/v agarose gel containing 250 ng/mL ethidium bromide immersed in 1X TRIS-acetate-EDTA (TAE) buffer and electrophoresed at 100 volts for 1 hour (Appendix 6). A 100bp marker (Promega, Madison WI, USA) was loaded together with amplified products to determine the relative product sizes. The DNA fragments were visualised on a G:BOX Gel Documentation System (Syngene, Cambridge, UK).

2.6 Automated DNA sequencing and analysis

2.6.1 DNA sequencing

Bidirectional automated DNA sequencing of PCR products and cloned inserts were performed at the Central Analytical Facility (CAF) of the University of Stellenbosch on the ABI Prism™ 3100 Automated Sequencer (Applied Biosystems, Forester City, CA, USA). The primers used for sequencing reactions were identical to the initial PCR primers (i.e. FLNA), while specific primers for pGemT-easy (T9 and Sp6), pGBKT7 and pGADT7 were used to test the sequence conformity by bidirectional sequencing (Table 2.2). The concentration of primers in the sequencing reaction was 1.1 pmol/µL and the reaction volume was 5 µL. Table 2.3 lists required concentration of starting material.

Table 2.3: Starting product size and required concentration for sequencing reactions

Product	Concentration required
< 500 bp	5 ng/µL
500 – 1000 bp	20 ng/µL
> 1000 bp	20 ng/µL
Plasmid DNA	100 ng/µL

2.6.2 Analysis of DNA fragments

Sequence analysis was done using the biological sequence alignment editor (BioEdit) version 7.0.5.3 (Sanchez-Villeda et al., 2008), to verify whether the sequence integrity of bait constructs, as well the interacting prey clone inserts identified during the Y2H screening, were intact and in-frame.

The nucleotide sequences of mycobacterial bait constructs were compared to the reference sequences obtained from Tuberculist (http://genolist.pasteur.fr/TubercuList/). The prey inserts were translated in the frame preceding the GAL4 AD reading frame. The identity of individual Y2H prey sequences was determined using the BLASTN and BLASTP programs (http://www.ncbi.nlm.nih.gov/BLAST/) to screen the GenBank database (www.ncbi.nlm.nih.gov/genbank/).

2.7 Generation of constructs

2.7.1 pGemT-easy cloning

PCR products were separated on a 1% TAE agarose gel as discussed in section 2.5. The PCR bands of the appropriate size were excised from agarose gel and was purified using the Wizard ® SV Gel and PCR clean-Up system (Promega Corp. Madison Wisconsin, USA) (Appendix 7). After purification, the concentration of the PCR products was quantified on the Nanodrop ND-1000 spectrophotometer (Labtech, UK). Ligation reactions were performed using the pGem T-easy cloning kit from Promega as per manufacturer's instructions: 5 µL of the 2X ligation buffer, 1 µL of pGem T-easy, 1 µL of T_4 ligase and 3 µL of purified PCR product. The ligation reactions

were carried out overnight at 4°C and transformed into electro-competent XL-1Blue *E.coli* cells as described in section 2.8.1 (see Appendix 8 for a detailed outline of section 2.7, as well as additional bait constructs made during this study).

The *E.coli* transformation mixture was plated on LB plates containing 100 µg/mL ampicillin with 100 µL of 0.1 M IPTG (Invitrogen, Carlsbad, CA, USA) and 100 µL of 20mg/mL X-gal (Roche, Germany) to enable blue/white colony selection. The plates were incubated at 37°C overnight. Isolated white colonies were verified by colony PCR (section 2.4.2) and the appropriate glycerol stocks cultures were made of all constructed plasmids. Sequence confirmed pGem-ESAT-6 and pGem-CFP-10 colonies were inoculated into 10 mL LB/Amp liquid medium and incubated overnight in a 37°C shaking incubator.

2.7.2 Restriction digest

Plasmid DNA was isolated from the overnight 10mL cultures of both pGem-ESAT-6 and pGem-CFP-10 constructs using the Wizard™ SV plus miniprep DNA purification system (section 2.9.1) (Promega Corp. Madison Wisconsin, USA) (Appendix 7). The isolated plasmid DNA of pGem-ESAT-6 and pGem-CFP-10 were digested with EcoRI and PstI, as well as the sub-cloning vector pGBKT7. The enzyme restriction reactions were set up as follows: 8 µL of plasmid (i.e. pGem-ESAT-6, pGem-CFP-10 and pGBKT7) was mixed with 1 µL of EcoRI (5 units/µL) and appropriate 1X restriction buffer. The reaction mixtures were incubated for 3 hours at 37°C. After digestion, the reaction mixtures were electrophoresed on a 1% w/v agarose gel containing 250 ng/mL ethidium bromide immersed in 1X TAE buffer. The EcoRI digested pGBKT7 and pGem plasmids were excised from the agarose gel and column purified using the Wizard™ SV Gel and PCR kit (Promega Corp. Madison Wisconsin, USA) (Appendix 7).

The samples were subsequently eluted in 25 µL dH_2O resulting in a residual volume of 15 µL, which was mixed with 2 µL PstI and 2 µL appropriate 1X restriction buffer. The reaction mixtures were incubated for 3 hours at 37°C. After digestion, the reaction mixtures were electrophoresed on a 1% agarose gel, excised from the gel and column purified using the Wizard™ SV gel kit (Promega Corp. Madison Wisconsin, USA). To prevent self-ligation, the vector was treated with shrimp alkaline phosphatase (SAP) (section 2.7.3).

2.7.3 Shrimp alkaline phosphatase treatment

The ends of the linearised construct were treated with SAP to catalyse the dephosphorylation of 5' phosphatase from DNA after the final restriction enzyme digestion step. The reaction was set up as follows: 19 µL linearised vector, 1 µL SAP (Roche, Mannheim, Germany), 3 µL of 10X buffer and 7 µL dH_2O. The reaction mixture was incubated at 37°C for 10 min and inactivated at 65°C for 15 min, followed by purification using the Wizard™ SV Gel and PCR kit as described above (Promega Corp. Madison Wisconsin, USA).

2.7.4 DNA ligation

The DNA ligation reactions were set up in 10 µL reaction volumes as follows: 1 µL T4 DNA ligase (Promega Corp. Madison Wisconsin, USA), 1 µL 10X ligase buffer and dH_2O to a final volume. The amount of double digested vector and insert was determined by the equation below.

$$\frac{ng\ vector}{kb\ size\ of\ vector} \times \text{kb size of insert} \times \frac{3}{1} = ng\ insert\ required$$

The reaction was then incubated overnight at 4°C. Following incubation, 2 µL of the ligation mix was transformed into electro-competent *E. coli* XL-1 stains, which was plated onto LB agar plates containing the appropriate antibiotics. After incubation, colony PCR (section 2.4.2) was performed to verify whether the colony forming units contained the inserts corresponding to both ESAT-6 and CFP-10.

2.8 Plasmid transformation

2.8.1 Bacterial plasmid transformation

Electro-competent XL-1 *E. coli* cells were thawed on ice and 45 µL of the cells were added to 2 µL of overnight ligation reaction. The mixture was transferred to a 1mm electroporation cuvette (BioRad), taking care to avoid the introduction of air bubbles. Electroporation was performed at 2.5 kV, 25 µF, 125 µFd and 200 Ω using the MicroPulser™ electroporator (Bio-Rad laboratories, Hercules, CA, USA). The electroporated mixture was re-suspended into 1 mL SOC medium (2% tryptone, 0.5% yeast extract, 0.05% NaCI, 20% glucose and 0.01% $MgCl_2$) and incubated at

37°C with shaking for 1 hour. The *E. coli* transformation mixture (50 – 100 µL) was plated on LB plates with appropriate antibiotics and incubated at 37°C overnight. Isolated colonies were verified by colony PCR (section 2.4.2) and glycerol stock cultures were made of all constructed plasmids.

2.8.2 Yeast plasmid transformation

Yeast transformation was performed by the standard LiAc method (Gietz and Woods, 2005). Briefly, a single colony (<2 mm) was inoculated in 10 mL SD medium lacking tryptophan (Trp^-) and leucine (Leu^-). The culture was incubated at 30°C overnight with shaking at 250 rpm. The following day, the culture was spin down, re-suspended in YPDA rich medium and incubated for 5 hours at 30°C with shaking. The cells were collected by centrifugation at 3000 rpm for 5 min and the appropriate amount of yeast cells (~20-50 µL) were re-suspended in 1 mL sterile dH_2O. The supernatant was removed and re-suspended in 1 mL 100mM LiAc solution. The cell mixture was incubated at 30°C for 5 min with gentle shaking and again centrifuged at 3000 rpm for 5 minutes. The excess amount of LiAc was removed by pelleting the cells at 10 000 rpm for 20 sec. The following layers were added to the yeast pellet in order: 240 µL 50% PEG, 36 µL 1M LiAc, 25 µL 2mg/mL Herring testes carrier DNA, 10 – 20 µL of purified bait/prey vector (100 ng – 5 µg) and sterile dH_2O up to a volume of 50 µL. The transformation complex was mixed for 1 minute and incubated in a 42°C water bath for 30 min. The transformed yeast suspension was plated on SD plates lacking the appropriate nutritional marker (see Appendix 9 for a detailed protocol).

2.9 Plasmid purification methods

2.9.1 Bacterial plasmid purification

Colonies confirmed by PCR to contain the correct recombinant plasmid were inoculated in 10 mL LB medium with appropriate antibiotics and incubated overnight at 37°C with shaking. The recombinant plasmid was isolated from 10 mL cultures using the Wizard ® SV plus miniprep DNA purification system (Promega, Madison WI, USA) (see Appendix 7 for a detailed protocol).

2.9.2 Yeast plasmid purification

Yeast cultures (10 mL) were pelleted at 10 000 rpm for 1 min and re-suspended in 200 µL of lysis buffer [3ml of 1 M sorbitol, 100 mM $NaPO_4$, 60 mM EDTA and 10 mg lyticase (Sigma, St. Louis, MO)] and incubated at 30°C overnight. After the first cell wall digest, the yeast cells were pelleted and plasmid isolation was performed using the Wizard ® SV plus miniprep DNA purification system (section 2.9.1) (Promega, Madison WI, USA) (see Appendix 7 for a detailed protocol).

2.10 Tissue culturing human cell lines

2.10.1 Culturing from frozen stocks

Frozen cell cultures were kept at -80°C for two days, followed by transfer to liquid nitrogen for long term storage. Cell cultures were rapidly defrosted in a water bath at 37°C for 10 min. The vial was sterilised with 70% ethanol and the defrosted cells were quickly re-suspended in 10 mL RPMI 1640 supplemented with 20% HI-FBS to dilute the DMSO. The cells were pelleted at 1000 rpm at 21°C for 5 minutes and re-suspended in 10 mL RPMI 1640 supplemented with 20% HI-FBS and 1% pen-strep. The 25 cm^2 culture flask containing cells were grown in a 37°C, 5% CO_2 incubator and checked every day.

2.10.2 Splitting the cell culture

Cell cultures were split every 2-4 days when they reached 80% density. The cells were transferred to 50 mL falcon tubes (Greiner) and pelleted at 1000 rpm at 21°C for 5 min. The cells were then re-suspended in 20 mL RPMI 1640 supplemented with 10% HI-FBS and 1% pen-strep solution and transferred to a 75 cm^2 culture flask. The tissue culture cells were grown in a 37°C, 5% CO_2 incubator and checked every day

2.10.3 Differentiation of THP-1 cells

THP-1 was differentiated using phorbol 12-myristate 13-acetate (PMA) (Sigma, St. Louis, MO) at a final concentration of 100 nM for 48 hours. The 100µM PMA stock was prepared by

dissolving 1 mg in 16.2 mL of 99.98% ethanol (Sigma, St. Louis, MO). PMA treatment stimulates Protein Kinase C which triggers THP-1 cells to differentiate into a macrophage like morphology. The cells become adherent, phagocytic and stop dividing.

2.10.4 Generating stock cultures

THP-1 and Jurkat cells were kept in a 37°C, 5% CO_2 incubator until the required cell density was reached. The flasks were pooled in 50 mL Falcon tubes (Greiner) and pipetted up-and-down to detach cells from another. The cells were pelleted at 1000 rpm at 21°C for 5 minutes, followed by removal of supernatant. The pellet was re-suspended in 1.5 mL fetal bovine serum and placed at 4°C for 5 min. Thereafter, RPMI 1640 containing 20% DMSO was added and 1 mL aliquots was stored at -80°C in liquid nitrogen for long term storage.

2.11 *In vivo* treatments

2.11.1 Etoposide-induced apoptosis

Differentiated THP-1 or Jurkat (1 X 10^6 cells/mL) cells in RPMI 1640 supplemented with 10% HI-FBS were incubated with etoposide (100 µg/mL) (Sigma, St. Louis, MO) for 6 hours at 37°C. Induction of apoptosis was established by binding of CaspACE FITC-VAD-fmk (section 2.14.1) (Promega Corp. Madison Wisconsin, USA).

2.12 Protein transfection

Human Jurkat cells were cultured in RPMI 1640 (Invitrogen, Carlsbad, CA) supplemented with 10% fetal bovine serum (Gibco), 1% penicillin-streptomycin solution (Sigma, St. Louis, MO) and incubated at 37°C with 5% $C0_2$. Pro-Ject protein transfection reagent was purchased from Thermo Scientific to effectively deliver recombinant mycobacterial proteins into cultured cells (Thermo Fisher Scientific, Rockford, IL). This experimental method was included to overcome the limitations of using a mammalian expression vector to express mycobacterial proteins.

Briefly, 5 µg of either recombinant ESAT-6 or CFP-10 was diluted in PBS and was used to re-hydrate the dried Pro-Ject film. Cells in suspension were counted (5 × 10^5 cells/mL), centrifuged

at 1200 rpm for 5 minutes and seeded in 900 µL RPMI free medium and 100 µL Pro-Ject hydration volumes. The transfection mix together with 5×10^5 cells/mL were then transferred to a 6-well plate and incubated for 4 hours at 37°C with 5% $C0_2$. After the incubation step, the reaction mixture was supplemented with 1 mL RPMI containing 20% fetal bovine serum. The transfection mixture was incubated overnight at 37°C with 5% $C0_2$. After protein transfection, cell lysates (section 2.16.2) and membrane protein extraction (section 2.16.3) was performed.

2.13 Evaluation of yeast strains and constructs

2.13.1 Phenotypic assessment of yeast strains

Before AH109 and Y187 were used in the Y2H analysis, the phenotypes were first assessed. Both yeast strains have defects in genes vital for the production of adenine, leucine, histidine and tryptophan, with neither having a deficiency in uracil production. As a result, these nutritional phenotypes were assessable by plating AH109 and Y187 on selection plates based on the nutritional requirements shown in the Table 2.4 (see Appendix 4B for a detailed protocol).

Table 2.4: Nutritional requirements for AH109 and Y187

Strain	SD Ade^-	SD Trp^-	SD Leu^-	SD His^-	SD Ura^-	YPDA
AH109	-	+	-	-	+	+
Y187	-	-	-	-	+	+

A single isolated colony from the verified working stock plate (YPDA) was propagated only if AH109 and Y187 displayed expected phenotypes. The verified working stock plates were sealed and stored at 4°C, until further use.

2.13.2 Testing the DNA-BD construct for transcriptional activation

Small scale transformation of pGBKT7-ESAT-6 and pGBKT7-CFP-10 were transformed into the Y187 yeast strains (section 2.8.2). The bait constructs were tested for transcriptional activation of ADE2 and HIS3 reporter genes by plating the transformed yeast strains on agar plates lacking essential amino acids: SD Trp^-/His^- and SD Trp^-/Ade^-.

2.13.3 Toxicity test of transformed yeast strains

To test whether the DNA-BD constructs had any toxic effect on yeast strains, growth rates in liquid culture of yeast strains transformed with the 'empty' DNA-BD vector and those containing the bait plasmid were compared. The growth curves were generated by inoculating one colony representing the appropriate bait plasmid into 50 mL SD Trp^- supplemented with 20 µg/mL kanamycin. The culture was incubated at 37°C with shaking (250-270 rpm) and measured every 2 hours for 8 hours, followed by incubation overnight. The measure OD_{600} was used to generate a linearised graph, comparing the slope of bait plasmids versus 'empty' plasmids.

2.14 Yeast two-hybrid analysis

2.14.1 Principles of the yeast two-hybrid (Y2H) technique

The yeast two-hybrid assay uses two separate domains, a sequence specific DNA binding domain (DNA-BD) and a transcription activation domain (AD). The known insert of interest is fused to the DNA-BD, known at the 'bait' and the interacting partner library is expressed as fusions to the AD, known as 'prey' peptides. If the prey and bait interact, the DNA-BD and AD are combined, activating transcription from the GAL4 responsive promoters. If the bait-prey interactions efficiently control transcription of reporter genes, putative binding partners can then be selected (Figure 2.1).

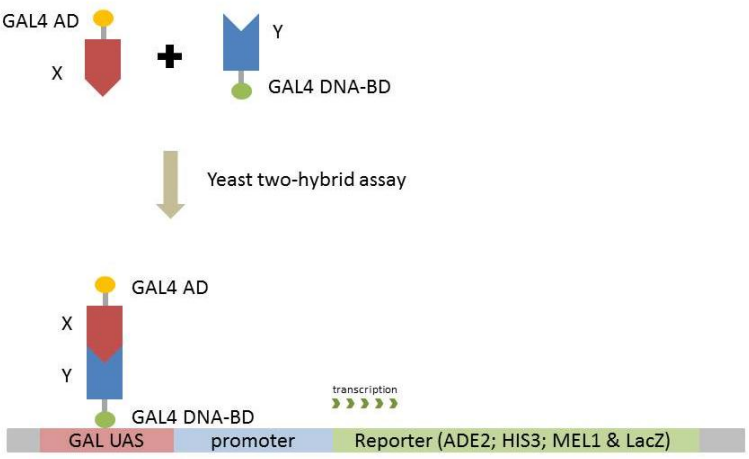

Figure 2.1: Principle of the yeast two-hybrid assay

2.14.2 Library construction

Human lung mRNA (catalog number: 636105, Clontech Laboratories Inc., Palo Alto, CA) was used to construct the cDNA library used in this study. The GAL4 activation domain (AD) fusion library was produced by co-transforming yeast with SMART generated ds cDNA (section 2.4.3) and *Sma*I-linearised pGADT7-Rec2 vector, as per manufacturer's instructions (Clontech Laboratories Inc., Palo Alto, CA). This process is outlined in Figure 2.2. One-step *in vivo* cloning using homologous recombination was possible using the BD SMART III and CDS III sequences incorporated during RT and LD-PCR. These sites have been engineered into the pGADT7-Rec2 vector. The transformation protocol as described under section 2.8.2 was used with a slight modification for volume adjustment (see Appendix 5 for a detailed protocol). Following homologous recombination, the transformants were spread on ~200 SD plates lacking leucine (SD-Leu$^-$) and incubated at 30°C for 5-7 days. Yeast transformants were harvested with 4 mL freezing medium (75% YPD and 5% glycerol) per library plate. Library transformants were scraped off the plates, pooled and stored as 1 mL aliquots at -80°C.

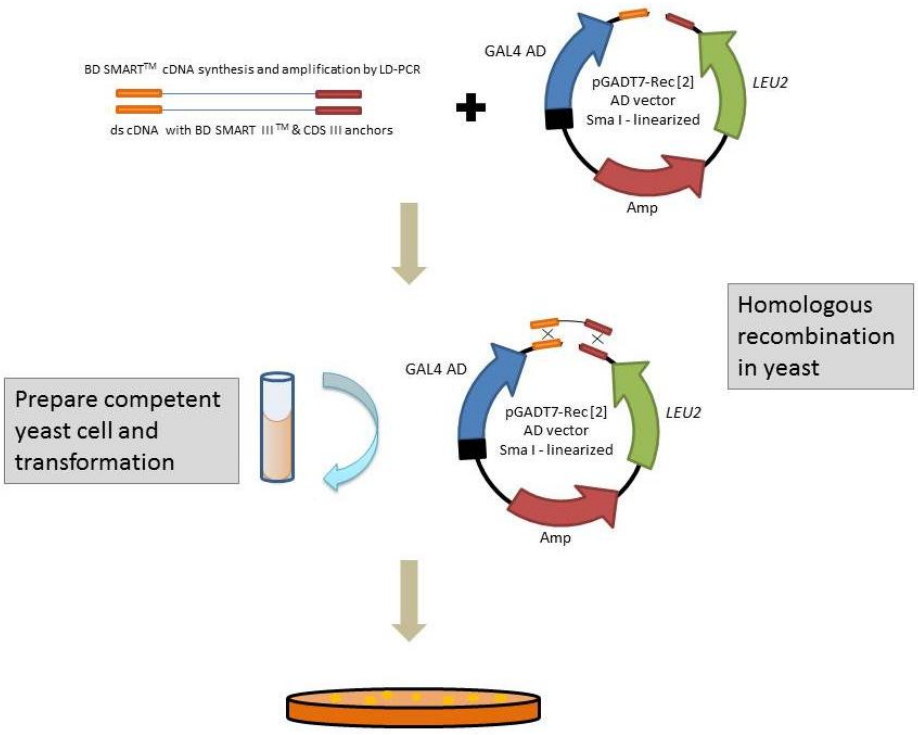

Figure 2.2: The construction of lung cDNA library using homologous recombination in yeast

The library titer was determined by spreading 100 µL of the following dilutions: 1:100, 1:1000 and 1:10000 on SD Leu$^-$ plates. The plates were incubated at 30°C until colonies developed ~2- 3 days later. The numbers of colony forming units (cfu) were counted and the numbers of clones in the library were determined using the formula below (transformation efficiency*):

$$number\ of\ \ cfu/mL^{\,*} = \frac{number\ of\ colonies}{plating\ vol\ (mL)\ \times dilution}$$

$$number\ of\ clones\ in\ library = number\ of\ \ cfu/mL\ \times vol\ final\ resuspension$$

The library titer plates were used to determine whether library construction was successful by colony PCR (section 2.4.2).

2.14.3 Establishment of bait culture

A single colony (< 2 mm) was selected on SD Trp$^-$ plates containing the transformed 'bait' plasmid (section 2.8.2) and inoculated in 50 mL SD Trp$^-$ liquid media. The culture was incubated overnight at 30°C with shaking. The yeast culture was centrifuged at 2500 rpm for 5 minutes and the supernatant was removed. The pellet was re-suspended in 5 mL SD Trp$^-$ liquid media and the numbers of cells were counted using a hemacytometer (cell density: ≥ 1 X 10^9 cells/mL).

2.14.4 Yeast two-hybrid assay

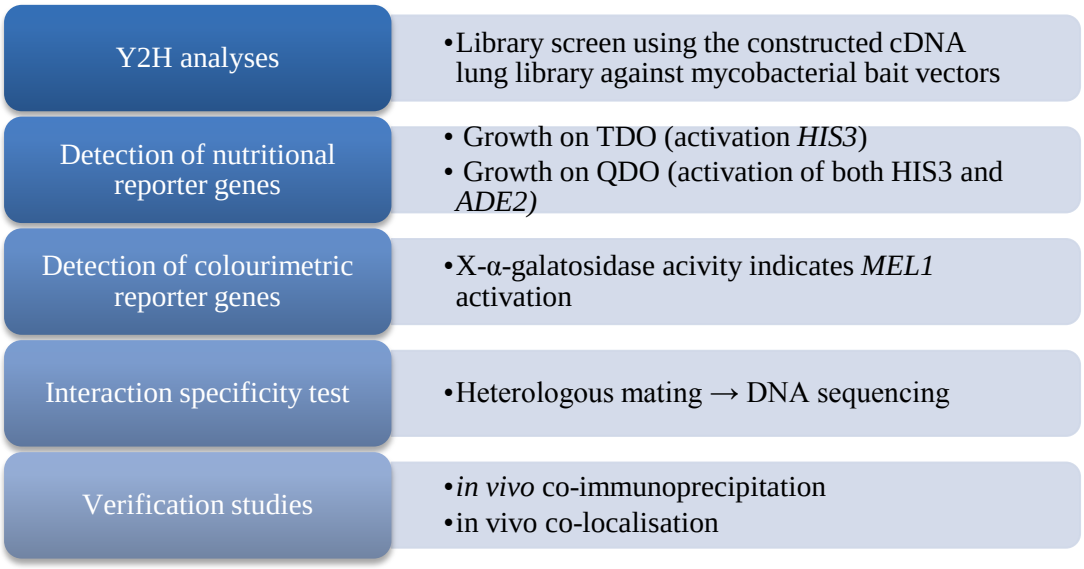

Figure 2.3: Schematic flow diagram of the Y2H analyses and verification studies

The Y2H process is outlined in Figure 2.3 (see Appendix 11 for a detailed protocol). For initial screenings, full length ESAT-6 and CFP-10 GAL4BD fusion constructs were used as baits and mated overnight with the constructed human lung cDNA library. Briefly, 1 ml of the AH109 library aliquot was thawed in a room temperature water bath and combined with 5 mL of Y187 'bait' culture in a sterile 2 L flask, together with 45 mL of 2X YPDA supplemented with 50 µg/mL kanamycin. The flask was incubated at 30°C for 24 hours in a shaking incubator (< 50 rpm). After mating, a drop of mating culture was checked under a phase contrast microscope to observe the formation of zygotes. The mating mixture was transferred to a sterile 50 mL Falcon tube (Greiner) and centrifuged at 2500 rpm for 10 minutes. The mating flask was rinsed with 0.5X YPDA liquid medium. The rinsed medium was used to re-suspend the mating pellet. Once again, the mixture was centrifuged and the pellet was re-suspended in 0.5X YPDA supplemented with 50 µg/mL kanamycin. The mating mixture was spread on triple dropout (TDO: lacking Trp, Leu and His) agar plates and incubated at 30°C until colonies appeared. The mating efficiency was determined by spreading 100 µL of the following dilutions: 1:100, 1:1000 and 1:10000 on SD Leu^-, SD Trp^-, and SD Leu^-/Trp^- plates. The colonies growing on TDO plates were replica-plated on quadruple dropout (QDO: lacking Trp, Leu, His and Ade) agar plates and incubated at 30°C for 2 weeks. Colonies positive for Ade and His were replica-plated on QDO containing X-α-gal and allowed to grow at 30°C for 4 days. Plates were sealed and stock cultures of diploid

cells were stored at -70°C. The AD library plasmid was isolated and heterologous mating with 'bait' was performed to confirm the phenotype. The library insert was amplified and the purified insert was determined by DNA sequencing (see Appendix 12 for a detailed protocol).

Control experiments were performed in parallel. The positive control was pGADT7-RecT (AH109) mated with pGBKT7-53 (Y187) and the negative control was pGADT7-RecT (AH109) mated with pGBKT7-Lam (Y187). The control mating efficiency was determined by spreading 100 µL of the following dilutions: 1:100, 1:1000 and 1:10000 on SD Leu^-, SD Trp^-, and SD Leu^-/Trp^- plates.

The Y2H and control dilution plates were used to determine the mating efficiency as follows:

$$number\ of\ (\#)\ viable\ \ cfu/mL = \frac{\#cfu}{plating\ vol\ (mL)\ \times dilution}$$

$$cfu/mL\ \ on\ SD\ Leu^- = viability\ of\ Y187\ partner$$
$$cfu/mL\ \ on\ SD\ Trp^- = viability\ of\ AH109\ partner$$
$$cfu/mL\ \ on\ SD\ Trp^-/Leu^- = viability\ of\ diploids$$

$$mating\ efficiency\ (\%\ diploid) = \frac{\#\ cfu/mL\ of\ diploids}{\#\ cfu/mL\ of\ library\ partners}\ \times\ 100$$

$$estimated\ \#clones\ screened = \#\ cfu/mL\ of\ diploids\ \times vol\ final\ resuspension$$

2.15 *In vivo* microscopy

In vivo co-localisation was performed in order to determine whether putative interacting binding partners shared the same cellular environment by labeling the proteins of interest with primary and secondary fluorescently labeled antibodies. Suspected co-localisation was accessed using immunofluorescence (see Appendix 13 for a detailed protocol).

2.15.1 Tissue culturing and staining for microscopy

For co-localisation studies, THP-1 cells were cultured in RPMI 1640 supplemented with 10% fetal bovine serum, 1% penicillin-streptomycin solution and incubated at 37°C with 5% $C0_2$. THP-1 cells were allowed to differentiate directly on microscope cover slips in 6-well tissue culture plates (CELLSTAR, Greiner Bio-One, LASEC, South Africa). The cover slips were transfected with either ESAT-6 or CFP-10 recombinant proteins using Pro-Ject protein transfection reagent (Thermo Fisher Scientific, Rockford, IL).

After 24 hours of incubation with recombinant proteins, cover slips were washed with pre-warmed RPMI 1640 medium, permeabilised by immersing coverslips in 100% methanol at -20°C and fixed in a 4% paraformaldehyde solution at room temperature. Various steps of washing with 1X PBS were performed, followed by incubation in blocking buffer (1% BSA in PBS) at room temperature. Primary and secondary antibodies for fluorescence instrumentation are listed in Table 2.5. All prepared slides were counterstained with 4',6-diamidino-2-phenylindole, dilactate (DAPI) nuclear stain (Invitrogen, Carlsbad, CA). Slides were mounted in Mowiol mounting medium with anti-fade (Calbiochem) and stored at 4°C until further use.

Table 2.5: Primary and secondary fluorescence labeled antibodies for use as immunofluorescent microscopy

Primary antibody
C1QA Goat polyclonal (1:200)
FLNA Rabbit monoclonal (1:200)
ESAT-6 Mouse monoclonal (1:200)
CFP-10Mouse monoclonal (1:200)
Secondary antibody
Goat anti-mouse Alexa 488 (1:500)
Donkey anti- Rabbit Cy3 (1:500)
Donkey anti-mouse Cy3 (1:500)
Donkey anti-goat FITC (1:500)

Similarly, differentiated THP-1 cells were treated with recombinant ESAT-6 and stained with FITC-VAD-fmk (according to the manufacturer's conditions) in culture to test for activation of caspase activity.

2.15.2 Fluorescence microscopy and *in vivo* co-localisation

Fluorescent imaging was performed using the Zeiss Axiovert 200M LSM-510 Meta confocal microscope system (Jena, Germany) at the Department of Anatomy, University of Cape Town, South Africa. Fluorescent signals of antibody tags were obtained by excitation using a 488 nm line of a multiline argon laser, the DPSS 561-nm laser and the Mai Tai 2-photon deep sea 750nm laser with a X63 oil-immersion objective with a numerical aperture of 1.4. The excitation and emission wavelengths are listed in Table 2.6. Quantitative co-localisation analyses were performed using the Ziess LSM 510 Meta software (Jena, Germany) to measure the co-localisation coefficient within a defined region of interest (ROI).

Table 2.6: Summary of fluorescent filters

Excitation	Emission	Filter set
488nm	519nm	FITC
494nm	570nm	Cy3
405nm	461nm	DAPI

2.16 *In vivo* co-immunoprecipitation

2.16.1 Principle

In vivo co-immunoprecipitation, outlined in Figure 2.4, is a method that examines *in vivo* protein complex formation between various proteins. This analysis provides evidence for the coexistence of proteins in a complex and further validation is required to prove the interaction *in vitro* experiments (Phizicky and Fields, 1995). The coexistence of protein complexes are important structures for many biological processes that give information about the molecular mechanisms of these biological processes.

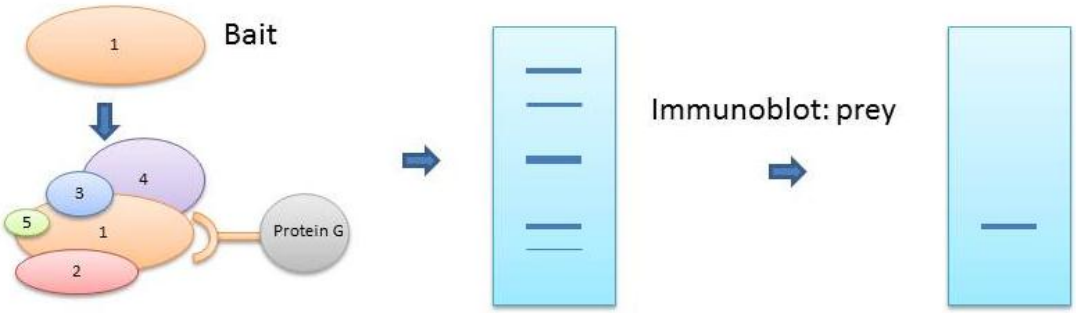

Figure 2.4: Principle of *in vivo* co-immunoprecipitation (Co-IP). *In vivo* Co-IP determines the dynamic protein interaction in living cells. A protein-specific antibody conjugated to protein G beads is used to purify the protein interest and its associated complex from cell lysates. The precipitate is eluted from the protein G beads and loaded on a sodium dodecyl sulfate-polyacrylamide gel electrophoresis (SDS-PAGE). The resulting SDS-PAGE, with separated protein partners, are transferred to a nitrocellulose membrane and Western blot analysis is performed with the protein-specific antibody against the interacting protein partner.

2.16.2 Preparation of cell lysates

Twenty four hours after protein transfection, discussed in section 2.12, cells were washed with PBS and lysed on ice with Tissue Protein Extraction Reagent (TPER, Thermo Fisher Scientific, Rockford, IL) supplemented with protease inhibitors (Calbiochem). The cellular debris was then centrifuged at 4°C for 10 min at 10 000 rpm and the total protein concentration of the supernatant were estimated using the Bradford Protein assay (Bio-Rad laboratories, Hercules, CA, USA). Lysates were stored at -20°C until needed.

2.16.3 Membrane protein extraction

Human Jurkat or THP-1 cells were cultured and transfected as discussed in sections 2.10 and 2.12. Twenty four hours after protein transfection, the cells were centrifuged and washed with 1X PBS. Membrane associated proteins were extracted using the membrane protein extraction kit (Mem-PER, Thermo Fisher Scientific, Rockford, IL). Briefly, pelleted cells were lysed using Reagent A, followed by re-suspension into one part Reagent B and two parts Reagent C at 4°C for 30 minutes. The extraction mix was centrifuged at 10 000 rpm for 3 minute at 4°C and transferred to a 1.5 mL centrifugation tube. The supernatant was incubated for 10 minutes in a 37°C water bath for phase separation of hydrophobic and hydrophilic fractions. The majority of

membrane proteins were located in the lower hydrophobic fraction and were stored at -20°C until needed.

2.16.4 *In vivo* semi-endogenous co-immunoprecipitation

Cell lysates and membrane fractions were prepared as described in sections 2.16.2 and 2.16.3. The protein fractions were pre-cleared with 20 µL of protein G Dynabeads (Invitrogen, Carlsbad, CA) for 1 hour at 4°C. The precipitating antibody (2-5 µg) was allowed to the bind protein G for 10 minutes at room temperature. Antibodies were cross-linked to Dynabeads using suberic acid bis (3-sulfo-N-hydroxysuccinimide ester) sodium salt (BS^3; Sigma, St. Louis, MO) to prevent co-elution of antibodies. The cross-linking reaction was stopped by the addition of 12.5 µL 1M Tris-HCI solution. The bead-antibody complex was washed twice using 1X PBS 0.01% Tween 20. The complex was incubated with the prepared lysate fractions for 10 minutes at room temperature. After several washing steps with 1X PBS 0.25 mM Lithium chloride (LiCl), the complex was suspended in 2X reducing sample buffer and denatured for 5 minutes at 95°C.

The levels of C1qA in both THP-1 and Jurkat cells were extremely low and not sufficient to perform precipitation experiments. Therefore, co-immunoprecipitation (Co-IP) experiments were performed with human serum and recombinant GST tagged C1QA. Serum was pre-cleared twice overnight at 4°C to remove excess amounts of immunoglobulin, followed by immunoprecipitation.

2.16.5 Western blot analysis

The denatured protein lysate containing the sample of interest was subjected to electrophoresis on 6% - 12% polyacrylamide gels. The proteins were separated using a Mini-Protean III System (Bio-Rad laboratories, Hercules, CA, USA), then electro-transferred from the gel to polyvinylidene difluoride (PVDF) membrane using the iBLOT semi-dry apparatus (Invitrogen, Carlsbad, CA). The membrane was blocked overnight with blocking buffer (1X PBS 0.05% Tween 20 5% non-fat milk powder). The membrane was incubated with the primary antibody overnight at 4°C, after which it was washed 3X for 30 minutes with 1X PBS. The secondary HRP-conjugated antibody was added for 1 hour at room temperature, followed by 3 washing

steps with 1X PBS for 30 minutes. The concentrations of primary and secondary antibodies combinations, diluted in blocking buffer, are listed in Table 2.7. The protein band was visualised by developing the membrane in SuperSignal West Pico Chemiluminescent substrate as per manufacturer's instructions (Thermo Fisher Scientific, Rockford, IL) (see Appendix 14 for a detailed protocol). Reciprocal immunoprecipitaion experiments were performed for bait and prey combinations.

Table 2.7: Primary and secondary antibody combinations for the detection of proteins using Western blot analysis.

Protein	Identification	Primary antibody	Secondary antibody
C1QA	Prey* [#]	Goat polyclonal (1:1000)	Donkey anti-goat IgG HRP (1:1000)
FLNA	Prey*	Mouse monoclonal (1:1000)	Goat anti-mouse IgG HRP (1:1000)
ESAT-6	Bait*	Mouse monoclonal (1:500)	Goat anti-mouse IgG HRP (1:1000)
CFP-10	Bait[#]	Rabbit polyclonal (1:500)	Goat anti-mouse IgG HRP (1:2000)
β-Tubulin	Control	Mouse monoclonal (1:500)	Goat anti-mouse IgG HRP (1:2000)

Identifiers*[#] illustrates binding partners

2.17 Case-Control study

2.17.1 Patient and control cohort

A case/control study was performed involving ~500 cases and ~500 controls. All study participants were from the South African Coloured (SAC) population. The origins of this mixed ancestry population date back numerous generations, with genetic contributions from San, Khoi, Malaysian, African black and European lineages (de Wit et al., 2010). This population was formed from different populations with different susceptibility features and offers a unique opportunity to dissect and identify TB susceptibility alleles, as this population has a high burden of tuberculosis (Barreiro et al., 2006). The study cohort in question has been shown to demonstrate no difference in substructure between cases and controls (Barreiro et al., 2006) and therefore may not influence the observed results. Participants diagnosed with tuberculosis were recruited from the Ravensmead-Uitsig an epidemiological field site near Cape Town in the Western Cape region of South Africa. Controls were healthy individuals with no history of TB, who live in the same catchment area as the patients. Informed consent was obtained from all study participants. All protocols were approved by the Health Research Ethics Committee of the

Faculty of Medicine and Health Sciences, Stellenbosch University (project number 95/072). All participants were HIV negative and all TB cases were bacteriologically confirmed.

2.17.2 Demographics of the study cohort

The mean age of TB cases was 33.7 years (SD 13.8); 52.3% were female and 47.7% were male. Patients diagnosed with Tuberculous Meningitis were commonly observed in children (mean age 7.26 [SD 5.24]); 58.7% were female and 41.3% were male. The mean age of the control group was 32.8 years [SD 10.88] with an unequal distribution of gender (females: 76.5% and males: 23.5%). Since the difference in age and gender was observed, as seen in Figure 2.5, we corrected our statistical analyses to account for these differences.

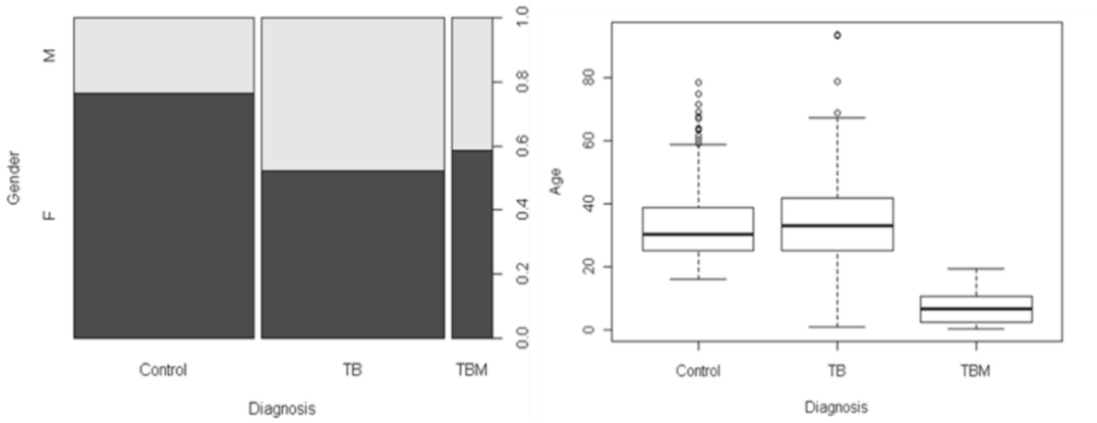

Figure 2.5: Distribution of gender and age of the study cohort

2.17.3 Promoter screening for functional variants

To initially screen for single nucleotide polymorphisms (SNPs), a PCR-based strategy was followed by direct sequence analysis. Human genomic DNA was amplified from 10 cases and 10 controls across the 5' flanking region of the human *FLNA* promoter. Primers were designed (section 2.3.1, Table 2.2) according to the *FLNA* gene sequence published on NCBI (http://www.ncbi.nlm.nih.gov/). PCR reactions were performed using sense primer 5' CTG ACA AGT CTT ATG GGA ACC 3' and anti-sense 5' CCG AGA GTG GGA GCT ACT CAT 3' according to the method described in section 2.4.1 (Tm 55°C, Table 2.2). The resulting PCR products were purified using the Wizard ® SV Gel and PCR clean-up system (Promega Corp.

Madison Wisconsin, USA) and sequenced in both directions using the PCR primers (section 2.6). Sequences were aligned and analysed using BioEdit (version 7.0.5.3).

2.17.4 SNP selection

The *C1QA* gene, identified as a TB susceptibility gene by means of yeast two-hybrid analyses, was investigated to test the hypothesis that SNPs within the genomic region spanning the C1q molecule may influence susceptibility to mycobacterial disease. Polymorphisms were selected from literature based on previous associations or functional effects. The selected SNPs were then further explored within the HapMap CEU and YRI population groups to check the frequency spectrum of the selected SNPs on the NCBI SNP database (db) (http://www.ncbi.nlm.nih.gov/snp). Table 2.6 represents the SNPs selected for this study as well as the individual TaqMan assay used to genotype each polymorphism.

Table 2.8: Selected dbSNP used for this study and the TaqMan assay used to type the particular variant.

C1q region	dbSNP	bp change	ABI TaqMan assay
5' C1qA	rs665691	C → G	C_3176793_10
5' C1qA	rs587585	A → G	C_3176797_10
3' C1qA	rs12033074	C → G	C_31443180_10
C1qA (exon 3)	rs172378	G → A	C_3176785_10
C1qB (intron 2)	rs631090	T → C	C_992968_10

2.17.5 TaqMan SNP genotyping

TaqMan® SNP genotyping assays consists of a primer set, which amplifies the sequence of interest, and two TaqMan probes for allele detection. Each TaqMan probe incorporates a non-fluorescent quencher attached to a minor groove binder (MGB) at the 3' end and a reporter dye for each allele at the 5' end. Hybridisation of the MGB molecule to the minor groove of the DNA helix improves the probe-template complex and increases stability. The final step of detection is achieved by 5' nuclease chemistry, which cleaves the allele-specific 5' dye that generates a permanent signal for allele discrimination (Figure 2.8).

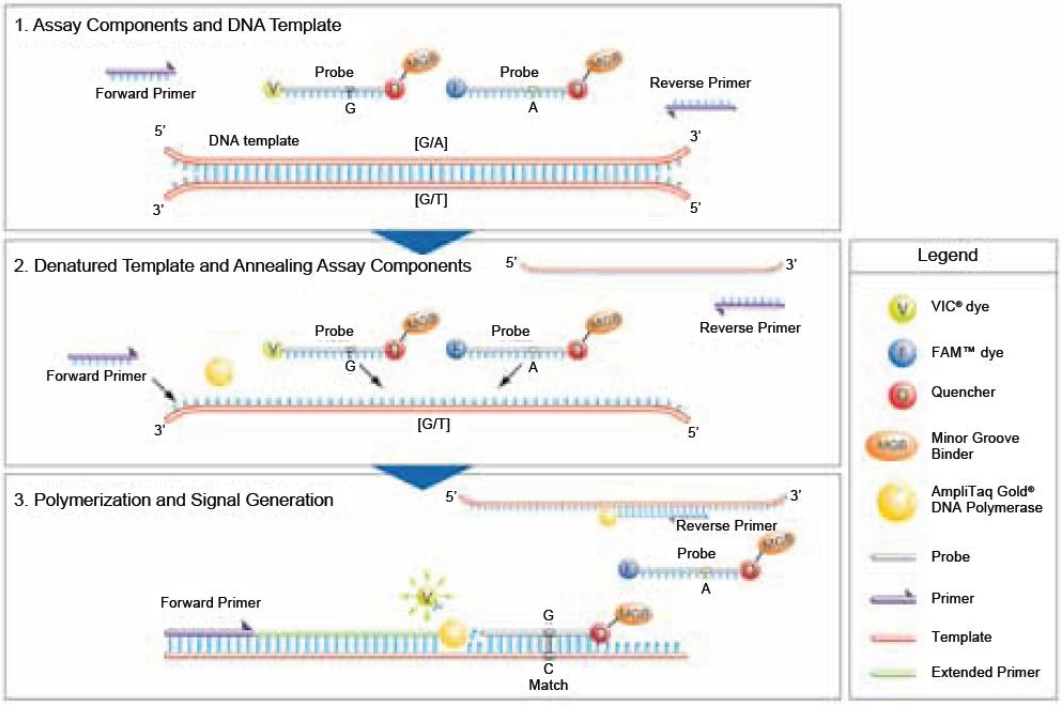

Figure 2.6: Allelic discrimination, achieved by selective annealing of TaqMan probes (http://www.appliedbiosystems.com)

2.17.6 Real Time PCR amplification

Real time PCR amplification for each individual pre-designed SNP assay was performed on a 384 well plate on an Applied Biosystems Prism 7900HT (Applied Biosystems Inc., Forster City CA, USA). The amplification mix was made up as follows: 2.5 µL ABI TaqMan Universal PCR master mix, 1.375 µL sterile dH_2O and 0.125 µL sequence-specific primers and probe mix. The master mix and DNA samples were loaded on a 384 well plate using the EpiMotion pipetting robot (Eppendorf, Hamburg, Germany). Each prepared plate contained 30 non-template controls, to test for contamination. PCR conditions were as follows: 50°C for 2 min; 95°C for 10 min, followed by 40 cycles of 95° for 15sec and 60°C for 1.5 min.

2.17.7 Allelic discrimination

After PCR amplification, allelic discrimination was performed by an end point plate read using the 7900HT Fast Real-Time PCR System (Applied Biosystems). The Sequence Detection Systems (SDS) 2.3 software was used to measure the amount of fluorescence during the plate

read. The software reads the fluorescence from each sample well and performs automated allelic discrimination to generate discrimination plots.

2.18 ELISA assay

Human complement component 1, q subcomponent, A (C1QA) was measured quantitatively using an ELISA assay according to a modified method previously described (Beards et al., 1984). Briefly, 96-well immunoassay plates (MaxiSorp, Nunc, Wiesban) were coated with 100 µL/well rabbit anti-human C1QA monoclonal antibody (0.5 µg/mL; R&D systems, Wiesban, Germany) and kept at 4°C overnight. The remaining protein binding sites were blocked at 4°C with blocking buffer (100 mM phosphate buffer saline [PBS], 0.05% Tween-20, 5% bovine serum albumin [BSA]). Human plasma was diluted 1:500 in blocking buffer and incubated for 90 min at 37°C in duplicate, together with diluted standards on the same ELISA plate. After sample incubation, 100 µL/well detection antibody was added (mouse anti-human C1QA, 200 ng/mL; Santa Cruz Biotechnology, Santa Cruz, California, USA), followed by 100 µL/well secondary horseradish peroxidase antibody (goat anti-mouse, 100 ng/mL; Santa Cruz Biotechnology, Santa Cruz, California, USA). Both of the antibody incubations were performed for 1 hour at room temperature. The assay was developed using 3, 3´, 5, 5´ - tetramethyl-benzidine (TMB; Sigma, St. Louis, MO) and hydrogen peroxide (H_2O_2; Sigma, St. Louis, MO) in a total reaction volume of 100 µL/well. The reaction was stopped by adding 100 µL of 2M sulphuric acid (H_2SO_4; Sigma, St. Louis, MO) per well. The absorbance was measured at a dual wavelength of 450 nm and 650 nm using the iMark microplate reader (Bio-Rad laboratories, Hercules, CA, USA). The standard curve was used to determine the mean absorbance of the relative levels of plasma C1QA in cases and controls. The data was normalised by subtracting the background absorbance from each sample well (see Appendix 15 for detailed protocol).

2.19 Statistical Analysis

Alleles and genotype frequencies for case and control groups were determined by direct counting, and frequencies among the groups were tested for conformity to Hardy-Weinberg equilibrium. Significant differences between cases and controls for the genotype and haplotype groups were tested using a general linear model (glm) – analysis of variance (ANOVA), adjusting for age and

gender. In addition, we evaluated whether additive and dominance effects can be assigned to a given SNP association. R (freely available from http://www.r-project.org) and the R package, genetics (Warnes et al., 2008) was used to test the above assumptions. A result corresponding to a p-value below 0.05 was described as statistically significant.

The precision of ELISA measurements was determined by the Shapiro Wilk test. The Levene test was used to verify the assumption that the variances are equal or differed across a sample population. All ELISA statistics were performed using SPSS software (version 11.5, SPSS, Chicago, IL, USA).

Chapter 3

3 Yeast two-hybrid analysis to identify host binding partners of ESAT-6 and CFP-10

3.1 Results

3.1.1 Construction of lung cDNA library

3.1.1.1 Integrity of lung RNA

The purity and integrity of RNA was evaluated using the Experion RNA StdSens Starter kit (Bio-Rad laboratories, Hercules, CA, USA), which requires only a small amount of sample material (25-500 ng/µL). Figure 3.1 shows two RNA bands corresponding to 18S and 28S ribosomal RNA's. The bands were clear and the brightness of the 28S band was approximately twice that of the 18S band, which demonstrates that the RNA was intact and free of RNA degradation. In addition, the RNA loaded onto the chip had no other visible bands, which suggest that the RNA sample was free of genomic DNA. The 260/280 ratio of the RNA sample was 1.96. Pure RNA has a 260/280 ratio of ~1.9-2.1 and the RNA used in this study thus corresponds to good quality RNA (http://www.qiagen.com). The assessment of RNA integrity was a critical first step in ensuring that good quality RNA was used for the generation of cDNA for further library construction.

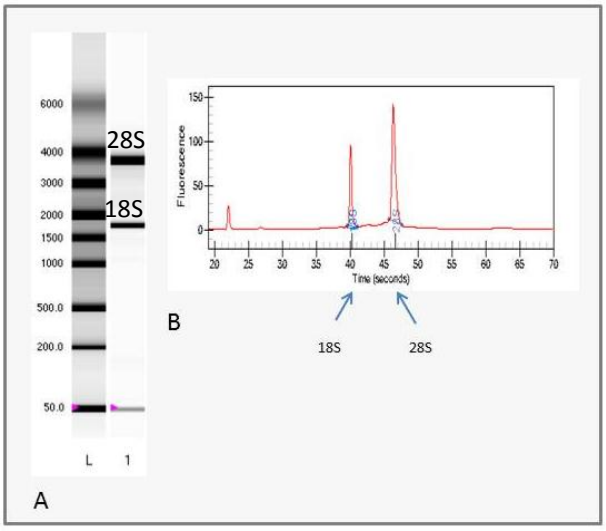

Figure 3.1: Assessment of RNA integrity and purity. (A) Virtual gel demonstrating the Experion RNA ladder in lane L and the RNA sample in lane 1 showing the 18S and 28S bands. (B) Electropherogram of the 18S and 28S peaks obtained using the Experion™ Automated Electrophoresis Station (Bio-Rad laboratories, Hercules, CA, USA).

3.1.1.2 cDNA amplification

Human lung RNA was reverse transcribed to cDNA using the BD SMART™ cDNA synthesis kit (BD Biosciences Pharmingen, San Diego, CA). Amplification was evaluated by loading 7 µL of the PCR product, alongside a 100bp DNA ladder (Fermentas, Burlington, Canada), on a 1.2% w/v agarose gel containing 250 ng/mL ethidium bromide immersed in 1X TAE buffer was (Figure 3.2A, lane 2). After amplification, the ds cDNA was purified using BD CHROMS SPIN™TE-400 columns to eliminate excess adaptors and fragments smaller than 400 bp (Figure 3.2B, lane 3). The purified ds cDNA was used for the construction of the lung cDNA library.

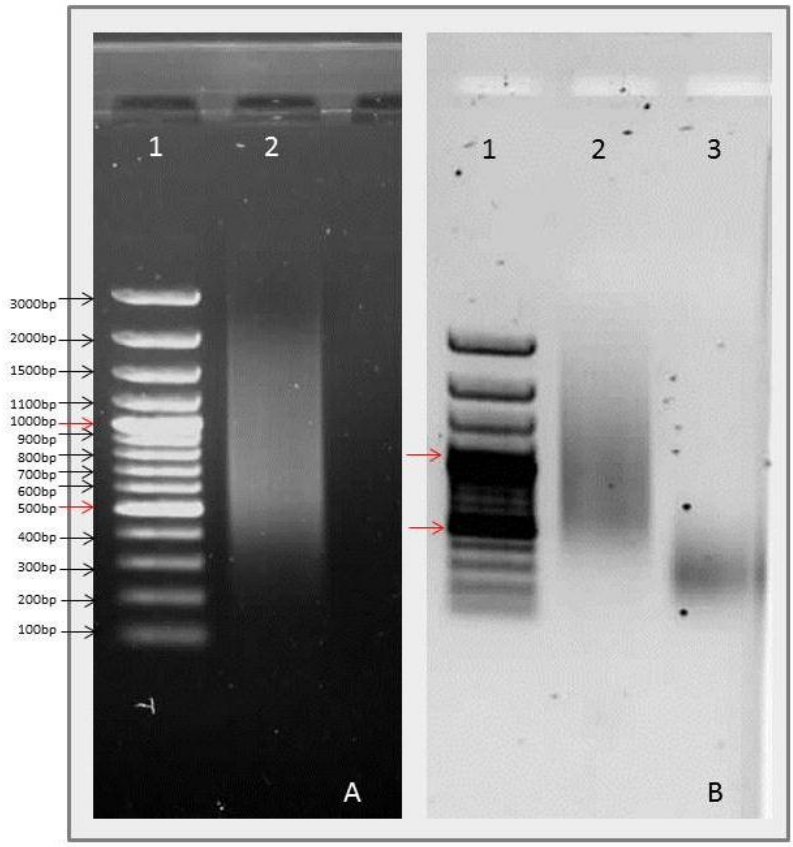

Figure 3.2: 1.2% TAE Agarose gel electrophoresis image of size fractionated ds cDNA before and after purification (A) Lane 1 contains a 100bp DNA ladder (Fermentas, Burlington, Canada) and lane 2 represents the unpurified double stranded (ds) cDNA amplification product. (B) Lane 1 contains a 100bp DNA ladder (Fermentas, Burlington, Canada) and lane 2 represents the ds cDNA after purification to exclude fragments smaller than 400 bp. Lane 3 represents the smaller fragments not retained by the BD columns.

3.1.1.3 Library construction

For library construction, purified ds cDNA and linearised SmaI-pGADT7 vector were co-transformed into freshly prepared competent AH109 yeast cells. The GAL4 fusion library was constructed in a single step reaction using homologous recombination as the cloning method in yeast. The transformation reaction was plated on 200 SD Leu$^-$ plates and incubated at 30°C until colonies developed (~3-6 days) (Figure 3.3A). The library titer was determined by counting the number of colonies on the 1:100 SD Leu$^-$ dilution plates. The library titer was determined using the equation in section 2.13.2 and yielded 1.73×10^9 cfu/mL. Fourteen colonies were randomly selected and amplified by PCR using primers listed in Table 2.2, to identify colonies containing cDNA inserts. Colony PCR of the 10 randomly selected colonies contained a PCR insert, which indicated that the transformation efficiency was above ~70%. The sizes of the PCR products were between 0.5-1kb (Figure 3.3B).

The yeast transformants were scraped from SD Leu$^-$ plates using glass balls and 4 mL freezing medium per library plate. The transformants from all the 200 library plates were pooled into one suspension. The total number of independent clones in the pooled library suspension was 4.87×10^8 clones (equation in section 2.13.2). The constructed library was stored as 1 mL aliquots containing $\sim 1 \times 10^9$ cfu's.

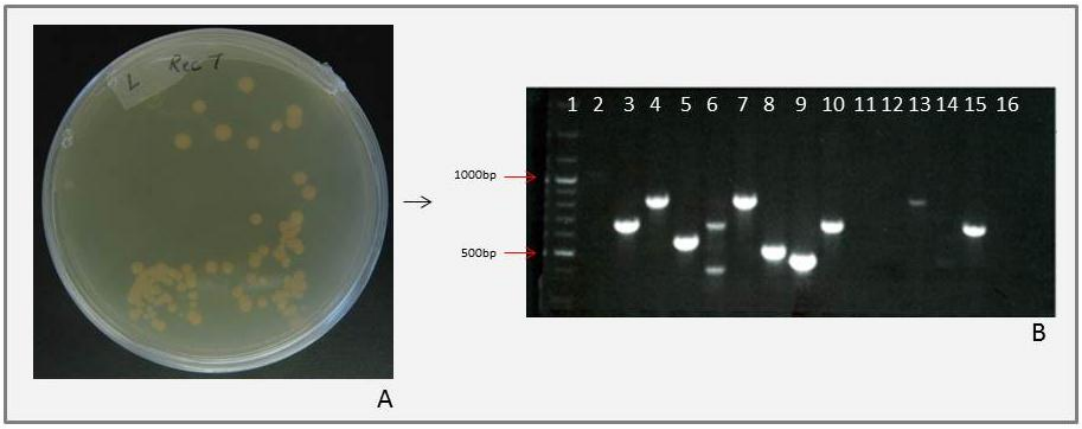

Figure 3.3: Screening of randomly selected yeast colonies for positive library transformants (A) Colony growth of library transformants allowing for restoration of the SmaI-linear vector to circular form, permitting growth on selection medium lacking leucine. (B) 1.5% TAE agarose gel of the PCR inserts from 14 randomly selected colonies. Lane 1 represents the 100bp DNA ladder (Fermentas, Burlington, Canada). Lanes 2-15 represents the PCR products of 14 randomly selected clones, illustrating the diversity in insert length. Lane 16 represents the negative control.

3.1.2 Bait construction

3.1.2.1 Amplification of ESAT-6 and CFP-10

The genes encoding ESAT-6 and CFP-10 were amplified from genomic DNA isolated from the laboratory strain, *Mycobacterium tuberculosis* H37Rv. The PCR products were resolved on a 2% agarose TAE/EtBr gel. The amplification of ESAT-6 generated a PCR product of 339 bp and a 414bp product for CFP-10 (Figure 3.4). Amplification products were purified using the Wizard ® SV gel and PCR purification kit (Promega Corp. Madison Wisconsin, USA).

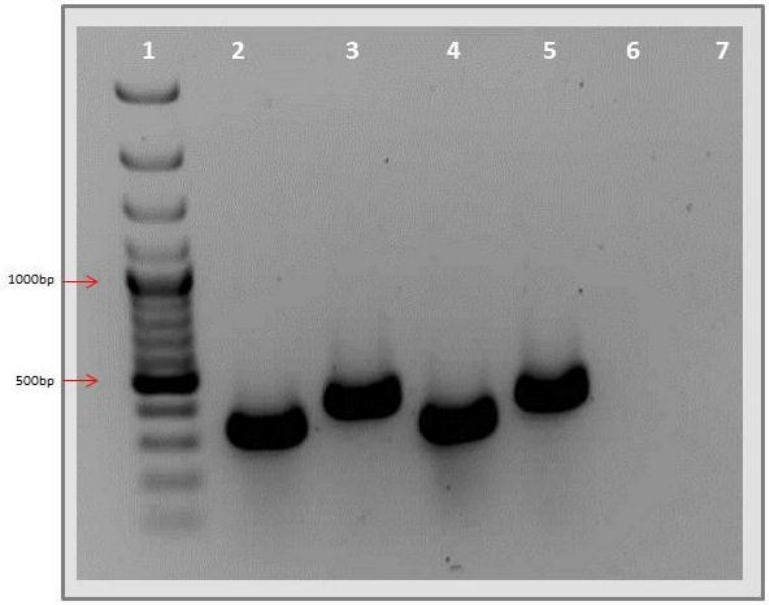

Figure 3.4: 1.5% TAE agarose gel of PCR products of ESAT-6 and CFP-10. Lane 1 contains the 100bp DNA ladder (Fermentas, Burlington, Canada). Lanes 2 and 4 contain the amplified PCR product of ESAT-6 (339bp). Lanes 3 and 5 contain the amplified PCR fragment of CFP-10 (414bp). Lanes 6&7 contain the negative control of each PCR reaction.

3.1.2.2 pGem-T-easy ligation and colony PCR

The purified PCR products were cloned into the pGem-T easy cloning vector (Promega Corp. Madison Wisconsin, USA) and transformed into *E. coli* XL-1 blue strain for blue/white selection (Figure 3.5). Bacterial colony PCR was performed in order to select for positive clones containing the inserts of interest. Stock cultures were prepared and the constructed plasmid was purified from *E. coli* using the Wizard ® SV plus miniprep DNA purification system (Promega, Madison WI, USA).

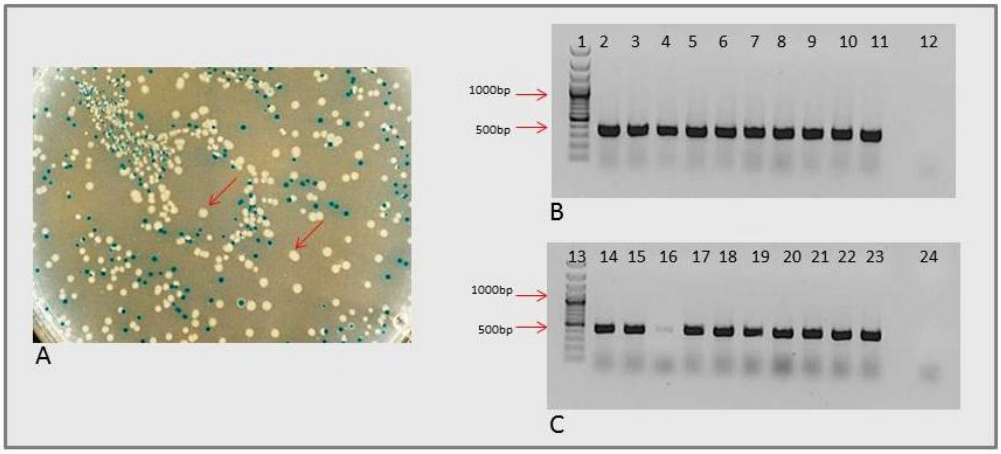

Figure 3.5: Screening of white pGem-T-ESAT-6 and pGem-T-CFP-10 colonies. (A) Recombinants were identified by blue/white screening and were confirmed by PCR. White colonies contained the insert of interest (indicated with the red arrows), while the blue colonies contained no insert. Blue colonies produce functional β-galactosidase and cleave the X-gal substrate plated on LB plates, whereas white colonies contain inserts that disrupts that functional LacZ gene that produces β-galactosidase. (B) Colony PCR of ESAT-6 (lanes 2-11, 339bp) and (C) CFP-10 (lanes 14-23, 414bp) positive clones. Lanes 1 and 13 represents the 100bp DNA ladder (Fermentas, Burlington, Canada). Lanes 12 and 24 represents the negative controls for each reaction.

3.1.2.3 Construction of pGBKT7 constructs

The pGem-T-ESAT-6 and pGem-T-CFP-10 were digested with EcoRI and PstI (Figure 3.6A). The restricted inserts were excised and gel purified using the Wizard ® SV plus miniprep DNA purification system (Promega, Madison WI, USA). The isolated inserts were sub-cloned into shrimp alkaline phosphatase (SAP) treated pGBKT7 vector restricted with EcoRI and PstI. The ligation reaction for each bait vector was transformed into *E. coli* cells. The pGBKT7-ESAT-6 and pGBKT7-CFP-10 were confirmed by colony PCR (Figure 3.6B) and sequenced to verify that the inserts were in-frame with the DNA-BD of pGBKT7. These recombinant plasmids were used to perform the yeast two-hybrid screens.

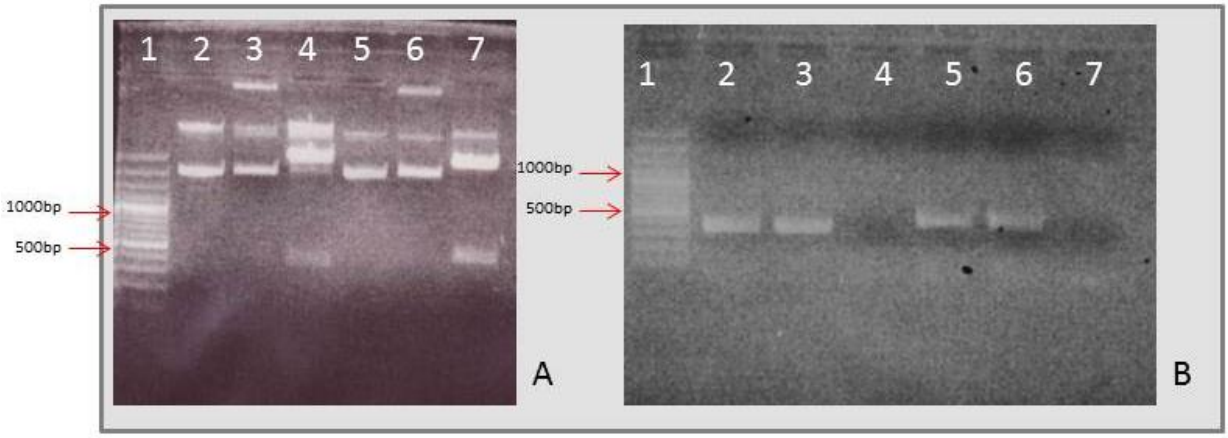

Figure 3.6: Construction of pGBKT7-ESAT-6 and pGBKT7-CFP-10 constructs. (A) The result of pGem-T-ESAT-6 and pGem-T-CFP-10 digested with EcoRI and PstI. Lane 1 contains the 100bp DNA ladder (Fermentas, Burlington, Canada). Lanes 2 and 5 contain the uncut pGemT vectors. Lanes 3 and 4 contains pGem-T-ESAT-6 after the final digest with EcoRI and PstI. Lanes 6 and 7 contains pGem-T-CFP-10 after the final digest with EcoRI and PstI. The insert from lanes 4 and 7 were purified using the Wizard ® SV Gel and PCR purification system (Promega Corp. Madison Wisconsin, USA). The purified insert of ESAT-6 and CFP-10 were sub-cloned into pGBKT7. (B) Bacterial colony PCR of pGBKT7-ESAT-6 (lanes 2 and 3) and pGBKT7-CFP-10 (lanes 5&6). Lane 1 contains the 100bp ladder (Fermentas, Burlington, Canada). Lanes 4 and 7 are the negative controls for each reaction.

3.1.3 Testing of pGBKT7 constructs

3.1.3.1 Testing pGBKT7 constructs for toxicity

The pGBKT7-ESAT-6 and pGBKT7-CFP-10 constructs were transformed into the Y187 yeast strains and the formation of colonies was compared to yeast containing the empty pGBKT7 vector. The colony morphology was normal in colour and size, when compared to yeast strains containing the empty pGBKT7 vector (Figure 3.7). An isolated colony from each plate was selected and inoculated into 50 mL SD Trp^- liquid medium. The growth rate was recorded to assess, whether pGBKT7-ESAT-6 and pGBKT7-CFP-10 constructs were toxic to the Y187 yeast strain.

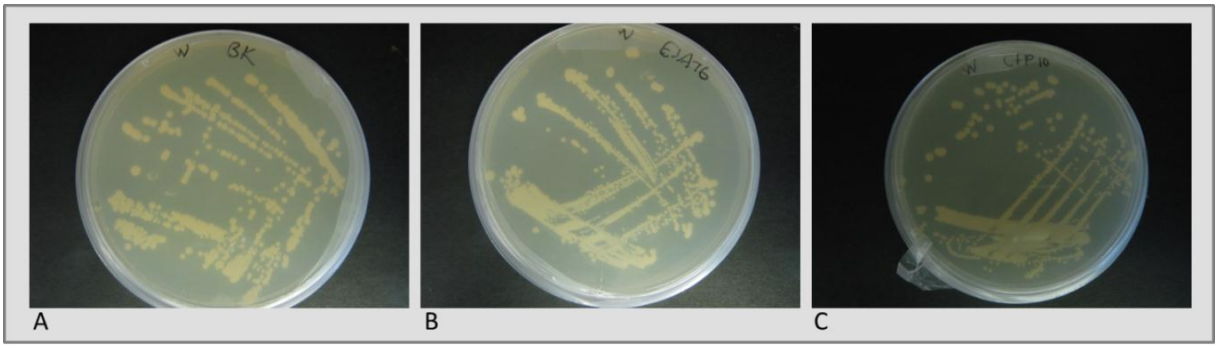

Figure 3.7: Recombinant pGBKT7-ESAT-6 and pGBKT7-CFP-10 constructs in Y187 yeast strains. Visual inspection of size and colour of yeast colonies containing (A) empty pGBKT7 vector, (B) pGBKT7-ESAT-6 and (C) pGBKT7-CFP-10 recombinant vectors. The yeast strains containing ESAT-6 and CFP-10 were normal in size and colour.

The log (OD_{600}) of ESAT-6 and CFP-10 were compared to the slope of the empty vector (Figure 3.8). Normally, if the growth rate of bait protein (i.e. ESAT-6 and CFP-10) is noticeably slower than the empty pGBKT7 vector, the fusion proteins would have been considered as toxic to the yeast strains. The colony morphology was normal and the transformed strains had compatible growth rate in culture, suggesting that the constructs were non-toxic. These strains were thus used for further analysis in the Y2H assays.

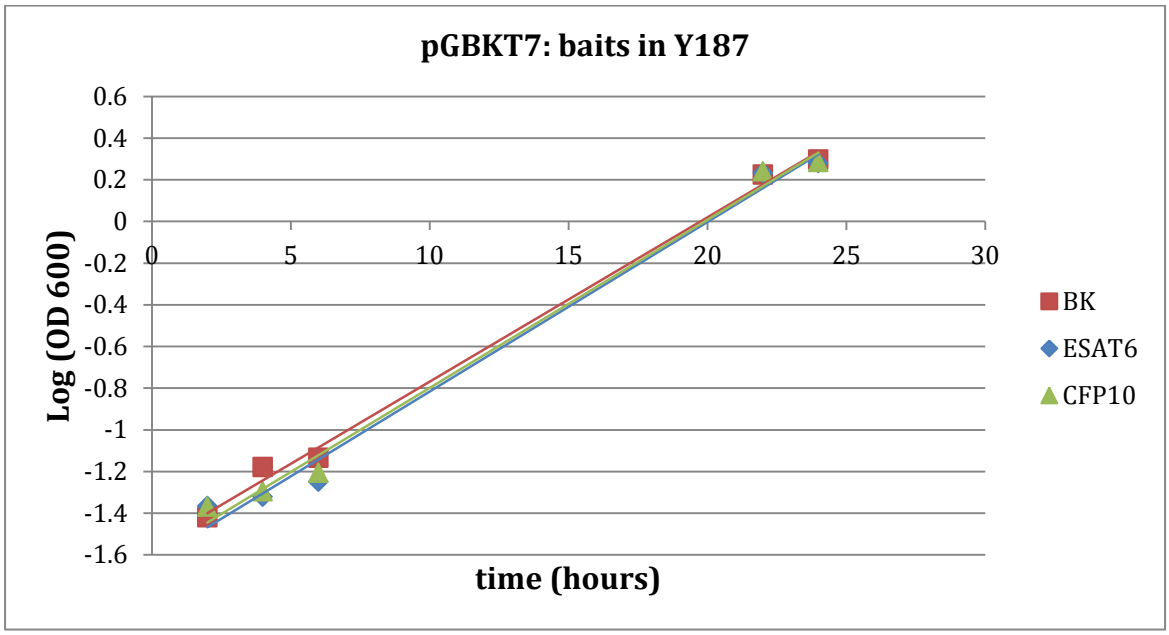

Figure 3.8: Growth rate of pGBKT7-ESAT-6 and pGBKT7-CFP-10. The log(OD_{600}) of the empty pGBKT7, pGBKT7-ESAT-6 and pGBKT7-CFP-10 constructs were plotted against time (hours). The observed growth rates were non-toxic.

3.1.3.2 *Testing pGBKT7 constructs for transcriptional activation*

In order to test whether pGBKT7-ESAT-6 and pGBKT7-CFP-10 were able to self-activate the *HIS*3 and *ADE*2 reporter genes, Y187-containing constructs were plated on SD/-Trp/-His and SD/-Trp/-Ade selection plates. pGBKT7-ESAT-6 and pGBKT7-CFP-10 demonstrated no growth on SD/-Trp/-Ade plates and did not autonomously activate the expression of *ADE2* reporter gene. However, growth was observed on SD/-Trp/-His for both ESAT-6 and CFP-10. The background expression of the *HIS3* reporter gene was suppressed by adding 3-aminotrizole (3-AT) to selection plates (Table 3.1). Colonies were plated on 10 mM 3-AT SD/-Trp/-His selection plates and demonstrated no growth. Therefore, the yeast two-hybrid screens were conducted using 10 mM 3-AT on TDO plates to select for putative interactions.

Table 3.1: Testing pGBKT7-ESAT-6 and pGBKT7-CFP-10 constructs for transcriptional activation of reporter genes. pGBKT7-ESAT-6 and pGBKT7-CFP-10 constructs were plated on SD/-Trp/-His and SD/-Trp/-Ade plates to test for transcriptional activation of reporter genes (i.e. –His and –Trp). pGBKT7-ESAT-6 and pGBKT7-CFP-10 constructs were active on SD/-Trp/-His, indicating the presence of transcriptional activation by ESAT-6 and CFP-10 fusion constructs. When these constructs were plated on 10mM 3-AT SD/-Trp/-His plates, no growth was observed.

		Selection		
	pGBKT7	**Trp/His**	**Trp/Ade**	**10mM 3-AT Trp/His**
Y187	**ESAT-6**	+	-	-
	CFP-10	+	-	-

3.1.4 Yeast-two-hybrid screen

3.1.4.1 ESAT-6

A yeast-two-hybrid screen was performed to identify potential targets that interact with ESAT-6. The GAL4AD lung cDNA plasmids in AH109 were mated overnight at 30°C with the GAL4BD ESAT-6 bait fusion protein expressed in Y187. The overnight mating culture was plated on 10mM 3-AT TDO selection plates and SD/Leu$^-$, SD/Trp$^-$ and SD/Leu$^-$/Trp$^-$ plates. The number of transformants screened was determined by counting the number of viable diploids on the SD/Leu$^-$/Trp$^-$ plates. In total, 1.8×10^5 transformants were screened (i.e. number of screened clones = cfu/ml of diploids (SD/Leu$^-$/Trp$^-$) x re-suspension volume (mL)). To identify the positive colonies containing an integrated library cDNA insert, a yeast colony PCR was performed by

using the primers listed in Table 2.2 (Figure 3.9). The positive bait-prey plasmids were extracted from yeast using the method described in section 2.9.2. The isolated plasmids were transformed into *E. coli* and plated on LB/ampicillin and LB/kanamycin, to separate the bait/prey plasmids. Each plasmid (i.e. pGADT7 and pGBKT7) was extracted from *E. coli* and re-transformed into yeast. The transformed yeast was used to perform heterologous bait-prey matings to re-test the putative phenotype (Figure 3.10). Sequence results of the 79 putative clones containing an integrated library cDNA insert were analysed using both BLASTN and BLASTP programs (http://www.ncbi.nlm.nih.gov/Entrez). Analyses revealed that only two inserts were in frame preceding the DNA-AD of the pGADT7 vector. These inserts matched the C-terminal side of filamin A (*FLNA*, corresponding to repeats 23-24) and the C-terminal side of complement component 1, q subcomponent, A chain (*C1QA*), respectively.

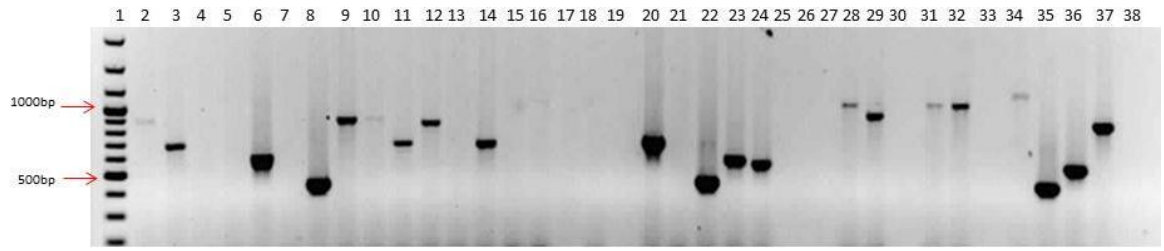

Figure 3.9: 1.5% TAE agarose gel of PCR products of candidate clones identified during the ESAT-6 screen. Yeast colony PCR amplification of candidate clones (lanes 2-37) identified during the ESAT-6 screen. Lane 1 contains a 100bp DNA ladder (Fermentas, Burlington, Canada) and lane 38 represents the negative control.

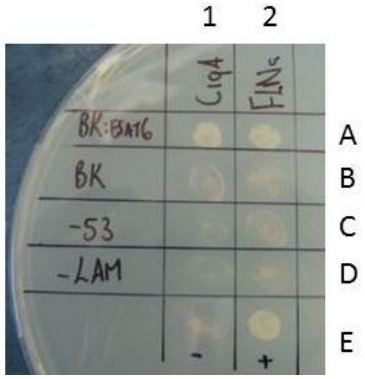

Figure 3.10: Heterologous mating to re-test the interaction of ESAT-6 and FLNA and C1QA. Small scale mating was performed between pGBKT7-ESAT-6 & C1QA (1A) and pGBKT7-ESAT-6 & FLNA (2A). Both C1QA and FLNA were mated with the empty pGBKT7 vector (1B and 2B). pGBKT7-53 (1C and 2C) and pGBKT7-LAM (1D and 2D) were mated with both C1QA and FLNA, separately to test specificity of the identified interactions. The negative control (1E) served as a mating between pGADT7-SV40 and pGBKT7-LAM and the positive control (2E) served as a mating between pGADT7-SV40 and pGBKT7-53.

3.1.4.2 CFP-10

Following large scale preparation of pGBKT7-CFP-10, an additional yeast two-hybrid screen was performed with the constructed lung library. Similar to the ESAT-6 screen, the GAL4AD lung cDNA plasmids were mated overnight at 30°C with the GAL4BD CFP-10 bait fusion protein. The overnight mating mixtures were plated on selection plates and the number of transformants was determined by counting the number of viable diploids. In total, 2.27×10^6 transformants were screened. To identify the positive colonies, a yeast colony PCR was performed using the primers listed in Table 2.2. The amplified insert displayed the same bp size repeatedly (Figure 3.11). The yeast colonies containing an integrated library cDNA insert was extracted using the yeast plasmid extraction method described in section 2.9.2 and was transformed into *E. coli* with appropriate antibiotics to separate the two interacting plasmids. The bait and prey plasmids were re-transformed into the appropriate yeast strains to re-test the putative interaction. Additionally, CFP-10 was sub-cloned into a low expression vector (pGBT9) and the interactions were re-tested by plating the heterologous small scale matings on 10mM 3-AT QDO (Figure 3.12) selection plates. The results demonstrated in Figure 3.12 depict the identification of a putative interaction, demonstrating minimal growth when C1QA was mated with the empty pGBKT7 vector. Sequence results of the 19 putative clones revealed that the library clones corresponded to the same insert, matching the C-terminal side of C1qA, also identified during the first initial yeast two-hybrid screen with ESAT-6.

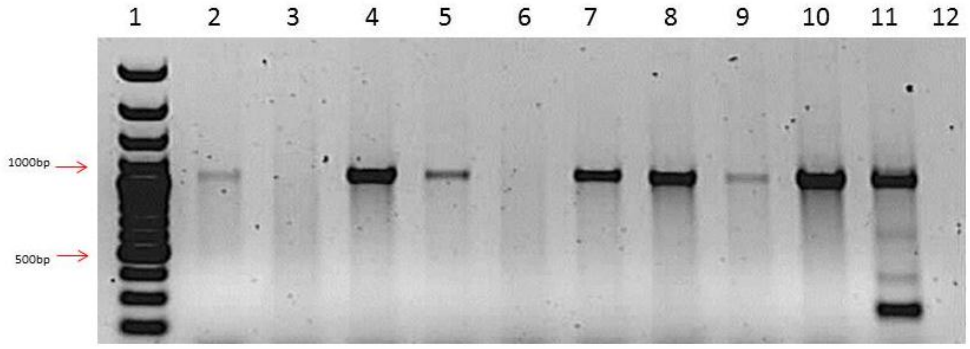

Figure 3.11: 1.5% TAE agarose gel of PCR products of candidate clones identified during the CFP-10 screen
Yeast colony PCR of candidate clones (lanes 2-11) identified during the CFP-10 screen. Lane 1 contains a 100bp DNA ladder (Fermentas, Burlington, Canada) and lane 12 represents the negative control.

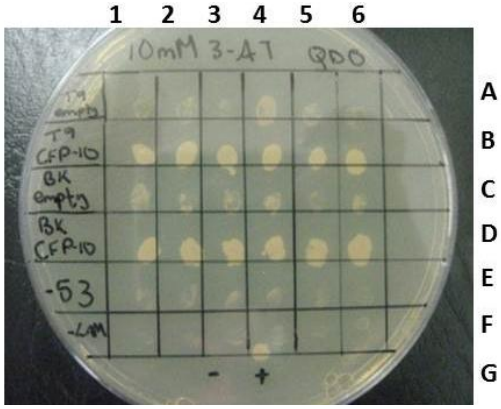

Figure 3.12: Heterologous mating to re-test the interaction of CFP-10 and C1QA of six randomly selected clones. Small scale mating was performed between pGBT9-CFP-10 & C1QA (1-6B) and pGBKT7-CFP-10 & C1QA (1-6D). The empty pGBT9 (1-6A) and pGBKT7 (1-6C) were mated with C1QA to evaluate non-specific binding to the bait vector. pGBKT7-53 (1-6E) and pGBKT7-LAM (1-6F) were mated with C1QA to test specificity of the identified interactions. The negative control (3G) served as a mating between pGADT7-SV40 and pGBKT7-LAM and the positive control (4G) served as a mating between pGADT7-SV40 and pGBKT7-53.

The putative interactions of ESAT-6 and CFP-10 were confirmed using heterologous mating and were further validated using *in vivo* techniques (Chapter 4).

3.2 Discussion

Understanding protein complexes in protein-protein interaction (PPI) studies are important research topics in cell biology and biochemistry. Protein complexes are composed of many subunits which perform the majority of biological processes inside host cells. The identification of these complexes is useful in deciphering the molecular mechanisms that translate into many cellular functions related to cell structure, signaling and metabolism. These interactions are generally recognised as the building blocks of cellular environments or complex cell networks. The immune system is also a complex network of cells functioning together to coordinate immune regulation. During the course of infection, these networks are interfered with by *M. tuberculosis* to facilitate effective dissemination of the tubercle bacilli.

The ESX-1 secretion system of *M. tuberculosis* is responsible for the secretion of ESAT-6 and CFP-10, and is thought to be involved in membrane lysis of host cells. Secretory proteins of *M. tuberculosis* are likely to play important roles in host-pathogen interactions, by taking advantage of its position within the cellular milieu to facilitate interactions with host cells. Despite the vast

amount of research performed on these secretory proteins, little is known about the host targets that they interact with. Therefore, the current study was designed to gain insights into the host targets that interact with ESAT-6 and CFP-10.

The yeast two-hybrid (Y2H) system is a simple, high-throughput and cost-effective approach to generate PPI data, making it the most popular screening tool for interactome studies (Vidalain et al., 2004). This method can help assign biological functions to proteins, without previous knowledge of potential binding partners, and was thus chosen as the preferred technique for the current study.

Upon inhalation into the lung, *M. tuberculosis* comes into contact with airway macrophages and a number of other cell types. The establishment of infection therefore depends on the initial interactions with host cells. In choosing the right strategy that is representative of the biological material of interest, a cDNA yeast two-hybrid library from lung mRNA was constructed to enable the identification of PPIs that occur within the lung alveoli.

A key feature of the library construction was the use of BD SMART^{TM} cDNA synthesis, which requires only small amounts of mRNA. This method allows for amplification of 5´ ends of genes, which tends to be under-represented during conventional cDNA library construction. The integration of Long-Distance (LD) PCR greatly improved the reliability of the PCR reaction and the length of PCR products (Barnes, 1994). As seen in Figure 3.2, most of the cDNA inserts ranged between 0.4 – ~2 kb. The library consisted of over 1×10^9 independent clones, which was sufficient to perform a yeast two-hybrid screen. Based on Clareke-Carbon's formula, a cDNA library should contain at least 1.7×10^5 independent clones for good coverage (Sambrook, 2001). Therefore, the constructed library should represent most transcribed genes, assuming that the human genome has about 20 000 to 25 000 protein-coding genes (Pertea and Salzberg, 2010).

In judging the quality of a library screen, the number of transformants screened (calculated from SD/Leu-/Trp- plates) should exceed number of independent clones within the library. This estimate is a measure of the completeness of the library screen (Conn, 2010). Approximately, 1.5×10^5 and 2.27×10^6 clones were screened for ESAT-6 and CFP-10,

respectively. The number of transformants screened was lower than the number of independent library clones. Therefore, it may be possible that a number of putative interactions could have been missed in both screens with ESAT-6 and CFP-10. The following situations may have occurred, resulting in the identification of fewer putative interactions: (1) the hybrid protein may not have been stably expressed in the yeast cell, (2) the GAL4 activation and binding domains could have blocked the site of interaction, (3) the hybrid proteins may have folded improperly; or (4) they did not localise to the yeast nucleus. Although the Y2H system is frequently used as the preferred method to identify PPIs, it is not without limitations, which will be discussed later in this section.

In this study, ESAT-6 was first used as a bait to screen the constructed lung cDNA library, to identify putative host targets of ESAT-6. From the 79 positive colonies, two inserts were translated in-frame preceding the GAL4 AD, which were further subjected to *in vivo* analyses to test for biological significance. Although the 77 isolated library clones contained significant DNA matches, these inserts did not reveal significant protein matches. When a random fragment library is constructed only one-sixth of clones will generate true in-frame fusion constructs with the GAL4 AD and most screening libraries provide only one reading frame for the generation of fusion constructs. A solution to circumvent this problem could be the new Gateway technology (discussed further in the future considerations of this section). The two in-frame inserts were identified as filamin A and complement component 1, q subcomponent, A chain (C1QA)

Filamin A was originally identified as a non-muscle actin-binding and polymerising protein (Figure 3.13). Three discrete FLNs have been identified in humans, namely, filamin A (FLNA), filamin B (FLNB) and filamin C (FLNC). Filamin A is expressed in T cells and has the ability to bind actin. The dimerisation domain of filamin A associates with the plasma membrane and numerous intracellular signaling intermediates, including enzymes and scaffolding proteins. These findings indicate that filamin plays an important role as an adapter molecule that links a wide variety of intracellular proteins to the actin cytoskeleton and cell membrane receptors (Hayashi and Altman, 2006).

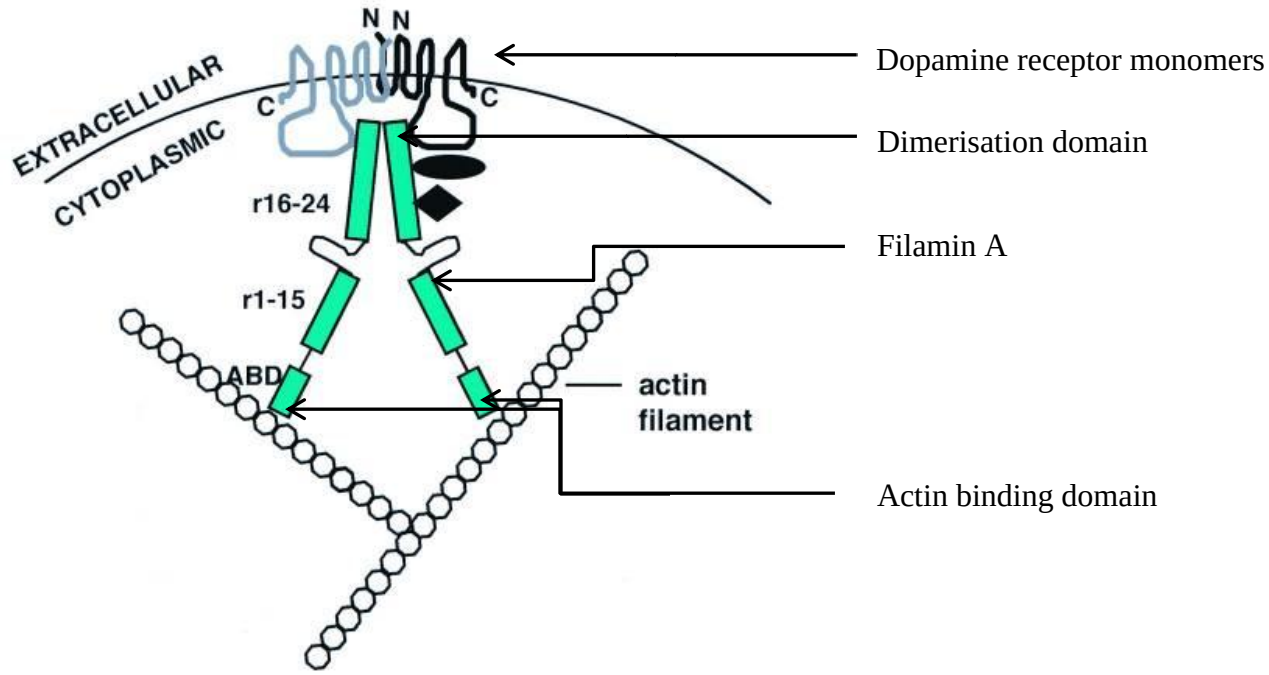

Figure 3.13: Representation of FLNA. Schematic representation of filamin A crosslinking actin filaments to the cytoplasmic region of host cell membranes (Lin et al., 2001).

The complement system is a central component of the innate immunity and functions to recognise foreign particles, to communicate and activate the adaptive immune response and to remove cellular debris. The complement system consists of a well-established complex of circulating and surface-bound proteins, which serves as substrates, enzymes or modulators of a sophisticated series of extracellular proteolytic cascades (Lambris et al., 2008). Complement is made up of three pathways: the classical, alternative and the lectin pathway, which involves the sequential activation of many proteins involved in the destruction of infecting microorganisms (Matsushita and Fujita, 2001). The initial event that triggers these pathways differs considerably between the three different systems. The classical pathway is initiated by C1Q recognition of antibody-antigen complexes and subsequent activation of the associated serine proteases C1r and C1s. The C1Q molecule is made up of three polypeptides chains, including C1QA, C1QB and C1QC (Figure 3.14).

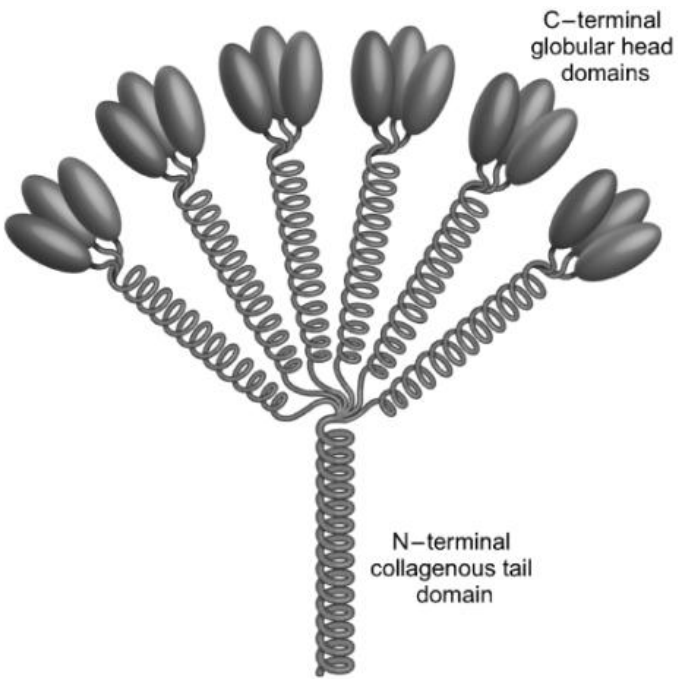

Figure 3.14: Structure of C1Q. The C1Q molecule is a glycoprotein consisting of 18 polypeptide chains (six C1QA chains, six C1QB chains and six C1QC chains). The chains associate as six heterodimers to form the functional C1q molecule. The C-terminal domain functions at the globular head and the N-terminal domain contains a collagen-like stalk region (Sontheimer et al., 2005).

An additional screen using CFP-10 as bait demonstrated that all 19 isolated clones activated the reporter genes and corresponded to the same insert, which was also C1QA, similar to what was observed with ESAT-6. In order to evaluate the interaction between CFP-10 and C1QA in yeast, 3-aminotrizole (3-AT) was added to selection plates, which is a competitive inhibitor of the *HIS3* gene product. The addition of 3-AT inhibits low background expression of *HIS3* reporter gene, which may lead to spurious results. CFP-10 was expressed in a GAL4 binding domain vectors – pGBKT7 (high expression) and pGBT9 (low expression) – to test for the interaction with C1QA using heterologous mating. High expression of bait proteins may allow yeast to overcome nutritional selection; therefore CFP-10 was evaluated in a low expression vector. The results presented in Figure 3.12 demonstrated a putative interaction between CFP-10 and C1QA. However, in all methods used to detect PPIs, false positives can occur. Many of these interactions are due to proteins having a tendency to generate non-specific binding. In Y2H studies, these are termed “sticky” proteins based on their frequent appearance among the isolation of prey proteins (Semple et al., 2002). If C1QA was indeed a sticky protein, growth should have been observed during the heterologous mating with pGBKT7-53 or pGBKT7-LAM (Figure 3.11). Given the

biological evidence that ESAT-6 and CFP-10 interact as a 1:1 heterodimer complex, the hypothesis that ESAT-6 and CFP-10 may share similar domains that interact with C1QA could not be excluded. Therefore, *in vivo* validation was performed to verify the putative interactions of C1QA with ESAT-6 or CFP-10. These results will be discussed in detail in Chapter 4.

The subcellular localisations of proteins are a crucial part in understanding their biological functions. When selecting the most plausible interactions, proteins should localise in compatible subcellular environments to support the possibility of direct interactions. Based on experimental evidence, ESAT-6 has been shown to be involved in pore formation of host cell membranes (Smith et al., 2008). Filamin A stabilises the actin filament network that links actin to the cellular membranes (Zhou et al., 2010). Therefore, the likelihood that ESAT-6 and Filamin A share the same subcellular location during *M. tuberculosis* infection could therefore not be excluded. With regards to C1QA, *M. tuberculosis* and *M. leprae* have been demonstrated to be activators of the complement system (Lahiri et al., 2008; Carroll et al., 2009). Evidence suggests that when *M. tuberculosis* is inhaled, the bacterium is opsonised by C3 via the activation of the classical pathway within the lung alveolus (Ferguson et al., 2004). For these reasons, a functional interaction and subcellular location exist between *M. tuberculosis* and the complement system, which provides evidence for further validation.

The desirable features of the Y2H approach (i.e. simple and cost effective) makes this system an excellent choice to identify PPIs; however it is not without limitations and strengths. The advantage of the Y2H is that it employs an *in vivo* method that detects interactions in live yeast cells, which has it disadvantages. As a eukaryote, yeast is a suitable host organism for investigating interactions of higher eukaryotes compared to most *in vitro* approaches or methods based on bacterial expression (Van Criekinge and Beyaert, 1999). When investigating host-pathogen interactions in a eukaryotic system, like the Y2H, it is not feasible to model interactions between bacterial and mammalian cells (Valdivia, 2004). However, multiple studies have demonstrated that it is possible to identify host-pathogen interactions using the Y2H approach (MacFarlane and Uhrig, 2008; Zhang et al., 2009; Dyer et al., 2010; de Barsy et al., 2011; Yang et al., 2011). Another appealing advantage of the Y2H system is the minimal requirements needed to initiate an interaction screen (Van Criekinge and Beyaert, 1999).

A limitation of the Y2H system is that the hybrid proteins are expressed artificially and may represent a possible risk in identifying false PPIs (Van Criekinge and Beyaert, 1999). Some interactions may be dependent on post-transcriptional modifications, which do not occur properly or not at all in yeast during artificial expression. These modifications include the formation of disulfide bridges, glycosylation and most commonly phosphorylation (Van Criekinge and Beyaert, 1999). However, alternative yeast two-hybrid methods co-expressing the modifying substrate that is responsible for post-transcriptional modification are available at the discretion of the researcher (Brückner et al., 2009). In addition, the incorporation of the GAL4 activation/binding domains during expression of hybrid proteins in yeast might influence their native conformation, possibly altering the activity and binding affinities of the hybrid proteins (Van Criekinge and Beyaert, 1999).

Another disadvantage of the Y2H system is the requirement of interacting bait and prey proteins to translocate to the nucleus, so that the reporter genes can be activated. The Y2H system requires that interactions be targeted to the nucleus and may be a disadvantage for extracellular or membrane proteins with a strong target signal to remain in their natural environment (Brückner et al., 2009). Therefore, the nucleus may not be the ideal cellular milieu to investigate particular proteins interactions. Other classes of proteins that are not suitable for Y2H analyses are transcriptional activators, as these proteins may activate the transcription of reporter genes without an interacting hybrid protein (Van Criekinge and Beyaert, 1999). In the present study, ESAT-6 and CFP-10 activated transcription of only the HIS3 reporter gene, and this was actively suppressed by the addition of 3-AT.

In addition, some bait proteins might become toxic upon expression in yeast, resulting in the loss of interactions being identified. Such proteins might proteolyse essential yeast proteins that are important for the maintenance of the Y2H system (Van Criekinge and Beyaert, 1999).

To address the described limitations of the present study a number of methods, including multiple reporters genes (i.e. *ADE2*, *HIS3* and *MEL1*), testing toxicity of bait constructs, performing heterologous mating, as well as the addition of 3-AT, were applied, to reduce the number of non-specific interactions during the Y2H screens.

Chapter 4

4 Verification studies of ESAT-6 and CFP-10 binding partners

4.1 Results

4.1.1 Recombinant mycobacterial proteins

Purified recombinant mycobacterial ESAT-6 and CFP-10 proteins were obtained from the infectious diseases research company BEI Resources (http://www.beiresources.org/) to ensure standardisation, repeatability and to minimise the effects of improper folding or formation of inactive protein. Recombinant proteins were received purified (done using standard non-denaturing chromatographic techniques followed by endotoxin removal procedures). Western blot analysis with mouse monoclonal antibody (mAb) to ESAT-6 (Santa Cruz Biotechnology, Santa Cruz, California, USA) and rabbit mAb to CFP-10 (Abcam, Cambridge, MA, USA) detected the protein bands at the expected molecular sizes, and as higher molecular weight bands representing dimers and multimers (Figure 4.1). This was expected, and confirms the correct structure of the prepared recombinant proteins, as these proteins are known to form aggregates in solution and form multimeric proteins (Wang et al., 2009).

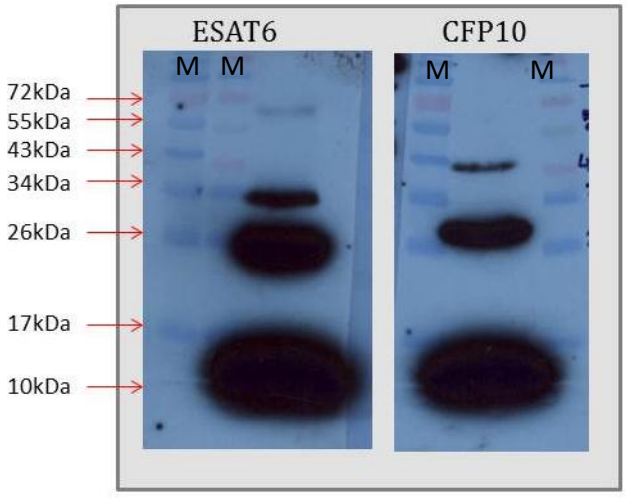

Figure 4.1: Western blot of ESAT-6 and CFP-10. The purified recombinant ESAT-6 (6 kDa) and CFP-10 (10 kDa) proteins were analysed by 12.5% SDS-PAGE and visualised through Western blot after electroblotting to a nitrocellulose membrane and blotted with ESAT-6 mouse mAb (1:500) and CFP-10 rabbit mAb (1:500). M: PageRuler™ Plus Prestained Protein Ladder (Fermentas, Burlington, Canada).

4.1.2 Transfection of recombinant proteins into cultured cells

To determine the efficiency of the protein delivery system, the cultured Jurkat cells were transfected with recombinant ESAT-6 using the Pro-Ject™ delivery system (Thermo Fisher Scientific, Rockford, IL), a lipid-based protein delivery system used to deliver recombinant proteins into the cytoplasm of cultured cells. After 12-24hrs of transfection, the cultured cells were thoroughly washed twice with 1X PBS to remove any undelivered recombinant proteins, and the cells were subsequently lysed using Tissue Protein Extraction Reagent (TPER, Thermo Fisher Scientific, Rockford, IL). Recombinant ESAT-6 was detected in the cell extracts of the Jurkat cells by Western blot (Figure 4.2), indicating that the recombinant proteins were successfully delivered into the cytoplasm of the cultured cells.

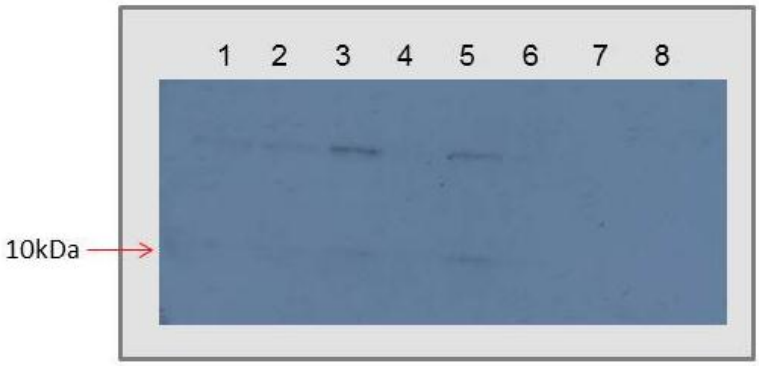

Figure 4.2: Western blot of Jurkat lysates transfected with recombinant ESAT-6. The efficiency of protein delivery using the Pro-Ject transfection reagent was analysed by 12.5% SDS-PAGE and visualised by Western blot after electroblotting to a nitrocellulose membrane and blotted with ESAT-6 mouse mAb (1:500). Lane 1 represent 100ng ESAT-6 (positive control for detection). Lanes 2-6 represents delivery of ESAT-6 into Jurkat cells. Lanes 7 and 8 represents un-transfected Jurkat cells (negative control), demonstrating no non-specific binding of ESAT-6 mAb to endogenous proteins.

The cultured THP-1 cells were differentiated into macrophage-like cells by stimulation with 100nM phorbol myristate acetate (PMA). For the delivery of recombinant proteins into cultured differentiated THP-1 cells, recombinant proteins was added exogenously and delivered into THP-1 cells taking advantage of the macrophage-like phenotype of engulfing exogenous components via phagocytosis. In addition, recombinant proteins were also transfected into THP-1 cells using the Pro-Ject transfecting reagent, to ensure that recombinant proteins are freely accesible in the cytosol to interact with host proteins for co-immunoprecipitation experiments. Cells were

subsequently lysed with Tissue Protein Extraction Reagent (TPER, Thermo Fisher Scientific, Rockford, IL) and membrane protein extraction kit (Mem-PER, Thermo Fisher Scientific, Rockford, IL). The extracted proteins were subjected to Western blot analysis, to evaluate the relative proportion of recombinant ESAT-6 and CFP-10 in tissue cell and membrane fractions. Figure 4.3A and B illustrates the detection of ESAT-6 and CFP-10 in whole cell extracts, demonstrating delivery of recombinants proteins into THP-1 cells. ESAT-6, but not CFP-10, was also detected in the membrane fractions of THP-1 cells, which was significant as it has been reported that purified ESAT-6 (but not CFP-10) associates with and disrupts membranes (Hsu et al., 2003; de Jonge et al., 2007; Derrick and Morris, 2007).

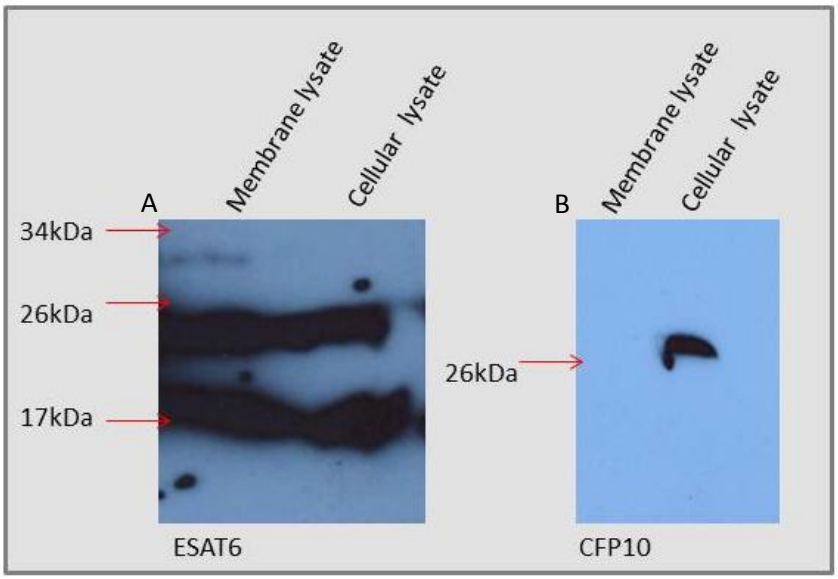

Figure 4.3: Western blot of differentiated THP-1 lysates treated with recombinant ESAT-6 and CFP-10. THP-1 cells at 1×10^6 cells/mL were differentiated with 100 nM PMA for 48 hours at 37°C, 5% CO_2. The uptake of recombinant proteins by PMA-differentiated THP-1 cells were analysed by 12.5% SDS-PAGE and visualised by Western blot after electroblotting to a nitrocellulose membrane and blotted with ESAT-6 mouse mAb (1:500) and CFP-10 rabbit mAb (1:500). ESAT-6 was detected in the total cell lysates and membrane extracts of the THP-1 cells, while CFP-10 was only detected in the cell lysates.

Further experiments showed that ESAT-6 exhibited a lytic phenotype (lysing both THP-1 and Jurkat cells); while the inverse was true for CFP-10, which demontrated no cytotoxic effect. Using fluorescence microscopy and a fluorescently labelled antibody specific for ESAT-6, it was shown that the lysed THP-1 cells associated with ESAT-6 (Figure 4.4). This lytic feature was further investigated and the results are described in Section 4.1.9. For subsequent co-

immunoprecipitation experiments, THP-1 and Jurkat cells were treated or transfected with 2.5 µg of ESAT-6 and incubated between 10-12 hrs, in order to minimise the cytolytic effects of ESAT-6.

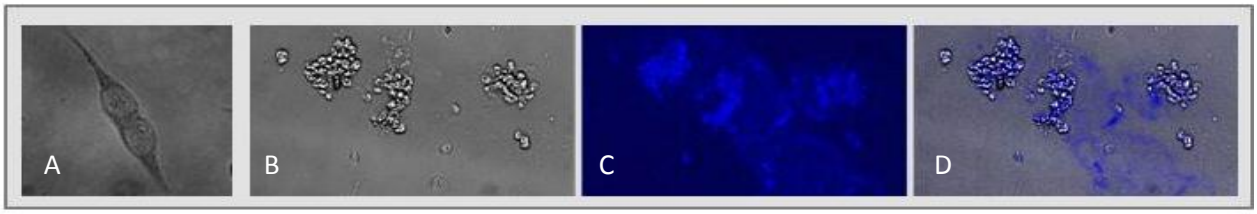

Figure 4.4: Cytolysis of differentiated THP-1 by recombinant ESAT-6. THP-1 cells at 1×10^6 cells/mL were differentiated with 100 nM PMA for 48 hours at 37°C, 5% CO_2. The PMA-differentiated THP-1 cells were left untreated or treated with 5 µg of ESAT-6. The culture cells were washed with 1X PBS, fixed and permeabilised. The fixed cells were stained with DyLight 350 to fluorescently labelled monoclonal antibody against ESAT-6 (mouse). (A) Differential interference contrast (DIC) image of un-treated and (B) treated THP-1 cells with 5 µg of ESAT-6, (C) fluorescent detection of ESAT-6 (labelled with Dylight 350 NHS Ester) and (D) overlay of DIC and fluorescent images, demonstrating a high fluorescent signal of ESAT-6 associated with lysed cells. The images were acquired at 20 µm.

4.1.3 Detection of endogenous proteins

For the detection of bait-prey interactions, cell lysates demonstrating the highest expression of endogenous prey proteins (i.e C1QA and filamin A) were used for subsequent co-localisation and co-immunoprecipitation experiments (see Section 4.1.4 and 4.1.5). THP-1 cells differentiated with PMA has been shown to have reduced production of C1Q (Walker, 1998). Therefore, the cells were stimulated with interferon-γ to induce production of C1Q in the THP-1 cells (Figure 4.5A). C1Q was detected in THP-1 lysates as complexes comprising the A-B and C-C dimers (Tenner and Volkin, 1986). Antibodies against C1QA (recognising the C-terminal side and the internal portion of the protein, respectively) were shown to be able to precipitate the protein form of C1QA using recombinant C1QA-GST tagged protein (Abcam, Cambridge, MA, USA)(Figure 4.5B). However, C1QA was not detected in Jurkat lysates (Figure 4.5B). Recombinant C1QA-GST tagged protein (Abcam, Cambridge, MA, USA) and serum associated C1QA were thus used to verify the interactions with ESAT-6 and CFP-10.

Endogenous filamin A was detected in Jurkat cell lysates using Western blot analysis (Figure 4.5C). In some experiments, filamin A was detected as a doublet (280 and 250 kDa) (data not shown). This is not uncommon, as the 250 kDa band has been identified previously as the proteolysed form of filamin A (Jiménez-Baranda et al., 2007).

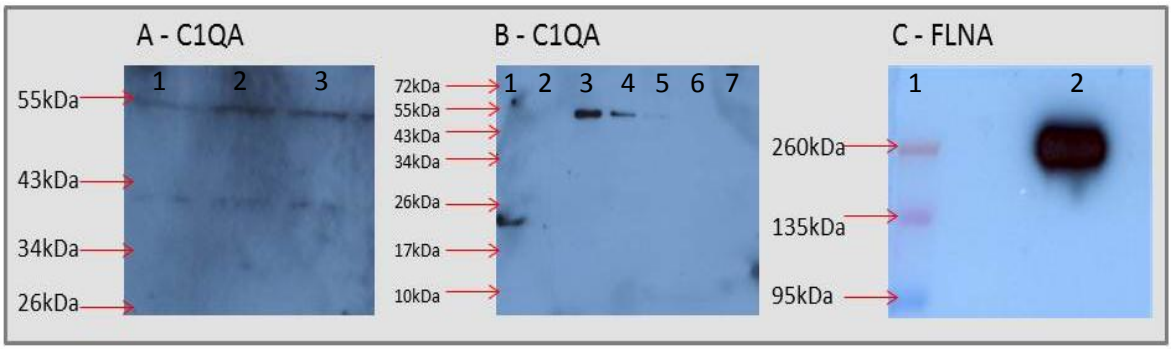

Figure 4.5: Western blot detection of prey proteins. (A) THP-1 cells at 1×10^6 cells/mL were differentiated with 100 nM PMA for 48 hours at 37°C, 5% CO_2. Following differentiation, THP-1 cells were stimulated with 25µg/mL interferon-γ for 12 hours to induce expression of C1QA. THP-1 lysates (lanes 1-3, 50 ng per well) were resolved on a 12.5% SDS-PAGE and visualised by Western blot with C1QA polyclonal goat antibody. (1:500). C1Q in THP-1 lysates were detected as A-B (55 kDa) and C-C (43 kDA) dimers. (B) Additional source of C1QA (12.5% SDS-PAGE): lane 1 represents human serum (1:2000 dilition in PBS) demonstrating the detection of C1QA at 23 kDa, lane 2 represents Jurkat lysates demonstrating no detection of C1QA, lane 3 represents recombinant C1QA-GST tagged protein, lane 4 represents immunoprecipitation of C1QA-GST using a C1QA polyclonal antibody recognising the C-terminal side and lane 5 represents immunoprecipitation of C1QA-GST using a C1QA polyclonal antibody recognising the internal portion. Lanes 4 and 5 demonstrate that antibodies against C1QA are able to precipitate the protein form of C1QA. Lanes 6-7 represent immunoprecipitation of Jurkat lysates using the two C1QA polyclonal antibodies (recognising the C-terminal side and the internal portion of C1QA, respectively). (C) Lane 1 represents the PageRuler™ Plus Prestained Protein Ladder (Fermentas, Burlington, Canada). Lane 2 represents Jurkat lysates resolved on a 6% SDS-PAGE and visualised by Western blot with filamin A mouse mAb (1:1000), demonstrating high levels of filamin A expression.

4.1.4 *In vivo* co-localisation of C1QA with ESAT-6 and CFP-10

In order to confirm the yeast two-hybrid results, it was necessary that the interactions between C1QA/ESAT-6 and C1QA/CFP-10 could be co-localised to the same sub-cellular environment. Since PMA reduced the expression of C1QA, interferon-γ treated THP-1 cells were used to test co-localisation of the putative bait and prey interactions. *In vivo* immunofluorescence was used to test this, however, sub-cellular localisation of C1QA in the THP-1 cells could not be detected

(Figure 4.6). Therefore, co-localisation of ESAT-6 and CFP-10 with endogenous C1QA could not be investigated. In the light of these findings, immunoprecipitation experiments were performed to verify whether the interaction could be physically demonstrated in THP-1 lysates (Section 4.1.5).

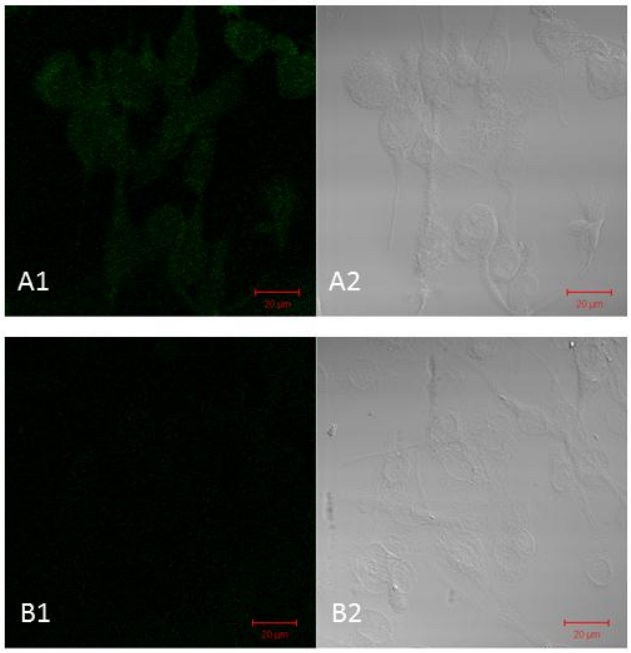

Figure 4.6: *In vivo* localisation of endogenous C1QA. THP-1 cells were grown in RPMI 1640 medium supplemented with 10% fetal bovine serum and 1% penicillin/streptomycin. THP-1 cells were differentiated for 48 hrs with 100nM PMA. The differentiated THP-1 cells were washed and treated overnight with interferon-γ. Non-specific background of slides were first analysed by acquiring fluorescent signals of prepared slides that received only donkey anti-goat FITC antibodies. A1 represents the non-specific background fluorescence and A2 the DIC image of A1. Once the baseline settings were determined, all images were aquired using these settings. Immunofluorescence staining, using a goat polyclonal antibody specific for endogenous C1QA, followed by staining with secondary donkey anti-goat labelled with FITC, demonstrated no detection of C1QA in THP-1 cells (B1 and B2). The scale bar represents 20 µm.

4.1.5 Co-immunoprecipitation of C1QA with ESAT-6 and CFP-10

Differentiated THP-1 cells were transfected with ESAT-6 and CFP-10, respectively. Co-immunoprecipitaion (Co-IP) experiments were performed using tissue cell lysate and membrane fractions, since literature suggest that a membrane form of C1Q exist (Martin et al., 1987). In order to determine whether the interactions could be demonstrated, immunoprecipitation with polyclonal C1QA antibodies were performed, followed by Western blotting with monoclonal

antibodies against CFP-10 (Figure 4.7A) and ESAT-6 (Figure 4.7B), respectively. Similar experiments were performed using reciprocal conditions, i.e. immunoprecipitation with CFP-10 (Figure 4.7C) and ESAT-6 (Figure 4.7D), respectively, followed by Western blotting with polyclonal C1QA antibodies. The interactions between C1QA and ESAT-6/CFP-10 could not be demonstrated *in vivo* with endogenous C1QA.

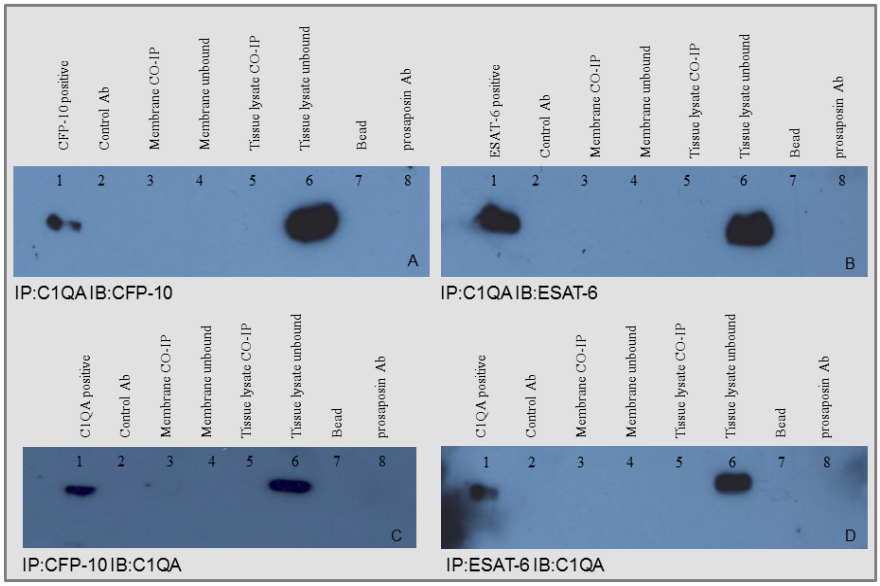

Figure 4.7: *In vivo* co-immunoprecipitation of C1QA with CFP-10 and ESAT-6. THP-1 cells were transfected with ESAT-6 and CFP-10, separately. Membrane and tissue cell lysate were prepared using the Membrane Protein Extraction kit (Thermo Fisher Scientific, Rockford, IL) and Tissue Protein Extraction Reagent (Thermo Fisher Scientific, Rockford, IL). The presence of ESAT-6, CFP-10 and C1QA were detected by Western blot with anti-ESAT-6 (lane B1), anti-CFP-10 (lane A1) and anti-C1QA (lanes C1 and D1), respectively. The membrane and tissue cell lysates were immunoprecipitated with anti-C1QA (lanes A3, A5, B3 and B5) conjugated to protein G and analysed for precipitation by Western blot using anti-CFP-10 (Image A) and anti-ESAT-6 (Image B). Similarly, the membrane and tissue cell lysates were immunoprecipitated with CFP-10 (lanes C3 and C5) and anti-ESAT-6 (lanes D3 and D5) conjugated to protein G and analysed for precipitation by Western blot using anti-C1QA (Images C and D). Unconjugated protein G and anti-prosaposin conjugated to protein G served as negative controls (lanes A7, A8, B7, B8, C7, C8, D7 and D8). Lanes A2, B2, C2 and D2 served as controls to test the crosslinking reaction that prevented co-elution of antibodies with precipitated proteins.

Using other approaches, several attempts were made using human serum and recombiant C1QA-GST tagged protein to precipitate the putative interations (each immunoprecipitaiton experiment with either total cell lysate, serum or GST-tagged C1QA protein were performed in triplicate). The human serum was pre-cleared twice overnight at 4°C with Dynabeads protein G to remove

excessive immunglobulins causing non-specific binding. The Western blot with human serum demonstrated no precipitated interaction using the different antibodies raised against the internal and C-terminal region of C1QA. Also, no band was detected when Co-IP experiments were performed with C1QA-GST tagged protein. Despite several attempts, the interactions identified with C1QA and ESAT-6/CFP-10 could not be confirmed in the subsequent Co-IP assays. These yeast two-hybrid defined interactions may thus be an example of a false positive result.

4.1.6 *In vivo* co-localisation of filamin A and ESAT-6

Filamin A crosslinks actin and stabilises the plasma membrane and the cell cortex. As previously demonstrated, ESAT-6 associated with the membrane fractions (Figure 4.3A), supporting the possibility that ESAT-6 and filamin A co-localise in the same cellular environment. Prior to determining co-localisation between ESAT-6 and filamin A, baseline fluorescent settings were first determined (Figure 4.8). These settings were used to acquire all images to avoid obtaining false-positive results.

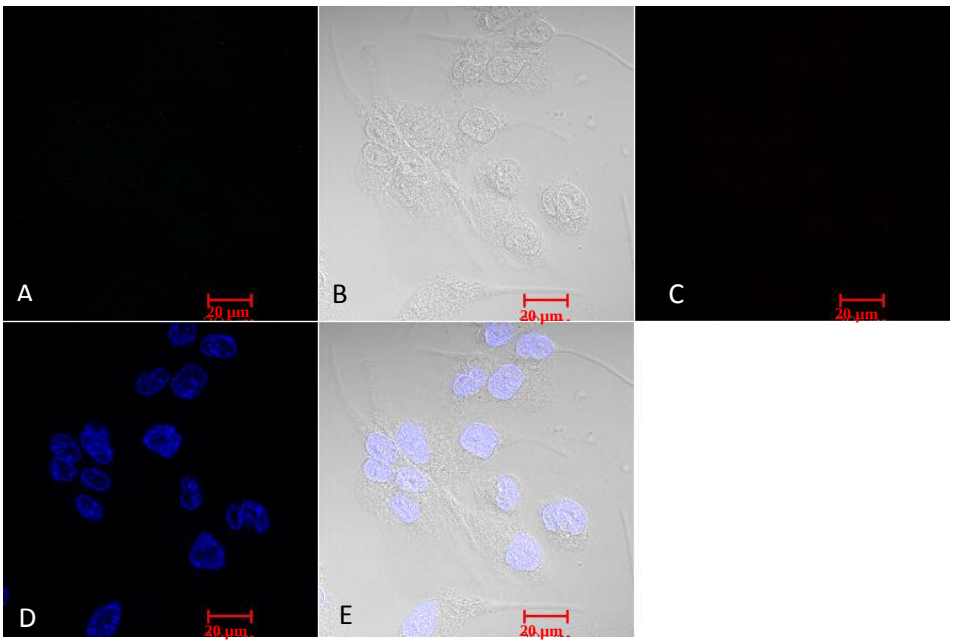

Figure 4.8: Non-specific background correction for ESAT-6 and filamin A co-localisation. Non-specific background of slides were first analysed by acquiring fluorescent signals of prepared slides that received only secondary antibodies (i.e. goat anti-mouse Alexa 488 and donkey anti-rabbit Cy3). A represents non-specific background fluorescence of goat anti-mouse Alexa 488, B represents the DIC image, C represents non-specific background fluorescence of donkey anti-rabbit Cy3, D represents DAPI staining for the cell nuclei and F represents the overlay of images A – D. The scale bar represents 20 µm.

Co-localisation images were recorded using a Zeiss LSM510-Meta laser scanning confocal microscope. The immunofluorescent staining for filamin A and ESAT-6 in THP-1 cells were granular and cytoplasmic (Figure 4.9).

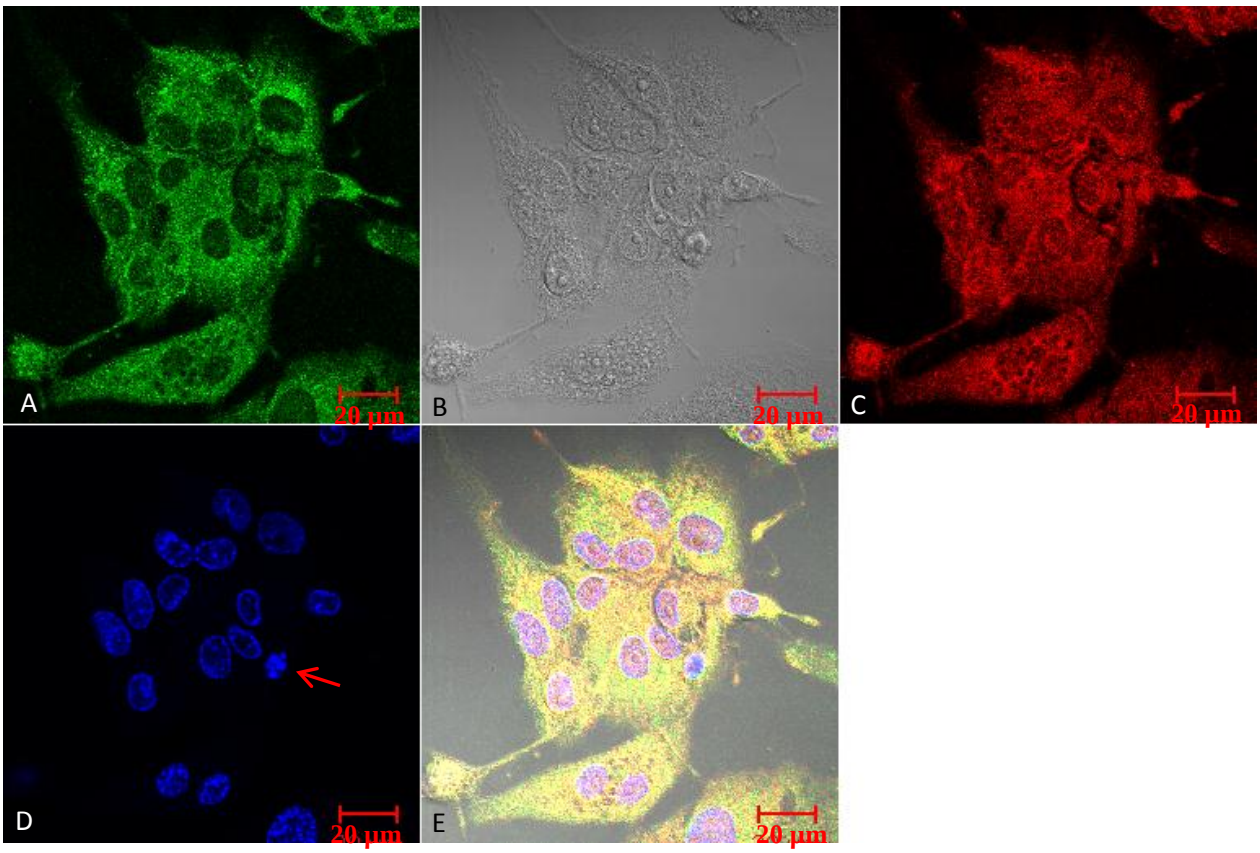

Figure 4.9: *In vivo* co-localisation of ESAT-6 and filamin A. THP-1 cells were grown in RPMI medium supplemented with 10% fetal bovine serum and 1% penicillin/streptomycin and differentiated for 48 hrs with 100nM PMA. The cells were teated with 2.5 µg/ml of ESAT-6 for 12hrs. The culture cells were washed with 1X PBS, fixed and permeabilised. The fixed cells were double stained with monoclonal antibodies against ESAT-6 (mouse) and filamin A (rabbit) and were detected with secondary fluorescent antibodies (i.e. goat anti-mouse Alexa 488 and donkey anti-rabbit Cy3). The prepared slides were counter stained with DAPI for cell nuclei and visualised using a Zeiss LSM 510 laser scanning confocal microscope. (A) represents the fluorescent signal for ESAT-6, (B) represents the DIC image, (C) represents the fluorescent signal for filamin A, (D) represents DAPI staining for the cell nuclei and (E) represents the overlay of images A – D. The scale bar represents 20 µm. The information in image D (red arrow) will be discussed in section 4.1.9).

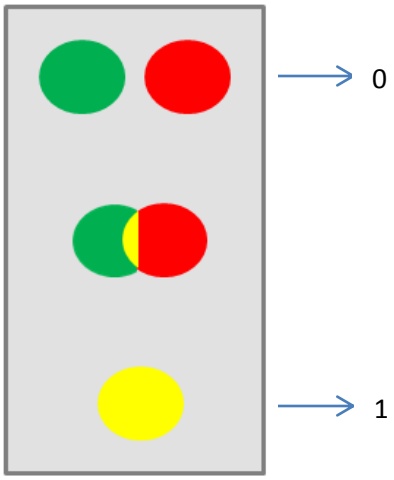

Figure 4.10: Example of co-localising pixels. The distribution of ESAT-6 (green) and filamin A (red) can be separate or close together, overlapping partially and overlapping completely (yellow) within the focal plane of the acquired image. The value of the co-localisation coefficient ranged between 0 - 1, where 0 represents no co-localisation and 1 represents pixels that co-localise. The co-localisation coefficient was analysed using acquired image of Figure 4.9E. The results is demonstrated in Figure 4.11.

Co-localisation analyses were performed using the Zeiss LSM 510 Meta software. The value of the co-localisation coefficient ranged between 0 - 1, where 0 represents no co-localisation and 1 represents pixels that co-localise (Figure 4.10). The number of co-localising pixels observed in channel 1 or 2, respectively, were compared to the total number of pixels above threshold and pixels with zero intensity were considered as background. In this experiment, the intensity of the threshold was set at a 100 and are indicated with the red arrows in Figure 4.11A. The pixels that co-localised are demonstrated in Figure 4.11B. The co-localisation coefficients for the green and red channels were 0.674 and 0.472, respectively, indicating that 67.4% of ESAT-6 co-localises with filamin A, whereas 47.2% of filamin A co-localised with ESAT-6 (Figure 4.11C). In other words, more than two-thirds of the total amount of ESAT-6 were specifically localised with filamin A. The staining of ESAT-6 and filamin A was specific and did not cross react or did not produce a signal bleed-through rendering separation of the fluorescent probes (Figure 4.12).

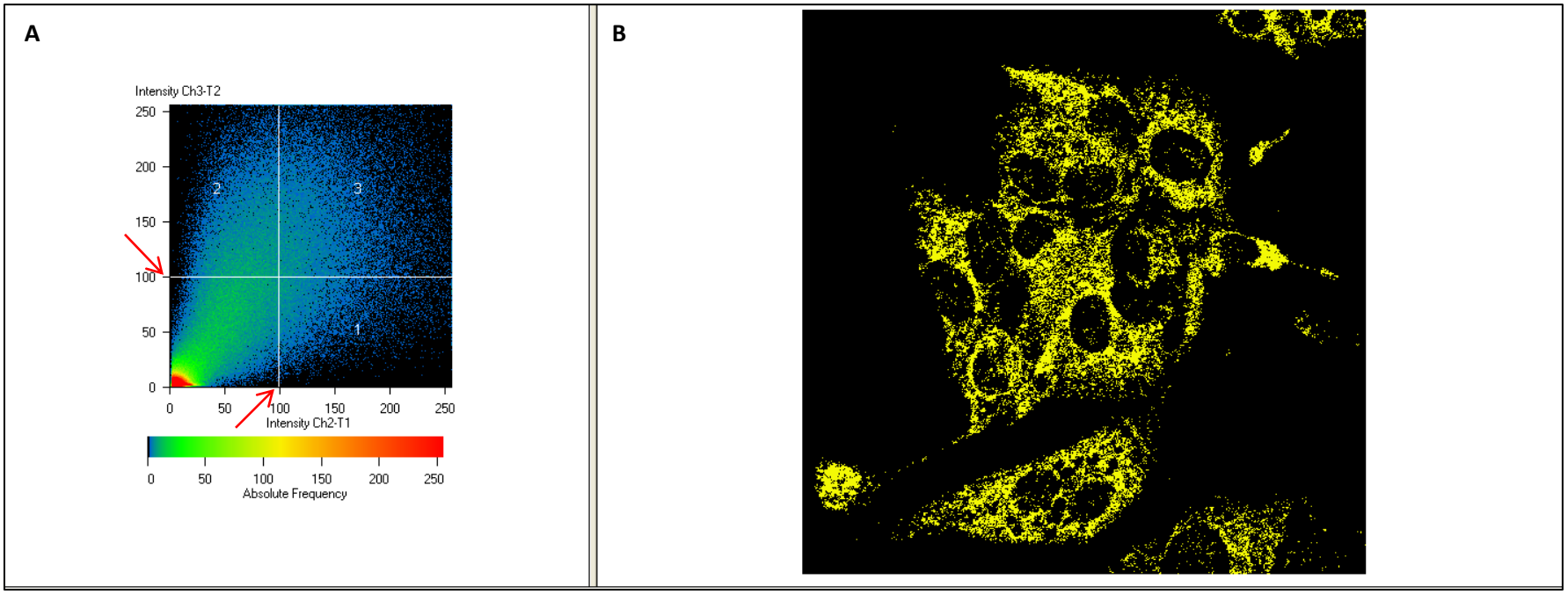

C

Colocalization Coefficient Ch2-T1	Colocalization Coefficient Ch3-T2
0.674	0.472

Figure 4.11: Measurement of co-localisation coefficient of ESAT-6 and filamin A. Ziess LSM 510 meta software was used to measure the co-localisation coefficients. Scatter region 1 represents the pixels for ESAT-6, scatter region 2 represents the pixels for filamin A and scatter region 3 represents the relative number of co-localising pixels containing a signal for both ESAT-6 and filamin A. The co-localisation coefficient range is 0 – 1, where 0 represents no co-localisation and 1 represents co-localisation. These results are based of Figure 4.9. Ch2 – channel for ESAT-6, Ch3 – channel for filamin A, T1 – scatter region for ESAT-6 pixels, T2 – scatter region for filamin A pixels and T3 – scatter region for co-localising pixels for ESAT-6 and filamin A.

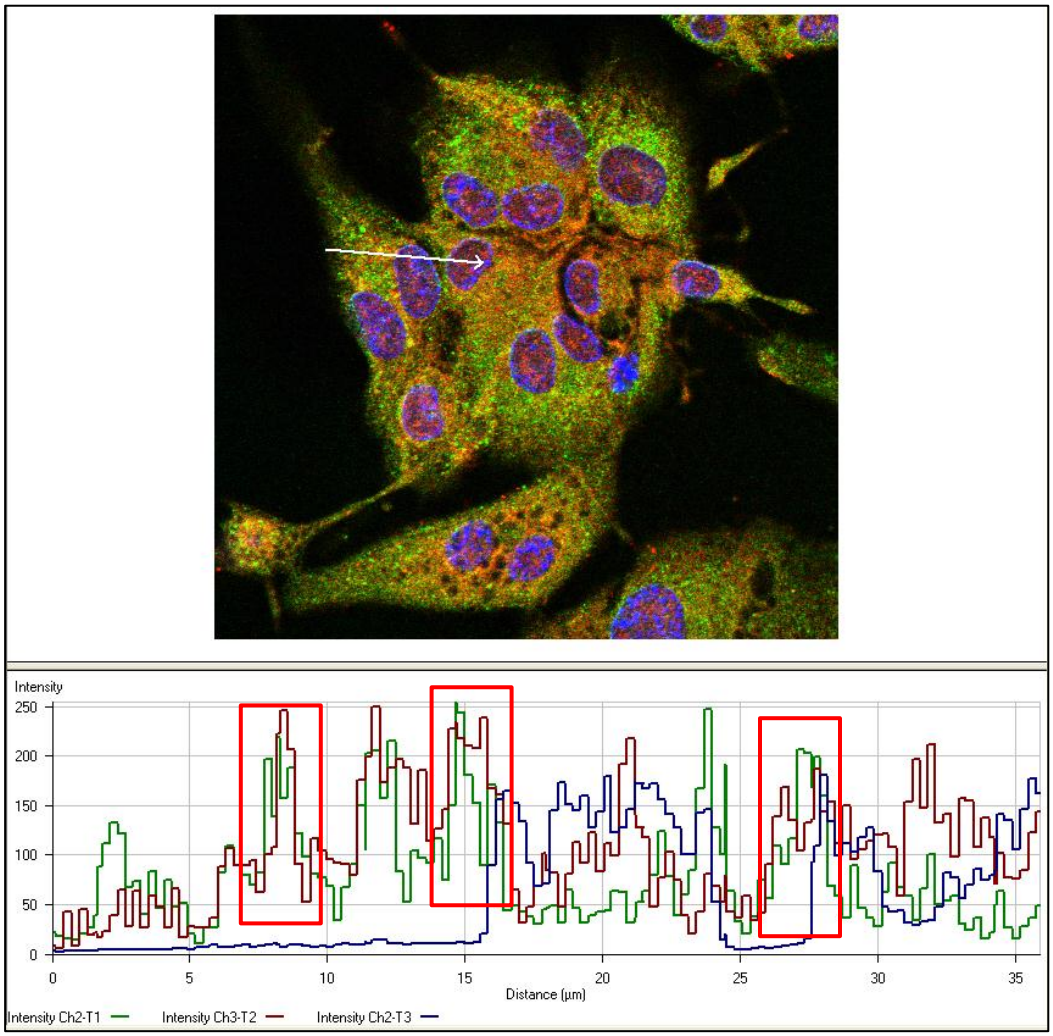

Figure 4.12: Spectral profile of ESAT-6, filamin A and the cell nuclei. (A) The cross section indicated with the white arrow indicates the (B) fluorescent spectral profile of ESAT-6, filamin A and the cell nuclei. The red blocks indicate where the fluorescent signal between ESAT-6 and filamin A co-localises. Note that the signal is different, excluding the possibility of cross reaction between antibodies or bleed through of the fluorescent probes.

Furthermore, during acquisition of images, strong signals for ESAT-6 were also observed in vacuolar inclusions, that seems to be at the membrane of THP-1 cells (Figure 4.13A). This was seen when recombinant ESAT-6 was added exogenously. To exclude the possiblity that these were not clumps on the outside of cells, an XYZ section throught the cell was analysed. From this analysis, the signal was observed in close proximity to the nucleus and was surrounded by the red signal, corresponding to filamin A (Figure 4.14). If this observation is true, ESAT-6 had to exhibit membrane lysing activity to be detected throughout the cytosol of THP-1 cells.

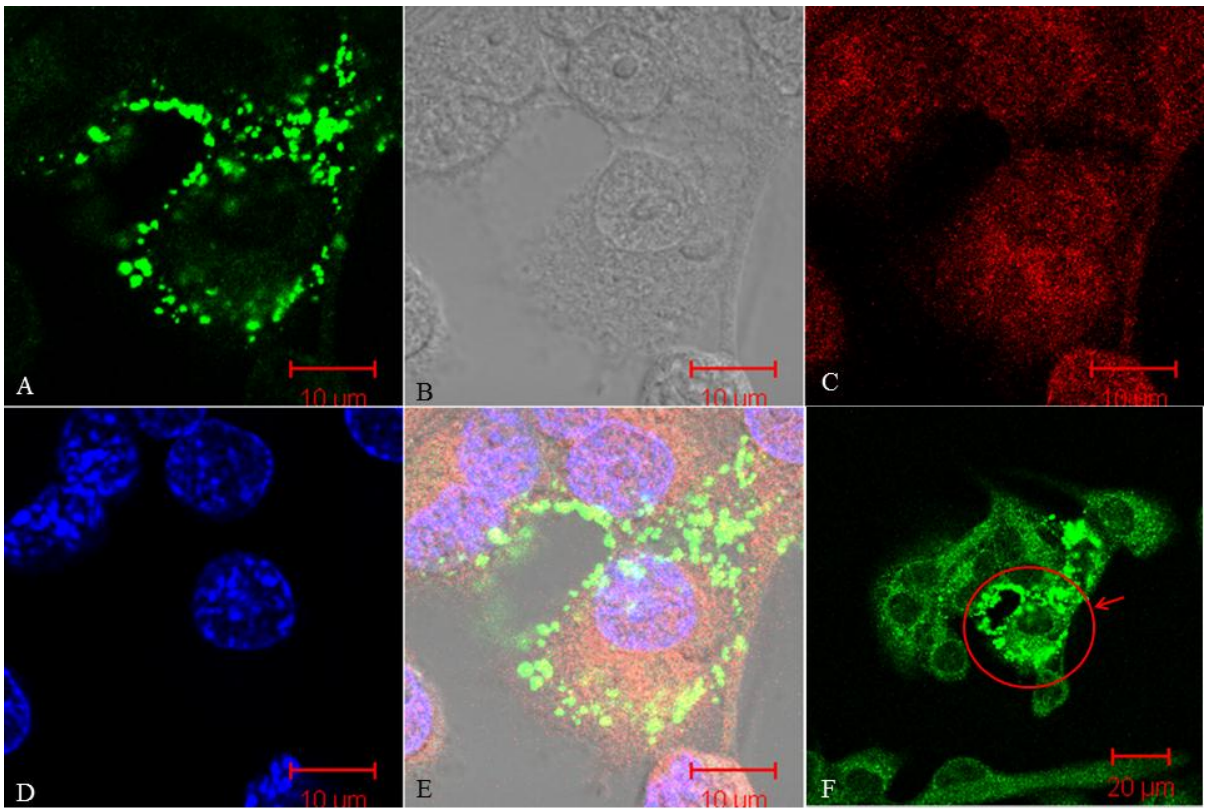

Figure 4.13 Inclusion bodies with ESAT-6. THP-1 cells were grown in RPMI medium supplemented with 10% fetal bovine serum and 1% penicillin/streptomycin and differentiated for 48 hrs with 100nM PMA. The cells were treated with 2.5 µg/ml of ESAT-6 for 6 hrs. The culture cells were washed with 1X PBS, fixed and permeabilised. The fixed cells were double stained with monoclonal antibodies against ESAT-6 (mouse) and filamin A (rabbit) and were detected with secondary fluorescent antibodies (i.e. goat anti-mouse Alexa 488 and donkey anti-rabbit Cy3). The prepared slides were stained with DAPI to visualise the cell nuclei. A Zeiss LSM 510 laser scanning confocal microscope was used to acquire images. (A) represents the fluorescent signal for ESAT-6 using the 100X objective lens, (B) represents the DIC image, (C) represents the fluorescent signal for filamin A, (D) represents DAPI staining for the cell nuclei, (E) represents the overlay of images A – D and (F) represents the staining for ESAT-6 of the same area using the lower magnification 63X objective lens. The scale bar of images A – E is 10 µm and F is 20 µm.

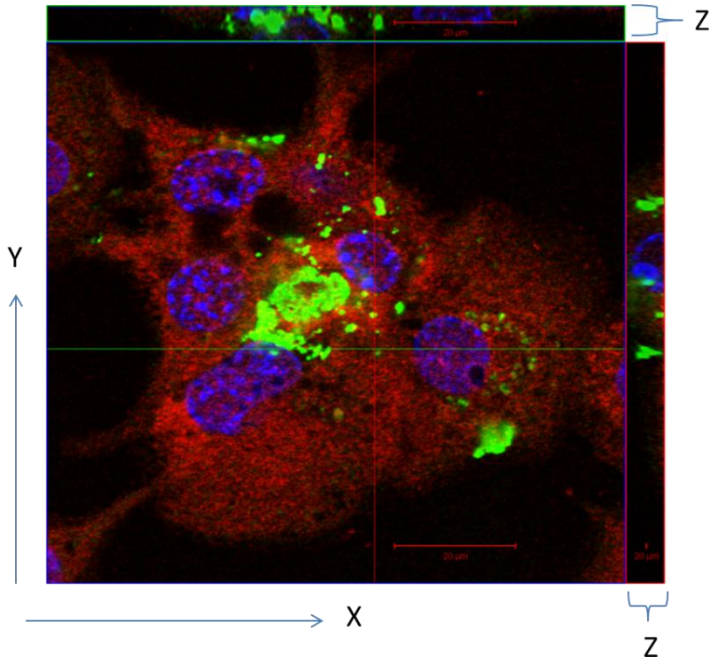

Figure 4.14: XYZ section through THP-1 cells containing ESAT-6 inclusion bodies. Figure represents data information from Figure 4.13E. The scale bar of the images is 20 µm. Images were enlarged using Zeiss LSM 510 Meta software.

4.1.7 *In vivo* co-immunoprecipitation of filamin A and ESAT-6

The interaction between ESAT-6 and filamin A was investigated in Jurkat cells, since these cells demonstrate effective expression of filamin A. Cells with a high expression of protein of interest are normally preferred when analysing interactions of endogenous proteins. Semi-endogenous *in vivo* Co-IP was performed by transfecting recombinant ESAT-6 into the cytosol of Jurkat cells using the Pro-Ject transfecting reagent (Thermo Fisher Scientific, Rockford, IL). Cell lysates were prepared using Tissue Protein Extraction Reagent (TPER, Thermo Fisher Scientific, Rockford, IL) and Membrane Protein Extraction Kit (Mem-PER, Thermo Fisher Scientific, Rockford, IL). Cell lysates were precipitated with monoclonal antibodies against filamin A and were then analysed by Western blot using anti-ESAT-6 antibodies. The results demonstrated that ESAT-6 and filamin A co-precipitate together (Figure 4.15A), confirming the interaction shown by the yeast-2-hybrid and *in vivo* co-localisation studies detailed above. The interaction between ESAT-6 and filamin A was also demonstrated in reciprocal experiments, where immunoprecipitation of ESAT-6 resulted in co-precipitation of filamin A (Figure 4.15B). A stronger interaction between ESAT-6 and filamin A was observed in the membrane fractions

compared to the tissue cell lysates. This result is supported by literature, demonstrating that filamin A is partially inserted into the hydrophobic domain of liposomes (Tempel et al., 1994). It has also been shown that ESAT-6 destabilises and lyses liposomes (de Jonge et al., 2007). Together, the results from the yeast-2-hybrid, *in vivo* co-localisation and co-immunoprecipitation studies, confirmed the biological interaction between mycobacterial ESAT-6 and host filamin A.

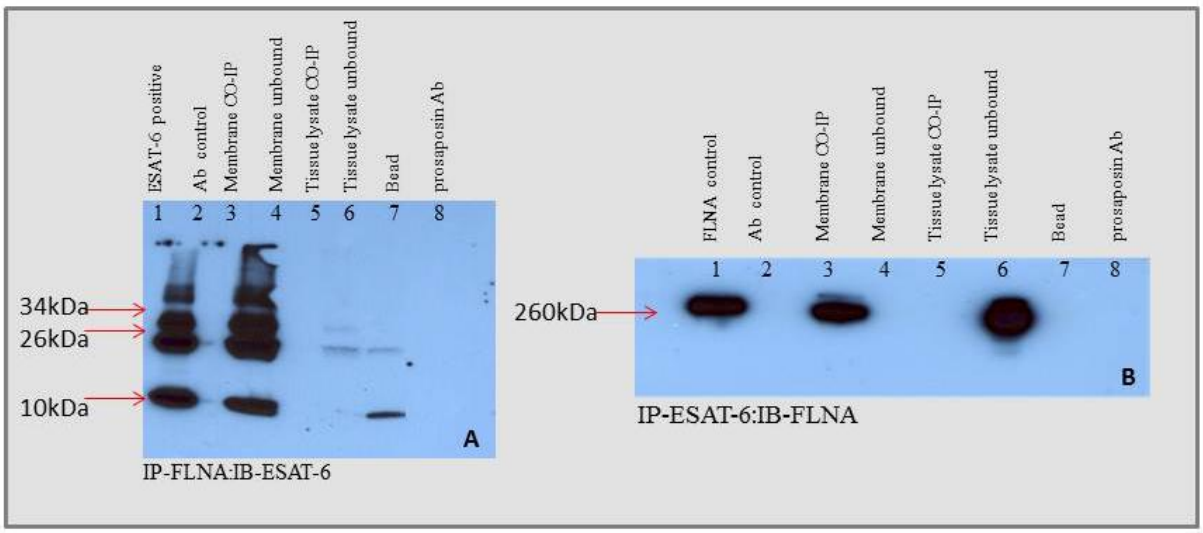

Figure 4.15: *In vivo* co-immunoprecipitation filamin A and ESAT-6. Jurkat cells were transfected with ESAT-6. Membrane and tissue cell lysates were prepared using the Membrane Protein Extraction kit (Thermo Fisher Scientific, Rockford, IL) and Tissue Protein Extraction Reagent (Thermo Fisher Scientific, Rockford, IL). The presence of ESAT-6 and filamin A was detected by Western blot with anti-ESAT-6 (lane A1) and anti-filamin A (lane B1), respectively.The membrane and tissue cell lysates were immunoprecipitated with anti-filamin A (lanes A3 and A5) and anti-ESAT-6 (lanes B3 and B5) conjugated to protein G and analysed for precipitation by Western blot using anti-ESAT-6 and anti-filamin A, respectively. Unconjugated protein G and anti-prosaposin conjugated to protein G served as negative controls (lanes A7, A8, B7 & B8). Lanes A2 and B2 served as a control to test the crosslinking reaction by preventing the co-elution of antibodies with precipitated proteins.

4.1.8 Effect of ESAT-6 on Jurkat cells and endogenous filamin A

A number of intracellular pathogens including *Salmonella*, *Yersinia*, *Shigella* and *Eschericia coli* are dependent on the manipulation of cytoskeletal dynamics for intracellular survival (Hestvik et al., 2005). Filamin A mediates interactions between cytoskeletal proteins and in a manner controls cytoskeletal dynamics of host cells. In this section, the next question was whether the protein levels of filamin A were affected by the presence of ESAT-6 in Jurkat cells.

Western blot was used to examine the endogenous level of filamin A in Jurkat cells treated with 1, 2.5 and 5 µg/mL of ESAT-6 and CFP-10. In each well, 1×10^6 cells were seeded. In order to verify whether any observed effect was dependent and specific to ESAT-6, treatment was performed with CFP-10 in a separate experiment to act as a control. Cells were lysed after 24 hrs of treatment with ESAT-6 and CFP-10, respectively. The same amounts of cell lysates were then analysed by Western blot with anti-filamin A antibodies. Anti-β-tubulin was used to equilibrate the loading amounts of cell lysates (Figure 4.16). When Jurkat cells were treated with higher concentrations of ESAT-6 (higher than 2.5 µg/mL), both filamin A and β-tubulin proteins disappeared and could not be detected by Western blotting anymore (lanes 4 and 5 in Figure 4.16A and B). However, the abundance of filamin A and β-tubulin remained unchanged in the presence of the same high concentrations of CFP-10, suggesting that the effect demonstrated is specific to ESAT-6. A possible reason for the fact that no observable protein bands were present at higher concentrations of ESAT-6, may be related to the cytolytic properties and induction of cell death by ESAT-6, which lead to the destruction of these cells and the concurrent loss of protein content.

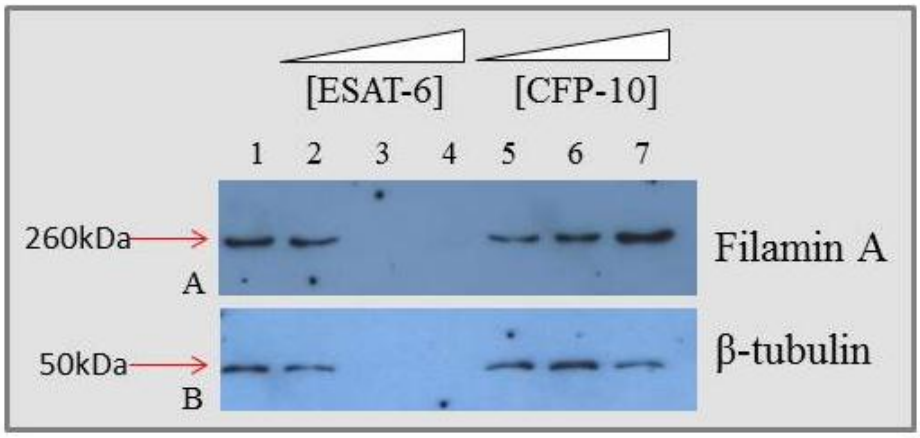

Figure 4.16: Expression levels of filamin A in the presence of ESAT-6 and CFP-10. Jurkat cells were seeded at a cell density of $5 \times 10^5$and treated with 1 µg/mL (lanes 2 and 5), 2.5 µg/mL (lanes 3 and 6) and 5 µg/mL (lanes 4 and 7) ESAT-6 or CFP-10, respectivly. Lane 1 is the untreatd control. Tissue cell lysates were prepared using the Tissue Protein Extraction Reagent (Thermo Fisher Scientific, Rockford, IL). The presence of Filamin A and β-tubulin were detected by Western blot with anti-filamin A and β-tubulin antibodies. Anti-β-tubulin was used to equilibrate the loading amounts of cell lysates. The abundance of filamin A and β-tubulin remained unchanged in the presence of varying levels of CFP-10, while the filamin A and β-tubulin were undetected at a higher concentrations of ESAT-6. This result is likely due to the cytolytic properties of ESAT-6.

In order to examine the events that occur at a higher concentration of ESAT-6, cells were treated with 2 μg/mL of ESAT-6 (and CFP-10 as a negative control) and lysates were prepared at various time points. ESAT-6 has been shown to induce expression of caspase genes in a dose-dependent manner, and filamin A, in turn, has been shown to be a substrate for cleavage by activated caspases (Browne et al., 2000; Umeda et al., 2001). Therefore, if ESAT-6 is involved in prompting a death signal that leads to the activation of proteases, cleavage of filamin A should be observed. Jurkat cells were also treated separately and in parallel with etoposide. Etoposide activates the apoptosis cascade by inducing the expression of caspase-related genes (de Bruin et al., 2003), and were thus used as a positive control for caspase activation and caspase-associated filamin A degradation. Cells were lysed at pre-determined time points (0, 1, 2, 4, 6, 12 and 24 hrs) after treatment with 2 μg/mL of ESAT-6. As shown in Figure 4.17, the levels of filamin A remained unchanged in the presence of CFP-10. However, in cells treated with ESAT-6, endogenous filamin A demonstrated significant breakdown (Figure 4.18B) compared CFP-10 treated Jurkat at 12 hrs (Figure 4.17). After 24 hrs, the protein content for both endogenous filamin A and β-tubulin could only be faintly detected, similar to the results observed in lanes 4 and 5 of Figure 4.16. This correlated well with the morphological changes seen in the case of etoposide-induced apoptosis used as a positive control (Figure 4.18A). The results demonstrate that treatment of Jurkat cells with ESAT-6 induces cleavage of filamin A.

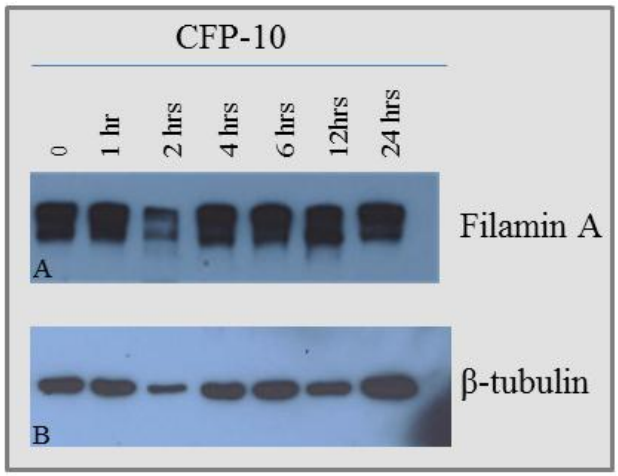

Figure 4.17 Expression level of filamin A and β-tubulin in the presence of CFP-10. Jurkat cells were seeded and treated with 2 μg/mL CFP-10. Tissue cell lysates were prepared using the Tissue Protein Extraction Reagent (Thermo Fisher Scientific, Rockford, IL). The presence of filamin A (Image A) and β-tubulin (Image B) was detected by Western blot with anti-filamin A and β-tubulin antibodies. Anti-β-tubulin was used to equilibrate the loading amounts of cell lysates. The abundance of filamin A remained unchanged in the presence of CFP-10.

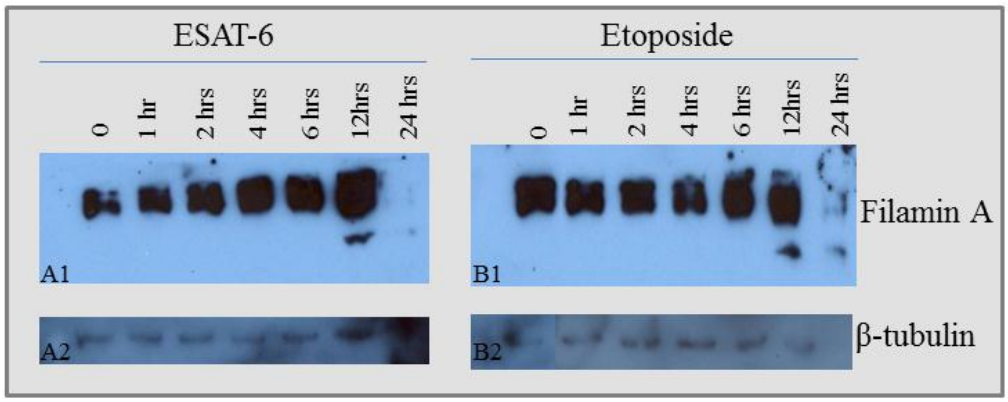

Figure 4.18 Expression level of filamin A and β-tubulin in the presence of ESAT-6 and etoposide. Jurkat cells were seeded and treated with 2 µg/mL ESAT-6 (A) or etoposide (B). Tissue cell lysates were prepared using the Tissue Protein Extraction Reagent (Thermo Fisher Scientific, Rockford, IL). The presence of filamin A (Images A1 and B1) and β-tubulin (Images A2 and B2) was detected by Western blot with anti-filamin A and β-tubulin antibodies. Anti-β-tubulin was used to equilibrate the loading amounts of cell lysates. At 12 hrs after treatment with ESAT-6 and etoposide, significant cleavage products of filamin A was observed (lanes 12 in images A1 and B1) and a 24 hrs after treatment the proteins were only barely detectable.

4.1.9 Cytotoxicity and cell death mediated by ESAT-6

An unusual morphological structure was observed for the cell nuclei of THP-1 cells treated with ESAT-6 during the co-localisation experiments. The nuclei demonstrated dot-like structures that are suggestive of DNA fragmentation (see Figure 4.9D). This feature is reminiscent of programmed cell death and also occurs during certain periods of necrosis (Gold et al., 1993). This observation is clearly portrayed in Figure 4.19, comparing nuclear morphology in cells treated and untreated with recombinant ESAT-6. The result demonstrates that access of ESAT-6 to the cytosol of THP-1 cells is associated with cell death (i.e. DNA fragmentation of the cell nuclei). This observation supports the hypothesis that ESAT-6 escapes inclusion bodies i.e. phagosomes and gain entry to the cytosol, leading to the induction of cell death (Simeone et al., 2012).

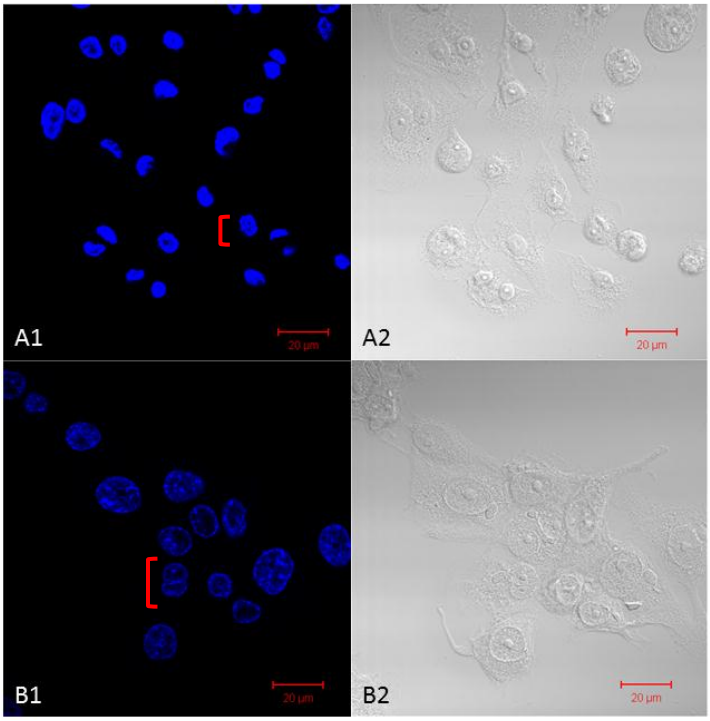

Figure 4.19: Comparison of THP-1 nuclear morphology in (A) treated and (B) untreated with recombinant ESAT-6. THP-1 cells treated with ESAT-6 demonstrated dot-like structures due to DNA fragmentation of the nucleas. Cell nuclei were stained with DAPI. The scale bar represents 20 µm.

4.2 Discussion

In order to identify host targets of the mycobacterial proteins ESAT-6 and CFP-10, a yeast two-hybrid system was used to screen the constructed human lung cDNA library. Both C1QA and filamin A were identified as ESAT-6 interacting proteins. In an additional screen, C1QA was also identified as a binding partner for CFP-10. However, the interactions of C1QA with ESAT-6 and CFP-10 could not be confirmed, despite numerous attempts. Unfortunately, even though C1QA was shown to interact with both ESAT-6 and CFP-10 in the yeast nucleus, this interaction could not be demonstrated by subsequent *in vitro* and *in vivo* experiments. The yeast two-hybrid system is known for producing high numbers of false positive results, which may result from improper folding during the expression of bait and prey fusion proteins. This may result in improper folding presenting as unnatural structures, causing non-specific binding. It is thus possible that the interaction with C1QA could be one of these false positives. On the other hand, it is also possible that there could be other factors involved in the confirmatory experiments, such as buffering conditions of lysis buffers, which are not suitable to identify the interaction, so that the

interaction of C1QA with ESAT-6 and CFP-10 might still be true interactions. The yeast two-hybrid systems detect interaction between bait and prey proteins expressed in yeast and present with the advantage that reporter genes may be activated by weak or transient interactions which are not detatable using *in vivo* detection methods. Alternative approaches to address the verification of weak or transient interactions are crosslinking- or label transfer-protein interaction analyses.

Nonetheless, the interaction between filamin A and ESAT-6 was confirmed by both *in vivo* co-localisation and co-immunoprecipitation, indicating that this was a true interaction between the mycobacterial and host proteins.

The findings from this section of the work conclusively confirmed the interaction between filamin A and ESAT-6 and showed that ESAT-6 co-localised and co-immunoprecipitated with filamin A in host Jurkat and THP-1 cells. The co-immunoprecipitation results indicated that the majority of ESAT-6 interacting with filamin A was associated with the membrane fraction of Jurkat cells, rather than the tissue cell lysate. This observation is strengthened with the result presented in Figure 4.3A, demonstrating that ESAT-6 associated with the membrane fraction of THP-1 lysates, and that filamin A is a membrane-associated cytoskeletal protein. As the co-immunoprecipitation result was not suitable to confirm a direct protein-protein interaction (as the precipitate may have consisted of a subset of proteins belonging to a larger protein complex), future studies using *in vitro* methods would be required to investigate whether there is in fact a direct interaction between ESAT-6 and filamin A.

It has previously been shown that filamin A binds F-actin and associates with the plasma membrane and with numerous other intracellular signaling intermediates, including enzymes and scaffolding proteins (Hayashi and Altman, 2006). These findings indicate that filamin A plays an important role as an adapter molecule that links a wide variety of intracellular proteins to the actin cytoskeleton and cell membrane receptors (Hayashi and Altman, 2006). Pathogenic species of mycobacteria have been found to interfere with the host cell's actin filament network, influencing cellular processes ranging from migration, phagocytosis, motility and cellular adherence (Hestvik et al., 2005). Phagosomes containing pathogenic *M. avium* coincide with the disorganisation of the F-actin distribution in macrophages compared to uninfected cells (Guérin

and de Chastellier, 2000). We have shown that the abundance and/or molecular composition of filamin A in Jurkat cells were altered in the presence of ESAT-6. This alteration caused by ESAT-6 on Jurkat cells was similar to etoposide-induced cell death. Exposure of cells to etoposide induces endonucleolytic cleavage of DNA during the early stages of cell death, which is followed by cytoskeleton degradation (Kaufmann, 1989). Therefore, the evidence suggests that disorganisation and induction of cell death via the action of ESAT-6 are events that are not mutually exclusive.

The ESX-1 system is required for secretion of effector proteins, including CFP-10 and ESAT-6, and is important for virulence of pathogenic mycobacterial species (McLaughlin et al., 2007). Mutants of *M. bovis*, *M. marinum* and *M. tuberculosis* lacking an intact ESX-1 secretion system or substrates necessary for secretion, have been shown to be attenuated in cultured macrophages and animal models of infection, demonstrating defects in cell-to-cell spread, altered cytokine profile or phagosomal maturation arrest (Gao et al., 2004; Smith et al., 2008; Kinhikar et al 2010; Welin et al., 2011). Moreover, it has been demonstrated that secretion of ESAT-6 by *M. marinum* causes the induction of membrane pores in bone marrow derived macrophages (Smith et al., 2008). Therefore, it is suggested that ESAT-6 secretion by the ESX-1 system of *M. marinum* could play a direct role in producing pores in membranes of cells that contain mycobacteria, facilitating the escape from the vacuole into the cytosol, and enabling cell-to-cell spread (Smith et al., 2008). In this study, recombinant ESAT-6 exhibited membrane lysing activity on both THP-1 (Figure 4.4) and Jurkat cells (data not shown, observed by visual inspection using light microscope), demonstrating the lytic phenotype of ESAT-6. Therefore, it suggests that ESAT-6 had to lyse vacuolar membranes in order to be detected throughout the cytosol of THP-1 cells (Figure 4.16F). This hypothesis is consistent with the potential role of ESAT-6 in the disruption of phagosomal membranes, to release bacterial content into cytosol of infected cells to facilitate spread (Derrick and Morris, 2007). The findings are also in agreement with literature demonstrating that purified ESAT-6 from *M. tuberculosis* results in disruption and lysis of artificial lipid bilayers and liposomes (Hsu et al., 2003; de Jonge et al., 2007). As seen in Figure 4.4, lysis of THP-1 cells correlated to a strong fluorescent signal of ESAT-6. Furthermore, the open reading frame for ESAT-6 from *M. tuberculosis* encodes a 95 amino-acid (aa) protein with 90.5% similarity to its *M. marinum* homologue (Gao et al., 2004). Therefore, ESAT-6 secreted by *M. tuberculosis* may potentially share the same function with *M. marinum*, resulting in the

translocation of *M. tuberculosis* from the phagosomal compartments to the cytosol of infected cells.

Recently, Simeone and coworkers (2012) have demonstrated that both *M. marinum* and *M. tuberculosis* gain access to the cytosol of infected macrophages, by taking advantage of a newly developed tool that allows for quantitative analysis of vacuolar rupture and cytosolic entry of bacteria. The authors revealed that phagosomal rupture was facilitated by ESAT-6 (Simeone et al., 2012). In addition, they demonstrated that phagosomal rupture precedes host cell death, which is in agreement with the work presented in this study (see Figures 4.23 and 4.25). Others have also demonstrated that ESAT-6 in its purified form induces cell death in macrophages (Derrick and Morris, 2007).

Given that cell death in the form of apoptosis is a mechanism that the human host employ to remove infected cells, while reducing cell death and tissue destruction in nearby uninfected cells has importance in the control of M. tuberculosis infection (Abebe et al., 2011). In addition, M. tuberculosis can directly interfere with the induction of apoptosis of cells in vitro and it appears to be related to virulence in vivo (Keane et al., 1997, 2000; Rojas et al., 1997; Santucci et al., 2000). Furthermore, M. tuberculosis is able to promote necrotic death in infected human macrophages (Wong and Jacobs, 2011). A suitable explanation is that necrosis is important for dissemination within the host and cell-to-cell spread, but also blocking it to allow the pathogen to persist in the human host. In both aspects, M. tuberculosis may manipulate responses to favour of apoptosis (reducing inflammation, allowing for persistent infection) or necrosis (promoting tissue destruction, dissemination and spread to uninfected cells) (Abebe et al., 2011). In the light of these findings and documented reports in literature, we suggest expanding the knowledge of how M. tuberculosis actively control pathways related to cell death and could potentially identify mycobacterial or host features that can be targeted for vaccine development

In conclusion, the results presented in this section show that ESAT-6 interacts with filamin A and precipitated a process which results in cell death. We suggest the following hypothesis for the progression of this process. ESAT-6 is an early-secreted antigen and is thus expressed and secreted from early after uptake of the bacterium by host cells, reaching a critical concentration required for vacuolar membrane destruction. It has been shown that secreted ESAT-6 has the

ability to facilitate phagosomal rupture, releasing the mycobacterium into the cytosol of infected cells (Simeone et al., 2012). As the process of phagosomal rupture is initiated, we speculate that small amounts of ESAT-6 leak into the cytosol via pore formation, preparing the cytosolic environment for mycobacterial entry. During this time, ESAT-6 interacts with filamin A and destabilises the actin cytoskeleton structure by inducing structural degradation of filamin A and inducing programmed cell death of the infected cells. As the mycobacterium enters the cytosol, the infected cells are unable to effectively recognise the pathogenic bacteria as a result of the initiation of cell death, leading to a deficiency in the acquired immune response. As *M. tuberculosis* exits the infected cell after cell death, it is taken up by newly arriving uninfected macrophages, resulting in disease progression. The results of the work presented here open the way to new exciting future studies to explore this and other hypotheses. This study highlights the importance of understanding the molecular events whereby *M. tuberculosis* manipulate and control cell death pathways, which can be exploited to gain insight into new approaches to control tuberculosis infection.

Chapter 5

5 Association studies of the C1Q gene cluster

5.1 Results

Filamin A and complement component 1q A (C1QA), identified during the yeast two-hybrid screens, were further investigated as genetic candidates for susceptibility to tuberculosis. The genetic analyses in this part of the study were completed before the outcome of the *in vivo* verification of the putative interactions was completed. A case-control study involving 604 cases, of which 109 were Tuberculous Meningitis (TBM) and 486 controls from the South African Coloured (SAC) population were selected from the Ravensmead-Uitsig sample cohort according to the description in section 2.17.1 (Chapter 2). The criteria for the selection of SNPs are discussed in sections 5.1.1 and 5.1.2.

5.1.1 *FLNA* gene

The filamin A (*FLNA)* gene is highly conserved and genetic evidence suggests that filamins are vital for human development. Filamin A is widely expressed in multiple organ types and controls actin cytoskeleton organisation by connecting integrins, transmembrane receptors and second messengers to the plasma membrane of host cells. Mutations found in the *FLNA* gene have been associated with human genetic developmental disease of the brain, bone, cardiovascular system, and many other organs in the human body (Feng and Walsh, 2004). Therefore, due to strong mutational influence resulting developmental disorders, only the promoter region of the *FLNA* (1kb upstream of ATG start site) was screened for SNPs that may possibly interfere with transcriptional binding sites or expression levels of filamin A that may contribute to tuberculosis susceptibility.

5.1.1.1 PCR amplification of the promoter of FLNA

DNA samples from 10 TB cases and 10 healthy individuals were amplified and sequenced using primers listed in Table 2.2 (Chapter 2). Due to the strong conservation of filamin A gene, only 20 samples were screened to identify polymorphic sites in the promoter region. The amplified

products were resolved on a 1% TAE agarose gel and yielded a product size of 1181 bp (Figure 5.1). The PCR products were purified and sequenced to screen for potential promoter variants.

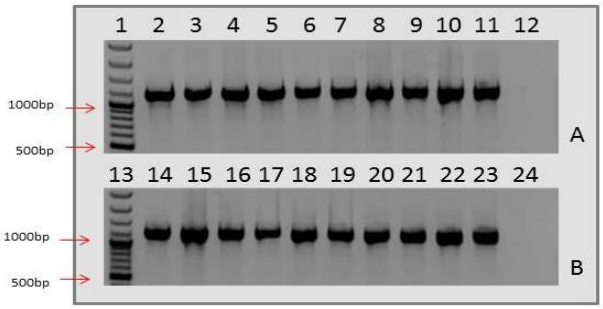

Figure 5.1: 1% TAE Agarose gel electrophoresis image of the PCR products of the FLNA promoter. (A) Lanes 1 and 13 contain the 100bp ladder (Fermentas, Burlington, Canada). Lanes 2-11 represent the PCR products of TB patients and (B) lanes 14-23 represent the PCR products of healthy individuals. Lanes 12 and 24 represent the negative control of each PCR reaction.

5.1.1.2 Sequence analysis

The sequence information obtained by bidirectional sequencing using primers listed in Table 2.2 (Chapter 2) was analysed using the BioEdit program to detect SNPs in the promoter region of the *FLNA* gene. Sequence analysis revealed a low-frequency SNP (G>C, 20%) indicated with arrow in Figure 5.2). Furthermore, sequence alignment demonstrated complete homology with the reference sequence of the *FLNA* gene (NCBI RefSeqGene NG_011506.1) (Figure 5.2). Due to the low frequency of variation across the promoter region of the *FLNA* gene; the investigation into the role of *FLNA* in tuberculosis susceptibility was discontinued.

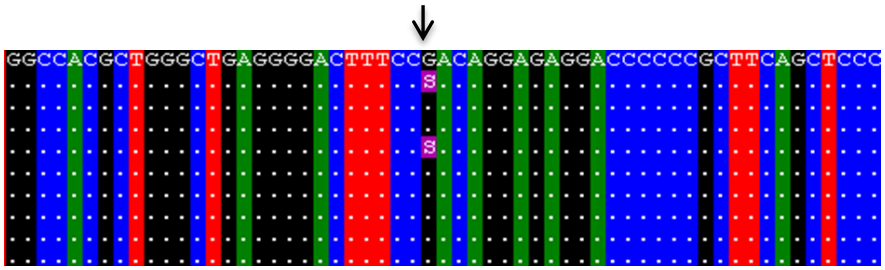

Figure 5.2: Sequence alignment of TB cases to the reference sequence of *FLNA*. Sequence alignment of the 10 TB patients to reference sequence of *FLNA* (NCBI RefSeqGene NG_011506.1) revealed a low frequency SNP (indicated with arrow). The full length alignment demonstrated low rates of variation.

5.1.2 *C1QA* gene

The most important molecular complexes affecting susceptibility to infectious disease are those related to immune defenses. Therefore, it was appropriate to investigate immune complexes that function during *M. tuberculosis* infection. It is well known that *M. tuberculosis* is phagocytosed via complement receptors expressed on human alveolar macrophages and that the classical pathway is more functional in the lungs than the alternative pathway (Ferguson et al., 2004). The C1Q molecule is the first component of the classical pathway that leads to activation of complement.

The coding region for *C1Q* has been mapped to chromosomal position 1p34-36 and is composed of three genes, *C1QA*, *C1QB* and *C1QC*. The protein product of each of the three genes associates as six heterotrimers in a 'bouquet-like' structure, forming the mature molecule (Figure 3.14, Chapter 3). This molecule participates in the clearance of immune complexes and apoptotic cells. Structurally, C1Q is related to the family of collectins that play key roles in the innate immune response and defense against invading pathogens. Therefore, we hypothesised that C1Q related polymorphisms may influence the biological function of the C1q protein and thus may confer genetic susceptibility to Tuberculosis.

For SNP selection, a literature search was done regarding associations between *C1Q* gene variants and various diseases in case control studies. The five selected SNPs were inspected for heterogeneity and minor allele frequencies (MAF) using the HapMap population groups (http://www.ncbi.nlm.nih.gov/snp). Table 5.1 lists the MAF of the five selected SNPs within the *C1Q* gene cluster. The power as a percentage of chance to detect risk associated effects is dependent on the MAF ≥ 0.05, which in this study was 90%. All selected SNPs complied with the requirements (see Table 5.1). Given the evidence in literature, the level of heterogeneity and the MAF ≥ 0.05, a case control study was designed to investigate the role of *C1Q* as a candidate for tuberculosis susceptibility in the South African Coloured Population.

Table 5.1: **HapMap MAF of the five selected SNPs.** The MAF of African, European and Asian populations of rs587585, rs665691, rs172378, rs12033074 and rs631090.

		MAF: NCBI			
Marker	Minor allele	CEU	YRI	HCB	JPT
rs587585	G	0.128	0.429	0.151	0.128
rs665691	C	0.438	0.841	0.64	0.669
rs172378*	A	0.583	0.169	-	0.367
rs12033074	G	0.350	0.425	0.467	0.511
rs631090	C	0.051	0.617	0.278	0.256

CEU – Utah residents with ancestry from northern and western Europe
YRI – Yoruba in Ibadan
HCB – Han Chinese in Beijing
JPT – Japanese in Tokyo
*low coverage population panel (CHB and JPT combined)

5.1.2.1 TaqMan allelic discrimination results

The selected variants spanning the *C1Q* gene complex were genotyped by PCR using pre-developed TaqMan SNP genotyping assays. After amplification, allelic discrimination was performed by end point plate reading using the ABI Real-time PCR system (http://www.appliedbiosystems.com/). The plate readings were analysed using the SDS 2.3 software to measure the amount of fluorescence and to convert the fluorescent signal into allelic discrimination plots. An example of the end point results of rs631090 is shown in Figure 5.3, representing the allelic discrimination plots obtained using the SDS software (http://www.appliedbiosystems.com). The plate readings of the end point analyses were exported and the sample IDs were assigned to each reading.

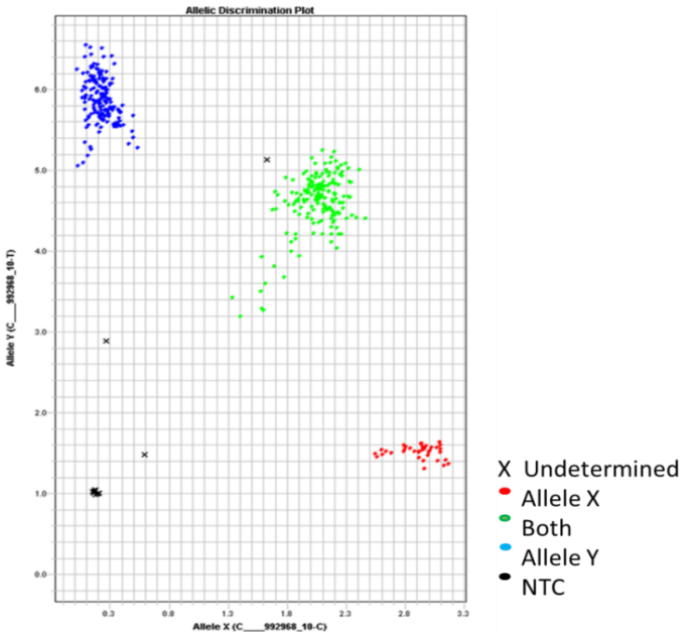

Figure 5.3: Representative result for a TaqMan allelic discrimination plot. Genotyping results for rs631090 representing the allelic discrimination plot generated using SDS software (Allele Y → T and Allele Y → C).

5.1.2.2 Genotype and allele frequencies

The success rate of genotyping (the percentage of samples that could be analysed) was >95% for all genetic variants in both cases and controls. The genotype and allele frequencies of the five SNPs in the controls, pulmonary tuberculosis (TB) and Tuberculous Meningitis (TBM) are shown in Table 5.2. The distributions of genotype and allele frequencies of the *C1Q* gene variants, in both case and control groups, were in Hardy-Weinberg Equilibrium ($P > 0.05$) and were subjected to further analysis.

Table 5.2: Genotype and allele frequencies of the *C1Q* gene variants in the control, tuberculosis and Tuberculous Meningitis group. Hardy Weinberg Equilibrium was determined for each individual SNP and the corresponding HWE *P* values are show at the bottom of each SNP section. All genetic variants segregated according to the assumption of Hardy Weinberg ($P > 0.05$) and were subjected to further analyses.

	Control	TB	TBM
rs587585			
AA	277 (0.58)	237 (0.49)	50 (0.46)
AG	179 (0.37)	205 (042)	48 (0.44)
GG	24 (0.05)	44 (0.09)	11 (0.10)
A	0.764	0.699	0.679
G	0.236	0.301	0.321
HWE *P* – VALUE	0.473	0.972	0.917
rs665691			
CC	59 (0.12)	49 (0.10)	9 (0.08)
CG	211 (0.44)	205 (0.42)	50 (0.46)
GG	213 (0.44)	235 (0.48)	49 (0.45)
C	0.341	0.310	0.315
G	0.659	0.690	0.685
HWE *P* – VALUE	0.547	0.663	0.447
rs172378			
AA	65 (0.14)	57 (0.12)	15 (0.14)
AG	221 (0.46)	224 (0.46)	44 (0.42)
GG	195 (0.41)	205 (0.42)	47 (0.44)
A	0.365	0.348	0.349
G	0.635	0.652	0.651
HWE *P* – VALUE	0.849	0.724	0.373
rs12033074			
CC	143 (0.30)	173 (0.36)	40 (0.37)
CG	241 (0.51)	221 (0.46)	54 (0.50)
GG	90 (0.19)	85 (0.18)	15 (0.14)
C	0.556	0.592	0.615
G	0.444	0.408	0.385
HWE *P* - VALUE	0.517	0.325	0.632
rs631090			
CC	50 (0.10)	69 (0.14)	20 (0.18)
TC	218 (0.45)	225 (0.46)	49 (0.45)
TT	213 (0.44)	191 (0.40)	40 (0.37)
C	0.331	0.374	0.331
T	0.669	0.626	0.669
HWE *P* – VALUE	0.598	0.834	0.598

Single SNP association tests were performed using allele, genotype, and dominant models. All analyses were adjusted to account for sampling differences in age and gender. The genotype and allelic frequencies of rs665691, rs172378 and rs631090 were similar in cases and controls and showed no significant association with TB or TBM cases (Table 5.3A). However, rs631090 demonstrated an association at allele level with TB, whereas rs587585 demonstrated an

association at both allele and genotype level with TB (genotype: *P* = 0.001 and allele *P* = 0.000). No significant associations were seen in the TBM cases with rs631090 and rs587585.

Although the G-allele frequencies for rs587585 were comparable between TB and TBM (0.301 and 0.321 vs. controls 0.236), rs587585 was associated with TB but not TBM, possibly due to the small sample number of TBM cases (n = 109). Furthermore, rs12033074 demonstrated a weak association in the TBM group, but as a result of the small sample size of the TBM group, no concrete conclusion could be made. No significant associations were observed with the dominant model demonstrating that the observed associations are likely additive. A summary of the significant additive effects of the associated allele are shown in Table 5.3B.

Table 5.3: Results from association analyses of rs587585, rs665691, rs172378, rs12033074 and rs631090. (A) Significant association at genotype, dominant and allelic level. (B) Additive effects of allelic associations (markers in table A are colour coded to markers in table B).

A Marker	Genotype		Dominant		Allelic	
	TB	TBM	TB	TBM	TB	TBM
rs587585	**0.001****	0.158	0.703	0.058	**0.000****	0.745
rs665691	0.186	0.424	0.558	0.822	0.082	0.197
rs172378	0.559	0.300	0.437	0.662	0.454	0.137
rs12033074	0.122	**0.045***	0.469	0.423	0.055	**0.018***
rs631090	0.050	0.881	0.590	0.946	**0.017***	0.618

P value less than 0.05* and 0.001**
TB – Tuberculosis
TBM – Tuberculous Meningitis

B Marker	Diagnosis	Allele	OR	95% CI	
rs587585	TB	G	1.48	1.21	1.82
rs12033074	TBM	G	4.98	1.30	24.31
rs631090	TB	C	1.25	1.04	1.51

Among the identified SNPs, the G allele of rs587585 was significantly associated with TB in the additive model (*P* = 0.002, OR: 1.48 95% CI 1.21 – 1.82). Similarly, the C allele of rs631090 was associated with TB (*P* = 0.018, OR 1.25 95% CI 1.04 – 1.51) using the same model. Given these results, it seems likely that rs587585 contributes more to tuberculosis susceptibility than rs631090.

In the current analysis we did not use Bonferroni correct for multiple testing, which refers to a situation that involves the simultaneous testing of more than one association within the same

sample population (Nyholt, 2004), with risk of eliminating important findings. The inappropriateness of Bonferroni, in this instance, is the unlikelihood that all genes important for susceptibility can be found *a priori* with tuberculosis (Perneger, 1998), whereas Bayesian methods for correction relies on prior knowledge of involvement, which is currently unknown for most genetic variants (Campbell and Rudan, 2002).

5.1.3 Linkage disequilibrium and haplotype analysis

To delineate the haplotype architecture of the *C1Q* gene complex, linkage disequilibrium and haplotype analyses were performed. The linkage disequilibrium, measured by D', suggested that rs587585 and rs665691 were in moderate disequilibrium across a genetic region of 2 kb (D' = 0.99, r^2 = 0.18, Figure 5.4). The haplotype frequencies within block 1 are shown in Table 5.4.

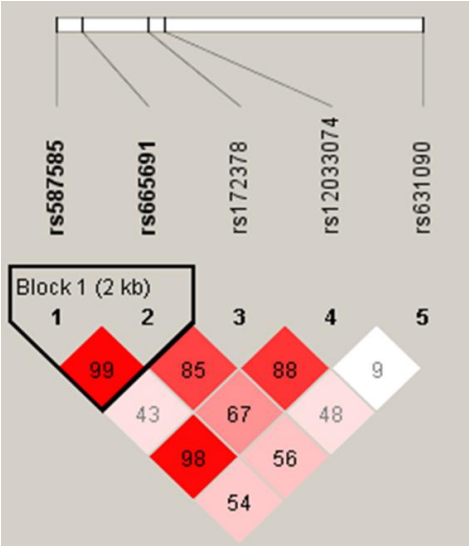

Figure 5.4: LD structure for rs587585, rs665691, rs172378, rs12033074 and rs631090. Linkage block (2kb) between marker rs587585-rs665691 was in moderate disequilibrium (D' = 0.99, r^2 = 0.18).

Table 5.4: Haplotype pairs of rs587585 and rs665691. Haplotype frequency of rs587585-rs665691 in case and controls. The odds ratio corresponding to the reference haplotype is 1. Note that if the odds ratio is significant, the 95% confidence intervals do not span 1. The data is interpreted as follows: G-G haplotype compared to the A-G haplotype increases the odds of TB with 45% (between 15 and 82%, with 95% confidence).

TB	Frequency		OR of TB, adjusted for age and gender		
Haplotype:	**Control**	**Case**	**OR**	**95% CI**	
A-C	0.34	0.31	0.97	0.79	1.19
G-G	0.24	0.30	1.45	1.15	1.82
A-G	0.42	0.38	1		

Haplotype analysis was performed to determine if certain haplotype pairs were transmitted together more frequently. Statistically significant haplotype pairs for all loci are listed in Table 5.5. Haplotype analysis revealed that the association from block 1 to block 5 decayed. This observation led to the conclusion that rs587585 contributed significantly to the association observed with haplotype rs587585-rs665691. To see whether rs587585 had any functional consequences, the serum levels of C1QA were assessed in 18 cases and 18 controls using an ELISA assay.

Table 5.5: Results of haplotype associations. Haplotype frequencies were determined in R-project using a GLM-ANOVA model; all analyses were adjusted for age and gender. The association from block 1-5 highlighted in orange demonstrates a decaying trend in association.

TB	Number in haplotype			
Starting SNP	**2**	**3**	**4**	**All**
rs587585	**0.0015**	**0.0140**	**0.0205**	0.0830
rs665691	0.2509	**0.0436**	0.0736	
rs172378	**0.0347**	0.0695		
rs12033074	**0.0233**			
rs631090				
Starting SNP	**2**	**3**	**4**	**All**
rs587585	0.3925	0.7953	0.5469	0.9326
rs665691	0.5632	0.3642	0.7344	
rs172378	0.1449	0.5343		
rs12033074	**0.0056**			
rs631090				

5.1.4 C1QA ELISA

5.1.4.1 Analysis of normality

In order to avoid inaccurate interpretation of the ELISA data, the normality was checked using the null hypothesis of the Shapiro-Wilk test that explores the distribution of samples and tests whether the data is distributed normally. In the analyses, a *P*-value of greater than 0.05 was considered as statistically significant. If the *P*-value was less than 0.05, then the null hypothesis that the data was distributed normally would be rejected, leading to inaccurate interpretation.

The ELISA data fitted the linear distribution and the null hypothesis was therefore not rejected (*P*-value of 0.101). The ELISA measurements were distributed normally and further subgroup analyses were performed as follows: (1) TB vs. controls and (2) subgroups of the different genotypes in relation to TB and controls (Figure 5.5).

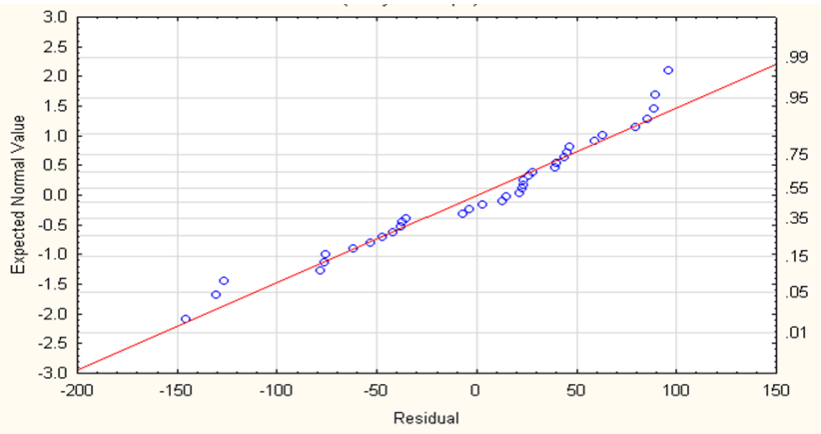

Figure 5.5: Representation of the ELISA data distribution. The ELISA data of the total group fitted the linear distribution. The null hypothesis that the data was not distributed normally was rejected (*P*-value of 0.101).

5.1.4.2 Group and subgroup analyses

The results from the ELISA analyses revealed that the serum levels of C1QA were higher in TB subjects compared to control individuals ($P = 0.037$, Figure 5.6A). A significant difference was observed in the distribution of serum C1QA across the three genotypes of rs587585 ($P = 0.0409$, Figure 5.6B). Adding a G allele of rs587585 was associated with an increased level of circulating C1QA in the total sample group.

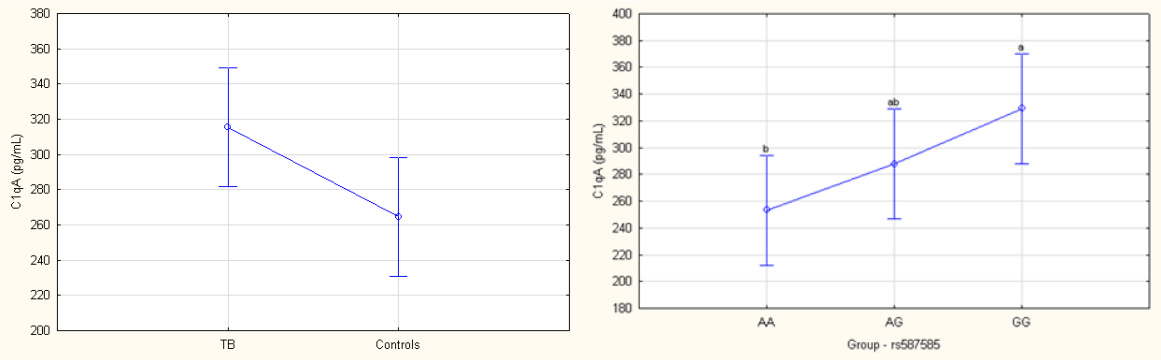

Figure 5.6: Levels of C1QA distribution between groups and subgroups. (A) Demonstrates an elevation in the serum levels in TB vs. controls. (B) Difference in serum levels of the three genotype of rs587585 in the total sample group. The GG genotype is associated with the highest C1QA levels.

We stratified the groups according to controls and TB patients, and observed a dosage effect of the G allele. The observation was not significant, but demonstrated a trend (*P* = 0.098). The serum levels of C1QA remained constant in the controls, while increasing in TB patients (Figure 5.7). This result demonstrated a functional trend associated with the GG genotype of rs587585. The apparent association of this SNP could also be due to linkage disequilibrium with the true functional variant or other genetic factors that could explain the elevation seen in GG individuals.

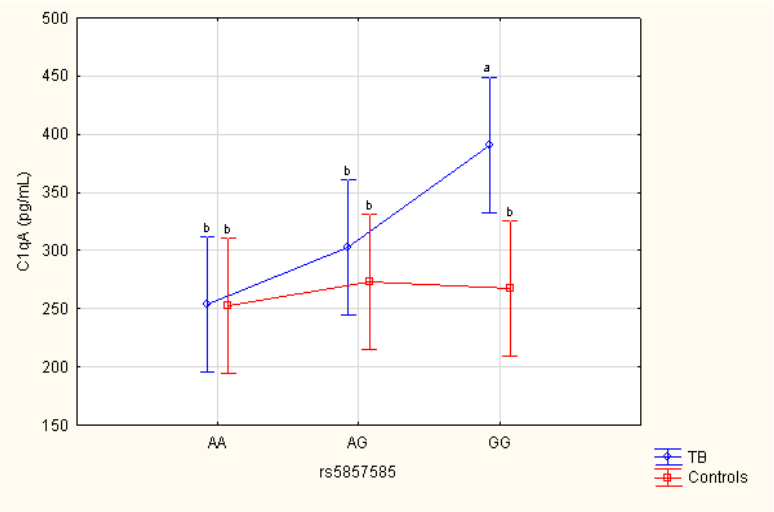

Figure 5.7: Levels of C1QA distribution stratified according to subgroups and rs587585 genotypes. Levels of C1QA stratified according to the rs5857585 genotype in the TB and control group, demonstrated an increase in serum C1QA in the TB group vs. controls. The observation was not significant, but demonstrates a trend (P = 0.098). The elevation of serum C1QA in individuals with the GG genotype in the TB group could be a result of linkage with a true functional SNP or other genetic factors (a vs. b: no significant difference, but demonstrates a trend).

5.2 Discussion

This study reports an association analysis of five polymorphisms of the *C1Q* gene cluster (i.e. *C1QA*, *C1QB* and *C1QC*) in ~500 cases and ~500 controls from the South African Coloured (SAC) population. The results showed a novel association of a regulatory variant located upstream of the *C1QA* gene and determined that C1QA serum levels showed a trend towards increased values in patients with the associated genotype.

In our association study we screened 486 cases and 480 controls and demonstrated an association at both genotype and allele level with rs587585 (genotype: $P = 0.001$ and allele: $P = 0.000$; OR = 1.48; 95% CI 1.21 – 1.82). We did not identify additional associations with *C1Q* and tuberculosis. One possible explanation is the incomplete polymorphism coverage of the *C1Q* gene cluster. The associations demonstrated were additive and together with other risk alleles may provide a synergistic interaction between multiple risk alleles.

The G-allele of rs587585, located upstream of *C1QA*, demonstrated a trend towards increased serum levels, but this difference was not statistically significant ($P = 0.0977$). In the control individuals carrying the G-allele of rs587585, no significant elevation in serum levels was observed. Thus, other genetic factors may contribute to the increase observed in GG individuals infected with tuberculosis. A potential explanation for this observation could be linked to the measure of linkage disequilibrium between rs587585 and rs665691 located in the promoter region of *C1QA* (D' = 0.99, $r^2 = 0.18$, Figure 5.5) that may possibly hold the true functional variant causing the increase in serum levels. Regulatory variants that are located hundreds of kb upstream can influence the control of gene expression (Forton et al., 2007; Stranger et al., 2007). Therefore it should be considered that other unidentified promoter variants could contribute to the observed phenotype, as well as other variants affecting the production of C1QA and ultimately the functional protein. In future studies the sample size of the ELISA cohort should be increased to verify the findings using freshly prepared serum from genotyped cases and controls. Currently, published methods for determining the levels of C1Q vary greatly in their application, results, and reproducibility. For further analysis, a protocol such as that described by Dillon et al., should be considered for the quantification of serum C1Q levels, as this method is an improvement in scale, theory, precision, reproducibility, cost efficiency and ease (Dillon et al., 2009).

The role of complement is very complex and serves the host by providing protection. It has been reported that C1Q binds both IgM and MBL, which co-operate to promote phagocytosis of apoptotic or necrotic cells (Xu et al., 2008). Therefore, one possible explanation for our finding is that the G allele of rs587585, is in linkage with the true functional variant and that higher levels of complement may facilitate opsonisation of dead or dying cells. The rapid clearance could possibly facilitate entry of *M. tuberculosis* into host cells via phagocytosis, and in so doing evade destruction by the host immune response. Another possible explanation has been recently described by Carroll and colleagues (2009). In this study, they demonstrated that *M. bovis* BCG is able to directly bind to C1Q, MBL and L-ficolin in both an antibody-dependent and independent manner (Carrol et al., 2009). It is thought that the activation of complement could be one of the mechanisms employed by macrophage-ingested mycobacteria to escape the immune system i.e. by remaining intracellular in the phagosome. Previous studies have shown that *M. tuberculosis* can activate complement and gain entry via macrophage complement receptors (Ramanathan et al., 1980; Schlesinger et al., 1990; Schlesinger, 1993; Ferguson et al., 2004). The involvement of the classical pathway has been demonstrated by the depletion of C1Q from serum, which significantly reduced the binding of C3 to *M. tuberculosis in vitro*. It has been shown that entry of *M. tuberculosis* is dependent on C3 opsonisation and that it is initiated by the classical pathway within the human alveolus (Ferguson et al., 2004).

The genetic variants reported on in this study, have not previously been investigated in tuberculosis susceptibility and represent an intriguing area for future research. Variants within the *C1Q* gene cluster are typically associated with systemic lupus erythematous (SLE). In this study, rs587585 G allele demonstrated a trend of increased serum C1QA levels. However, Martens and co-workers demonstrated that the G-allele of rs587585 is associated with low serum C1Q levels and total hemolytic complement activity (CH50) in SLE Caucasian patients (Martens et al., 2009). Similarly, in animal studies, a polymorphism in this regulatory region was also found to be associated with low C1Q levels in a murine model of New Zealand Black (NZB) mice; therefore the authors suggest that the region upstream of the *C1Q* gene cluster may possibly be important (Miura-Shimura et al., 2002), keeping in mind that functional variants may act differently within ethnically diverse populations. This difference in reported serum levels can be explained by the fact that our cohort is infected with tuberculosis compared to SLE patients and the sample cohort

are SAC compared to Caucasians or NZB mice. In addition, low C1Q and CH50 levels may also be a reflection of complement consumption by the disease activity of lupus (Martens et al., 2009).

The etiology of lupus remains unknown and is characterised by autoantibodies against self-antigens, leading to inflammation-mediated multi-organ failure. The majority of deaths in SLE patients are caused by infection, renal failure and cardiovascular diseases. In most cases, infections are caused by gram-positive or gram-negative bacteria, with an increased prevalence of *M. tuberculosis* infection. These opportunistic infections explain the increase of mortality observed in lupus patients (Agrawal and Prabu, 2010).

The surge of *M. tuberculosis* infection in SLE is caused by a defective immune system and the treatment of immunosuppressive therapy, including high doses of corticosteroids. Normally the response to infection involves cellular immunity and in lupus patients this system is deficient, which is due to the features of the disease and the effects of immunosuppression (Agrawal and Prabu, 2010). The clinical presentation of tuberculosis and lupus may present with similar phenotypes and at times, mimic each other. The probability of lupus patients developing tuberculosis depends on the population prevalence and incidence of tuberculosis within a geographical area (Agrawal and Prabu, 2010). In some instances tuberculosis may precipitate lupus, especially in a genetically predisposed individual living in endemic areas (Ghosh et al., 2009).

Wadee and colleagues reported that in South African hospitals, death in lupus patients is mainly associated with infections and documented that three of the 18 infection-related deaths were due to tuberculosis (Wadee et al., 2007). A similar observation was demonstrated in lupus patients hospitalised in KwaZulu-Natal (Mody et al., 1994). In a retrospective review of tuberculosis in SLE patients from South Africa, they reported that 13.6% of all lupus and lupus-like patients contracted tuberculosis during the course of follow up, of which 26.4% had extra-pulmonary disease (Wadee et al., 2007).

It is interesting to speculate that there exists interplay on a biological level where the one disease precipitates the other and vice versa, and this may possibly lead to the identification of genes and pathways involved in both diseases.

Lastly, the work presented in this section of the work demonstrates a novel association with the regulatory variant, rs587585, located upstream of the *C1QA* gene. The associated genotype demonstrates an increased trend with elevated levels of C1qA in patients infected with *M. tuberculosis*. In any situation, there may be additional complement related genes and an undefined cluster of genes in close vicinity to the *C1Q* gene complex that may be involved in tuberculosis susceptibility and warrants further investigation.

6 Conclusion

Tuberculosis (TB) is one of the most ancient diseases known to mankind and has re-emerged in recent years as one of the leading causes of death worldwide. Mycobacterial pathogenesis is characterised by a high rate of infectivity and long periods of persistence without disease. The co-habitation of the mycobacterial and host immune cells, results in the regulation of sophisticated mechanisms that are advantageous to either the host or microbe. Defining these relationships offers rich opportunities to reveal relevant human-mycobacterial interactions. The elucidation of these mechanisms is critical in understanding how disease phenotypes manifest during infection. As such interactions can either facilitate or neutralise intracellular growth of the mycobacterium, the characterisation thereof provides new ventures for therapeutic strategies through the understanding of mycobacterial physiology and biological interactions that can be manipulated to control tuberculosis infection.

In this study, a systematic high-throughput technique called the yeast two-hybrid system was employed to identify host interacting binding partners of secretory antigens, ESAT-6 and CFP-10. Although our data demonstrated a high level of false positive hits, this study did identify at least two possible host interacting proteins of ESAT-6 and CFP-10, of which one was subsequently confirmed through *in vivo* and *in vitro* methods. This raised new questions and demonstrates the usefulness of the yeast two-hybrid assays, to capture potential protein-protein interactions. The opening hypothesis of this study was to gain insight into the functions of ESAT-6 and CFP-10, and their role in host-pathogen interactions. More specifically, we aimed to obtain some level of understanding on how *M. tuberculosis* evades immune responses and how secreted substrates regulate the host infection.

The results from this study illustrated the plausible interaction between ESAT-6 and the host protein, filamin A. This finding was confirmed using co-localisation and co-immunoprecipitation. The co-immunoprecipitation results showed that the majority of ESAT-6 interacting with filamin A associated with the membrane fraction, rather than the cell lysate. This observation is in agreement with literature validating the role of purified ESAT-6 from *M. tuberculosis* causing disruption and lysis of artificial lipid bilayers and liposomes by the interaction of ESAT-6 with host membranes (Hsu et al., 2003; de Jonge et al., 2007). Furthermore, ESAT-6 induced cleavage

of filamin A and we therefore suggest that ESAT-6 influences the dynamics of cytoskeletal proteins for intracellular survival, as was previously observed in *Salmonella*, *Yersinia*, *Shigella* and *Eschericia coli* (Hestvik et al., 2005). In addition, we emphasise the role of ESAT-6 in influencing cell death pathways in order to replicate and spread. From these results, we conclude that the release of ESAT-6 into the cytosol of infected cells and induction of cell death are events which are not mutually exclusive and are prerequisites for cell-to-cell spread. Furthermore, we hypothesise that during the release the interaction between ESAT-6 and filamin A weakens the cytoskeletal structure by inducing structural degradation of filamin A. This study, together with others (Lee et al., 2011; Simeone et al., 2012), highlights the importance of understanding the molecular events whereby *M. tuberculosis* manipulate and control cell death pathways, which can be exploited to gain insight into new approaches to control tuberculosis infection.

In addition to the research question to identify host targets that interact with secretory substrates of *M. tuberculosis*, we designed an additional study to investigate the identified binding partners (filamin A and C1QA) as possible genetic markers for susceptibility studies to tuberculosis. A case-control study involving 486 cases and 480 controls from the South African Coloured population within the Ravensmead-Uitsig area (an epidemiological field site near Cape Town) were selected to investigate the role of selected gene variants and tuberculosis susceptibility. In our analysis, we demonstrated a novel association of a regulatory variant located upstream of the *C1QA* gene. Furthermore, we stratified the control and tuberculosis patients according to the rs587585 genotype and demonstrated that the associated genotype displayed an increasing trend towards increased levels of C1q in tuberculosis patients. The complement system functions by providing the host with initial protection by promoting phagocytosis of apoptotic or necrotic cells. Consequently, the elevated levels of C1q as a result of the associated genotype may facilitate opsonisation of dead or dying cells, facilitating rapid uptake of *M. tuberculosis* into host cells via phagocytosis, and thereby escaping host immune responses. This is the first study to initiate the investigation of *C1Q* gene polymorphisms in tuberculosis susceptibility and presents as an interesting area for further research.

In an effort to better understand the results presented in this dissertation, the following future research should be considered.

To address and expand our knowledge of host-pathogen interactions, appropriate tools should be in place to strengthen the throughput of identifying PPIs. A weakness of the present study was the problem of out-of-frame constructs. Future studies should consider the use of Gateway vectors to address this problem. This technology, which was not available at the time when our study was initiated, uses site-specific recombination functions of phage λ. The bait insert or cDNA material is cloned into the donor (pDONR) vector. Using site-specific LR reactions, the sequences are shuttled into Gateway modified pGBKT7 or pGADT7 vectors (Figure 6.1 A & B). The recombination reactions are highly efficient, quick and simple. The addition of one and two nucleotides (Figure 6.1 C & D) enables correct expression of the bait and prey vectors in all three reading frames (Maier et al., 2008).

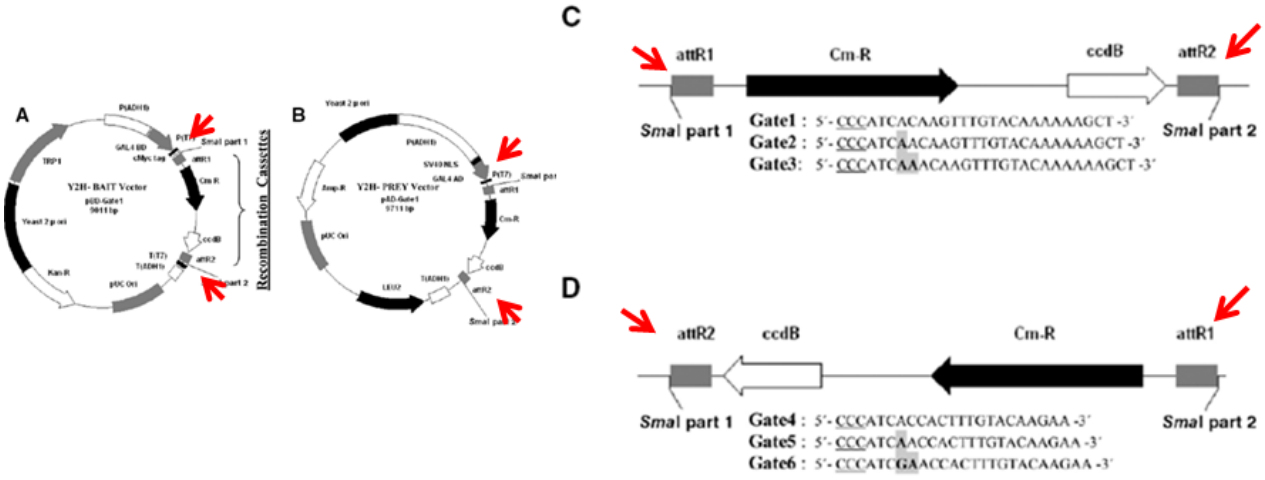

Figure 6.1: Illustration and description of the set of six Gateway-compatible yeast two-hybrid (Y2H) pGBKT7 bait vector (A) and pGADT7 prey vector (B). Each vector was constructed using blunt-end cloning using the three Gateway cassettes in forward (C) and reverse (D) direction into the original *Sma*I restriction site. The first part of the *Sma*I site is underlined and the bases inserted to shift the reading frame are highlighted in gray (Maier et al., 2008).

The modified Gateway Y2H vectors are fully functional and do not influence the selection system in yeast or activate transcription of reporter genes (Maier et al., 2008). The total number of positive transformants will be divided across three pGADT7 vectors via Gateway 1, 2 and 3 making this approach more laborious. However, this technique may increase the number of correct fusion proteins and therefore ultimately the number of in-frame interactions. As mentioned before, this technique was only published in 2008 and was not available when the

study commenced. It could therefore not be applied to the present study, since the experimental work was already well in progress when it became available.

The combination of Gateway vectors and appropriate mRNA for the construction of a screening library, in future, may increase the specificity and coverage of a cDNA library screen. The libraries prepared should be representative of the biological content of interest, as in the case of this study, using lung mRNA to construct a cDNA library. Future studies may also focus on mRNA extracted from *M. tuberculosis* infected macrophages or T-cells, to enrich the expression of mRNA transcripts specific to *M. tuberculosis* infection. The construction of such a library will be uniquely descriptive of the gene expression pattern that defines the response to *M. tuberculosis* infection.

The classical Y2H is created to reconstruct a transcription factor and is not suitable for proteins that can activate transcription. The use of such baits would trigger transcription and would not be ideal for screening purposes. In future, if bait vectors enable self-activation of selection genes (i.e. HIS3, ADE2 and MEL1); then alternative yeast two-hybrid methods should be considered.

Alternative systems to analyse proteins like these can be based on methods suppressing transcription, using an alternative polymerase III transcription pathway or the split-ubiquitin type-systems. However, all of the above systems require that interaction takes place in the nucleus, which is not suitable for membrane associated, integral membrane and soluble cytosolic proteins. Table 6.1 provides a brief description of the current available Y2H techniques to aid in choosing the right strategy and condition to increase the sensitivity of the Y2H screen for future studies (Brückner et al., 2009).

Table 6.1: Variations of Y2H systems and their specificities (Brückner et al., 2009).

Year	Y2H method	Possible baits	Response	Location
1989	Classical Y2H	Non-transactivating proteins capable of entering nucleus	Transcriptional activation	Nucleus
1994	SOS recruitment	Transactivating, cytosolic proteins	Ras signaling	Membrane periphery
1994	Split-ubiquitin	Nuclear, membrane and cytosolic proteins	Uracil auxotrophy and 5-FoA resistance	Cytosol
1998	Membrane split-ubiquitin	Membrane proteins	Transcriptional activation	Membrane periphery
1998	Ras recruitment	Transactivating, cytosolic	Ras signaling	Membrane
1999	Dual bait	Two non-transactivating proteins capable of entering nucleus	Transcriptional activation	Nucleus
2000	G-protein fusion	Membrane proteins	Inhibition of proteinG signaling	Membrane periphery
2001	RNA polymerase III based	Transactivating proteins (in the RNA pol II pathway)	Transcriptional activation	Nucleus
2001	Repressed transactivator	Transactivating proteins capable of entering nucleus	Inhibition of transcriptional activation	Nucleus
2001	Reverse Ras recruitment	Membrane proteins	Ras signaling	Membrane periphery
2003	SCINEX-P	Extracellular and transmembrane proteins	Downstream signaling and transcriptional activation	Endoplasmic reticulum (ER)
2004	Split-Trp	Cytosolic, membrane proteins	Trp1p activity	Cytosol
2007	Cytosolic split-ubiquitin	Transactivating, cytosolic proteins	Transcriptional activation	ER membrane periphery

Further work could also be done with regard to the further elucidation of the filamin A-ESAT-6 interactions. Since the results of the co-immunoprecipitation may consist of a subset of proteins belonging to a larger protein complex, future studies should aim to validate the direct protein-protein interaction between ESAT-6 and filamin A.

Experimentally, the precipitated protein complex could possibly be analysed by combining Blue Native (BN)-PAGE retardation assay and mass spectrometry analyses to identify interactions of biomolecules within a protein complex. Following the results of mass spectrometry, each identified target should be validated by *in vitro* methods to identify the true binding partner. This

approach would me more favourable since physiological host-pathogen interactions are more likely to occur in complexes and therefore the importance should not be disregarded.

Given that we observed DNA fragmentation of nuclei in cells treated with ESAT-6 and the evidence that ESAT-6 is involved in the induction of cell death pathways, future studies may focus on isolating nuclear RNA from tissue culture cells treated with ESAT-6 in a time course manner. The up and down regulated genes may then be extracted from the dataset to identify the biological pathways involved in the induction of cell death pathways, specific to mycobacterial infection. The information taken from this study may further promote our understanding of how *M. tuberculosis* manipulates host mechanisms in favour of itself.

Future studies should also be conducted to confirm the association between rs587585 and tuberculosis, by exploring the associations in other populations (i.e. Caucasians and Black individuals) before firm conclusions can be drawn on the true genetic association. Furthermore, additional *C1Q* polymorphisms should be genotyped in a larger sample cohort to increase coverage of the *C1Q* gene complex and to improve statistical power. In this study, rs587585 was associated with C1QA serum levels and since the function of this variant was not identified in this study, future studies should focus on confirming the levels of C1QA in a larger cohort of genotyped cases and controls to identify the true function of this variant. In addition, reporter gene assays should be considered to evaluate the promoter activity of rs587585 and the effect of gene expression of *C1QA*.

Given the evidence that lupus and tuberculosis may at times mimic each other (Agrawal and Prabu, 2010), it is interesting to speculate that genes and molecular pathways may exist that could explain the similarities between tuberculosis and lupus. Therefore, follow up studies should focus on investigating genes involved in the classical complement pathway (for example C1Q, C3 and C4) in TB, since numerous studies have focused on investigating the role of complement in SLE patients (Miura-Shimura et al., 2002; Martens et al., 2009; Namjou et al., 2009; Mok et al., 2010; Rafiq et al., 2010; Said et al., 2010; Hayakawa et al., 2011; Katsumata et al., 2011) and together with the existing body of evidence that document an increase in tuberculosis susceptibility among SLE patients, could therefore be a worthwhile research direction. This study should be designed to include significant SNP coverage of genes, a larger study cohort and the measurement of

serum complement levels of genes under investigation. Given the design of the study, it provides the possibility of investigating gene-gene interactions within the classical pathway.

In conclusion, the present study represents a noteworthy contribution to the field of host-pathogen interaction research. It identified at least one confirmed interaction of a mycobacterial virulence-associated protein with a host protein and paved the way to further investigate the physiological role of the interaction between ESAT-6 and filamin A. In addition, this study has initiated and demonstrated the novel role of complement related genes in tuberculosis susceptibility, which has unlocked exciting areas for additional research.

References

Abdallah, A. M., Gey van Pittius, N. C., Champion, P. A., Cox, J., Luirink, J., Vandenbroucke-Grauls, C. M., Appelmelk, B. J., and Bitter, W. (2007). Type VII secretion--mycobacteria show the way. Nat.Rev.Microbiol. *5*, 883-891.

Abebe, M., Kim, L., Rook, G., Aseffa, A., Wassie, L., Zewdie, M., Zumla, A., Engers, H., Andersen, P., and Doherty, T.M. (2011). Modulation of Cell Death by M. tuberculosis as a Strategy for Pathogen Survival. Clinical and Developmental Immunology 2011, 1–11.

Abel, B., Thieblemont, N., Quesniaux, V. J. F., Brown, N., Mpagi, J., Miyake, K., Bihl, F., and Ryffel, B. (2002). Toll-like receptor 4 expression is required to control chronic Mycobacterium tuberculosis infection in mice. J. Immunol. *169*, 3155-3162.

Adam, A., Petit, J. F., and Wietzerbin-Falszpan, J. (1969). L'acide N-glycolyl-muramique, constituant des parois de Mycobacterium smegmatis: Identification par spectrometrie de masse. FEBS letters *4*, 87-92.

Aderem, A., and Underhill, D. M. (1999). Mechanisms of phagocytosis in macrophages. Annual review of immunology *17*, 593–623.

Agrawal, S., and Prabu, V. . (2010). Systemic lupus erythematosus and tuberculosis: A review of complex interactions of complicated diseases. Journal of Postgraduate Medicine *56*, 244.

Ahmad, N. (2011). Stop TB strategy- DOTS. International Journal of Students' Research *1*, 16-18.

Akira, S., Uematsu, S., and Takeuchi, O. (2006). Pathogen recognition and innate immunity. Cell *124*, 783-801.

Alexander, K. A., Laver, P. N., Michel, A. L., Williams, M., van Helden, P. D., Warren, R. M., and Gey van Pittius, N. C. (2010). Novel Mycobacterium tuberculosis complex pathogen, M. mungi. Emerging Infect. Dis. *16*, 1296-1299.

Allen, L.-A. H. (2003). Mechanisms of pathogenesis: evasion of killing by polymorphonuclear leukocytes. Microbes Infect. *5*, 1329-1335.

Altare, F., Jouanguy, E., Lamhamedi, S., Döffinger, R., Fischer, A., and Casanova, J. L. (1998). Mendelian susceptibility to mycobacterial infection in man. Curr. Opin. Immunol. *10*, 413-417.

Anes, E., Kühnel, M. P., Bos, E., Moniz-Pereira, J., Habermann, A., and Griffiths, G. (2003). Selected lipids activate phagosome actin assembly and maturation resulting in killing of pathogenic mycobacteria. Nat. Cell Biol. *5*, 793-802.

Bafica, A., Scanga, C. A., Feng, C. G., Leifer, C., Cheever, A., and Sher, A. (2005). TLR9 regulates Th1 responses and cooperates with TLR2 in mediating optimal resistance to Mycobacterium tuberculosis. J Exp Med *202*, 1715-1724.

Barreiro, L. B., Neyrolles, O., Babb, C. L., Tailleux, L., Quach, H., McElreavey, K., Helden, P. D. van, Hoal, E. G., Gicquel, B., and Quintana-Murci, L. (2006). Promoter Variation in the DC-SIGN–Encoding Gene CD209 Is Associated with Tuberculosis. PLoS Med *3*, e20.

Beards, G. M., Campbell, A. D., Cottrell, N. R., Peiris, J. S., Rees, N., Sanders, R. C., Shirley, J. A., Wood, H. C., and Flewett, T. H. (1984). Enzyme-linked immunosorbent assays based on polyclonal and monoclonal antibodies for rotavirus detection. J Clin Microbiol *19*, 248-254.

Behr, M. A., Wilson, M. A., Gill, W. P., Salamon, H., Schoolnik, G. K., Rane, S., and Small, P. M. (1999). Comparative genomics of BCG vaccines by whole-genome DNA microarray. Science *284*, 1520-1523.

Bellamy, R., Beyers, N., McAdam, K. P., Ruwende, C., Gie, R., Samaai, P., Bester, D., Meyer, M., Corrah, T., Collin, M., et al. (2000). Genetic susceptibility to tuberculosis in Africans: a genome-wide scan. Proc. Natl. Acad. Sci. U.S.A. *97*, 8005-8009.

Bellamy, R., Ruwende, C., Corrah, T., McAdam, K. P., Thursz, M., Whittle, H. C., and Hill, A. V. (1999). Tuberculosis and chronic hepatitis B virus infection in Africans and variation in the vitamin D receptor gene. J. Infect. Dis. *179*, 721-724.

Bellamy, R., Ruwende, C., McAdam, K. P., Thursz, M., Sumiya, M., Summerfield, J., Gilbert, S. C., Corrah, T., Kwiatkowski, D., Whittle, H. C., et al. (1998). Mannose binding protein deficiency is not associated with malaria, hepatitis B carriage nor tuberculosis in Africans. QJM *91*, 13-18.

Bernardo, J., Billingslea, A. M., Blumenthal, R. L., Seetoo, K. F., Simons, E. R., and Fenton, M. J. (1998). Differential Responses of Human Mononuclear Phagocytes to Mycobacterial Lipoarabinomannans: Role of CD14 and the Mannose Receptor. Infect Immun *66*, 28-35.

Blackwell, J. M., Black, G. F., Peacock, C. S., Miller, E. N., Sibthorpe, D., Gnananandha, D., Shaw, J. J., Silveira, F., Lins-Lainson, Z., Ramos, F., et al. (1997). Immunogenetics of leishmanial and mycobacterial infections: the Belem Family Study. Philos. Trans. R. Soc. Lond., B, Biol. Sci. *352*, 1331-1345.

Blasco, B., Stenta, M., Alonso-Sarduy, L., Dietler, G., Peraro, M. D., Cole, S. T., and Pojer, F. (2011). Atypical DNA recognition mechanism used by the EspR virulence regulator of Mycobacterium tuberculosis. Molecular Microbiology *82*, 251-264.

Bowdish, D. M. E., Sakamoto, K., Kim, M.-J., Kroos, M., Mukhopadhyay, S., Leifer, C. A., Tryggvason, K., Gordon, S., and Russell, D. G. (2009). MARCO, TLR2, and CD14 Are Required for Macrophage Cytokine Responses to Mycobacterial Trehalose Dimycolate and Mycobacterium tuberculosis. PLoS Pathog *5*.

Brennan, P. J., and Nikaido, H. (1995). The envelope of mycobacteria. Annu. Rev. Biochem *64*, 29-63.

Briken, V. (2008). Molecular Mechanisms of Host-Pathogen Interactions and their Potential for the Discovery of New Drug Targets. Curr Drug Targets *9*, 150-157.

Brodin, P., de Jonge, M. I., Majlessi, L., Leclerc, C., Nilges, M., Cole, S. T., and Brosch, R. (2005). Functional analysis of early secreted antigenic target-6, the dominant T-cell antigen of Mycobacterium tuberculosis, reveals key residues involved in secretion, complex formation, virulence, and immunogenicity. J.Biol.Chem. *280*, 33953-33959.

Brooks, M. N., Rajaram, M. V. S., Azad, A. K., Amer, A. O., Valdivia-Arenas, M. A., Park, J.-H., Núñez, G., and Schlesinger, L. S. (2011). NOD2 controls the nature of the inflammatory response and subsequent fate of Mycobacterium tuberculosis and M. bovis BCG in human macrophages. Cellular Microbiology *13*, 402-418.

Brosch, R., Gordon, S. V., Buchrieser, C., Pym, A. S., Garnier, T., and Cole, S. T. (2000). Comparative genomics uncovers large tandem chromosomal duplications in Mycobacterium bovis BCG Pasteur. Yeast *17*, 111-123.

Brosch, R., Gordon, S. V., Garnier, T., Eiglmeier, K., Frigui, W., Valenti, P., Dos Santos, S., Duthoy, S., Lacroix, C., Garcia-Pelayo, C., et al. (2007). Genome plasticity of BCG and impact on vaccine efficacy. Proc. Natl. Acad. Sci. U.S.A. *104*, 5596-5601.

Brückner, A., Polge, C., Lentze, N., Auerbach, D., and Schlattner, U. (2009). Yeast two-hybrid, a powerful tool for systems biology. Int J Mol Sci *10*, 2763-2788.

Brueggemann, A. B., Griffiths, D. T., Meats, E., Peto, T., Crook, D. W., and Spratt, B. G. (2003). Clonal relationships between invasive and carriage Streptococcus pneumoniae and serotype- and clone-specific differences in invasive disease potential. J. Infect. Dis. *187*, 1424-1432.

Bulut, Y., Michelsen, K. S., Hayrapetian, L., Naiki, Y., Spallek, R., Singh, M., and Arditi, M. (2005). Mycobacterium tuberculosis heat shock proteins use diverse Toll-like receptor pathways to activate pro-inflammatory signals. J. Biol. Chem. *280*, 20961-20967.

Campbell, H., and Rudan, I. (2002). Interpretation of genetic association studies in complex disease. Pharmacogenomics J *2*, 349-360.

Carlson, T. K., Torrelles, J. B., Smith, K., Horlacher, T., Castelli, R., Seeberger, P. H., Crouch, E. C., and Schlesinger, L. S. (2009). Critical role of amino acid position 343 of surfactant protein-D in the selective binding of glycolipids from Mycobacterium tuberculosis. Glycobiology *19*, 1473-1484.

Caron, E., and Hall, A. (1998). Identification of two distinct mechanisms of phagocytosis controlled by different Rho GTPases. Science *282*, 1717-1721.

Carroll, M.V., Lack, N., Sim, E., Krarup, A., and Sim, R.B., (2009) Multiple routes of complement activation by Mycobacterium bovis BCG. Mol Immunol. 46, 3367-3378.

Casanova, J.-L., and Abel, L. (2002). Genetic dissection of immunity to mycobacteria: the human model. Annu. Rev. Immunol. *20*, 581-620.

Chaisson, R. E., and Martinson, N. A. (2008). Tuberculosis in Africa--combating an HIV-driven crisis. N. Engl. J. Med. *358*, 1089-1092.

Chamaillard, M., Hashimoto, M., Horie, Y., Masumoto, J., Qiu, S., Saab, L., Ogura, Y., Kawasaki, A., Fukase, K., Kusumoto, S., et al. (2003). An essential role for NOD1 in host recognition of bacterial peptidoglycan containing diaminopimelic acid. Nat. Immunol. *4*, 702-707.

Champion, P. A. D., Stanley, S. A., Champion, M. M., Brown, E. J., and Cox, J. S. (2006). C-terminal signal sequence promotes virulence factor secretion in Mycobacterium tuberculosis. Science *313*, 1632-1636.

Cole, S. T., Brosch, R., Parkhill, J., Garnier, T., Churcher, C., Harris, D., Gordon, S. V., Eiglmeier, K., Gas, S., Barry, C. E., et al. (1998). Deciphering the biology of Mycobacterium tuberculosis from the complete genome sequence. Nature *393*, 537-544.

Comas, I., and Gagneux, S. (2011). A role for systems epidemiology in tuberculosis research. Trends in Microbiology. Available at: http://www.cell.com/trends/microbiology/abstract/S0966-842X(11)00139-9 [Accessed September 19, 2011].

Comas, I., and Gagneux, S. (2009). The past and future of tuberculosis research. PLoS.Pathog. *5*, e1000600.

Comstock, G. W. (1978). Tuberculosis in twins: a re-analysis of the Prophit survey. Am. Rev. Respir. Dis. *117*, 621-624.

Cooper, A. M. (2009). Cell-Mediated Immune Responses in Tuberculosis. Annual Review of Immunology *27*, 393-422.

Coscolla, M., and Gagneux, S. (2010). Does M. tuberculosis genomic diversity explain disease diversity? Drug Discov Today Dis Mech *7*, e43-e59.

Cossart, P., and Roy, C. R. (2010). Manipulation of host membrane machinery by bacterial pathogens. Curr Opin Cell Biol *22*, 547-554.

Coulombe, F., Divangahi, M., Veyrier, F., de Léséleuc, L., Gleason, J. L., Yang, Y., Kelliher, M. A., Pandey, A. K., Sassetti, C. M., Reed, M. B., et al. (2009). Increased NOD2-mediated recognition of N-glycolyl muramyl dipeptide. The Journal of Experimental Medicine *206*, 1709 -1716.

van Crevel, R., Ottenhoff, T. H. M., and van der Meer, J. W. M. (2002). Innate Immunity to Mycobacterium tuberculosis. Clinical Microbiology Reviews *15*, 294 -309.

Das, C., Ghosh, T. S., and Mande, S. S. (2011). Computational Analysis of the ESX-1 Region of Mycobacterium tuberculosis: Insights into the Mechanism of Type VII Secretion System. PLoS ONE *6*, e27980.

Davila, S., Hibberd, M. L., Hari Dass, R., Wong, H. E. E., Sahiratmadja, E., Bonnard, C., Alisjahbana, B., Szeszko, J. S., Balabanova, Y., Drobniewski, F., et al. (2008). Genetic association and expression studies indicate a role of toll-like receptor 8 in pulmonary tuberculosis. PLoS Genet. *4*, e1000218.

Davis, F. P., Barkan, D. T., Eswar, N., McKerrow, J. H., and Sali, A. (2007). Host pathogen protein interactions predicted by comparative modeling. Protein Sci. *16*, 2585-2596.

Deretic, V., Singh, S., Master, S., Harris, J., Roberts, E., Kyei, G., Davis, A., de Haro, S., Naylor, J., Lee, H.-H., et al. (2006). Mycobacterium tuberculosis inhibition of phagolysosome biogenesis and autophagy as a host defence mechanism. Cell. Microbiol *8*, 719-727.

Derrick, S.C., and Morris, S.L. (2007). The ESAT6 protein of Mycobacterium tuberculosis induces apoptosis of macrophages by activating caspase expression. Cellular Microbiology 9, 1547–1555.

de Wit, E., Delport, W., Rugamika, C.E., Meintjes, A., Möller, M., van Helden, P.D., Seoighe, C., and Hoal, E.G. (2010). Genome-wide analysis of the structure of the South African Coloured Population in the Western Cape. 145–153.

DiGiuseppe Champion, P. A., Champion, M. M., Manzanillo, P., and Cox, J. S. (2009). ESX-1 secreted virulence factors are recognized by multiple cytosolic AAA ATPases in pathogenic mycobacteria. Mol. Microbiol. *73*, 950-962.

Dillon, S. P., D'Souza, A., Kurien, B. T., and Scofield, R. H. (2009). SLE and C1q: A quantitative ELISA for determining C1q levels in serum. Biotechnol J *4*, 1210-1214.

Downing, J. F., Pasula, R., Wright, J. R., Twigg, H. L., 3rd, and Martin, W. J., 2nd (1995). Surfactant protein a promotes attachment of Mycobacterium tuberculosis to alveolar macrophages during infection with human immunodeficiency virus. Proc. Natl. Acad. Sci. U.S.A. *92*, 4848-4852.

Drecktrah, D., Knodler, L. A., Howe, D., and Steele-Mortimer, O. (2007). Salmonella Trafficking is Defined by Continuous Dynamic Interactions with the Endolysosomal System. Traffic *8*, 212-225.

Drennan, M. B., Nicolle, D., Quesniaux, V. J. F., Jacobs, M., Allie, N., Mpagi, J., Frémond, C., Wagner, H., Kirschning, C., and Ryffel, B. (2004). Toll-like receptor 2-deficient mice succumb to Mycobacterium tuberculosis infection. Am. J. Pathol. *164*, 49-57.

Dubos, J. (1986). The White Plague: Tuberculosis, Man and Society (Rutgers University Press).

Duclos, S., and Desjardins, M. (2000). Subversion of a young phagosome: the survival strategies of intracellular pathogens. Cell. Microbiol *2*, 365-377.

Dufner, A., Pownall, S., and Mak, T. W. (2006). Caspase recruitment domain protein 6 is a microtubule-interacting protein that positively modulates NF-kappaB activation. Proc. Natl. Acad. Sci. U.S.A. *103*, 988-993.

Dunne, D. W., Resnick, D., Greenberg, J., Krieger, M., and Joiner, K. A. (1994). The type I macrophage scavenger receptor binds to gram-positive bacteria and recognizes lipoteichoic acid. Proc. Natl. Acad. Sci. U.S.A. *91*, 1863-1867.

Dunsmore, S. E., and Rannels, D. E. (1996). Extracellular matrix biology in the lung. Am. J. Physiol. *270*, L3-27.

Dye, C., and Floyd, K. (2006). Chapter 16 - Tuberculosis. In Disease Control Priorities in Developing Countries, 2nd edition (Washington DC: World Bank; Oxford University Press USA), pp. 289-309.

van der Eijk, E. A., van de Vosse, E., Vandenbroucke, J. P., and van Dissel, J. T. (2007). Heredity versus Environment in Tuberculosis in Twins: The 1950s United Kingdom Prophit Survey Simonds and Comstock Revisited. Am. J. Respir. Crit. Care Med. *176*, 1281-1288.

El, G. M., Bouhss, A., Blanot, D., and Mengin-Lecreulx, D. (2004). The bacA gene of Escherichia coli encodes an undecaprenyl pyrophosphate phosphatase activity. J.Biol.Chem. *279*, 30106-30113.

Ernst, J. D. (1998). Macrophage receptors for Mycobacterium tuberculosis. Infect. Immun *66*, 1277-1281.

Feltcher, M. E., Sullivan, J. T., and Braunstein, M. (2010). Protein export systems of Mycobacterium tuberculosis: novel targets for drug development? Future Microbiol *5*, 1581-1597.

Feng, Y., and Walsh, C. A. (2004). The many faces of filamin: a versatile molecular scaffold for cell motility and signalling. Nat.Cell Biol. *6*, 1034-1038.

Ferguson, J. S., and Schlesinger, L. S. (2000). Pulmonary surfactant in innate immunity and the pathogenesis of tuberculosis. Tuber. Lung Dis. *80*, 173-184.

Ferguson, J. S., Martin, J. L., Azad, A. K., McCarthy, T. R., Kang, P. B., Voelker, D. R., Crouch, E. C., and Schlesinger, L. S. (2006). Surfactant protein D increases fusion of Mycobacterium tuberculosis-containing phagosomes with lysosomes in human macrophages. Infect. Immun. *74*, 7005-7009.

Ferguson, J. S., Voelker, D. R., McCormack, F. X., and Schlesinger, L. S. (1999). Surfactant protein D binds to Mycobacterium tuberculosis bacilli and lipoarabinomannan via carbohydrate-lectin interactions resulting in reduced phagocytosis of the bacteria by macrophages. J. Immunol. *163*, 312-321.

Ferguson, J. S., Weis, J. J., Martin, J. L., and Schlesinger, L. S. (2004). Complement protein C3 binding to Mycobacterium tuberculosis is initiated by the classical pathway in human bronchoalveolar lavage fluid. Infect.Immun. *72*, 2564-2573.

Ferrari, G., Langen, H., Naito, M., and Pieters, J. (1999). A coat protein on phagosomes involved in the intracellular survival of mycobacteria. Cell *97*, 435-447.

Fieschi, C., Dupuis, S., Catherinot, E., Feinberg, J., Bustamante, J., Breiman, A., Altare, F., Baretto, R., Le Deist, F., Kayal, S., et al. (2003). Low penetrance, broad resistance, and favorable outcome of interleukin 12 receptor beta1 deficiency: medical and immunological implications. J. Exp. Med. *197*, 527-535.

Filipe-Santos, O., Bustamante, J., Chapgier, A., Vogt, G., de Beaucoudrey, L., Feinberg, J., Jouanguy, E., Boisson-Dupuis, S., Fieschi, C., Picard, C., et al. (2006). Inborn errors of IL-12/23- and IFN-gamma-mediated immunity: molecular, cellular, and clinical features. Semin. Immunol. *18*, 347-361.

Flynn, J. L., and Chan, J. (2001). I MMUNOLOGY OF T UBERCULOSIS. Annual Review of Immunology *19*, 93-129.

Forton, J. T., Udalova, I. A., Campino, S., Rockett, K. A., Hull, J., and Kwiatkowski, D. P. (2007). Localization of a long-range cis-regulatory element of IL13 by allelic transcript ratio mapping. Genome Res. *17*, 82-87.

Fortune, S. M., Jaeger, A., Sarracino, D. A., Chase, M. R., Sassetti, C. M., Sherman, D. R., Bloom, B. R., and Rubin, E. J. (2005). Mutually dependent secretion of proteins required for mycobacterial virulence. Proc. Natl. Acad. Sci. U.S.A. *102*, 10676-10681.

Fransen, F., Heckenberg, S. G. B., Hamstra, H. J., Feller, M., Boog, C. J. P., van Putten, J. P. M., van de Beek, D., van der Ende, A., and van der Ley, P. (2009). Naturally occurring lipid A mutants in neisseria meningitidis from patients with invasive meningococcal disease are associated with reduced coagulopathy. PLoS Pathog. *5*, e1000396.

Fratti, R. A., Chua, J., Vergne, I., and Deretic, V. (2003). Mycobacterium tuberculosis glycosylated phosphatidylinositol causes phagosome maturation arrest. Proc.Natl.Acad.Sci.U.S.A *100*, 5437-5442.

Frigui, W., Bottai, D., Majlessi, L., Monot, M., Josselin, E., Brodin, P., Garnier, T., Gicquel, B., Martin, C., Leclerc, C., et al. (2008). Control of M. tuberculosis ESAT-6 secretion and specific T cell recognition by PhoP. PLoS Pathog. *4*, e33.

Gagneux, S., and Small, P. M. (2007). Global phylogeography of Mycobacterium tuberculosis and implications for tuberculosis product development. Lancet Infect Dis *7*, 328-337.

Gagneux, S., DeRiemer, K., Van, T., Kato-Maeda, M., de Jong, B. C., Narayanan, S., Nicol, M., Niemann, S., Kremer, K., Gutierrez, M. C., et al. (2006). Variable host–pathogen compatibility in Mycobacterium tuberculosis. Proceedings of the National Academy of Sciences of the United States of America *103*, 2869 -2873.

Ganguly, N., Siddiqui, I., and Sharma, P. (2008). Role of M. tuberculosis RD-1 region encoded secretory proteins in protective response and virulence. Tuberculosis (Edinb) *88*, 510-517.

Gao, L. Y., Guo, S., McLaughlin, B., Morisaki, H., Engel, J. N., and Brown, E. J. (2004). A mycobacterial virulence gene cluster extending RD1 is required for cytolysis, bacterial spreading and ESAT-6 secretion. Mol.Microbiol. *53*, 1677-1693.

Gatfield, J., and Pieters, J. (2000). Essential role for cholesterol in entry of mycobacteria into macrophages. Science *288*, 1647-1650.

Gehring, A. J., Dobos, K. M., Belisle, J. T., Harding, C. V., and Boom, W. H. (2004). Mycobacterium tuberculosis LprG (Rv1411c): a novel TLR-2 ligand that inhibits human macrophage class II MHC antigen processing. J. Immunol. *173*, 2660-2668.

Geldmacher, C., Zumla, A., and Hoelscher, M. (2012). Interaction between HIV and Mycobacterium tuberculosis: HIV-1-induced CD4 T-cell depletion and the development of active tuberculosis. Curr Opin HIV AIDS 7, 268–275.

Gey van Pittius, N. C., Gamieldien, J., Hide, W., Brown, G. D., Siezen, R. J., and Beyers, A. D. (2001). The ESAT-6 gene cluster of Mycobacterium tuberculosis and other high G+C Gram-positive bacteria. Genome Biol *2*, research0044.1-research0044.18.

Ghosh, K., Patwardhan, M., and Pradhan, V. (2009). Mycobacterium tuberculosis infection precipitates SLE in patients from endemic areas. Rheumatology International *29*, 1047-1050.

Gietz, R. D., and Woods, R. A. (2005). Yeast Transformation by the LiAc/SS Carrier DNA/PEG Method. In Yeast Protocols (New Jersey: Humana Press), pp. 107-120. Available at: http://www.springerprotocols.com/Full/doi/10.1385/1-59259-958-3:107?encCode=Q0lNOjcwMTozLTg1OS05NTI5NS0x&tokenString=VakU7kkxmMT93eggGCi7ag==&access=denied [Accessed April 24, 2011].

Girardin, S. E., Boneca, I. G., Viala, J., Chamaillard, M., Labigne, A., Thomas, G., Philpott, D. J., and Sansonetti, P. J. (2003). Nod2 Is a General Sensor of Peptidoglycan through Muramyl Dipeptide (MDP) Detection. Journal of Biological Chemistry *278*, 8869 -8872.

Gomes, M. G. M., Franco, A. O., Gomes, M. C., and Medley, G. F. (2004). The reinfection threshold promotes variability in tuberculosis epidemiology and vaccine efficacy. Proc Biol Sci *271*, 617-623.

Greenwood, C. M., Fujiwara, T. M., Boothroyd, L. J., Miller, M. A., Frappier, D., Fanning, E. A., Schurr, E., and Morgan, K. (2000). Linkage of tuberculosis to chromosome 2q35 loci, including NRAMP1, in a large aboriginal Canadian family. Am. J. Hum. Genet. *67*, 405-416.

Guinn, K. M., Hickey, M. J., Mathur, S. K., Zakel, K. L., Grotzke, J. E., Lewinsohn, D. M., Smith, S., and Sherman, D. R. (2004). Individual RD1-region genes are required for export of ESAT-6/CFP-10 and for virulence of Mycobacterium tuberculosis. Mol.Microbiol. *51*, 359-370.

Guérin, I., and de Chastellier, C. (2000). Disruption of the actin filament network affects delivery of endocytic contents marker to phagosomes with early endosome characteristics: The case of phagosomes with pathogenic mycobacteria. Eur J Cell Biol. 735–749.

Guo, J., Zheng, X., Xu, L., Liu, Z., Xu, K., Li, S., Wen, T., Liu, S., and Pang, H. (2010). Characterization of a novel esterase Rv0045c from Mycobacterium tuberculosis. PLoS ONE *5*. Available at: http://www.ncbi.nlm.nih.gov/pubmed/20957207 [Accessed September 24, 2011].

Gustincich, S., Manfioletti, G., Del Sal, G., Schneider, C., and Carninci, P. (1991). A fast method for high-quality genomic DNA extraction from whole human blood. BioTechniques 11, 298–300, 302.

Haberzettl, P., Schins, R. P. F., Höhr, D., Wilhelmi, V., Borm, P. J. A., and Albrecht, C. (2008). Impact of the FcγII-receptor on quartz uptake and inflammatory response by alveolar macrophages. American Journal of Physiology - Lung Cellular and Molecular Physiology *294*, L1137 -L1148.

Havlir, D.V., and Barnes, P.F. (1999). Tuberculosis in patients with human immunodeficiency virus infection. N. Engl. J. Med. 340, 367–373.

Hart, G. T., Ramani, A. K., and Marcotte, E. M. (2006). How complete are current yeast and human protein-interaction networks? Genome Biol. *7*, 120.

Hayakawa, J., Migita, M., Ueda, T., Itoh, Y., and Fukunaga, Y. (2011). An infantile case of early manifestation of SLE-like symptoms in complete C1q deficiency. J Nippon Med Sch. *78*, 322-328.

Hayashi, K., and Altman, A. (2006). Filamin A is required for T cell activation mediated by protein kinase C-theta. J.Immunol. *177*, 1721-1728.

Heil, F., Hemmi, H., Hochrein, H., Ampenberger, F., Kirschning, C., Akira, S., Lipford, G., Wagner, H., and Bauer, S. (2004). Species-Specific Recognition of Single-Stranded RNA via Toll-like Receptor 7 and 8. Science *303*, 1526 -1529.

Hemmi, H., Takeuchi, O., Kawai, T., Kaisho, T., Sato, S., Sanjo, H., Matsumoto, M., Hoshino, K., Wagner, H., Takeda, K., et al. (2000). A Toll-like receptor recognizes bacterial DNA. Nature *408*, 740-745.

Hoal-Van Helden, E. G., Epstein, J., Victor, T. C., Hon, D., Lewis, L. A., Beyers, N., Zurakowski, D., Ezekowitz, A. B., and Van Helden, P. D. (1999). Mannose-binding protein B allele confers protection against tuberculous meningitis. Pediatr. Res. *45*, 459-464.

Horn, C., Namane, A., Pescher, P., Rivière, M., Romain, F., Puzo, G., Bârzu, O., and Marchal, G. (1999). Decreased capacity of recombinant 45/47-kDa molecules (Apa) of Mycobacterium tuberculosis to stimulate T lymphocyte responses related to changes in their mannosylation pattern. J. Biol. Chem. *274*, 32023-32030.

Hou, B., Reizis, B., and DeFranco, A. L. (2008). Toll-like Receptors Activate Innate and Adaptive Immunity by using Dendritic Cell-Intrinsic and -Extrinsic Mechanisms. Immunity *29*, 272-282.

Hsu, T., Hingley-Wilson, S. M., Chen, B., Chen, M., Dai, A. Z., Morin, P. M., Marks, C. B., Padiyar, J., Goulding, C., Gingery, M., et al. (2003). The primary mechanism of attenuation of bacillus Calmette-Guerin is a loss of secreted lytic function required for invasion of lung interstitial tissue. Proc.Natl.Acad.Sci.U.S.A *100*, 12420-12425.

Hu, C., Mayadas-Norton, T., Tanaka, K., Chan, J., and Salgame, P. (2000). Mycobacterium tuberculosis Infection in Complement Receptor 3-Deficient Mice. The Journal of Immunology *165*, 2596 - 2602.

Jayachandran, R., Sundaramurthy, V., Combaluzier, B., Mueller, P., Korf, H., Huygen, K., Miyazaki, T., Albrecht, I., Massner, J., and Pieters, J. (2007). Survival of mycobacteria in macrophages is mediated by coronin 1-dependent activation of calcineurin. Cell *130*, 37-50.

Jiménez-Baranda, S., Gómez-Moutón, C., Rojas, A., Martínez-Prats, L., Mira, E., Ana Lacalle, R., Valencia, A., Dimitrov, D. S., Viola, A., Delgado, R., et al. (2007). Filamin-A regulates actin-dependent clustering of HIV receptors. Nat. Cell Biol. *9*, 838-846.

Jones, B. W., Means, T. K., Heldwein, K. A., Keen, M. A., Hill, P. J., Belisle, J. T., and Fenton, M. J. (2001). Different Toll-like receptor agonists induce distinct macrophage responses. J. Leukoc. Biol. *69*, 1036-1044.

de Jong, B. C., Hill, P. C., Aiken, A., Awine, T., Antonio, M., Adetifa, I. M., Jackson-Sillah, D. J., Fox, A., Deriemer, K., Gagneux, S., et al. (2008). Progression to active tuberculosis, but not transmission, varies by Mycobacterium tuberculosis lineage in The Gambia. J. Infect. Dis. *198*, 1037-1043.

de Jonge, M. I., Pehau-Arnaudet, G., Fretz, M. M., Romain, F., Bottai, D., Brodin, P., Honore, N., Marchal, G., Jiskoot, W., England, P., et al. (2007). ESAT-6 from Mycobacterium tuberculosis dissociates from its putative chaperone CFP-10 under acidic conditions and exhibits membrane-lysing activity. J.Bacteriol. *189*, 6028-6034.

Kapetanovic, R., and Cavaillon, J.-M. (2007). Early events in innate immunity in the recognition of microbial pathogens. Expert Opin Biol Ther *7*, 907-918.

Kapogiannis, B. G., Satola, S., Keyserling, H. L., and Farley, M. M. (2005). Invasive infections with Haemophilus influenzae serotype a containing an IS1016-bexA partial deletion: possible association with virulence. Clin. Infect. Dis. *41*, e97-103.

Karaolis, D. K., Johnson, J. A., Bailey, C. C., Boedeker, E. C., Kaper, J. B., and Reeves, P. R. (1998). A Vibrio cholerae pathogenicity island associated with epidemic and pandemic strains. Proc. Natl. Acad. Sci. U.S.A. *95*, 3134-3139.

Karp, C. L., Wysocka, M., Wahl, L. M., Ahearn, J. M., Cuomo, P. J., Sherry, B., Trinchieri, G., and Griffin, D. E. (1996). Mechanism of suppression of cell-mediated immunity by measles virus. Science *273*, 228-231.

Katsumata, Y., Miyake, K., Kawaguchi, Y., Okamoto, Y., Kawamoto, M., Gono, T., Baba, S., Hara, M., and Yamanaka, H. (2011). Anti-C1q antibodies are associated with systemic lupus erythematosus global activity but not specifically with nephritis: a controlled study of 126 consecutive patients. Arthritis Rheum. *63*, 2436-2444.

Kaufmann, S. H. E. (2011). Intracellular pathogens: living in an extreme environment. Immunological Reviews *240*, 5-10.

Kaufmann, S. H. E., and Parida, S. K. (2007). Changing funding patterns in tuberculosis. Nat Med *13*, 299-303.

Kaufmann, S.H. (1989). Induction of endonucleolytic DNA cleavage in human acute myelogenous leukemia cells by etoposide, camptothecin, and other cytotoxic anticancer drugs: a cautionary note. Cancer Res. 49, 5870–5878.

Kawai, T., and Akira, S. (2010). The role of pattern-recognition receptors in innate immunity: update on Toll-like receptors. Nat Immunol *11*, 373-384.

Keane, J., Balcewicz-Sablinska, M.K., Remold, H.G., Chupp, G.L., Meek, B.B., Fenton, M.J., and Kornfeld, H. (1997). Infection by Mycobacterium tuberculosis promotes human alveolar macrophage apoptosis. Infect. Immun. 65, 298–304.

Keane, J., Remold, H. G., and Kornfeld, H. (2000). Virulent Mycobacterium tuberculosis Strains Evade Apoptosis of Infected Alveolar Macrophages. The Journal of Immunology *164*, 2016 -2020.

Kinhikar, A. G., Verma, I., Chandra, D., Singh, K. K., Weldingh, K., Andersen, P., Hsu, T., Jacobs, W. R., and Laal, S. (2010). Potential role for ESAT6 in dissemination of M. tuberculosis via human lung epithelial cells. Mol.Microbiol. *75*, 92-106.

Kleinnijenhuis, J., Joosten, L. A. B., van de Veerdonk, F. L., Savage, N., van Crevel, R., Kullberg, B. J., van der Ven, A., Ottenhoff, T. H. M., Dinarello, C. A., van der Meer, J. W. M., et al. (2009). Transcriptional and inflammasome-mediated pathways for the induction of IL-1beta production by Mycobacterium tuberculosis. Eur. J. Immunol. *39*, 1914-1922.

Kleinnijenhuis, J., Oosting, M., Joosten, L. A. B., Netea, M. G., and Van Crevel, R. (2011). Innate immune recognition of Mycobacterium tuberculosis. Clin. Dev. Immunol. *2011*, 405310.

Krieger, M., Acton, S., Ashkenas, J., Pearson, A., Penman, M., and Resnick, D. (1993). Molecular flypaper, host defense, and atherosclerosis. Structure, binding properties, and functions of macrophage scavenger receptors. J. Biol. Chem. *268*, 4569-4572.

Krogh, A., Larsson, B., von Heijne, G., and Sonnhammer, E. L. (2001). Predicting transmembrane protein topology with a hidden Markov model: application to complete genomes. J. Mol. Biol. *305*, 567-580.

Kumar, D., Nath, L., Kamal, M. A., Varshney, A., Jain, A., Singh, S., and Rao, K. V. S. (2010). Genome-wide analysis of the host intracellular network that regulates survival of Mycobacterium tuberculosis. Cell *140*, 731-743.

Kumar, K., Tharad, M., Ganapathy, S., Ram, G., Narayan, A., Khan, J. A., Pratap, R., Ghosh, A., Samuchiwal, S. K., Kumar, S., et al. (2009). Phenylalanine-rich peptides potently bind ESAT6, a virulence determinant of Mycobacterium tuberculosis, and concurrently affect the pathogen's growth. PLoS ONE *4*, e7615.

Kumar, R., and Nanduri, B. (2010). HPIDB - a unified resource for host-pathogen interactions. BMC Bioinformatics *11*, S16.

Kumar, Y., and Valdivia, R. H. (2009). Leading a sheltered life: intracellular pathogens and maintenance of vacuolar compartments. Cell Host Microbe *5*, 593-601.

Kumararatne, D. S. (2006). Mendelian susceptibility to mycobacterial disease. Respiration *73*, 280-282.

Kyei, G. B., Vergne, I., Chua, J., Roberts, E., Harris, J., Junutula, J. R., and Deretic, V. (2006). Rab14 is critical for maintenance of Mycobacterium tuberculosis phagosome maturation arrest. EMBO J. *25*, 5250-5259.

Lee, B.-Y., Clemens, D. L., and Horwitz, M. A. (2008). The metabolic activity of Mycobacterium tuberculosis, assessed by use of a novel inducible GFP expression system, correlates with its

capacity to inhibit phagosomal maturation and acidification in human macrophages. Mol. Microbiol. *68*, 1047-1060.

Lee, J., Repasy, T., Papavinasasundaram, K., Sassetti, C., and Kornfeld, H. (2011). Mycobacterium tuberculosis induces an atypical cell death mode to escape from infected macrophages. PLoS ONE *6*, e18367.

Lewinsohn, D. M., Grotzke, J. E., Heinzel, A. S., Zhu, L., Ovendale, P. J., Johnson, M., and Alderson, M. R. (2006). Secreted Proteins from Mycobacterium tuberculosis Gain Access to the Cytosolic MHC Class-I Antigen-Processing Pathway. The Journal of Immunology *177*, 437 -442.

Li, Q., and Cherayil, B. J. (2004). Toll-like receptor 4 mutation impairs the macrophage TNFalpha response to peptidoglycan. Biochem. Biophys. Res. Commun. *325*, 91-96.

Lightbody, K. L., Ilghari, D., Waters, L. C., Carey, G., Bailey, M. A., Williamson, R. A., Renshaw, P. S., and Carr, M. D. (2008). Molecular features governing the stability and specificity of functional complex formation by Mycobacterium tuberculosis CFP-10/ESAT-6 family proteins. J. Biol. Chem. *283*, 17681-17690.

Lightbody, K., Renshaw, P., Collins, M., Wright, R., Hunt, D., Gordon, S., Hewinson, R., Buxton, R., Williamson, R., and Carr, M. (2004). Characterisation of complex formation between members of the complex CFP-10/ESAT-6 protein family: towards an understanding of the rules governing complex formation and thereby functional flexibility. FEMS Microbiology Letters *238*, 255-262.

Ligon, B. L. (2002). Robert Koch: Nobel laureate and controversial figure in tuberculin research. Semin Pediatr Infect Dis *13*, 289-299.

Lin, R., Karpa, K., Kabbani, N., Goldman-Rakic, P., and Levenson, R. (2001). Dopamine D2 and D3 receptors are linked to the actin cytoskeleton via interaction with filamin A. Proceedings of the National Academy of Sciences *98*, 5258 -5263.

Lönnroth, K., Jaramillo, E., Williams, B. G., Dye, C., and Raviglione, M. (2009). Drivers of tuberculosis epidemics: the role of risk factors and social determinants. Soc Sci Med *68*, 2240-2246.

Luthra, A., Mahmood, A., Arora, A., and Ramachandran, R. (2008). Characterization of Rv3868, an essential hypothetical protein of the ESX-1 secretion system in Mycobacterium tuberculosis. J. Biol. Chem. *283*, 36532-36541.

MacGurn, J. A., Raghavan, S., Stanley, S. A., and Cox, J. S. (2005). A non-RD1 gene cluster is required for Snm secretion in Mycobacterium tuberculosis. Mol. Microbiol. *57*, 1653-1663.

MacMicking, J. D., Taylor, G. A., and McKinney, J. D. (2003). Immune control of tuberculosis by IFN-gamma-inducible LRG-47. Science *302*, 654-659.

Maglione, P. J., Xu, J., Casadevall, A., and Chan, J. (2008a). Fc gamma receptors regulate immune activation and susceptibility during Mycobacterium tuberculosis infection. J. Immunol *180*, 3329-3338.

Mahairas, G. G., Sabo, P. J., Hickey, M. J., Singh, D. C., and Stover, C. K. (1996). Molecular analysis of genetic differences between Mycobacterium bovis BCG and virulent M. bovis. J. Bacteriol. *178*, 1274-1282.

Maier, R., Brandner, C., Hintner, H., Bauer, J., and Onder, K. (2008). Construction of a reading frame-independent yeast two-hybrid vector system for site-specific recombinational cloning and protein interaction screening. BioTechniques *45*, 235-244.

Manca, C., Reed, M. B., Freeman, S., Mathema, B., Kreiswirth, B., Barry, C. E., and Kaplan, G. (2004). Differential Monocyte Activation Underlies Strain-Specific Mycobacterium tuberculosis Pathogenesis. Infect Immun *72*, 5511-5514.

Martens, H. A., Zuurman, M. W., de Lange, A. H. M., Nolte, I. M., van der Steege, G., Navis, G. J., Kallenberg, C. G. M., Seelen, M. A., and Bijl, M. (2009). Analysis of C1q polymorphisms suggests association with systemic lupus erythematosus, serum C1q and CH50 levels and disease severity. Ann. Rheum. Dis *68*, 715-720.

Marth, T., and Kelsall, B. L. (1997). Regulation of interleukin-12 by complement receptor 3 signaling. J. Exp. Med *185*, 1987-1995.

Martin, H., Heinz, H., Reske, K., and Loos, M. (1987). Macrophage C1q: characterization of a membrane form of C1q and of multimers of C1q subunits. The Journal of Immunology *138*, 3863 -3867.

Martinez-Pomares, L., Linehan, S. A., Taylor, P. R., and Gordon, S. (2001). Binding properties of the mannose receptor. Immunobiology *204*, 527-535.

McCarthy, T. R., Torrelles, J. B., MacFarlane, A. S., Katawczik, M., Kutzbach, B., Desjardin, L. E., Clegg, S., Goldberg, J. B., and Schlesinger, L. S. (2005). Overexpression of Mycobacterium tuberculosis manB, a phosphomannomutase that increases phosphatidylinositol mannoside biosynthesis in Mycobacterium smegmatis and mycobacterial association with human macrophages. Mol. Microbiol. *58*, 774-790.

McLaughlin, B., Chon, J. S., MacGurn, J. A., Carlsson, F., Cheng, T. L., Cox, J. S., and Brown, E. J. (2007). A mycobacterium ESX-1-secreted virulence factor with unique requirements for export. PLoS.Pathog. *3*, e105.

Means, T. K., Jones, B. W., Schromm, A. B., Shurtleff, B. A., Smith, J. A., Keane, J., Golenbock, D. T., Vogel, S. N., and Fenton, M. J. (2001). Differential effects of a Toll-like receptor antagonist on Mycobacterium tuberculosis-induced macrophage responses. J. Immunol. *166*, 4074-4082.

Meher, A. K., Bal, N. C., Chary, K. V. R., and Arora, A. (2006). Mycobacterium tuberculosis H37Rv ESAT-6-CFP-10 complex formation confers thermodynamic and biochemical stability. FEBS J. *273*, 1445-1462.

Mészáros, B., Tóth, J., Vértessy, B. G., Dosztányi, Z., and Simon, I. (2011). Proteins with Complex Architecture as Potential Targets for Drug Design: A Case Study of Mycobacterium tuberculosis. PLoS Comput Biol *7*, e1002118.

Metchnikoff, E. (1905). Immunity to Infective Disease (Cambridge: Cambridge University Press).

MISAWA, K. (1952). Detection and acid-fast forms of tubercle bacilli in sputum in relation to varying staining conditions in Ziehl-Neelsen stain. Sci Rep Res Inst Tohoku Univ Med *3*, 307-325.

Miura-Shimura, Y., Nakamura, K., Ohtsuji, M., Tomita, H., Jiang, Y., Abe, M., Zhang, D., Hamano, Y., Tsuda, H., Hashimoto, H., et al. (2002). C1q regulatory region polymorphism down-regulating murine c1q protein levels with linkage to lupus nephritis. J. Immunol. *169*, 1334-1339.

Mody, G. M., Parag, K. B., Nathoo, B. C., Pudifin, D. J., Duursma, J., and Seedat, Y. K. (1994). High mortality with systemic lupus erythematosus in hospitalized African blacks. Br. J. Rheumatol. *33*, 1151-1153.

Mofenson, L.M., and Laughon, B.E. (2007). Human Immunodeficiency Virus, Mycobacterium Tuberculosis, and Pregnancy: A Deadly Combination. Clin Infect Dis. 45, 250–253.

Mok, C. C., Ho, L. Y., Leung, H. W., and Wong, L. G. (2010). Performance of anti-C1q, antinucleosome, and anti-dsDNA antibodies for detecting concurrent disease activity of systemic lupus erythematosus. Transl Res *156*, 320-325.

Molle, V., Saint, N., Campagna, S., Kremer, L., Lea, E., Draper, P., and Molle, G. (2006). pH-dependent pore-forming activity of OmpATb from Mycobacterium tuberculosis and characterization of the channel by peptidic dissection. Mol.Microbiol. *61*, 826-837.

Möller, M., de Wit, E., and Hoal, E. G. (2010). Past, present and future directions in human genetic susceptibility to tuberculosis. FEMS Immunol. Med. Microbiol. *58*, 3-26.

Mollick, J. A., Miller, G. G., Musser, J. M., Cook, R. G., Grossman, D., and Rich, R. R. (1993). A novel superantigen isolated from pathogenic strains of Streptococcus pyogenes with aminoterminal homology to staphylococcal enterotoxins B and C. J Clin Invest *92*, 710-719.

Mostowy, S., and Cossart, P. (2011). Autophagy and the cytoskeleton: New links revealed by intracellular pathogens. Autophagy *7*. Available at: http://www.ncbi.nlm.nih.gov/pubmed/21464614 [Accessed May 8, 2011].

Motulsky, A. G. (1989). Metabolic polymorphisms and the role of infectious diseases in human evolution. 1960. Hum. Biol. *61*, 835-869; discussion 870-877.

Mounier, J., Ryter, A., Coquis-Rondon, M., and Sansonetti, P. J. (1990). Intracellular and cell-to-cell spread of Listeria monocytogenes involves interaction with F-actin in the enterocytelike cell line Caco-2. Infect. Immun. *58*, 1048-1058.

Murray, J. F. (2004). A Century of Tuberculosis. Am. J. Respir. Crit. Care Med. *169*, 1181-1186.

Nam, D. K., Lee, S., Zhou, G., Cao, X., Wang, C., Clark, T., Chen, J., Rowley, J. D., and Wang, S. M. (2002). Oligo(dT) primer generates a high frequency of truncated cDNAs through internal poly(A) priming during reverse transcription. Proceedings of the National Academy of Sciences *99*, 6152 - 6156.

Namjou, B., Gray-McGuire, C., Sestak, A. L., Gilkeson, G. S., Jacob, C. O., Merrill, J. T., James, J. A., Wakeland, E. K., Li, Q.-Z., Langefeld, C. D., et al. (2009). Evaluation of C1q genomic region in minority racial groups of lupus. Genes Immun. *10*, 517-524.

Newport, M. J., Goetghebuer, T., Weiss, H. A., Whittle, H., Siegrist, C.-A., and Marchant, A. (2004). Genetic regulation of immune responses to vaccines in early life. Genes Immun *5*, 122-129.

Neyrolles, O., Hernández-Pando, R., Pietri-Rouxel, F., Fornès, P., Tailleux, L., Payán, J. A. B., Pivert, E., Bordat, Y., Aguilar, D., Prévost, M.-C., et al. (2006). Is Adipose Tissue a Place for Mycobacterium tuberculosis Persistence? PLoS ONE *1*, e43.

Nguyen, L., and Pieters, J. (2005). The Trojan horse: survival tactics of pathogenic mycobacteria in macrophages. Trends in Cell Biology *15*, 269-276.

Nicol, M. P., and Wilkinson, R. J. (2008). The clinical consequences of strain diversity in Mycobacterium tuberculosis. Trans. R. Soc. Trop. Med. Hyg. *102*, 955-965.

Nigou, J., Gilleron, M., and Puzo, G. (2003). Lipoarabinomannans: from structure to biosynthesis. Biochimie *85*, 153-166.

Noss, E. H., Pai, R. K., Sellati, T. J., Radolf, J. D., Belisle, J., Golenbock, D. T., Boom, W. H., and Harding, C. V. (2001). Toll-like receptor 2-dependent inhibition of macrophage class II MHC expression and antigen processing by 19-kDa lipoprotein of Mycobacterium tuberculosis. J. Immunol. *167*, 910-918.

Nyholt, D.R. (2004). A simple correction for multiple testing for single-nucleotide polymorphisms in linkage disequilibrium with each other. Am J Hum Genet. *74*, 765-769

Ohashi, K., Burkart, V., Flohé, S., and Kolb, H. (2000). Cutting edge: heat shock protein 60 is a putative endogenous ligand of the toll-like receptor-4 complex. J. Immunol. *164*, 558-561.

Ohol, Y. M., Goetz, D. H., Chan, K., Shiloh, M. U., Craik, C. S., and Cox, J. S. (2010). Mycobacterium tuberculosis MycP1 protease plays a dual role in regulation of ESX-1 secretion and virulence. Cell Host Microbe *7*, 210-220.

Ojha, A. K., Baughn, A. D., Sambandan, D., Hsu, T., Trivelli, X., Guerardel, Y., Alahari, A., Kremer, L., Jacobs, W. R., and Hatfull, G. F. (2008). Growth of Mycobacterium tuberculosis biofilms containing free mycolic acids and harbouring drug-tolerant bacteria. Mol Microbiol *69*, 164-174.

Okkels, L. M., Müller, E.-C., Schmid, M., Rosenkrands, I., Kaufmann, S. H. E., Andersen, P., and Jungblut, P. R. (2004). CFP10 discriminates between nonacetylated and acetylated ESAT-6 of Mycobacterium tuberculosis by differential interaction. Proteomics *4*, 2954-2960.

Patel, N.R., Zhu, J., Tachado, S.D., Zhang, J., Wan, Z., Saukkonen, J., and Koziel, H. (2007). HIV impairs TNF-alpha mediated macrophage apoptotic response to Mycobacterium tuberculosis. J. Immunol. 179, 6973–6980.

Pandey, A. K., and Sassetti, C. M. (2008). Mycobacterial persistence requires the utilization of host cholesterol. Proc. Natl. Acad. Sci. U.S.A. *105*, 4376-4380.

Pasteur, L., Chamberland, and Roux (2002). Summary report of the experiments conducted at Pouilly-le-Fort, near Melun, on the anthrax vaccination, 1881. Yale J Biol Med *75*, 59-62.

Pathak, S. K., Basu, S., Basu, K. K., Banerjee, A., Pathak, S., Bhattacharyya, A., Kaisho, T., Kundu, M., and Basu, J. (2007). Direct extracellular interaction between the early secreted antigen ESAT-6 of Mycobacterium tuberculosis and TLR2 inhibits TLR signaling in macrophages. Nat. Immunol. *8*, 610-618.

Pawlowski, A., Jansson, M., Sköld, M., Rottenberg, M.E., and Källenius, G. (2012). Tuberculosis and HIV Co-Infection. PLoS Pathog 8, 1-7.

Pecora, N. D., Gehring, A. J., Canaday, D. H., Boom, W. H., and Harding, C. V. (2006). Mycobacterium tuberculosis LprA is a lipoprotein agonist of TLR2 that regulates innate immunity and APC function. J. Immunol. *177*, 422-429.

Perneger, T.V. (1998). What's wrong with Bonferroni adjustments. BMJ. *316*, 1236-1238

Pennini, M. E., Pai, R. K., Schultz, D. C., Boom, W. H., and Harding, C. V. (2006). Mycobacterium tuberculosis 19-kDa Lipoprotein Inhibits IFN-γ-Induced Chromatin Remodeling of MHC2TA by TLR2 and MAPK Signaling. The Journal of Immunology *176*, 4323 -4330.

Pertea, M., and Salzberg, S. L. (2010). Between a chicken and a grape: estimating the number of human genes. Genome Biol. *11*, 206.

Peyron, P., Bordier, C., N'Diaye, E. N., and Maridonneau-Parini, I. (2000). Nonopsonic phagocytosis of Mycobacterium kansasii by human neutrophils depends on cholesterol and is mediated by CR3 associated with glycosylphosphatidylinositol-anchored proteins. J. Immunol. *165*, 5186-5191.

Phizicky, E. M., and Fields, S. (1995). Protein-protein interactions: methods for detection and analysis. Microbiol Rev *59*, 94-123.

Pieters, J., and Gatfield, J. (2002). Hijacking the host: survival of pathogenic mycobacteria inside macrophages. Trends Microbiol. *10*, 142-146.

Pompei, L., Jang, S., Zamlynny, B., Ravikumar, S., McBride, A., Hickman, S. P., and Salgame, P. (2007). Disparity in IL-12 release in dendritic cells and macrophages in response to Mycobacterium tuberculosis is due to use of distinct TLRs. J. Immunol. *178*, 5192-5199.

Portevin, D., Gagneux, S., Comas, I., and Young, D. (2011). Human Macrophage Responses to Clinical Isolates from the Mycobacterium tuberculosis Complex Discriminate between Ancient and Modern Lineages. PLoS Pathog *7*, e1001307.

Proell, M., Riedl, S. J., Fritz, J. H., Rojas, A. M., and Schwarzenbacher, R. (2008). The Nod-like receptor (NLR) family: a tale of similarities and differences. PLoS ONE *3*, e2119.

Pryor, P. R., and Raines, S. A. (2010). Manipulation of the host by pathogens to survive the lysosome. Biochem. Soc. Trans *38*, 1417-1419.

Pugin, J., Heumann, I. D., Tomasz, A., Kravchenko, V. V., Akamatsu, Y., Nishijima, M., Glauser, M. P., Tobias, P. S., and Ulevitch, R. J. (1994). CD14 is a pattern recognition receptor. Immunity *1*, 509-516.

Rafiq, S., Frayling, T. M., Vyse, T. J., Cunninghame Graham, D. S., and Eggleton, P. (2010). Assessing association of common variation in the C1Q gene cluster with systemic lupus erythematosus. Clin. Exp. Immunol *161*, 284-289.

Raghavan, S., Manzanillo, P., Chan, K., Dovey, C., and Cox, J. S. (2008). Secreted transcription factor controls Mycobacterium tuberculosis virulence. Nature *454*, 717-721.

Rajaram, M. V. S., Brooks, M. N., Morris, J. D., Torrelles, J. B., Azad, A. K., and Schlesinger, L. S. (2010). Mycobacterium tuberculosis Activates Human Macrophage Peroxisome Proliferator-Activated Receptor γ Linking Mannose Receptor Recognition to Regulation of Immune Responses. J Immunol *185*, 929-942.

Ramakrishnan, L., and Falkow, S. (1994). Mycobacterium marinum persists in cultured mammalian cells in a temperature-restricted fashion. Infect Immun *62*, 3222-3229.

Ramanathan, V. D., Curtis, J., and Turk, J. L. (1980). Activation of the alternative pathway of complement by mycobacteria and cord factor. Infect. Immun. *29*, 30-35.

Raynaud, C., Papavinasasundaram, K. G., Speight, R. A., Springer, B., Sander, P., Bottger, E. C., Colston, M. J., and Draper, P. (2002). The functions of OmpATb, a pore-forming protein of Mycobacterium tuberculosis. Mol.Microbiol. *46*, 191-201.

Reiling, N., Hölscher, C., Fehrenbach, A., Kröger, S., Kirschning, C. J., Goyert, S., and Ehlers, S. (2002). Cutting edge: Toll-like receptor (TLR)2- and TLR4-mediated pathogen recognition in resistance to airborne infection with Mycobacterium tuberculosis. J. Immunol. *169*, 3480-3484.

Renshaw, P. S., Lightbody, K. L., Veverka, V., Muskett, F. W., Kelly, G., Frenkiel, T. A., Gordon, S. V., Hewinson, R. G., Burke, B., Norman, J., et al. (2005). Structure and function of the complex formed by the tuberculosis virulence factors CFP-10 and ESAT-6. EMBO J. *24*, 2491-2498.

Renshaw, P. S., Panagiotidou, P., Whelan, A., Gordon, S. V., Hewinson, R. G., Williamson, R. A., and Carr, M. D. (2002). Conclusive evidence that the major T-cell antigens of the Mycobacterium tuberculosis complex ESAT-6 and CFP-10 form a tight, 1:1 complex and characterization of the structural properties of ESAT-6, CFP-10, and the ESAT-6*CFP-10 complex. Implications for pathogenesis and virulence. J. Biol. Chem. *277*, 21598-21603.

Risch, N., and Merikangas, K. (1996). The future of genetic studies of complex human diseases. Science *273*, 1516-1517.

Rohde, K., Yates, R. M., Purdy, G. E., and Russell, D. G. (2007). Mycobacterium tuberculosis and the environment within the phagosome. Immunological Reviews *219*, 37-54.

Rojas, M., Barrera, L.F., Puzo, G., and Garcia, L.F. (1997). Differential induction of apoptosis by virulent Mycobacterium tuberculosis in resistant and susceptible murine macrophages: role of nitric oxide and mycobacterial products. J. Immunol. 159, 1352–1361.

Roth, D. E., Soto, G., Arenas, F., Bautista, C. T., Ortiz, J., Rodriguez, R., Cabrera, L., and Gilman, R. H. (2004). Association between vitamin D receptor gene polymorphisms and response to treatment of pulmonary tuberculosis. J. Infect. Dis. *190*, 920-927.

Rosas-Taraco, A.G., Arce-Mendoza, A.Y., Caballero-Olín, G., and Salinas-Carmona, M.C. (2006). Mycobacterium tuberculosis upregulates coreceptors CCR5 and CXCR4 while HIV modulates CD14 favoring concurrent infection. AIDS Res. Hum. Retroviruses 22, 45–51.

Roxas, B. A., and Li, Q. (2009). Acid stress response of a mycobacterial proteome: insight from a gene ontology analysis. Int.J.Clin.Exp.Med. *2*, 309-328.

Said, S. M., Cornell, L. D., Valeri, A. M., Sethi, S., Fidler, M. E., Cosio, F. G., and Nasr, S. H. (2010). C1q deposition in the renal allograft: a report of 24 cases. Mod.Pathol. Available at: PM:20473274.

Samten, B., Townsend, J. C., Sever-Chroneos, Z., Pasquinelli, V., Barnes, P. F., and Chroneos, Z. C. (2008). An antibody against the surfactant protein A (SP-A)-binding domain of the SP-A receptor inhibits T cell-mediated immune responses to Mycobacterium tuberculosis. J. Leukoc. Biol. *84*, 115-123.

Sánchez, D., Rojas, M., Hernández, I., Radzioch, D., García, L. F., and Barrera, L. F. (2010). Role of TLR2- and TLR4-mediated signaling in Mycobacterium tuberculosis-induced macrophage death. Cellular Immunology *260*, 128-136.

Sanchez-Villeda, H., Schroeder, S., Flint-Garcia, S., Guill, K., Yamasaki, M., and McMullen, M. (2008). DNAAlignEditor: DNA alignment editor tool. BMC Bioinformatics *9*, 154-158.

Santucci, M.B., Amicosante, M., Cicconi, R., Montesano, C., Casarini, M., Giosuè, S., Bisetti, A., Colizzi, V., and Fraziano, M. (2000). Mycobacterium tuberculosis-induced apoptosis in monocytes/macrophages: early membrane modifications and intracellular mycobacterial viability. J. Infect. Dis. 181, 1506–1509.

Sasindran, S. J., and Torrelles, J. B. (2011). Mycobacterium tuberculosis infection and inflammation: what is beneficial for the host and for the bacterium? Front Microbiol. *2*, 1-16.

Sassetti, C.M., and Rubin, E.J. (2003). Genetic requirements for mycobacterial survival during infection. Proc Natl Acad Sci. 12989–12994.

Sawant, S.S., Agrawal, S.R., Shastri, J.S., Pawaskar, M., and Kadam, P. (2011). Human Immunodeficiency Virus Infection Among Tuberculosis Patients in Mumbai. J Lab Physicians 3, 12–14.

Schaible, U. E., Sturgill-Koszycki, S., Schlesinger, P. H., and Russell, D. G. (1998). Cytokine activation leads to acidification and increases maturation of Mycobacterium avium-containing phagosomes in murine macrophages. J.Immunol. *160*, 1290-1296.

Schlesinger, L. S. (1993). Macrophage phagocytosis of virulent but not attenuated strains of Mycobacterium tuberculosis is mediated by mannose receptors in addition to complement receptors. J. Immunol. *150*, 2920-2930.

Schlesinger, L. S., Bellinger-Kawahara, C. G., Payne, N. R., and Horwitz, M. A. (1990). Phagocytosis of Mycobacterium tuberculosis is mediated by human monocyte complement receptors and complement component C3. J. Immunol. *144*, 2771-2780.

Schlesinger, L. S., Hull, S. R., and Kaufman, T. M. (1994). Binding of the terminal mannosyl units of lipoarabinomannan from a virulent strain of Mycobacterium tuberculosis to human macrophages. J. Immunol *152*, 4070-4079.

Scholl, P., Diez, A., Mourad, W., Parsonnet, J., Geha, R. S., and Chatila, T. (1989). Toxic shock syndrome toxin 1 binds to major histocompatibility complex class II molecules. Proc. Natl. Acad. Sci. U.S.A. *86*, 4210-4214.

Schumann, G., Schleier, S., Rosenkrands, I., Nehmann, N., Hälbich, S., Zipfel, P. F., Jonge, M. I., Cole, S. T., Munder, T., and Möllmann, U. (2006). Mycobacterium tuberculosis secreted protein ESAT-6 interacts with the human protein syntenin-1. Central European Journal of Biology *1*, 183-202.

Semple, J. I., Sanderson, C. M., and Campbell, R. D. (2002). The jury is out on "guilt by association" trials. Brief Funct Genomic Proteomic *1*, 40-52.

Sethi, S., and Murphy, T. F. (2008). Infection in the pathogenesis and course of chronic obstructive pulmonary disease. N.Engl.J.Med. *359*, 2355-2365.

Shi, S., Nathan, C., Schnappinger, D., Drenkow, J., Fuortes, M., Block, E., Ding, A., Gingeras, T. R., Schoolnik, G., Akira, S., et al. (2003). MyD88 primes macrophages for full-scale activation by interferon-gamma yet mediates few responses to Mycobacterium tuberculosis. J. Exp. Med. *198*, 987-997.

Sibley, L. D. (2004). Intracellular parasite invasion strategies. Science *304*, 248-253.

Simeone, R., Bobard, A., Lippmann, J., Bitter, W., Majlessi, L., Brosch, R., and Enninga, J. (2012). Phagosomal Rupture by Mycobacterium tuberculosis Results in Toxicity and Host Cell Death. PLoS Pathog 8, e1002507.

Simeone, R., Bottai, D., and Brosch, R. (2009). ESX/type VII secretion systems and their role in host-pathogen interaction. Curr.Opin.Microbiol. *12*, 4-10.

Singh, S. P., Mehra, N. K., Dingley, H. B., Pande, J. N., and Vaidya, M. C. (1983). Human leukocyte antigen (HLA)-linked control of susceptibility to pulmonary tuberculosis and association with HLA-DR types. J. Infect. Dis. *148*, 676-681.

Smith, J., Manoranjan, J., Pan, M., Bohsali, A., Xu, J., Liu, J., McDonald, K.L., Szyk, A., LaRonde-LeBlanc, N., and Gao, L.Y. (2008). Evidence for pore formation in host cell membranes by ESX-1-secreted ESAT-6 and its role in Mycobacterium marinum escape from the vacuole. Infect.Immun. *76*, 5478–5487.

Sontheimer, R. D., Racila, E., and Racila, D. M. (2005). C1q: its functions within the innate and adaptive immune responses and its role in lupus autoimmunity. J. Invest. Dermatol *125*, 14-23.

Sørensen, T. I., Nielsen, G. G., Andersen, P. K., and Teasdale, T. W. (1988). Genetic and environmental influences on premature death in adult adoptees. N. Engl. J. Med. *318*, 727-732.

Spear, G.T., Kessler, H.A., Rothberg, L., Phair, J., and Landay, A.L. (1990). Decreased oxidative burst activity of monocytes from asymptomatic HIV-infected individuals. Clin. Immunol. Immunopathol. 54, 184–191.

Stanley, S. A., Johndrow, J. E., Manzanillo, P., and Cox, J. S. (2007). The Type I IFN Response to Infection with Mycobacterium tuberculosis Requires ESX-1-Mediated Secretion and Contributes to Pathogenesis. The Journal of Immunology *178*, 3143 -3152.

Stanley, S. A., Raghavan, S., Hwang, W. W., and Cox, J. S. (2003). Acute infection and macrophage subversion by Mycobacterium tuberculosis require a specialized secretion system. Proc.Natl.Acad.Sci.U.S.A *100*, 13001-13006.

Stead, W. W., Senner, J. W., Reddick, W. T., and Lofgren, J. P. (1990). Racial differences in susceptibility to infection by Mycobacterium tuberculosis. N. Engl. J. Med. *322*, 422-427.

Sterling, T.R., Pham, P.A., and Chaisson, R.E. (2010). HIV Infection–Related Tuberculosis: Clinical Manifestations and Treatment. Clinical Infectious Diseases 50, S223–S230.

Stewart, G. R., Patel, J., Robertson, B. D., Rae, A., and Young, D. B. (2005). Mycobacterial mutants with defective control of phagosomal acidification. PLoS Pathog. *1*, 269-278.

Stranger, B. E., Nica, A. C., Forrest, M. S., Dimas, A., Bird, C. P., Beazley, C., Ingle, C. E., Dunning, M., Flicek, P., Koller, D., et al. (2007). Population genomics of human gene expression. Nat. Genet. *39*, 1217-1224.

Sutterwala, F. S., Noel, G. J., Clynes, R., and Mosser, D. M. (1997). Selective suppression of interleukin-12 induction after macrophage receptor ligation. J. Exp. Med *185*, 1977-1985.

Tan, T., Lee, W. L., Alexander, D. C., Grinstein, S., and Liu, J. (2006). The ESAT-6/CFP-10 secretion system of Mycobacterium marinum modulates phagosome maturation. Cell Microbiol. *8*, 1417-1429.

Taylor, G. M., Stewart, G. R., Cooke, M., Chaplin, S., Ladva, S., Kirkup, J., Palmer, S., and Young, D. B. (2003). Koch's Bacillus – a look at the first isolate of Mycobacterium tuberculosis from a modern perspective. Microbiology *149*, 3213 -3220.

Taylor, P. R., Gordon, S., and Martinez-Pomares, L. (2005). The mannose receptor: linking homeostasis and immunity through sugar recognition. Trends in Immunology *26*, 104-110.

Tenner, A. J., and Volkin, D. B. (1986). Complement subcomponent C1q secreted by cultured human monocytes has subunit structure identical with that of serum C1q. Biochem J *233*, 451-458.

Thoma-Uszynski, S., Stenger, S., Takeuchi, O., Ochoa, M. T., Engele, M., Sieling, P. A., Barnes, P. F., Rollinghoff, M., Bolcskei, P. L., Wagner, M., et al. (2001). Induction of direct antimicrobial activity through mammalian toll-like receptors. Science *291*, 1544-1547.

Todar, N. (2011). Mycobacterium tuberculosis and Tuberculosis. In Online Textbook of Bacteriology.

Torrelles, J. B., and Schlesinger, L. S. (2010). Diversity in Mycobacterium tuberculosis mannosylated cell wall determinants impacts adaptation to the host. Tuberculosis (Edinb) *90*, 84-93.

Torrelles, J. B., Azad, A. K., and Schlesinger, L. S. (2006). Fine discrimination in the recognition of individual species of phosphatidyl-myo-inositol mannosides from Mycobacterium tuberculosis by C-type lectin pattern recognition receptors. J. Immunol. *177*, 1805-1816.

Tuberculosis in Twins (1965). Postgraduate Medical Journal *41*, 54.

Underhill, D. M., Ozinsky, A., Smith, K. D., and Aderem, A. (1999). Toll-like receptor-2 mediates mycobacteria-induced proinflammatory signaling in macrophages. Proc. Natl. Acad. Sci. U.S.A. *96*, 14459-14463.

Valdivia-Arenas, M., Amer, A., Henning, L., Wewers, M., and Schlesinger, L. (2007). Lung infections and innate host defense. Drug Discov Today Dis Mech *4*, 73-81.

Vandal, O. H., Nathan, C. F., and Ehrt, S. (2009a). Acid resistance in Mycobacterium tuberculosis. J.Bacteriol. *191*, 4714-4721.

Vandal, O. H., Pierini, L. M., Schnappinger, D., Nathan, C. F., and Ehrt, S. (2008). A membrane protein preserves intrabacterial pH in intraphagosomal Mycobacterium tuberculosis. Nat.Med. *14*, 849-854.

Vandal, O. H., Roberts, J. A., Odaira, T., Schnappinger, D., Nathan, C. F., and Ehrt, S. (2009b). Acid-susceptible mutants of Mycobacterium tuberculosis share hypersusceptibility to cell wall and oxidative stress and to the host environment. J.Bacteriol. *191*, 625-631.

Vandivier, R. W., Ogden, C. A., Fadok, V. A., Hoffmann, P. R., Brown, K. K., Botto, M., Walport, M. J., Fisher, J. H., Henson, P. M., and Greene, K. E. (2002). Role of surfactant proteins A, D, and C1q in the clearance of apoptotic cells in vivo and in vitro: calreticulin and CD91 as a common collectin receptor complex. J. Immunol. *169*, 3978-3986.

Velayati, A. A., Masjedi, M. R., Farnia, P., Tabarsi, P., Ghanavi, J., Ziazarifi, A. H., and Hoffner, S. E. (2009). Emergence of new forms of totally drug-resistant tuberculosis bacilli: super extensively drug-resistant tuberculosis or totally drug-resistant strains in iran. Chest *136*, 420-425.

Velmurugan, K., Chen, B., Miller, J. L., Azogue, S., Gurses, S., Hsu, T., Glickman, M., Jacobs, W. R., Porcelli, S. A., and Briken, V. (2007). Mycobacterium tuberculosis nuoG Is a Virulence Gene That Inhibits Apoptosis of Infected Host Cells. PLoS Pathog *3*, e110.

Vergne, I., Chua, J., and Deretic, V. (2003). Tuberculosis toxin blocking phagosome maturation inhibits a novel Ca2+/calmodulin-PI3K hVPS34 cascade. J.Exp.Med. *198*, 653-659.

Via, L. E., Fratti, R. A., McFalone, M., Pagan-Ramos, E., Deretic, D., and Deretic, V. (1998). Effects of cytokines on mycobacterial phagosome maturation. J.Cell Sci. *111 (Pt 7)*, 897-905.

Vidalain, P.-O., Boxem, M., Ge, H., Li, S., and Vidal, M. (2004). Increasing specificity in high-throughput yeast two-hybrid experiments. Methods *32*, 363-370.

Vieira, O. V., Botelho, R. J., Rameh, L., Brachmann, S. M., Matsuo, T., Davidson, H. W., Schreiber, A., Backer, J. M., Cantley, L. C., and Grinstein, S. (2001). Distinct roles of class I and class III phosphatidylinositol 3-kinases in phagosome formation and maturation. J.Cell Biol. *155*, 19-25.

Wadee, S., Tikly, M., and Hopley, M. (2007). Causes and predictors of death in South Africans with systemic lupus erythematosus. Rheumatology *46*, 1487 -1491.

Wahl, S.M., Allen, J.B., Gartner, S., Orenstein, J.M., Popovic, M., Chenoweth, D.E., Arthur, L.O., Farrar, W.L., and Wahl, L.M. (1989). HIV-1 and its envelope glycoprotein down-regulate chemotactic ligand receptors and chemotactic function of peripheral blood monocytes. J. Immunol. 142, 3553–3559.

Walker, D. G. (1998). Expression and regulation of complement C1q by human THP-1-derived macrophages. Mol. Chem. Neuropathol. *34*, 197-218.

Wang, X., Barnes, P. F., Dobos-Elder, K. M., Townsend, J. C., Chung, Y.-tae, Shams, H., Weis, S. E., and Samten, B. (2009). ESAT-6 Inhibits Production of IFN-γ by Mycobacterium tuberculosis-Responsive Human T Cells. The Journal of Immunology *182*, 3668 -3677.

Wards, B. J., de Lisle, G. W., and Collins, D. M. (2000). An esat6 knockout mutant of Mycobacterium bovis produced by homologous recombination will contribute to the development of a live tuberculosis vaccine. Tuber. Lung Dis. *80*, 185-189.

Warnes G, Gorman D, Leisch F, Man M. Genetics: population genetics. http://CRAN.R-project.org/package=genetics , 2008.

Warren, R., de Kock, M., Engelke, E., Myburgh, R., Gey van Pittius, N., Victor, T., and van Helden, P. (2006). Safe Mycobacterium tuberculosis DNA Extraction Method That Does Not Compromise Integrity. Journal of Clinical Microbiology *44*, 254 -256.

Welin, A., Eklund, D., Stendahl, O., and Lerm, M. (2011). Human Macrophages Infected with a High Burden of ESAT-6-Expressing M. tuberculosis Undergo Caspase-1- and Cathepsin B-Independent Necrosis. PLoS ONE *6*, e20302.

Wong, K.-W., and Jacobs, W.R., Jr (2011). Critical role for NLRP3 in necrotic death triggered by Mycobacterium tuberculosis. Cell. Microbiol. *13*, 1371–1384.

Xu, J., Laine, O., Masciocchi, M., Manoranjan, J., Smith, J., Du, S. J., Edwards, N., Zhu, X., Fenselau, C., and Gao, L. Y. (2007). A unique Mycobacterium ESX-1 protein co-secretes with CFP-10/ESAT-6 and is necessary for inhibiting phagosome maturation. Mol.Microbiol. *66*, 787-800.

Xu, W., Berger, S. P., Trouw, L. A., de Boer, H. C., Schlagwein, N., Mutsaers, C., Daha, M. R., and van Kooten, C. (2008). Properdin Binds to Late Apoptotic and Necrotic Cells Independently of C3b and Regulates Alternative Pathway Complement Activation. The Journal of Immunology *180*, 7613 -7621.

Yates, R. M., Hermetter, A., and Russell, D. G. (2005). The kinetics of phagosome maturation as a function of phagosome/lysosome fusion and acquisition of hydrolytic activity. Traffic *6*, 413-420.

Zimmerli, S., Edwards, S., and Ernst, J. D. (1996). Selective receptor blockade during phagocytosis does not alter the survival and growth of Mycobacterium tuberculosis in human macrophages. Am. J. Respir. Cell Mol. Biol. *15*, 760-770.

Appendix 1

Preparing buffers and media for *E. coli* cultures

Reagents and materials

IPTG stock solution (0.1M)

- Dissolve 1.2 g of IPTG into 50 mL of dH_2O.
- Filter-sterilise, aliquot and store at 4°C.

X-Gal (20 mg/mL)

- Dissolve 40 mg of 5-bromo-4chloro-3-indolyl-β-D-galactoside into 2 mL N, N'-dimethyl-formamide.
- Cover with aluminium foil and store at 4°C.

Ampicillin (100 mg/mL)

- Dissolve 1 g of ampicillin into 10 mL of dH_2O.
- Filter-sterilise and store at -20°C

Kanamycin (50 mg/mL)

- Dissolve 0.5 g of kanamycin into 10 mL of dH_2O.
- Filter-sterilise and store at -20°C

LB medium (per liter)

- 10 g Bacto® -tryptone
- 5 g Bacto® -yeast extract
- 5 g NaCl
- Adjust pH to 7.0 with NaOH

LB plates with ampicillin

- Add 12 g agar to 1L of LB medium, autoclave.
- Allow the medium to cool to 50°C before adding ampicillin to a final concentration of 100 µg/mL.
- Pour 30-35 mL of medium into 85mm petri dishes.
- Let agar harden.
- Store at 4°C (1 month) or at room temperature (1 week)

LB plates with ampicillin/IPTG/X-Gal

- Add 100 µL of 0.1M of IPTG and 100 µL of 20mg/mL X-Gal, spread over the surface of LB-ampicillin plate.
- Allow to absorb for 30 minutes prior to use.

SOB medium

- 20 g Bacto-Tryptone
- 5 g Bacto-Yeast extract
- 0.5 g NaCl

- 2.5 mL 1M KCl

- Dissolve into 800 mL dH_2O.
- Adjust pH to 7.0 with 10M NaOH.
- Adjust volume to 990 mL with dH_2O.
- Sterilise by autoclaving and store at room temperature.
- Before use, add 10 mL sterile 1M $MgCl_2$.

SOC medium

- Identical to SOB media, except that it contains 20 mL sterile 1M glucose

1M $MgCl_2$ (1 L)

- Dissolve 203.31 g of magnesium chloride-$6H_2O$ into 800 mL dH_2O.
- Adjust volume to 1 L with dH_2O.
- Divide in aliquots of 100 mL and sterilise by autoclaving.
- Store at room temperature.

1M KCl (1 L)

- Dissolve 74.56 g of potassium chloride into 800 mL dH_2O.
- Adjust volume to 1 L with dH_2O.
- Sterilise by autoclaving.
- Store at room temperature.

Preparing buffers and media yeast culturing

YPDA Liquid (1 L)

- 50 g YPD
- 15 ml of 0.2% stock solution L-adenine hemisulphate
- Dissolve into 900 mL dH_2O.
- Adjust pH to 6.5 if necessary.
- Adjust volume to 1 L with dH_2O.
- Sterilise by autoclaving.

YPDA Agar (1 L)

- 50 g YPD
- 20 g Bacto Agar
- 15 ml of 0.2% stock solution L-adenine hemisulphate
- Dissolve into 900 mL dH_2O.
- Adjust pH to 6.5 if necessary.
- Adjust volume to 1 L with dH_2O.
- Sterilise by autoclaving.

2X YPDA Liquid (1 L)

- 100 g YPD
- 15 ml of 0.2% stock solution L-adenine hemisulphate
- Dissolve into 900 mL dH_2O.

- Adjust pH to 6.5 if necessary.
- Adjust volume to 1 L with dH_2O.
- Sterilise by autoclaving.

0.5 X YPDA Liquid (1 L)

- 25 g YPD
- 15 ml of 0.2% stock solution L-adenine hemisulphate
- Dissolve into 900 mL dH_2O.
- Adjust pH to 6.5 if necessary.
- Adjust volume to 1 L with dH_2O.
- Sterilise by autoclaving.

0.2% L-Adenine Hemisulphate stock

- Dissolve 0.2 g of L-adenine hemisulphate into 100 mL of dH_2O.
- Filter-sterilise and store at room temperature

Synthetic Defined (SD) Dropout (DO) Liquid (1L)

- 26.7 g of minimal SD base.
- Add the amount supplement required (see list below*)
- Dissolve into 900 mL dH_2O.
- Adjust pH to 5.8.
- Adjust volume to 1 L with dH_2O.
- Sterilise by autoclaving.
- Store plates at 4°C

SD/-DO Agar (1L)

- 46.7 g of minimal SD base supplemented with agar.
- Add the amount supplement required (see list below*)
- Dissolve into 900 mL dH_2O.
- Adjust pH to 5.8.
- Adjust volume to 1 L with dH_2O.
- Sterilise by autoclaving.
- Store plates at 4°C

Supplement*

- -Leu DO suppl 0.69 g
- -Trp DO suppl 0.74 g
- -Leu/-Trp DO suppl 0.64 g
- -His/-Leu/-Trp TDO suppl 0.62 g
- -Ade/-His/-Leu/-Trp QDO suppl 0.60 g
- -His/-Trp
  - Use media prepared with 0.62 g of -His/-Leu/-Trp DO suppl
  - Dissolve 6.55 g of L-Leucine into 500 ml dH_2O.
  - Sterilise by autoclaving (use at 16.7 mL LEU stock per 1 L of SD-His/-Leu/-Trp media)

- -Ade/-Trp
  - Use media prepared with 0.6 g of -Ade/-His/-Leu/-Trp DO suppl
  - Dissolve 200 mg L-Histidine HCl monohydrate and 1000 mg L-Leucine into 1 L of dH_2O.
  - Sterilise by autoclaving
  - Store at 4°C up to 1 year
  - Add 100 mL of 10X His/Leu to 900 mL autoclaved media

Appendix 2

Maps of vectors used in this study

Reagents and materials

pGem T-easy

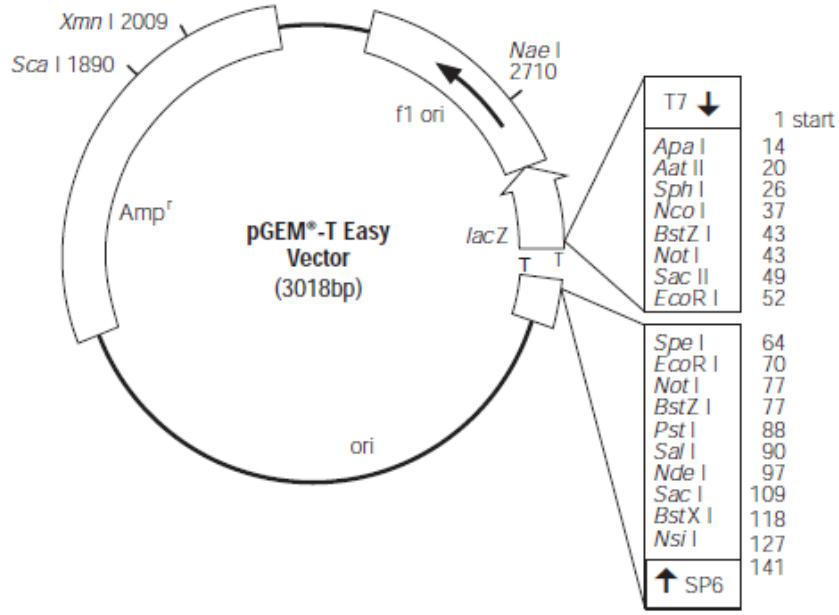

pGBKT7 (bait vector)

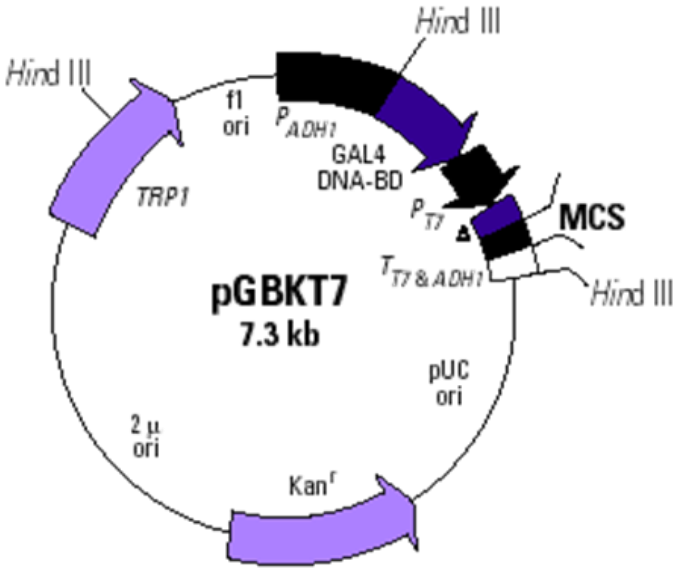

pGADT7-Rec (Library (prey) vector)

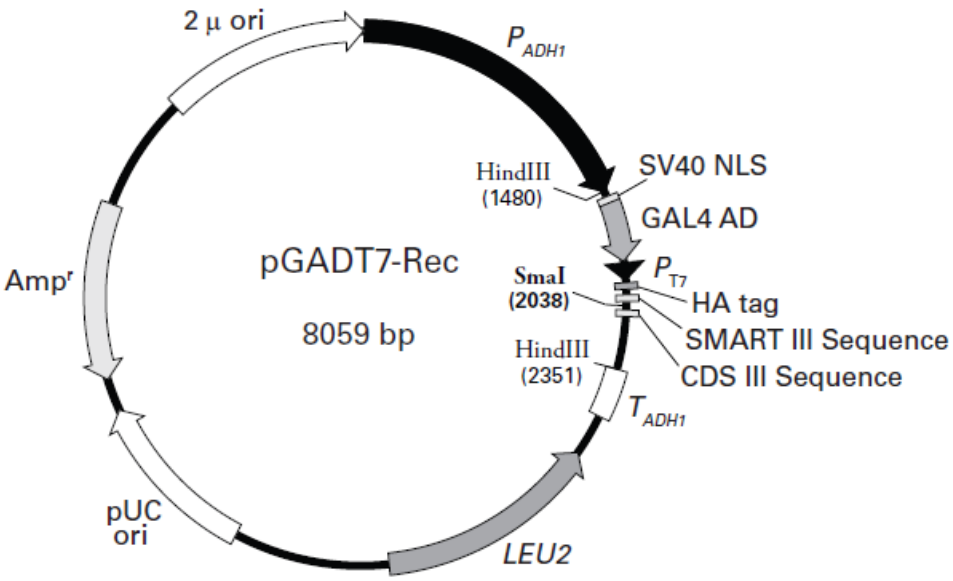

pGADT7-SV40 (control activation domain (AD) vector)

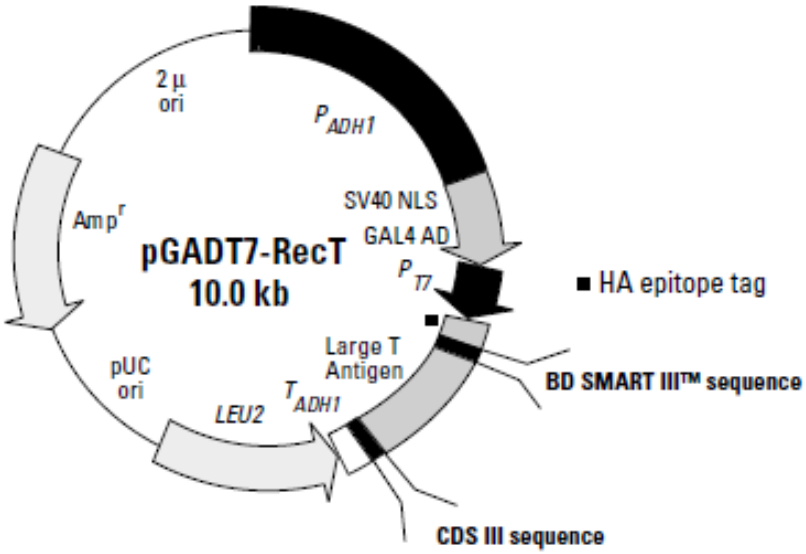

pGBKT7-p53 (control binding domain (BD) vector)

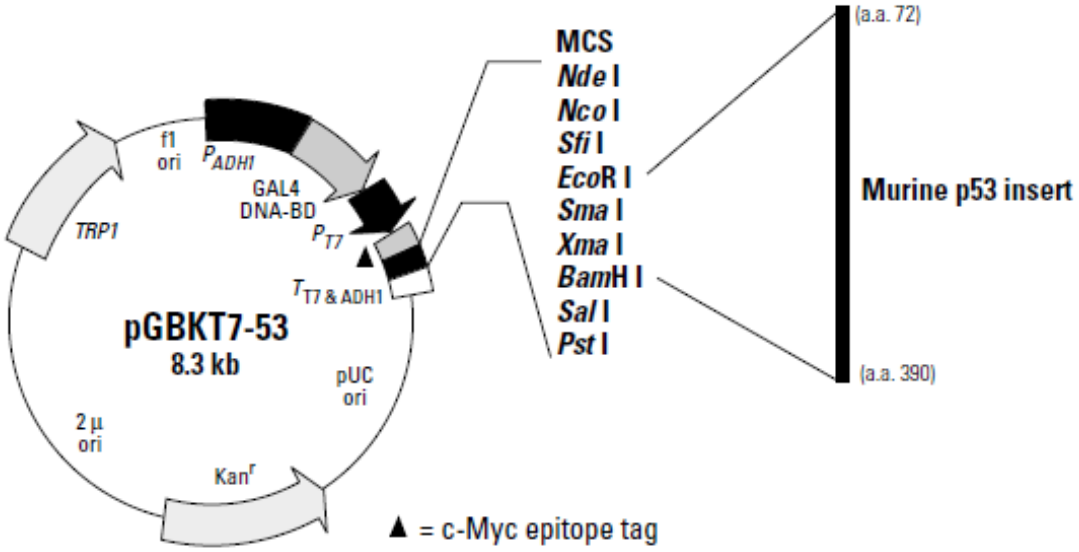

pGBKT7-LAM (control BD vector)

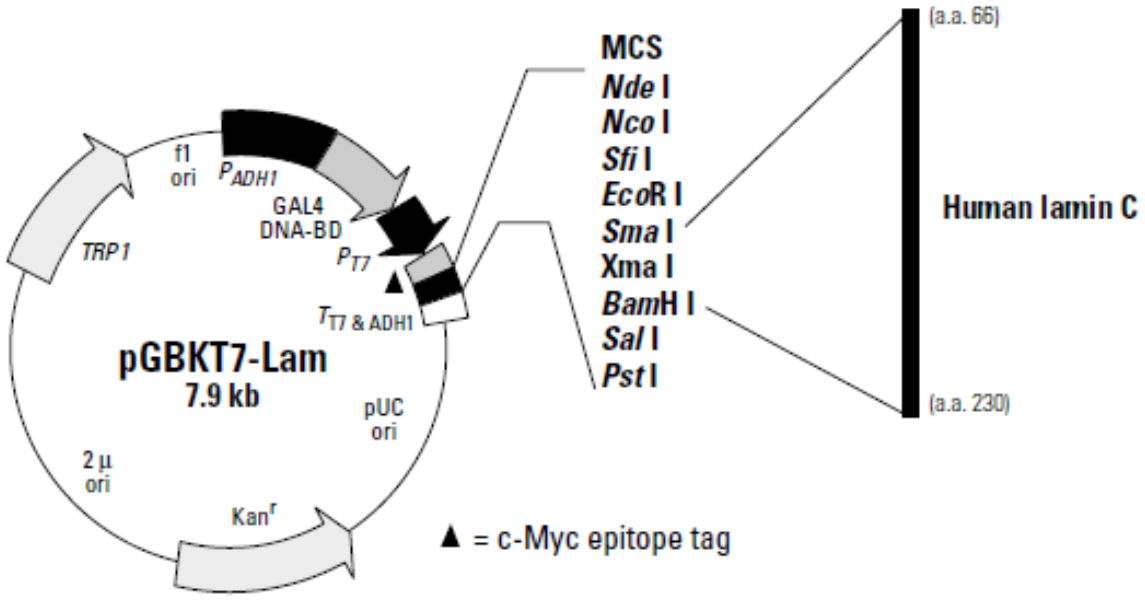

Appendix 3

Tissue culturing

Reagent and Material

RPMI 10% heat inactivated fetal bovine serum (HI-FBS) 1% penicillin/streptomycin

- 500 mL of RPMI-1640
- 50 mL of HI-FBS
- 5 mL of pen/strep

100µM Phorbol 12-myristate 13-acetate (PMA)

- Dissolve 1 mg of PMA into 16.3 mL 100% ethanol.
- Cover with aluminium foil and store at 4°C.
- Use at a final concentration of 1:100 (100nM)

PMA treatment stimulates Protein kinase C which triggers the THP-1 cells to differentiate into a macrophage like morphology, the cells become adherent and phagocytic and stops diving.

Protocol

Defrosting cells (THP-1 cells are kept in liquid nitrogen for long term storage)

1. Hold tube in water bath (or warm hands), taking care not to overheat
2. Cells should be defrosted but not warm
3. Dilute DMSO in stock culture ASAP
4. Place cells in 50mL tube with 9mL media
5. Pellet cells at 1000 rpm at 21°C for 5 min
6. Remove supernatant
7. Add 10 mL media and pipet in to a tissue culture flask
8. Incubate in a 37°C, 5% CO_2 incubator
9. Check cells every day and add fresh media when cells are too many

Differentiation of THP-1 cells with PMA

1. Harvest cells and re-suspend in 10mL RPMI lacking antibiotics and count using a haemocytometer
2. Adjust the concentration of cells to 1 X 10^6 cells per mL

3. Add PMA to final concentration of 100nM
4. Vortex 3X for 10sec
5. Add 1 mL of cells to each 24 well plate
6. Incubate for 2 days and remove non-adherent cells by washing with 2X RPMI/FBS media
7. Add fresh medium incubate for 4 hrs or overnight

Preparation of THP-1 and Jurkat stock cultures

1. Pool flask in 50 mL tube
2. Centrifuge at room temperature at 1000-1500 rpm for 5min
3. Remove and discard the supernatant
4. Re-suspend pellet in 100% FBS (1.5 mL per 50 mL flask) and cool on ice for 5 min
5. Prepare 20% DMSO/RPMI and add to FBS cell mixture
6. Aliquot 1 mL into cryovials
7. Freeze at -80°C and transfer to liquid nitrogen for long term storage

Appendix 4

Electro-competent *E. coli*

Reagents and materials

XL1-Blue genotype

- *recA1 endA1 gyrA96 thi-1 hsdR17 supE44 relA1 lac [F´ proAB lacI$_q$ZΔM15* Tn*10 (Tet$_r$)]*

Tetracycline 5 mg/mL

- Dissolve 5 mg of tetracycline into 1 mL 100% ethanol
- Store at -20°C, protected from light

10% Glycerol

- Take 1 volume of molecular-biology-grade glycerol in 9 volumes of sterile dH_2O.
- Sterilise by passing it through a 0.22µm filter.
- Store at 4°C

Protocol

1. Spread competent cells onto a LB plate containing tetracycline (10 µL/mL of a 5 mg/mL stock in methanol). Incubate overnight at 37°C.

2. Inoculate into 50 mL LB containing tetracycline for a starter culture. Incubate overnight at 37°C with shaking. Also prepare 4X 250 mL flasks containing LB with tetracycline and pre-warm overnight at 37°C with shaking.

3. Inoculate the above pre-warmed (37°C) in 4X 250 mL flasks containing LB with tetracycline, with 1/100 of starter culture. Incubate 3-4 hrs at 37°C with shaking.

4. Grow until OD_{600} reaches 0.7 (not higher than 0.8). Put on ice. All steps from this point forward must be performed under icy-cold conditions.

5. Harvest cells by spinning in GSA rotor for 10 minutes at 5000 rpm at 4°C.

6. Re-suspend pellet very carefully (cells are extremely fragile) in a volume of ice-cold 10% glycerol equal to the original culture volume.

7. Spin at 5000 rpm for 10 minutes at 4°C.

8. Carefully pour off the supernatant (pellet will be quite loose), re-suspend cells again in 10% glycerol equal to the original culture volume.

9. Spin at 5000 rpm for 10 minutes at 4°C.

10. Carefully pour off the supernatant, re-suspend cells in the volume if glycerol remaining in the centrifuge bottle. Pool the cells in one small centrifuge tube (SS34).

11. Spin for 10 minutes at 7000 rpm in SS34 rotor at 4°C.

12. Carefully pour off supernatant and re-suspend cells in 10% glycerol using a volume of 2mL per liter of initial culture.

13. Aliquot to micro-centrifuge tubes (100 µL per tube) and freeze quickly in a liquid nitrogen bath.

14. Store cells at -80°C.

Preparation of Competent Yeast Cells (LiAc Method)

Yeast strain genotypes

- AH109: *MAT*a *trp1-901 leu2–3,112 ura3*-52 *his3*-200 *gal4*Δ*gal80*Δ *LYS2*::*GAL1*$_{UAS}$-*GAL1*$_{TATA}$-*HIS3 MEL1 GAL2*$_{UAS}$-*GAL2*$_{TATA}$-*ADE2, URA3*::*MEL1*$_{UAS}$-*MEL1*$_{TATA}$-*lacZ*

- Y187: *MATα, ura3-52, his3-200, ade2-101, trp1-901, leu2-3, 112, gal4Δ, met-, gal80Δ, URA3::GAL1*$_{UAS}$-*GAL1*$_{TATA}$-*lacz*

1M LiAc (10X)

- Dissolve 5.1 g of LiAc into 50 mL dH_2O
- Filter-sterilise.
- Store at room temperature

10X TE buffer (1 L)

- Prepare from 1 M stock of Tris-HCl (pH 7.5) and 500 mM stock of EDTA (pH 8.0).
- To make 1 liter 10X TE (Tris-EDTA) Buffer, mix following:
  - 100 mL 1M Tris-HCl (pH7.5)
  - 20 mL 500mM EDTA (pH8)
  - Add 880 mL with sterile dH_2O
- Store at room temperature

1.1X TE/LiAc solution

- Mix the following: 1.1 mL of 10X TE with 1.1 mL of 1M LiAc
- Bring the total volume to 10 mL using sterile, dH_2O.

50% PEG

- Dissolve 25g of polyethyleneglycol 4000 into 50 mL dH_2O by stirring
- Sterilise by autoclaving
- Store at 4°C

Protocol

1. Prepare YPDA agar plates

2. To recover strains from frozen stock, scrape a small amount of cells from the surface with a sterile loop or wooden stick and streak them onto YPDA plates.

3. Incubate plates at 30°C for 3 - 5 days until colonies appear. Propagate additional cultures only from isolated colonies on this working stock plate.

4. Using a sterile loop or toothpick, streak 3–4 colonies from the working stock onto separate appropriate SD selection plates as indicated in the table.

Strain	SD/–Ade	SD/–Met	SD/–Trp	SD/–Leu	SD/–His	SD/–Ura	YPDA
AH109	–	+	–	–	–	+	+
Y187	–	–	–	–	–	+	+

5. Incubate plates at 30°C for 4 - 6 days. Yeast grows slower on SD selection medium than on YPDA.

6. Compare the results with those shown in the Table. Proceed only if AH109 and Y187 have the expected phenotypes.

7. Use well-isolated colonies from the verified working stock plate to inoculate liquid cultures for mating or for preparing competent cells. Seal the verified working stock plate with Parafilm and store at 4°C.

8. Streak a well-isolated colony (AH109 or Y187) from the verified working stock plate on YPDA agar plate

9. Incubate the plate upside down at 30°C until colonies appear (~3 days). (Note: yeast strains can be stored for up to 1 month at 4°C on YPDA culture plates sealed with parafilm)

10. Prepare 1.1X TE/LiAc Solution.

11. Inoculate one colony (< 4 weeks old, 2–3 mm in diameter) into 3 mL of YPDA medium in a sterile, 15 mL centrifuge tube. Incubate at 30°C with shaking for 8 hrs.

12. Transfer 5 µL of the culture to a 250 mL flask containing 50 mL of YPDA medium. Incubate at 30°C with shaking at 230–250 rpm for 16–20 hrs. The OD_{600} should reach 0.15–0.3.

13. Centrifuge the cells at 700 x g for 5 min at room temperature. Discard the supernatant and re-suspend the cell pellet in 100 mL of YPDA medium.

14. Incubate at 30°C for 3 - 5 hrs (OD600 = 0.4 - 0.5).

15. Centrifuge the cells at 700 x g for 5 min at room temperature. Discard the supernatant and re-suspend the cell pellet in 60 mL of sterile, dH_2O.

16. Centrifuge the cells at 700 x g for 5 min at room temperature. Discard the supernatant and re-suspend the cells in 3 mL of 1.1X TE/LiAc Solution.

17. Split the re-suspension between two 1.5 mL micro-centrifuge tubes (1.5 mL per tube). Centrifuge each tube at high speed for 15 sec.

18. Discard the supernatant and re-suspend each pellet in 600 µl of 1.1X TE/LiAc Solution.

19. Competent cells should be used for transformation immediately following preparation; however, if necessary, they can be stored at room temperature for a few hours without significantly affecting the competency.

Appendix 5

cDNA Generation

Reagents and Materials

BD Matchmaker™ Library Construction & Screening Kit

95% ethanol (-20°C)

Bromophenol blue loading dye

- Bromophenol blue 0.2% (w/V)
- Glycerol 50%
- Tris (pH8) 10mM
- Dissolve bromophenol blue, and Tris in 49 mL of dH_2O.
- Stir in 50 mL of glycerol to make 100 mL total solution.

Protocol

Synthesise First-Strand cDNA using an Oligo (dT) Primer

1. Combine the following reagents in a sterile 0.25ml microcentrifuge tube:
   1-2 µL RNA sample (0.025–1.0 µg poly A+ or 0.10–2.0 µg total RNA)
   1.0 µL CDS III Primer
   1-2 µL H_2O to bring volume up to 4.0 µL.
   4.0 µL Total volume

2. Mix contents and spin briefly. Incubate at 72°C for 2 min. Cool on ice for 2 min. Spin briefly

3. Add the following to the reaction tube:
   2.0 µL 5x First-Strand Buffer
   1.0 µL DTT (20 mM)
   1.0 µL dNTP Mix (10 mM)
   1.0 µL MMLV Reverse Transcriptase
   9.0 µL Total volume

4. Mix gently by tapping. Spin briefly and incubate at 42°C for 10 min.

5. Add 1.0 µL BD SMART III Oligonucleotide.

6. Incubate at 42°C for 1 hr in an hot-lid thermal cycler.

7. Place the tube at 75°C for 10 min to terminate first-strand synthesis.

8. Cool the tube to room temperature, then add 1.0 µL (2 units) RNase H. Incubate at 37°C for 20 min.

9. 2 µL of first-strand cDNA is necessary to generate enough ds cDNA. Take a 2µL aliquot from the Oligo (dT) first-strand synthesis and place it in a clean, pre-chilled, 0.5 mL tube. Place the tube on ice until the second first-strand generating reaction (using the random primer) is finished.

10. Store the rest of the first-strand reaction mixture at -20°C for up to three months.

Synthesise First-Strand cDNA using a Random Primer

1. Combine the following reagents in a sterile 0.5 mL microcentrifuge tube:
   1-2 µL RNA sample (0.025–1.0 µg poly A+ or 0.10–2.0 µg total RNA)
   1.0 µL CDS III/6 Primer
   1-2 µL Deionised H_2O to bring volume up to 4.0 µL.
   4.0 µL Total volume

2. Mix contents and spin briefly. Incubate at 72°C for 2 min. Cool on ice for 2 min. Spin briefly.

3. Keep the tube at room temperature and add the following:
   2.0 µL 5X First-Strand Buffer
   1.0 µL DTT (20 mM)
   1.0 µL dNTP Mix (10 mM)
   1.0 µL MMLV Reverse Transcriptase
   9.0 µL Total volume

4. Mix gently by tapping. Spin briefly.

5. Incubate at 25–30°C for 10 min at room temperature, and thereafter at 42°C for 10 min.

6. Add 1.0 µL BD SMART III Oligonucleotide, and Incubate at 42°C for 1 hr in a hot-lid thermal cycler.

7. Place the tube at 75°C for 10 min to terminate first-strand synthesis.

8. Cool the tube to room temperature, then add 1.0 µL (2 units) RNase H and incubate at 37°C for 20 min

9. Take a 2 µL aliquot from the Random Primed first-strand synthesis and place it in a clean, pre-chilled, 0.5 mL tube.

10. Store the rest of the first-strand reaction mixture at -20°C for up to three months.

Amplify ds cDNA by Long Distance PCR (LD-PCR)

1. The next table shows the optimal number of thermal cycles to use based on the amount of RNA used in the first-strand synthesis. Fewer cycles generally mean fewer nonspecific PCR products.

Total RNA (μg)	Poly A^+ RNA (μg)	Number of Cycles
1.0–2.0	0.5–1.0	15–20
0.5–1.0	0.25–0.5	20–22
0.25–0.5	0.125–0.25	22–24
0.05–0.25	0.025–0.125	24–26

2. Preheat the PCR thermal cycler to 95°C.

3. To prepare sufficient ds cDNA for transformation, two 100 μL PCR reactions are usually set up for each experimental sample. As we are generating ds cDNA from both the Oligo (dT) and Random primers (i.e. two reactions), this will act as two reactions and after the ds cDNA is pooled should be sufficient for transformation. Set up one reaction for the Control sample. In each reaction tube, combine the following components:

2 μL	First-Strand cDNA
70 μL	Deionised H2O
10 μL	10X BD Advantage 2 PCR Buffer
2 μL	50X dNTP Mix
2 μL	5' PCR Primer
2 μL	3' PCR Primer
10 μL	10X GC-Melt Solution
2 μL	50X BD Advantage 2 Polymerase Mix
100 μL	Total volume

4. Mix gently by flicking the tube. Centrifuge briefly, place in a preheated (95°C) thermal cycler and cycle as follows:

95°C for 30 sec

X cycles
95°C for 10 sec
68°C for 6 min
68°C for 5 min

where x is the amount of cycles from the table above

Program the cycler to increase the extension time by 5 sec with each successive cycle. For example, in the second cycle, the extension should last 6 min and 5 sec; in the third, 6 min and 10 sec.

5. When the cycling is complete, analyze a 7 μL aliquot of the PCR product from each sample alongside 0.25 μg of a 1 kb DNA size marker on a 1.2% agarose/EtBr gel. This should appear as a moderately strong smear from $\geq$ 0.1 kb to 4 kb (or more).

6. ds cDNA can be stored at -20°C until use.

Purify ds cDNA with a BD CHROMA SPIN™ TE-400 Column

1. Remove the BD CHROMA SPIN Column from the protective plastic bag and invert it several times to re-suspend the gel matrix completely. Use one column for each ~95 µL cDNA sample.

2. Holding the BD CHROMA SPIN Column upright, grasp the break-away end between your thumb and index finger and snap off. Place the end of the spin column into one of the 2 mL micro-centrifuge tubes, and lift off the top cap. Save the top cap and the white-end cap.

3. Centrifuge at 700 x g for 5 min in a swinging bucket or horizontal rotor.

4. After centrifugation, the column matrix will appear semi-dry. This step purges the equilibration buffer from the column and re-establishes the matrix bed.

5. Remove the spin column and collection tube from the centrifuge rotor, and discard the collection tube and column equilibration buffer.

6. Place the spin column into a 1.5 mL micro-centrifuge tube. Carefully and slowly apply your cDNA sample (~95µL) to the center of the gel bed's flat surface. Do not allow any sample to flow along the inner wall of the column.

7. Centrifuge at 700 x g for 5 min in a swinging bucket or horizontal rotor.

8. Remove the spin column and collection tube from the rotor and detach them from each other. The purified sample is at the bottom of the collection tube.

9. Combine the two samples (one from the Oligo (dT) priming and the other from the Random priming) in a single tube.

10. Add the following reagents:
    1/10 vol. Sodium Acetate (3 M; pH 4.8)
    2.5 vol. 95% ethanol (-20°C)

11. Mix gently by rocking the tube back and forth.

12. Place the tube in a -20°C freezer or a dry-ice/ethanol bath for 1 hr. Better recoveries are obtained at -20°C overnight.

13. Centrifuge the tube at 14,000 rpm for 20 min at room temperature.

14. Carefully remove the supernatant with a pipette. Do not disturb the pellet. Briefly centrifuge the tube to bring all remaining liquid to the bottom.

15. Carefully remove all liquid and allow the pellet to air dry for ~10 min. Re-suspend the pellet in 20 µL of dH_2O and mix gently. The cDNA is now ready for in vivo recombination (library construction) with pGADT7-Rec or pGADT7-Rec2.

16. cDNA can be stored at -20°C.

Library Construction

Reagents and Materials

100% Glycerol

Freezing Medium: YPD medium with 25% (v/v) glycerol

- Combine 25 mL 100% glycerol with 75 mL of prepared YPD media

Sterile glass beads

SD/–Leu ~200 150-mm plates

SD/–Leu ~5–10 100-mm plates

PEG/LiAc Solution

- Combine the following
  - 8 mL 50% PEG
  - 1 mL 10x TE buffer
  - 1 mL 10x LiAc

Protocol:

Transform yeast strain AH109 with ds cDNA and pGADT7-Rec

1. **NB!** Prepare competent AH109 yeast cells before starting library construction (see Section 8)

2. Transfer ~50 µL of Herring DNA to a micro-centrifuge tube and heat at 100°C for 5 min. Then, immediately chill the DNA by placing the tube in an ice bath. Repeat once more before using the DNA in the next reaction.

3. In a sterile, pre-chilled, 15 mL tube combine the following:
   20 µL ds cDNA
   6 µL pGADT7-Rec (0.5 µg/µL)
   20 µL Herring Testes Carrier DNA, denatured

4. Add 600 µL of competent AH109 cells to the DNA and gently mix by vortexing

5. Add 2.5 mL PEG/LiAc Solution and gently mix by vortexing.

6. Incubate at 30°C for 45 min. Mix cells every 15 min. Add 160 µL DMSO, mix, and then place the tube in a 42°C water bath for 20 min. Mix cells every 10 min.

7. Centrifuge at 700 x g for 5min, discard the supernatant and re-suspend in 3 mL of YPD Plus Liquid Medium.

8. Incubate at 30°C with shaking for 90 min.

9. Centrifuge at 700 x g for 5 min, discard the supernatant and re-suspend in 30 mL of NaCl Solution (0.9%).

Select transformants on SD/–Leu plates.

1. Spread 150 µL on each 150mm plate (~200 plates total). To check the transformation efficiency, spread 100µl of a 1:10, 1:100, 1:1 000, and 1:10 000 dilution on 100mm SD/–Leu plates.

2. Incubate plates upside down at 30°C until colonies appear (~3–6 days).

3. Calculate the transformation efficiency - expected results: ≥1 x 106 transformants / 3 µg pGADT7-Rec

Harvest (pool) transformants.

1. Chill plates at 4°C for 3–4 hrs, and then add 5 mL Freezing Medium to each plate.

2. Use sterile glass beads and gentle swirling to dislodge the cells into the liquid, and combine all liquids in a sterile flask. Mix well.

3. Check the cell density using a hemacytometer. If the cell density ≤ 2 x 10^7 cells/mL, reduce the volume of the suspension by centrifuging.

4. Aliquot (1 mL) and store at –80°C (not longer than 1 year). To determine the library titer, spread 100 µL of a 1:100, 1:1 000, and 1:10 000 dilution on 100mm SD/–Leu plates. Incubate at 30°C until colonies appear (~2–3 days). Count the colonies (cfu) and calculate the number of clones in your library.

Appendix 6

Electrophoresis solutions, loading dyes and agarose gels

Reagents and materials

50X TAE (500 mL)

- Dissolve 121 g of Tris base into 250 mL dH_2O, stir to dissolve
- Add 28.6 mL acetic acid
- Add 50 mL 0.5M EDTA (pH 8)
- Make up to 500mL

Bromophenol blue loading dye

- Bromophenol blue 0.2% (w/V)
- Glycerol 50%
- Tris (pH8) 10mM
- Dissolve bromophenol blue, and Tris in 49 mL of dH_2O.
- Stir in 50 mL of glycerol to make 100 mL total solution.

Ethidium bromide solution (5 mg/mL)

- Dissolve 5 mg of ethidium bromide into 1 mL dH_2O
- Cover with aluminium foil and store at room temperature
- Add 5 µL to final volume of 100 mL agarose gel solution (see list below for % agarose gels):
- Agarose concentration
  - 1% = 1g + 100mL 1X TAE buffer
  - 1.5% = 1.5g + 100mL 1X TAE buffer
  - 2% = 2g + 100mL 1X TAE buffer

Appendix 7

Promega Wizard® SV PCR, Gel and Plasmid Clean-up

Reagents and materials

Wizard® SV Gel and PCR Clean-Up System (kit)

Wizard® Plus SV Minipreps DNA Purification System (kit)

Protocol

Wizard® SV PCR Clean-Up

1. Add an equal volume of Membrane Binding Solution to the PCR reaction

2. Incubate at room temperature for 1 min

Wizard® SV Gel Clean-Up

1. Excise DNA band from gel and place gel slice in a 1.5 mL tube

2. Add 10 µL Membrane Binding Solution per 10 mg gel slice. Vortex and incubate at 50-65°C

Wizard® Plus SV Minipreps

1. Harvest 1–5 mL (high-copy-number plasmid) or 10 mL (low-copy-number plasmid) of bacterial culture by centrifugation for 5 minutes at 10,000 x *g*. Pour off the supernatant.

2. Add 250 µL of Cell Re-suspension Solution and completely re-suspend the cell pellet by vortexing or pipetting.

3. Add 250 µL of Cell Lysis Solution and mix by inverting the tube 4 times. Incubate until the cell suspension clears (approximately 1–5 min).

4. Add 10 µL of Alkaline Protease Solution and mix by inverting the tube 4 times. Incubate for 5 minutes at room temperature.

5. Add 350 µL of Neutralisation Solution and immediately mix by inverting the tube 4 times.

Follow the next instructions for each above

1. Insert SV mini-column into Collection tube.

2. Transfer prepared PCR/gel/bacterial solution to the Mini-column. Incubate at room temperature for 1 min.

3. Centrifuge at 10 000 x g for 1 min. Discard flow through and re-insert Mini-column into Collection Tube.

4. Add 700 µL Membrane Wash Solution (ethanol added). Centrifuge at 10 000 x g for 1 minute. Discard flow through and re-insert Mini-column into Collection Tube.

5. Repeat with 500 µL Membrane Wash Solution. Centrifuge at 10 000 x g for 5 min.

6. Carefully transfer Mini-column to a clean 1.5 mL micro-centrifuge tube.

7. Add 25 µL of Nuclease-Free Water (Promega Corp. Madison Wisconsin, USA) to the Mini-column. Incubate at room temperature for 1 min. Centrifuge at 10 000 x g for 1 min.

8. Discard Mini-column and store DNA at 4°C or -20°C.

High yield DNA extraction from larger volumes of bacterial culture

Reagents and materials

NucleoBond® PC 100 Midi High Yield Plasmid DNA purification (MACHEREY-NAGEL GmbH & Co. KG) from *E.coli* 50mL culture

1. Cultivate and harvest bacterial cells
   - Centrifuge LB culture at 3000 X g for 15 min at 4°C

2. Cell lysis
   - Re-suspend the pellet of bacterial cells in 4 mL S1 buffer + RNase A
     - Mix using pipette
   - Add 4 mL S2 buffer, invert 6-8 times. Incubate at RT (20-25°C) for 2-3 min (max 5min). [Do not vortex]
   - Add 4 mL pre-cooled S3 Buffer (4°C), invert 6-8 times until the homogenous suspension containing an off-white flocculate is formed. Incubate on ice for 5min.

3. Equilibration of the column
   - Equilibrate the AX 100 (Midi) column with 2.5 mL N2 buffer. Allow column to empty by gravity flow and discard the flow-through.

4. Clarification of the lysate
   - Filter the suspension (25min)
     - Place a NucleoBond® folded filter in a funnel and pre-wet the filter with a few drops of sterile dH_2O. Load the bacterial lysate onto the wet filter and collect the flow-through.

5. Binding
   - Load the cleared lysate from step 4 onto the NucleoBond® column. Allow the column to empty by gravidity flow.

6. Washing

- Wash the column with 10 mL N3 buffer. Discard the flow-through.

7. Elution
   - Elute the plasmid DNA using 5 mL N5 buffer into a new tube

8. Precipitation
   - Prepared 6X 1.5 mL eppendorf tubes with 680µL room temperature iso-propanol. Add 840 µL of the eluted plasmid. Mix and centrifuge at top speed for 30min at 4°C.

9. Wash and dry DNA pellet
   - Once centrifuged, remove pellets from iso-propanol with tip and place in new eppendorf with 500 µL 70% ethanol. Mix briefly and centrifuge at top speed for 10min at room temperature (20-25°C).
   - Remove ethanol and allow pellet to air dry at RT

10. Reconstitute DNA
    - Re-dissolve the DNA pellet in 50 µL sterile dH_2O

Yeast plasmid extraction

Reagents and materials

1M $NaPO_4$ [pH 7]

- Dissolve 138 g NaH_2PO_4 into 1 L of dH_2O
- Dissolve 142 g Na_2HPO_4 into 1 L of dH_2O
- Autoclave to sterilise each solution, store at room temperature
- Combine 423 mL of 1M NaH_2PO_4 and 577 mL 1M Na_2HPO_4. Store at room temperature.

2M sorbitol

- Dissolve 36.4 g of Sorbitol into 100mL dH_2O to a final volume of 100mL
- Autoclave to sterilise, store at room temperature

250 mM EDTA

- Dissolve 93.06 g of EDTA into 800 mL dH_2O
- Bring to pH 8 with 4M NaOH
- Adjust volume to 1 L
- Autoclave to sterilise, store at room temperature

Lysis buffer (100mM NaPO4 [pH 7], 1M sorbitol, 60mM EDTA)

- Combine the following:
  - 50 mL of 2M Sorbitol
  - 10 mL of 1M NaPO4
  - 24 mL of 250mM EDTA

Wizard® Plus SV Minipreps DNA Purification System (kit)

Protocol

1. Collect yeast from a liquid culture (10ml) and re-suspend in 200µL of lysis buffer (100mM $NaPO_4$ [pH 7], 1M sorbitol, 60mM EDTA). Mix vigorously by vortexing.

2. Digest the cell wall by adding lyticase (0.33 mg/mL, Sigma, St. Louis, MO Cat.# L2524) to each tube. Incubate at 37°C overnight without shaking.

3. Collect yeast by centrifugation for 5 min at 4000 rpm. Remove and discard the supernatant.

4. Perform plasmid DNA isolation on the yeast pellet with the Wizard® Plus SV Minipreps DNA Purification System as described.

Appendix 8

Bait Construction

Reagents and Materials

pGBKT7
Electro-competent *E. coli* cells.
T4 DNA ligase and 10X T4 ligation buffer
LB/amp plates
Restriction enzymes: EcoRI and PstI
Wizard SV Promega Plasmid isolation kit

Protocol

1. Design primers for in-frame cloning of both ESAT-6 (esxA), CFP-10 (esxB) in pGBKT7.

2. Primers look like follows:

		EcoRI
ESXA f	5'	G|AA TTC ATG ACA GAG CAG CAG TGG AAT 3' (27 bases)
ESXA r	5'	CTG CA|G ATC CCG TGT TTC GCT ATT CT 3' (26 bases)
		PstI

		EcoRI
ESXB f	5'	G|AA TTC ATG GCA GAG ATG AAG ACC GAT 3' (27 bases)
ESXB r	5'	CTG CA|G TGA CAT TTC CCT GGA TTG C 3' (25 bases)
		PstI

3. The amplified PCR fragments of ESXA = 339bp, ESXB = 414bp was purified and cloned into pGem-T Easy vector for propagation and sequence confirmation.

4. Recombinant pGem-ESAT6 and pGem-CFP-10 were digested with with appropriate enzymes and purify.

5. The DNA-BD vector, pGBKT7, were digested with EcoRI and PstI, and treated with phosphatase (see below method), and the DNA concentration were determined.

Phosphatase treatment

- Combine the following reaction mixture:
  - 19 µL vector (sub cloning vector)
  - 1 µL SAP
  - 3 µL Buffer
  - 7 µL H_2O
- Incubate the reaction mixture for 10 min at 37°C, followed by an additional incubation for 10min at 65°C

6. Ligations of the following reactions were performed: esxA and esxB inserts into pGBKT7 to obtain bait contructs. Transform ligation mixtures into *E. coli*.
    a. The ligation reaction were set up using the equation described below and the T4 DNA ligase kit

$$\frac{ng\ vector}{kb\ size\ of vector} \times \text{kb size of insert} \times \frac{3}{1} = ng\ insert\ required$$

7. Restriction digest product of ESAT-6 and CFP-10 were cloned in frame using the enzyme sites. See multiple cloning sites (MCS) below:

8. The insert-containing plasmids were identified by restriction enzyme analysis, PCR, and sequencing

9. Resulting clones to be used in the two-hybrid analyses.

List of additional constructs made during this study

1. proline-glutamic (PE) family related protein (PE35; Rv3872)
2. proline-proline-glutamic (PPE) family related protein (PPE68; Rv3873)
3. PPE family, MPTR subfamily (PPE-MPTR62; Rv1917c)
4. PE family, PGRS subfamily (PE-PGRS33; Rv1818c)

Growth curves of recombinant pGBKT7-PE35, -PPE68, -MPTR62 and –PGRS33

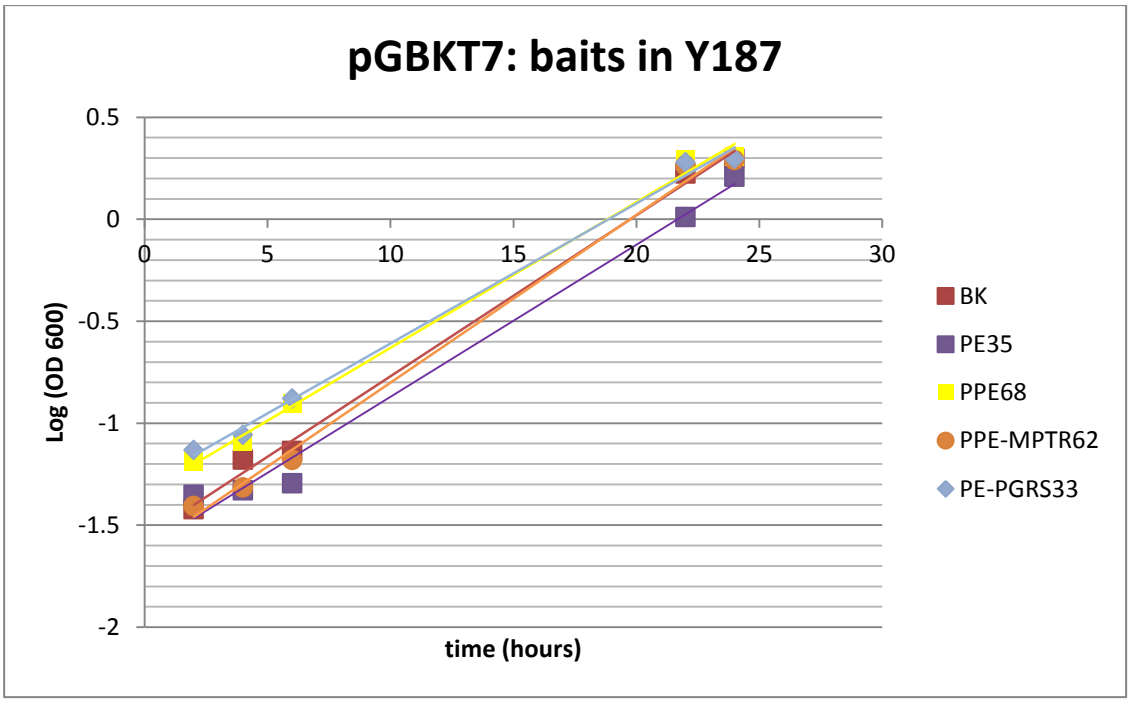

Figure 3.8: Growth curves of recombinant pGBKT7-PE35, -PPE68, -MPTR62 and –PGRS33 versus empty pGBKT7 vector to test the toxic effects of the recombinant constructs in the Y187 yeast strain. These constructs did not produce any toxic effects, as measured by growth curves compared the empty pGBKT7 vector (BK)

Table: Testing recombinant baits for transcriptional activation. Bait constructs were plated on SD/-Trp/-His and SD/-Trp/-Ade to test for transcriptional activation of reporter genes. Bait constructs PE35 and PPE68 were active on SD/-Trp/-His and grew on TDO plates. No growth was observed on QDO selection plates. Background growth on –His media was eliminated by adding 10mM 3-AT to TDO selection media

				mating with empty pGADT7:AH109	
	pGBKT7	**Trp/His**	**Trp/Ade**	**TDO**	**QDO**
Y187	PE35	+	-	+	-
	PPE68	+	-	+	-
	PGRS33	-	-	-	-
	MPTR62	-	-	-	-
	leaky HIS3 expression suppressed with 10mM 3-AT				

Appendix 9

Transform into yeast

Reagents and materials

Appropriate recombinant vectors for transformation into yeast cell

Appropriate SD agar plates

YPDA

- 50 g YPD
- 20 g Bacto Agar
- 15 ml of 0.2% stock solution L-adenine hemisulphate
- Dissolve into 900 mL dH_2O.
- Adjust pH to 6.5 if necessary.
- Adjust volume to 1 L with dH_2O.
- Sterilise by autoclaving.

2 mg/mL Herring Testes Carrier DNA (Clontech Laboratories Inc., Palo Alto, CA)

1M LiAc (10X)

- Dissolve 5.1 g of LiAc into 50 mL dH_2O
- Filter-sterilise.
- Store at room temperature

50% PEG

- Dissolve 25g of polyethyleneglycol 4000 into 50 mL dH_2O by stirring
- Sterilise by autoclaving
- Store at 4°C

Protocol

1. Inoculate a large yeast colony into 10 mL appropriate medium in 50mL sterile tube

2. Grow overnight at 30°C shaking at ~250 rpm

3. Centrifuge at 3000rpm for 10 min, decant the supernatant and re-suspend the pellet into 10 mL YPDA liquid media, vortex and allow to grow for 5 hrs

4. Centrifuge the cell suspension, if the yeast cell volume is estimated to be between 20-50 µL, proceed with the next steps.

5. Re-suspend the pellet of 20-50 µL yeast cells into 1 mL sterile dH_2O, vortex and pellet the cells for 30sec at 1500 rpm

6. Remove supernatant and re-suspend the pellet into 1 mL of 100mM LiAc solution

7. Incubate at 30°C for 5 min, without shaking and pipette the 20-50 µL yeast suspension into a 2 mL eppendorf tube

8. Pellet cells (top speed for 20sec) and remove all LiAc supernatant

9. Add the following in order:
   - 240 µL 50% PEG
   - 36 µL 1M LiAc
   - 25 µL of a 2 mg/mL Herring Testes Carrier DNA
   - 10-20 µL plasmid prep (100 ng – 5 µg) together with sterile dH_2O up to volume of 50 µL

10. Vortex for 1 min and incubate in water bath at 42°C for 30min

11. Plate transformed suspension onto appropriate SD agar plates

Appendix 10

Testing of DNA-BD Fusions

Reagents and materials

2 mg/mL Herring Testes Carrier DNA (Clontech Laboratories Inc., Palo Alto, CA)

DMSO (Sigma, St. Louis, MO)

YPD Plus Medium (Clontech Laboratories Inc., Palo Alto, CA)

NaCl
- Dissolve 58.44 g of NaCl into 1 L of dH_2O
- Sterilise by autoclaving

1 g/mL X-α-gal
- Dissolve 10 g of X-α-gal into 10 mL DMSO.
- Store at -20°C for long term storage. Protect from light.

Appropriate SD agar plates

1M 3-Amino-1,2,4-triazole (Sigma, St. Louis, MO)
- Dissolve 8.41 g of 3-AT into 100 mL dH_2O
- Do not autoclave, but filter sterilise the solution.
- Store at 4°C for up to 1 year

Kanamycin
- Dissolve 0.5 g of kanamycin into 10 mL of dH_2O.
- Filter-sterilise and store at -20°C

AH109 and Y187 yeast strains

Protocol

Test the DNA-BD Fusion for Transcriptional Activation

1. Transfer ~50 µL of Herring Testes DNA to a micro-centrifuge tube and heat at 100°C for 5 min. Immediately chill the DNA by placing the tube in an ice bath. Repeat once more before using the DNA in the transformation reaction described below.

2. Transform AH109 and Y187 with the constructs by setting up twelve 1.5 mL micro-centrifuge tubes and adding components using the volumes indicated in the table:

Component	1	2	3	4	5	6	7	8	9	10	11	12
pGBKT7esxA (500 ng/µL)	0.5	0.5	-	-	-	-	-	-	-	-	-	-
pGBKT7esxB (500 ng/µL)	-	-	0.5	0.5	-	-	-	-	-	-	-	-
pGBKT7 (500 ng/µL)	-	-	-	-	-	-	-	-	0.5	0.5	-	-
pBridge (500 ng/µL)	-	-	-	-	-	-	-	-	-	-	0.5	0.5
Herring Testes Carrier DNA (10 mg/mL), denatured*	5	5	5	5	5	5	5	5	5	5	5	5
AH109 competent yeast	50	-	50	-	50	-	50	-	50	-	50	-
Y187 competent yeast	-	50	-	50	-	50	-	50	-	50	-	50
PEG/LiAc Solution	500	500	500	500	500	500	500	500	500	500	500	500

3. Mix thoroughly by gently vortexing, and incubate at 30°C for 30 min. Vortex gently every 10 min.

4. Add 20 µL of DMSO to each tube, mix, and then place the tube in a 42°C waterbath for15 min. Vortex gently every 5 min.

5. Centrifuge at high speed in a micro-centrifuge for 15 sec.

6. Remove supernatant and re-suspend in 1 mL of YPD Plus Liquid Medium.

7. Incubate at 30°C for 90 min, centrifuge at high speed for 15 sec.

8. Discard the supernatant and re-suspend in 1 mL of NaCl Solution by gently pipetting up and down.

9. Spread 100 µL of a 1:10, 1:100, and 1:1000 dilution onto 100mm plates containing
   SD/–Trp/X-α-Gal
   SD/–His/–Trp/X-α-Gal
   SD/–Ade/–Trp/X-α-Gal

10. Incubate the plates at 30°C (face down) for 2–4 days, until colonies appear.

11. Bait protein is inactive if the transformant colonies are white and grow on SD/–Trp/X-α-Gal, but do not grow on SD/–His/–Trp or SD/–Ade/–Trp.

12. Bait protein is active if the transformant colonies are blue and grow on SD/–His/–Trp or SD/–Ade/–Trp.

13. If a bait strain exhibits background growth on –His medium, you may be able to eliminate (or reduce) the leaky His3 background expression by adding 3-AT to the selection medium (see below). Alternatively, use –Ade/–His/–Leu/–Trp medium for the library screening.

14. If a bait strain exhibits background growth on –Ade and –His medium, it will be difficult to use this bait protein in a two-hybrid library screening.

15. To test for transcriptional activation induced by the 3rd protein in the pBridge vectors, spread 100 µL of a 1:10, 1:100, and 1:1000 dilution of only the AH109 transformations (the Y187 is a methionine auxotroph and will not grow on –Met medium) onto 100mm plates containing:
    SD/–Met/–Trp/X-α-Gal
    SD/–His/–Met/–Trp/X-α-Gal

16. Incubate the plates at 30°C (face down) for 2–4 days, until colonies appear.

17. 3rd protein is inactive if the transformant colonies are white and grow on SD/–Met/–Trp/X-α-Gal, but do not grow on SD/–His/–Met –Trp.

18. 3rd protein is active if the transformant colonies are blue and grow on SD/–His/–Met/–Trp. See below for eliminating leaky HIS3 expression.

Leaky HIS3 expression – optimisation of the 3-AT concentration in the selection medium

1. Plate AH109 yeast transformants on a series of SD/–His/–Trp (or SD/–His/–Met/–Trp, if applicable) plates containing different concentrations of 3-AT.

2. start by testing [3-AT] in the range 0 to 15 mM (e.g. 0, 2.5, 5, 7.5, 10, 12.5, and 15 mM).

3. Use the lowest concentration of 3-AT that, after one week, allows only small (<1 mm) colonies to grow. Too much 3-AT in the medium can kill freshly transformed cells.

Testing the DNA-BD Fusion for Toxicity

1. Compare the growth rate in liquid culture of Y187 and AH109 cells transformed with the "empty" DNA-BD vector and cells transformed with the DNA-BD/bait plasmid. If the bait strain grows noticeably slower, your DNA-BD/bait protein may be toxic.

2. Select transformants from the SD/–Trp transformation plates above, then prepare an overnight culture as follows:

3. Inoculate 50 ml of SD/–Trp/Kan (20 µg/mL) with one large (2–3 mm) colony.

4. Incubate at 30°C overnight (16–24 hrs) with shaking at 250–270 rpm.

5. Check the OD_{600} of the culture; it should be ≥0.8. If the OD_{600} is much less than 0.8, the DNA-BD fusion may be toxic**.** If the fusion does not appear to hamper yeast growth—i.e. is nontoxic, carry on.

Preparation of DNA-BD transformants for Mating with the cDNA library-containing AH109

1. Centrifuge transformed Y187 culture at 600 x g for 5 min.

2. Remove supernatant.

3. Re-suspend in ~5 mL SD/–Trp liquid medium. Count cells using a hemacytometer. The cell density should be $\geq 1 \times 10^9$ cells/mL.

4. Mate this bait strain with your AD fusion library host strain.

Appendix 11

Yeast Two-Hybrid Assays

Reagents and Materials

Appropriate SD plates and recombinant vectors

2X YPDA Liquid

0.5 X YPDA Liquid

Kanamycin

X-α-gal

Protocol

Mate the library host strain with your bait strain.
(NB: Controls should be done in parallel with experimental work)

1. Thaw a 1ml aliquot (≥ 2 x 10^7 cells) of the AH109[library] in a room temperature waterbath.

2. Combine the 5 mL Y187 [bait] culture (≥ 1 x 10^9 cells/mL) and the 1 mL aliquot of AH109 [library] cells (≥ 2 x10^7 cells/mL) in a sterile 2 L flask.

3. Add 45 mL 2X YPDA/Kan (50 μg/mL). Swirl gently.

4. Rinse cells from library vial with two 1 mL aliquots of 2X YPDA/Kan (50 μg/mL).

5. Incubate at 30°C for 20–24 hrs with gentle swirling (30–50 rpm). Low-speed swirling is necessary to keep cells from settling to the bottom of the flask. However, shaking the culture at speeds > 50 rpm will significantly reduce mating efficiency.

6. After 20 hrs of mating, check a drop of the mating culture under a light microscope (40X). If zygotes (a zygote typically has a three-lobed shape, the lobes representing the two haploid (parental) cells and the budding diploid cell) are present, allow mating to continue for four more hours. Otherwise, continue.

7. Transfer the mating mixture to a sterile 100 mL centrifuge bottle. Centrifuge at 1000 x g for 10 min. Meanwhile, rinse the mating flask twice (50ml each rinse) with 0.5X YPDA/Kan (50 μg/mL). Combine the rinses and use them to re-suspend the pellet.

8. Centrifuge at 1000 x g for 10 min. Re-suspend the cell pellet in 10 mL of 0.5X YPDA/Kan (50 μg/mL) and measure the total volume of cells + medium.

Select for yeast diploids expressing interacting proteins

1. To determine the mating efficiency (see below), spread 100 µL of a 1:10 000, 1:1 000, 1:100, and 1:10 dilution of the mating mixture on three media (100mm plates):
   SD/–Leu
   SD/–Trp
   SD/–Leu/–Trp

2. Spread remaining mating mixture on Triple Dropout Medium (TDO) **or** Quadruple Dropout Medium (QDO) plates (200 µL cells / 150mm plate):
   For pGBKT7
   TDO: SD/–His/–Leu/–Trp
   QDO: SD/–Ade/–His/–Leu/–Trp

3. Incubate at 30°C until colonies appear. After 2–3 days, some colonies will be visible, but plates should be incubated for at least 5 days to allow slower growing colonies (i.e., weak positives) to appear. Ignore the small, pale colonies that may appear after 2 days but never grow to > 1 mm in diameter. True Ade+, His+ colonies are robust and can grow to > 2 mm. Also, Ade+ colonies are white or light pink, whereas Ade– colonies will slowly turn red on adenine-limited medium.

4. Score for growth on SD/–Leu, SD/–Trp, and SD/–Leu/–Trp. Calculate Mating Efficiency and Number of Colonies Screened (see below).

5. For colonies growing on TDO medium: Replica plate colonies onto QDO medium. Incubate at 30°C for 3–8 days.

6. Choose Ade+, His+ colonies for further analysis.

7. Streak out Ade+/His+ colonies on fresh SD/–Ade/–His/–Leu/–Trp/X-α-Gal master plates and grow for 2–4 days at 30°C. This enables the testing of the Ade+/His+ colonies for the activation of a third reporter: MEL1, which encodes α-galactosidase, a secreted enzyme that hydrolyzes X-α-Gal to produce a blue end product.

8. Seal the master plates with Parafilm and store at 4°C. If desired, prepare glycerol stock cultures of interesting clones and freeze at –70°C for long-term storage.

Control Matings

1. Pick one colony of each type prepared in Section 12 - i.e., AH109 [pGBKT7-RecT], Y187 [pGBKT7-53], and Y187 [pGBKT7-Lam] - to use in the mating. Use only large (2–3 mm), fresh (< 2 weeks old) colonies from the master plates.

2. Place both colonies in one 1.5 mL micro-centrifuge tube containing 0.5 mL of 2X YPDA medium. Vortex the tube for 1 min to completely re-suspend the cells.

3. Incubate at 30°C overnight (20–24 hrs) with shaking. Use the lowest shaking speed possible to prevent cells from settling. Vigorous shaking can reduce the mating efficiency

4. Plate cells on SD minimal media (see Table below; 100 µL cells/100mm plate). Use sterile 5mm glass beads to promote even spreading of the cells

Cross	**Plate on SD Minimal Media**[a] (100mm plates)	**Phenotype**	
		Mel1	**His/Ade**
Positive Control AH109[pGADT7-RecT] x Y187[pGBKT7-53]	–Leu[b] –Trp[b] –Leu/–Trp[b] –Ade/–His/–Leu/–Trp/X-α-Gal	Blue	+
Negative Control AH109[pGADT7-RecT] x Y187[pGBKT7-Lam]	–Leu[b] –Trp[b] –Leu/–Trp[b] –Ade/–His/–Leu/–Trp/X-α-Gal	no colonies	–

a Spread 100 µL aliquots of 1:10 and 1:100 dilutions of the mating culture.
b Use these plates to calculate the mating efficiency.

5. Incubate plates (colony side down) at 30°C for 3–5 days to allow diploid cells to form visible colonies.

6. Score for growth. Calculate the mating efficiency

7. Confirm nutritional and reporter phenotypes of diploids. Pick representative colonies from selection plates. Streak onto fresh medium.

8. After colonies have grown, seal plates with Parafilm and store at 4°C. For long term storage (> 2 weeks), prepare glycerol stock cultures and freeze at –70°C. These diploids are useful as reference strains when you wish to check a new batch of SD selection medium

Calculate Mating Efficiency & Number of Clones Screened

1. Count the colonies (cfu) growing on the SD/–Leu, SD/–Trp, and SD/–Leu/–Trp dilution plates that have 30–300 cfu

2. Calculate the viable cfu/ml on each type of SD medium:

$$\frac{\text{cfu}}{\text{Vol. plated (mL)} \times \text{dilution factor}} = \text{\# viable cfu/mL}$$

cfu/mL on SD/–Leu = viability of Y187 partner
cfu/mL on SD/–Trp = viability of AH109 partner
cfu/mL on SD/–Leu/–Trp = viability of diploids

3. Compare the viable cfu/mL of the two mating partners. The strain with the lower viability is the "limiting" partner. In this library screening protocol, the AH109[library] strain

should be the limiting partner to ensure that the maximum number of library cells find a mating partner. In a control cross, either strain could be limiting.

4. Calculate the mating efficiency (i.e., % Diploid):

$$\frac{\text{\# cfu/mL of diploids}}{\text{\# cfu/mL of limiting partner}} \times 100 = \% \text{ Diploid}$$

5. Estimate the number of clones screened:

cfu/mL of diploids x re-suspension volume (mL) = # of clones screened

Appendix 12

Verification and Analyses of Positive Interactions

Reagents and Materials

BD Matchmaker GAL4 AD LD-Insert Screening Amplimer Set (9103-1)
Appropriate SD plates

Protocol

Retest the Phenotype

Library transformants may contain more than one AD/library plasmid, which can complicate the analysis of putative positive clones. Thus, it is a good idea to restreak the positive colonies on SD dropout plates 2–3 times to segregate the AD/library plasmids.

1. Restreak positive two-hybrid clones on TDO medium.
   TDO = SD/–Ade/–Leu/–Trp or SD/–His/–Leu/–Trp

2. Incubate plates at 30°C for 4–6 days.

3. Replica plate or transfer well-isolated colonies to SD/–Ade/–His/– Leu/–Trp plates containing X-α-Gal to verify that they maintain the correct phenotype and to test for the expression of MEL1

4. Collect the re-streaked and retested positive colonies in a grid fashion on fresh master plates

5. Incubate plates at 30°C for 4–6 days.

6. After colonies have grown, seal plates with Parafilm, and store at 4°C for up to 4 weeks.

Rescue the Library cDNA Insert by Plasmid Isolation

1. Isolate plasmid DNA from yeast using method described in Appendix 7.

2. Because the plasmid DNA isolated from each yeast colony will be a mixture of the bait plasmid and at least one type of AD/library plasmid, you will need to separate the plasmids by selection in *E. coli*.

3. Transform the isolated plasmid extract from yeast into *E. coli*

4. For matings with pGBKT7 (Kanamycin-resistance), plate the transformants on LB medium containing ampicillin to select for the AD/library plasmid only.

5. Purify the AD/library plasmid using any suitable method

6. Amplify the cDNA insert by PCR using the BD Matchmaker AD LD-Insert Screening Amplimer Set (#9103-1) and the BD Advantage 2 PCR Kit (#K1910-1).

7. Analyze the cDNA Insert by Agarose/EtBr Gel Electrophoresis (see below)

Rescue the Library cDNA Insert by PCR Colony Screening

1. Preheat a PCR thermal cycler to 94°C

2. Place the BD Advantage 2 PCR Kit components and GAL4 AD LD-Insert Screening Amplimers on ice and allow them to thaw completely. Mix each component thoroughly before use

3. Prepare a Master Mix by combining the components as specified in the Table below:

Reagent	**1 rxn**
PCR-grade deionised H2O	41 mL
10X Advantage 2 PCR Buffer	5 µL
5' LD Amplimer (20 µM)	1 µL
3' LD Amplimer (20 µM)	1 µL
50X dNTP Mix (10 mM ea.)	1 µL
50 X Advantage 2 Polymerase Mix	1 µL
Total	**50 µL**

4. Using a sterile pipette tip, scrape a few cells from a colony that you wish to analyze. Place the cells in the bottom of a clean 250 µL PCR tube

5. Add 50 µL of Master Mix to the tube. Gently pipette up and down to disperse the cells, and PCR as follows:
   94°C 3 min
   25–30 cycles:
      94°C 30 sec
      68°C 3 min
   68°C 3 min
   Soak at 15°C

6. Analyze the PCR product by Agarose/EtBr Gel Electrophoresis (see below)

Analyze the cDNA Insert by Agarose/EtBr Gel Electrophoresis

1. Analyze a 5 µL aliquot of the PCR product alongside DNA size markers on a 0.8% 1X TAE agarose/EtBr gel

2. To distinguish the PCR product from similar size inserts in other AD/library plasmids, digest the PCR product with a frequent-cutter restriction enzyme such as Alu I or Hae III.

3. Run a small sample on a 2% agarose/EtBr gel. Compare the digestion pattern with that of other inserts

4. If a high percentage of the colonies appear to contain the same AD/library insert, expand the PCR analysis to another batch of 50 colonies.

5. If the PCR product consists of more than one band, segregate the library plasmids by isolating the plasmids from yeast using any standard method, transforming it into *E. coli* and selecting on LB/amp plates. Pick individual colonies..

6. If the PCR product consists of a single band, prepare a new master plate with a representative clone from each group.

7. Prepare a glycerol stock of each unique type of clone. Store at –80°C

8. Purify the PCR product with the Wizard SV PCR purification kit and sequence using the BD Matchmaker AD LD-Insert Screening Amplimer Set (#9103-1) or T7 Sequencing Primer

Retesting the Interaction

Protein-protein interactions can be retested in yeast (by either co-transformation or yeast mating), *in vitro* (by co-immunoprecipitation - Co-IP), and/or in mammalian cells.

Appendix 13

Protocol for Immunofluorescence-Labelling of Cultured Cells

Reagents and materials

RPMI 1640 media (Sigma, St. Louis, MO)

Methanol (Sigma, St. Louis, MO)

1X PBS

- Dissolve the following in 800 mL dH_2O.
  - 8g of NaCl
  - 0.2g of KCl
  - 1.44g of Na_2HPO_4
  - 0.24g of KH_2PO_4
- Adjust pH to 7.4.
- Adjust volume to 1L with additional dH_2O.
- Sterilise by autoclaving

4% Paraformaldehyde in PBS

- Take 1.25 mL of 32% w/v paraformaldehyde solution to a final volume of 10 ml in 1X PBS

1% Bovine serum albumin (BSA)

- Dissolve 1 g of BSA into 100 mL 1X PBS
- Filter-sterilise.
- Store at 4°C

Appropriate primary and secondary (labelled) antibodies

DAPI nuclear stain (Invitrogen)

- Dissolve the content of one vial (10 mg) in 2 mL deionised H_2O
- Aliquot and store at -20°C for long term storage

Mowiol mounting medium with anti-fade (Calbiochem)

Protocol

NOTE: General protocol that can be modified to give optimal results

Coverslip fixation of cultures of cells

1. Briefly rinse cell cultures in pre-warmed culture medium.

2. Alcohol permeabilisation: immerse coverslips carrying cells in absolute Methanol (5 min, -20°C).

3. Fix cells in 4% Paraformaldehyde in PBS (5 min, RT).

4. Wash cultures in PBS (3 x 10 min), then continue with Step 1 below:

Coverslip staining of cultures of cells

1. Incubate sections/cells in Blocking Solution: 1% bovine serum albumin (BSA) in PBS (optional and depending on antigen to be labelled: add 0.1% Triton X-100) (1 h, RT; blocking step to reduce non-specific staining).

2. Incubate sections/cells with appropriate pair of Primary Antibodies diluted in Blocking Solution (dilutions are antibody-specific and have to be established. As a rule of thumb, a good starting concentration for polyclonal ABs is 2 micrograms/ml; for monoclonals 20 micrograms/ml).

3. Seal in a humidified chamber and incubate overnight at 4^{o}C. Free-floating sections should be placed on a nutator for gentle agitation – but avoid this for mounted sections or cells on coverslips, as they may dislodge.

4. Wash sections/cells in PBS (3 x 10 min, RT)

5. Incubate sections/cells in Secondary Antibodies (e.g. donkey-anti-rabbit Cy3 and goat-anti-mouse ALEXA 488, both 1:500, diluted *together* in Blocking Solution). Incubate (90 min, RT) in a humidified chamber in the dark.

6. Wash sections/cells in PBS (3 x 10 min, RT)

7. Counterstain with DAPI Nuclear Stain (0.5 µg/ml in PBS) for 10min

8. Wash sections/cells in PBS (1 x 10 min, RT)

9. Mount sections/cells with Mowiol mounting medium with anti-fade (Calbiochem) (retards fading of fluorescence)

10. Store sections in the dark at 4°C until viewing

Appendix 14

SDS polyacrylamide gel electrophoresis

Reagent and materials

SDS PAGE BUFFERS:

1.5M Tris, pH8.8

- Dissolve 181.65 g of Tris base with 700 ml of dH_2O by stirring.
- Adjust the pH by adding the concentrated HCl.
- Adjust the final volume to 1 L with dH_2O.
- Autoclave to sterilise.

1 M Tris, pH 6.8

- Dissolve 121.4 g of Tris base with 700 ml of dH2O by stirring.
- Adjust the pH by adding the concentrated HCl.
- Adjust the final volume to 1 L with dH2O.
- Autoclave to sterilise.

10% SDS

- Dissolve 10 g of SDS (ultra-pure grade SDS) in 90 mL of ddH2O.
- Bring up to final volume of 100 mL

20% SDS

- Dissolve 20 g of SDS (ultra-pure grade SDS) in 90 mL of ddH2O.
- Bring up to final volume of 100 mL

2X reducing SDS sample buffer

- Combine the following
  - Tris (1M, pH 6.8) 3.4 mL
  - Glycerol 2 mL
  - SDS (20%) 3 mL
  - Bromophenol blue (0.75%) 500 µL
  - EDTA (0.5 M) 200 µL
  - β-Mercaptoethanol (BME) 1 mL

Store at -20°C or 4°C

Running bufferfor SDS-PAGE gels

- Combine the following

	2 litres:	4 litres:
25mM Tris	6 g	12 g
192mM Glvcine	28.8 g	57.6 g
0.1% SDS (10%)	20 mL	40 mL
H_2O	to 2 L	to 4 L

- DO NOT adjust pH. Store at 4°C or RT.

Acrylamide-BIS (30% w/v)

- Combine the following
  - Acrylamide 30 g
  - BIS 0.8 g
  - ddH_20 to 100mL

- Store at 4°C in dark container.

Ammonium persulphate (APS) (10% w/v)

- Dissolve 1 g of ammonium persulphate into 10 mL sterile dH_2O
- Store at 4°C.

Protocol

Preparation of the sample

1. Add an equal volume of 2 x SDS Sample Buffer to the protein sample (5-10 μg).

2. Mix and place in boiling water bath for 5 min.

3. If reduced and unreduced samples are to be run on same slab the reduced samples must be alkylated with iodoacetimide (l0 μL of a 1M solution per sample well, i.e. per 25 μL reducing sample buffer).

4. IAA added to samples after boiling, just prior to loading.

Preparation of the gel

1. Assemble gel apparatus as per manufacturer's instructions, and prepare separating and stacking gels as follows:

(a) Separating gel (for 2 x 0.75 mm mini-slab gels):

Component	7.5%	10%	12%	15%	18%
Acrylamide/bisacrylamide 30:0.8 (% w/v)	2.5 mL	3.33 mL (2.5ml of a 40% stock)	4.0 mL	5.0 mL	6.0 mL
1.5M Tris-HCI pH 8.8	2.5 mL	2.5 mL	2.5 mL	2.5 mL	2.5 mL
10% SDS	0.1 μL	0.1 μL	0.1 μL	0.1 μL	0.1 μL
H_20	4.85 mL	4.0 mL	3.35 m	2.35 mL	1.35 m
TEMED	10 μL	10 μL	l0 μL	l0 μL	l0 μL
10% ammonium persulphate	50 μL	50 μL	50 μL	50 μL	50 μL

2. Add water to the top of the gel to help separating gel set. After setting, pour off water and pour on stacking gel.

(b) 3% Stacking gel: (enough for 4) :

Components	Volumes
Acrylamide/bisacrylamide 30:0.8 (% w/v)	1.3 mL (0.8 ml of a 40% stock)
1M Tris-HCI pH 6.8	1.25 mL
10% SDS	0.1 µL
H_20	7.4 mL
TEMED	20 µL
10% ammonium persulphate	50 µL

Running of the samples

1. Pour running buffer into upper and lower chambers of apparatus so that top and bottom of gel and both electrodes are covered.

2. Load samples into the wells (approximately 15 - 20 uL), including a molecular weight marker in one lane.

3. Electrophorese at 200V (constant voltage) until the dye front reaches the end of the gel (45 min - 1 hr).

4. After electrophoresis the gel may be stained or used for Western Blotting.

Western Blotting

Reagent and materials

TBS-T wash buffer (0.1 % Tween)

– Combine the following

▪ 20mM Tris (1M 111 7.6)	50 mL	20 mL
▪ 137mM NaCl (5M)	137 mL / 40.03 g	16.01 g
▪ Tween	5 mL	2 mL
▪ H_2O	to 5 L	to 2 L

Blocking buffer

– Combine the following
  - 200 mL TBS-T wash buffer
  - 20 g fat free milk powder
  - 2 g of BSA

Stripping buffer (for Western membranes)

– β-Mercaptoethanol	100mM (21 mL 1.433M)
– SDS	2% (6 mL 10%)
– Tris (pH 6.7)	62.5mM (18.75 mL lM)
– ddH20	Make up to 300 mL

Protocol

Transfer of protein to nitrocellulose membrane:

1. The transfer stack is assembled as follows in Figure 1 and placed in the iBlot blotting system (Figure 2)

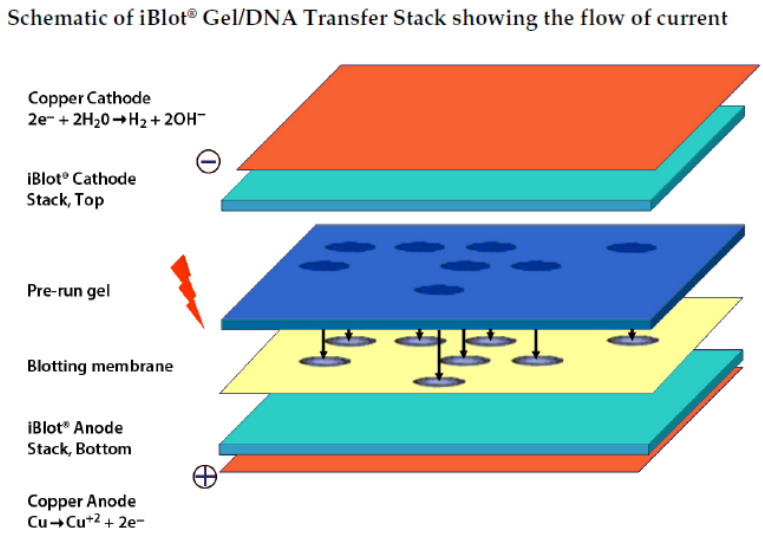

Figure 1. How iBlot® dry blotting works.

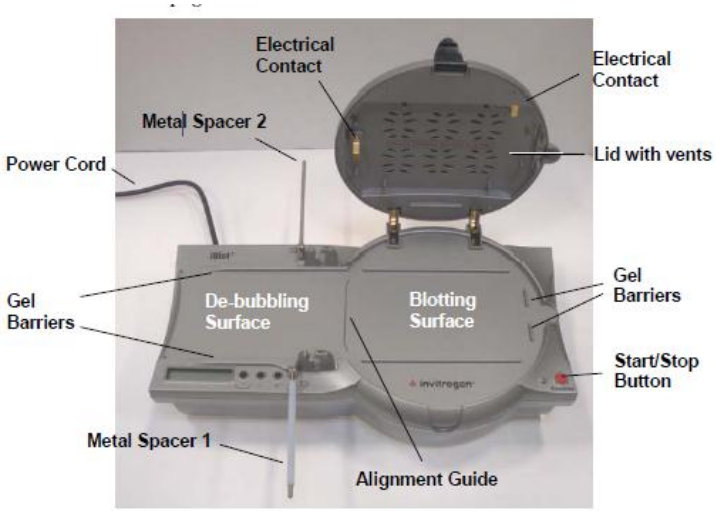

Figure 2. iBlot® dry blotting system (Invitrogen, Carlsbad, CA; http://www.Invitrogen, Carlsbad, CA.com)

2. After the transfer, the membrane is blocked overnight in 20 mL Blocking buffer (0.1% Tween).

Western detection

1. After overnight blocking step, the blocked membrane is rinsed with TBS-T buffer (0.1% Tween)

2. Incubate the blocked membrane with primary Ab diluted in TBS-T buffer at appropriate dilution for 60 min at RT

3. Wash step: rinse membrane 2x in TBS-T buffer, then wash 3x 10 min in TBS-T buffer with shaking

4. Incubate with dilution of secondary antibodies 60 min at RT.

5. Repeat the Wash step

6. Incubate in ECL detection fluid (5 mL of solution A with 5 mL of solution B)for 5 min

7. Wrap membrane in plastic wrap, stick to piece of Whatmann paper that fits into cassette

8. Detect 10 sec - 10 min with auto-radiographic film and develop autorads

Stripping and reprobing of blot (Safe to do once)

1. Incubate membrane in preheated Stripping buffer at 50°C in shaking water bath for 30' (70°C for high affinity antibodies)

2. Wash membrane 2x in TBS-T buffer at RT

3. Continue with blocking in Block buffer and proceed with Western Blot detection as outlined above.

Appendix 15

Sandwich ELISA protocol

Reagents and materials

96-Well Microtiter Nunc Maxisorb plates

3,3',5,5'-tetramethyl-benzidine (Sigma, St. Louis, MO T-2885)

Hydrogen peroxide 30% solution (Sigma, St. Louis, MO H-1009)

Dimethyl sulfoxide (DMSO), minimum 99.5% GC (Sigma, St. Louis, MO D5879-100ml)

Sulphuric acid 96% H_2SO_4

Sodium azide NaN_3

Adhesive plastic

2X anti-human C1qA primary antibodies (capture and detection) (two different epitopes)

1x secondary

Standard C1qA

Carbonate Buffer pH 9.5, 1L – store at 4°C

- Combine the following
  - 1.59 g of Na_2CO_3
  - 29.3 g of $NaHCO_3$
  - 2 mL of 10% NaN_3
- Adjust the volume 1 L with dH_2O.
- Store at 4°C.

Blocking buffer 0.05% Tween-20, 5% BSA, PBS – store at 4°C

- Dissolve 100 mg of BSA into 10 mL PBS-Tween
- Filter-sterilise and store at 4°C

TMB solution for 1mL– store at 4°C

- Dissolve 10 mg of TMB into 1 mL DMSO
- Filter-sterilise and store at 4°C

TMB buffer pH 5.5, 1L, 0.1M Na-acetate

- Dissolve 13.6 g of $CH_3COONa*3H_2O$ into 900 mL dH_2O
- Adjust pH to 5.5 with Acetic acid
- Adjust volume to 1 L with dH_2O

4M H_2SO_4 1L

- Carefully pour 392 mL H_2SO_4 stock solution in 608ml dH_2O (always pour acid into water)

2M H_2SO_4 100mL

- Combine 50 mL of the 4M H_2SO_4 solution with 50 mL dH_2O

Protocol

Day One

Antibody coating (capture)

1. Coat wells (Nunc Maxisorb plates) with capture antibody @ [1-10 µg/mL] carbonate/bicarbonate buffer pH 7.4 overnight at 4°C.

2. Remove coating solution and wash plate 3X 200 µL PBS/Tween

Day Two

Blocking

3. Block remaining protein binding sites in coated wells by adding 200-300 µL blocking buffer.

4. Incubate covered overnight at 4°C.

Day Three

Adding samples (duplicates)

5. Wash plate 3X 200-300µL PBS/Tween

6. Adding samples:
   a. Add 100 µL of diluted sample (blocking buffer) to each well.
   b. Set up standard curve (load 100 µL of each)
      - 4000, 2000, 1000, 500, 250, 125, 62.5, 31.25 pg/mL (blocking buffer)

7. Incubate for 90 min (or overnight) at 37°C

8. Remove samples and wash 3X with 200-300 µL PBS/Tween

Incubation with detection antibody and secondary antibody

9. Add 100 µL of diluted detection antibody to each well

10. Cover plates and incubate for 2hrs at room temperature

11. Wash plate 4X 200-300 µL PBS/Tween

12. Add 100 µ of secondary antibody conjugated with HRP, diluted in blocking buffer

13. Cover plates and incubate for 1-2 hrs at room temperature

14. Wash plate 4X 200-300 µL PBS/Tween

Detection

15. Add 100 µL TMB developing solution to wells
    a. 1 ELISA plate mix:
        - 11 mL TMB buffer
        - 110 µL TMB solution
        - 22 µL H_2O_2
    b. Incubate for 15-30min

16. Add 100 µL 2M H_2SO_4 to stop the reaction

17. Read absorbance at 450nm
    a. Positive wells will change to a blue color depending on signal intensity
    b. The blue will change to yellow when the reaction is stopped
    c. Read multiple plates in the order the color development was stopped
        - reaction is stopped after 5 min

Appendix 16

Haplotype frequencies

rs.172378-rs12033074

TB	Frequency		OR of TB, adjusted for age and gender		
Haplotype:	**Control**	**case**	**OR**	**95% CI**	
A-G	0.02	0.02	0.84	0.38	1.87
A-C	0.34	0.33	1.06	0.86	1.30
G-C	0.21	0.26	1.39	1.09	1.77
G-G	0.43	0.39	1		

rs12033074-rs631090

TB	Frequency		OR of TB, adjusted for age and gender		
Haplotype:	**Control**	**case**	**OR**	**95% CI**	
C-C	0.19	0.25	1.37	1.02	1.83
G-C	0.15	0.13	0.99	0.73	1.34
G-T	0.30	0.27	0.91	0.71	1.18
C-T	0.37	0.35	1.00	1.00	1.00

rs587585-rs665691-rs.172378

TB	Frequency		OR of TB, adjusted for age and gender		
Haplotype:	**Control**	**case**	**OR**	**95% CI**	
A-C-A	0.31	0.28	0.99	0.79	1.22
A-C-G	0.03	0.03	0.94	0.55	1.60
A-G-A	0.01	0.01	1.83	0.50	6.75
G-G-A	0.05	0.06	1.41	0.92	2.15
G-G-G	0.19	0.24	1.48	1.16	1.89
A-G-G	0.41	0.38	1.00	1.00	1.00

rs665691-rs.172378-rs12033074

TB	Frequency		OR of TB, adjusted for age and gender		
Haplotype:	**Control**	**case**	**OR**	**95% CI**	
C-A-C	0.29	0.27	1.00	0.80	1.24
C-A-G	0.02	0.01	0.68	0.29	1.59
C-G-G	0.03	0.03	0.94	0.55	1.61

G-A-C	0.06	0.07	1.35	0.89	2.02
G-G-C	0.21	0.26	1.40	1.09	1.78
G-G-G	0.39	0.36	1.00	1.00	1.00

rs587585-rs665691-rs.172378-rs12033074

TB	**Frequency**		**OR of TB, adjusted for age and gender**		
Haplotype:	**Control**	**Case**	**OR**	**95% CI**	
A-C-A-C	0.29	0.26	0.99	0.80	1.24
A-C-A-G	0.02	0.02	0.84	0.40	1.79
A-C-G-G	0.03	0.04	0.98	0.58	1.67
A-G-G-C	0.02	0.03	1.38	0.73	2.62
G-G-A-C	0.05	0.06	1.44	0.94	2.21
G-G-G-C	0.19	0.24	1.45	1.13	1.86
A-G-G-G	0.39	0.35	1.00	1.00	1.00

rs12033074-rs631090

TBM	**Frequency**		**OR of TB, adjusted for age and gender**		
Haplotype:	**Control**	**Case**	**OR**	**95% CI**	
C-C	0.19	0.27	0.20	0.02	2.34
G-C	0.15	0.14	9.48	1.09	82.67
G-T	0.30	0.25	2.04	0.34	12.24
C-T	0.37	0.34	1.00	1.00	1.00